LA-7709-T
Thesis

C.3

Thermal-Hydraulic Analysis Techniques for Axisymmetric Pebble Bed Nuclear Reactor Cores

LOS ALAMOS SCIENTIFIC LABORATORY
Post Office Box 1663 Los Alamos, New Mexico 87545

This thesis was accepted by the Department of Mechanical Engineering, Colorado State University, Fort Collins, Colorado, in partial fulfillment of the requirements for the degree of Doctor of Philosophy. It is the independent work of the author and has not been edited by the Technical Information staff.

This work was supported by the US Department of Energy, Division of Nuclear Research and Applications.

LA-7709-T
Thesis

UC-80
Issued: March 1979

Thermal-Hydraulic Analysis Techniques for Axisymmetric Pebble Bed Nuclear Reactor Cores

Kenneth R. Stroh

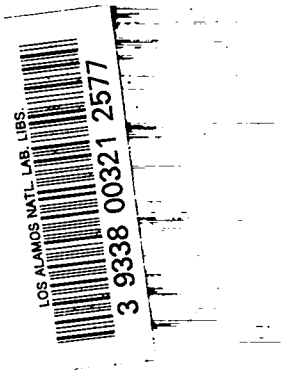

TABLE OF CONTENTS

TABLE OF CONTENTS (continued)

LIST OF FIGURES

LIST OF FIGURES (continued)

LIST OF FIGURES (continued)

ABSTRACT OF THESIS

THERMAL-HYDRAULIC ANALYSIS TECHNIQUES FOR

AXISYMMETRIC PEBBLE BED NUCLEAR REACTOR CORES

The pebble bed reactor's cylindrical core volume contains a random bed of small, spherical fuel-moderator elements. These graphite spheres, containing a central region of dispersed coated-particle fissile and fertile material, are cooled by high pressure helium flowing through the connected interstitial voids. A mathematical model and numerical solution technique have been developed which allow calculation of macroscopic values of thermal-hydraulic variables in an axisymmetric pebble bed nuclear reactor core. The computer program PEBBLE is based on a mathematical model which treats the bed macroscopically as a generating, conducting porous medium. The steady-state model uses a nonlinear Forchheimer-type relation between the coolant pressure gradient and mass flux, with newly derived coefficients for the linear and quadratic resistance terms. The remaining equations in the model make use of mass continuity, and thermal energy balances for the solid and fluid phases. None of the usual simplifying assumptions, such as constant properties, constant velocity flow, or negligible conduction and/or radiation are used.

PEBBLE solves a coupled set of nonlinear finite difference equations, derived by integrating the corresponding nonlinear elliptic partial differential equations over a finite area, based on assumptions about the distribution of the variables between the nodes of the grid. This approach ensures that conservation laws are obeyed over

arbitrarily large or small portions of the field. In addition, this approach is most appropriate for a macroscopic porous medium model of the packed sphere bed, which already includes the assumption that the variables in a given bed volume are well characterized by macroscopically-averaged values. The finite difference equations are solved by a successive substitution technique.

The code has been used to analyze the full-scale mockup of the Oak Ridge National Laboratory's Pebble Bed Reactor Experiment, and the flow predictions have been compared with data. The code PEBBLE is shown to predict distributions of velocity and pressure adequately for high Reynolds number flows in packed sphere beds. A fully coupled thermal-hydraulic analysis of a large power reactor design has also been completed, using calculated fission power profiles. The code calculated a mixed-mean outlet coolant temperature which is within one degree K of the analytic value. Limitations of the code, and its ability to calculate the distributions of the thermal-hydraulic variables in large pebble bed power reactors are discussed.

Kenneth R. Stroh
Department of Mechanical Engineering
Colorado State University
Fort Collins, Colorado 80523
Fall, 1978

I. INTRODUCTION

A. Pebble Bed Nuclear Reactor Concept

On October 11, 1945 Farrington Daniels filed a U.S. Patent application (granted October 15, 1957) describing a nuclear fission reactor using uranium carbide as fuel, graphite as moderator, thorium as fertile material and helium as the coolant [1]. The fuel and moderator were to be roughly spherical pebbles ($\sim$0.02 to 0.07 m in diameter) randomly arranged in a "pebble bed." Means were provided for charging at the top and discharging at the bottom, in part or in whole, at intervals as required. Coolant was assumed to pass uniformly through the entire cross section of the pile.

Since that time, work on the pebble bed reactor (PBR) concept has proceeded worldwide, primarily at the Oak Ridge National Laboratory (ORNL) in the early 1960's, and more recently in the Federal Republic of Germany. The program in Germany has seen more than nine years of operation of the 15 MW(e) Arbeitsgemeinschaft Versuch-Reaktor GmbH (AVR) reactor and the on-going construction of the 300 MW(e) Thorium High Temperature Reactor (THTR). In February, 1974 the mixed-mean outlet temperature of the AVR was increased to 1223 K without major problems, raising the possibility that a pebble bed Very High Temperature Reactor (VHTR) could supply helium at temperatures appropriate for process heat applications [2,3]. A section of a large PBR core is shown in Fig. 1.

The latest German designs use a spherical fuel-moderator element with small particles of fissile (or fertile) material, coated with pyrolytic carbon or SiC, embedded in a graphite matrix. In the

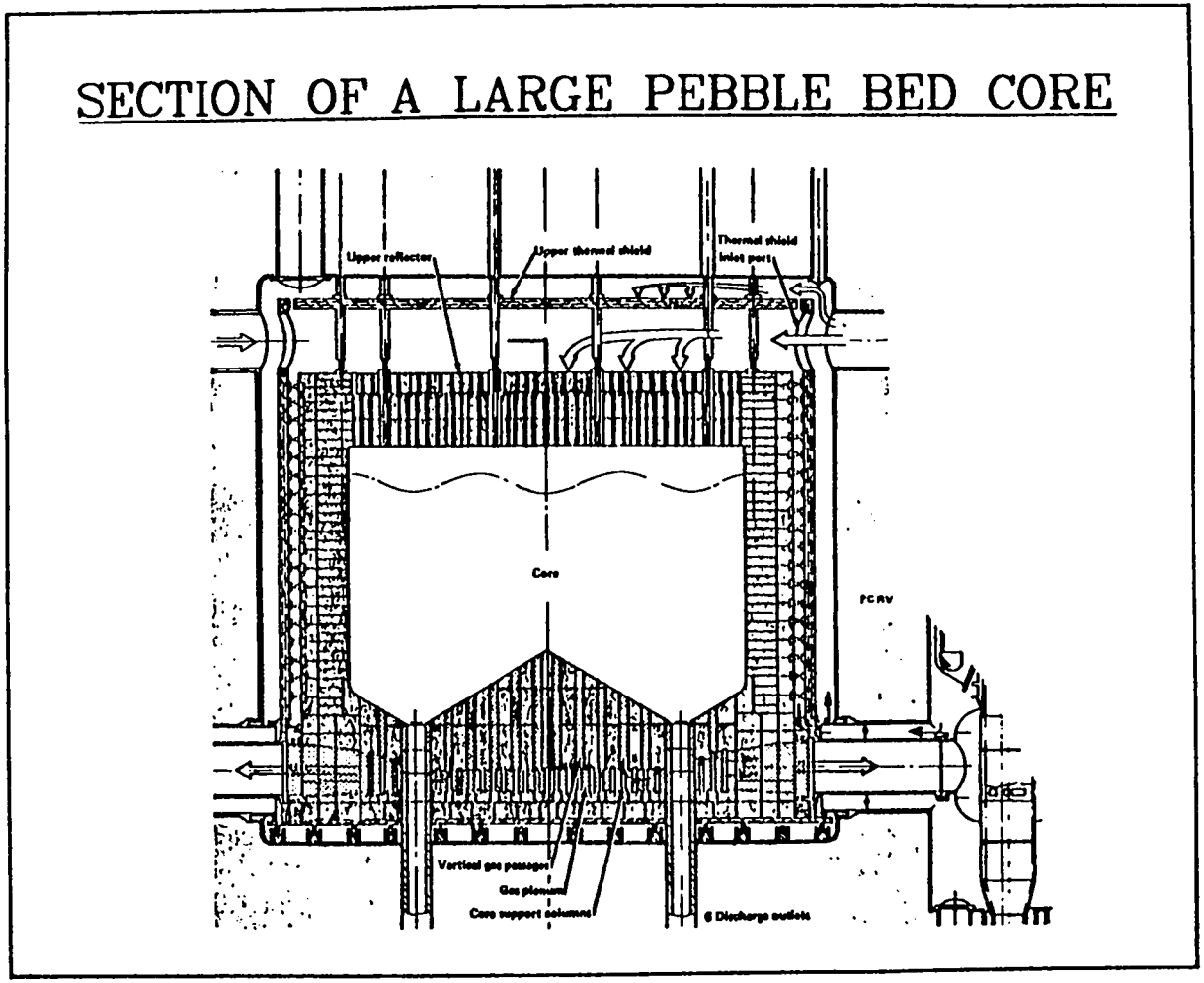

Fig. 1. A section view of a large power reactor design showing the graphite reflector structure, the pebble bed core with free surface, and the ball discharge structures [4].

reference fuel, the coated particles are dispersed throughout the 0.05 m diameter central region of the 0.06 m diameter graphite ball. In the advanced fuel-moderator element design the coated particles are dispersed in a spherical shell within the graphite ball. The fuel-moderator element types are shown in Fig. 2.

The bed is cooled by helium at an inlet pressure of about 4 MPa flowing downward through the core. The pebbles also flow slowly downward due to the continuous addition of fresh elements to the top of the bed and continuous removal of spent elements from the bottom of the bed. Most designs are based on the Once Through Then Out (OTTO) fuel cycle, in which the fuel elements reach their design burnup in a single pass through the reactor core. This fuel cycle, combined with downflowing coolant, results in approximately 90% of the thermal power being generated in the upper half of the core. Thus, near the outlet, where pebble surface and coolant temperatures are highest, internal generation is low. This results in acceptable maximum fuel particle temperatures and temperature gradients for very high helium temperatures at the core outlet.

B. Motivation of the Study

The Systems Analysis Study for Nuclear Process Heat is an on-going program in the Reactor and Advanced Heat Transfer Technology Group of the Energy Division of the Los Alamos Scientific Laboratory (LASL). A task of the program has been the development of appropriate calculational models for the analysis of various nuclear process heat systems. The status of the PBR thermal-hydraulic modeling effort is the subject of this paper. Sufficient detail is included to allow this paper to serve as a user's manual for the computer code PEBBLE.

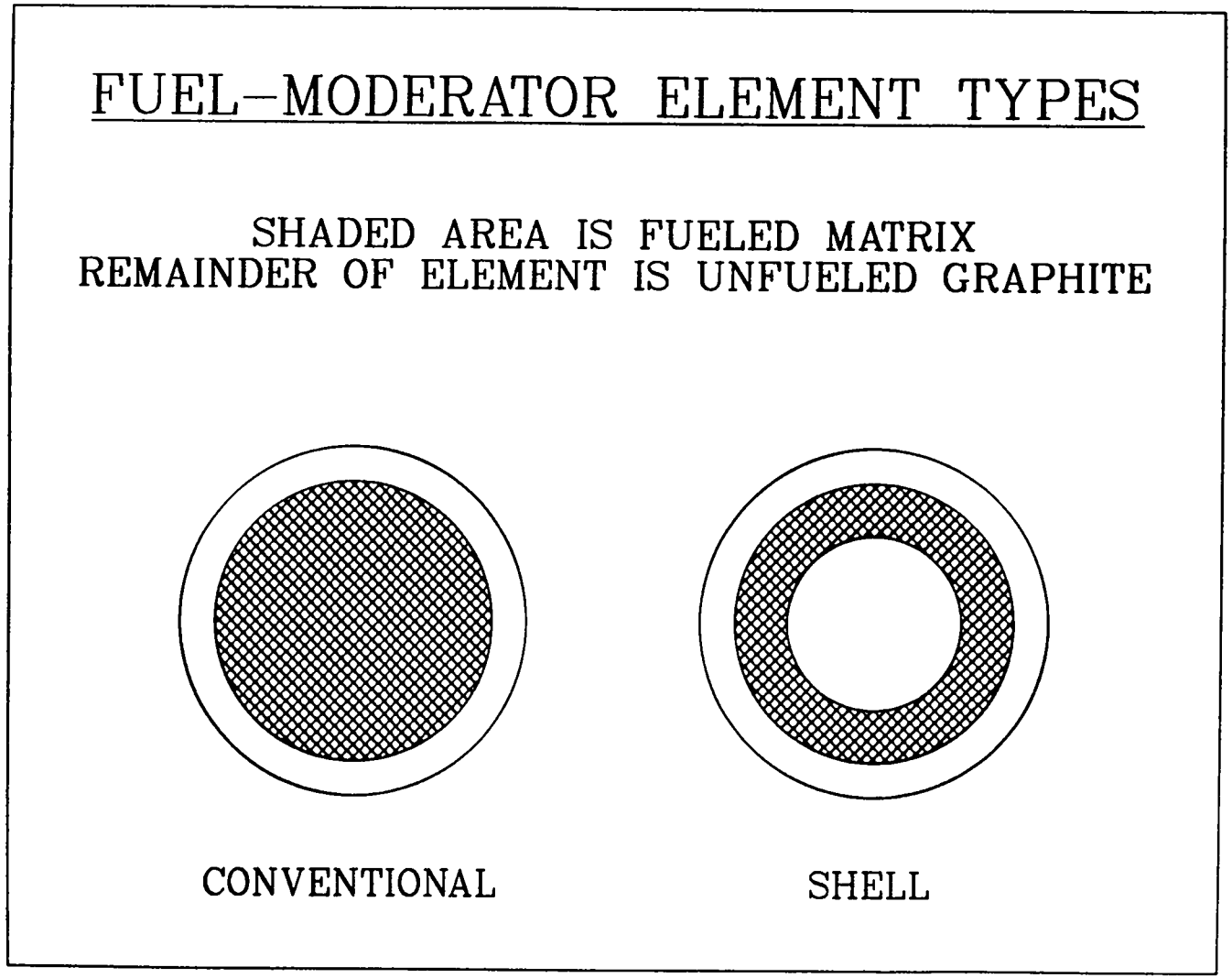

Fig. 2. Fuel-moderator element types proposed for pebble bed nuclear reactors [3].

The near-term requirements of the code are that when given the axisymmetric power distribution (from an existing neutronics model), the core geometry, and the helium inlet temperature, pressure and mass flow rate (from design information), the following steady-state information can be calculated:

1) the axisymmetric coolant velocity distribution,
2) the coolant pressure distribution and overall core pressure drop,
3) the distribution of coolant bulk temperature, and
4) the distributions of pebble average surface temperature, fueled/unfueled interface temperature, and maximum fuel temperature.

The task requires a numerical model which includes all important transport mechanisms, which is flexible enough to handle wide ranges of parameter variation as required by sensitivity analyses, and has the potential for eventual coupling to the neutronics model. Though specifically oriented toward nuclear reactor analysis, the techniques developed may be adaptable to many chemical engineering processes involving fluid flow through packed beds.

II. REVIEW OF THE LITERATURE

A. Introduction

Extensive literature exists in the chemical engineering journals regarding the flow of gases, the transfer of heat and mass, and the pressure drop in fluids flowing through packed beds. Most existing reaction engineering analyses, however, are for stagnant beds, for low Reynolds number flows or assume plugflow of the gas. The heat transfer analyses reported generally have no generation term (or at most a surface reaction), some neglect turbulent mixing, and many assume the solids temperature equals the gas temperature. No analysis was found which approached the complexity required in a pebble bed nuclear reactor analysis, however, many portions of the mathematical model have been previously derived. A partial review of the applicable literature published prior to 1975 has been performed by Badur and Giersch [5]. Techniques for the thermal-hydraulic analysis of a nuclear PBR have been developed in Germany, but the methodology (mathematical model or numerical method) has not been reported in the open literature.

B. Packed Bed Fluid Flow and Pressure Drop

Exact mathematical modeling of a packed bed reactor system is impossible, as the arrangement assumed by uniform spheres in a container with a sufficiently large bed to ball diameter ratio cannot be predetermined. Any approach which attempts to describe the bed geometry on a scale on the order of the particle diameter, introduces a regularity into the packing which does not physically exist. This can be avoided by treating the bed macroscopically as a porous medium; that is, each region of space contains a mixture of both a solid phase and a fluid phase, with the

respective fractions of each phase determined by a volume-averaged distribution of the phases representing the physical packed bed.

Though purely statistical approaches to porous media flow, such as random walk models [6,7] and random media models [6,8] hold promise for a fundamental understanding of the flow phenomena, results to date are inconclusive. The complexity of these models makes coupling of the fluid flow and heat transfer problems impractical.

It is more appropriate for engineering analyses to calculate the flow from differential equations. Though originally empirical, these differential equations have recently been derived theoretically [9,10]. Numerous solutions to porous media flow problems are available based on Darcy's law and various intuitive extensions thereof. Darcy's law states an empirical linear relationship between the flow rate and pressure gradient such that "the volume rate of flow is directly proportional to the pressure drop and inversely proportional to the thickness of the bed." It was observed very early that this linear relationship is only valid for the "seepage velocity" domain. Various investigators place the upper limit for validity of Darcy's law at Reynolds numbers, based on the particle diameter and superficial velocity (a velocity based on a void fraction of 1.0) of from 1 to 10 [6].

High velocity porous media flow analyses have most often used a quadratic equation of the type first proposed by Forchheimer [6]

$$\frac{\Delta P}{L} = a_1 V + a_2 V^2 \qquad (1)$$

for the non-linear flow regime, where V is the fluid velocity, P is the fluid pressure, L is the length of the medium, and a_1 and a_2 are factors which depend on both fluid and porous medium properties.

Ahmed [10] has derived a macroscopic one-dimensional Forchheimer-type equation from a dimensionless form of the turbulent Navier-Stokes equations. This analysis assumes an incompressible fluid and steady flow without body forces. He argues that the kinetic energy dissipation due to turbulent fluctuations is very small (~5%) compared to the energy represented by convective accelerations, and assumes the turbulent losses can be safely ignored for flow through porous media. The resulting equation is of the form

$$\frac{dP}{dx} = b_1 \frac{\mu}{D} V + b_2 \frac{\rho}{D} V^2, \tag{2}$$

where x is the spatial coordinate, D is a characteristic length for the flow, b_1 and b_2 are factors dependent on media properties, and μ and ρ represent the fluid dynamic viscosity and density, respectively. The origin of the terms in Eq. (2) indicates that the linear term represents a flow resistance due to viscous shear. The quadratic term represents losses caused by separation, and sudden enlargement of the flow area, as the fluid traverses the continuously changing interstitial pore geometry. Throughout this paper, the terms a_1V and a_2V^2 in Eq. (1) are referred to as the linear and quadratic resistance terms.

The most frequently used (and recommended) Forchheimer-type equation is the semi-empirical Ergun equation [11],

$$\frac{\Delta P}{L} = \frac{1-\varepsilon}{\varepsilon^3} \left[150\,(1-\varepsilon) \frac{\mu V}{d_p^2} + 1.75 \frac{\rho}{d_p} V^2 \right], \tag{3}$$

where V is the superficial velocity, ε is the bed void fraction and d_p

is the particle diameter. The equation is formed by adding the Blake-Kozeny equation for purely laminar (viscous) flow through a porous medium modeled as an assembly of capillaries, to the Burke-Plummer equation derived for the fully turbulent limit in a capillaric medium.

In recent years there has been a growing interest in the development of modeling equations for representing flow maldistribution in packed beds, primarily in chemical catalytic reactors and iron blast furnaces. There has been general agreement in the literature that the mathematical models of such systems make use of the differential, vectorial form of the Ergun equation. See for example Radestock and Jeschar [12,13], and Stanek and Szekely [14-16]. Moreover, in recent papers, Szekely and Povermo [17] presented direct experimental evidence for the validity of this approach.

The differential, vectorial form of the Ergun equation may be written as

$$\vec{\nabla}P = -\vec{V}\,(k_1 + k_2\,|\vec{V}|), \tag{4}$$

where the functions k_1 and k_2 can be deduced from Eq. (3). In recent papers, however, Shvydkii, et al. [18] suggested that this form is an oversimplification. They argued that the terms on the right-hand side of Eq. (4) represent a flow resistance, and that inertial terms should be explicitly included. When written in two-dimensional axisymmetric cylindrical coordinates, the equations proposed by Shvydkii take the following form

$$V_r \frac{\partial V_r}{\partial r} + V_z \frac{\partial V_r}{\partial z} = -\frac{1}{\rho}\frac{\partial P}{\partial r} - \frac{k_1}{\rho} V_r - \frac{k_2}{\rho} V_r V, \tag{5}$$

and

$$V_r \frac{\partial V_z}{\partial r} + V_z \frac{\partial V_z}{\partial z} = -\frac{1}{\rho} \frac{\partial P}{\partial z} - \frac{k_1}{\rho} V_z - \frac{k_2}{\rho} V_z V, \tag{6}$$

where

$$V = (V_r^2 + V_z^2)^{0.5}. \tag{7}$$

They did not present a numerical solution of the full set of equations containing these inertial terms, but assumed irrotational flow, making it impossible to compare directly the results obtained from the two different formulations given by Eq. (4) and Eqs. (5-7).

Choudhary, Propster and Szekely [19] have performed numerical experiments to allow direct comparison of the two flow models. They noted that in contrast to the laminar Navier-Stokes equations, where one would expect the inertial terms to predominate at high velocities (and at a distance from solid surfaces), the terms on the left- and right-hand sides of Eqs. (5) and (6) are both of the order (V^2), making it impossible to draw conclusions readily regarding the relative importance of these terms. As expected, the two solutions are essentially identical for parallel flow through uniformly packed beds. As a critical test, they performed an isothermal flow analysis of a blast furnace with alternate "V" shaped layers of different size packing, where the fluid was introduced through a side stream nozzle (perpendicular to the exit flow direction). They reported that the two flow models gave quite similar results, with the differences between calculated point values of the velocity ranging from 2 to 12%. They concluded that the calculated difference would be difficult to detect experimentally. The inclusion of

these inertial terms greatly increased the computational labor, and they questioned whether the refinement in the calculation justified the additional effort for the majority of engineering calculations. It can be noted that the flow maldistribution in the blast furnace problem is more extreme than would be expected in a pebble bed nuclear reactor core, even with radial power peaks and hot-spot formation.

Early pressure drop studies through sphere beds intended to mock-up pebble bed reactors indicated, however, that the Ergun equation considerably over-predicts the pressure drop in the Reynolds number range of interest. Defining a friction factor

$$f = \left(\frac{d_p \, \Delta P}{4L}\right) \Big/ \left(\frac{\rho V^2}{2}\right), \tag{8}$$

offers a basis for comparison of the Ergun equation with pressure drop data from Denton [20] and the ORNL Pebble Bed Reactor Experiment (PBRE) [21]. Figure 3 shows this comparison in a plot of friction factors versus Reynolds number. The Reynolds number used throughout this paper is based on the superficial mass flux, $G = \rho V$, and the pebble diameter, d_p, so that

$$N_{Re} = \frac{G \, d_p}{\mu} . \tag{9}$$

C. Packed Bed Heat Transfer

The rate of heat transfer in a generating, conducting porous medium with a flowing fluid phase is controlled by a number of mechanisms, including bulk movement of the fluid, conduction in both the solid and fluid phases, convective transfer between phases, dispersion of the fluid in the interstices of the porous medium, and in the case of a gaseous

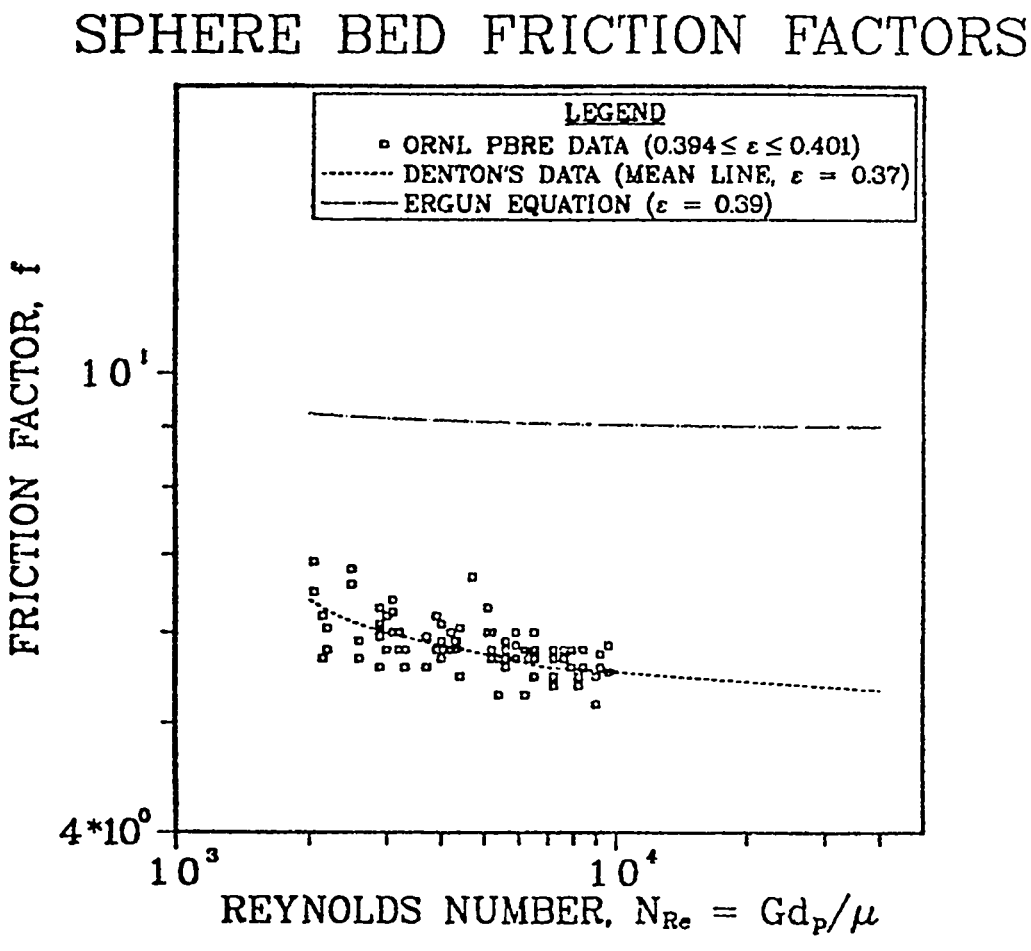

Fig. 3. Comparison of the Ergun equation with data from sphere bed flow experiments. The ORNL PBRE data was taken on a series of beds assembled by different methods in the same vessel.

fluid, radiant exchange. Because of the complexities of the solids packing and the interconnected interstitial spaces, a porous medium approach to thermal modeling is required. Thus, the dependent variables are the average temperature of the pebble surface and local value of the coolant bulk (mixing cup) temperature.

Several investigators have derived differential equations for these temperatures from thermal energy balances on the solid phase, on the fluid phase, or on a unit volume of the bed containing both phases. Choudhury [22] has derived ordinary differential equations in his study of porous-metal nuclear fuel elements, assuming uniform generation, constant coefficients and negligible radiant heat transfer. Experimentally determined effective thermal conductivities were used. Singer and Wilhelm [23] have derived vectorial differential temperature equations for packed bed chemical reactors, and have presented analytical solutions for certain restricted cases where constant coefficients can be assumed and some terms can be neglected.

There are numerous correlations and models in the literature for packed bed heat transfer coefficients and effective conductivities. One review by Barker [24] lists 244 references on subjects related to heat transfer in particulate systems, including fluid-to-particle heat transfer coefficients, mass transfer coefficients, mixing studies and effective conductivity experiments.

III. MATHEMATICAL MODEL

A. Hydraulic Model

In formulating this model, the core volume was treated as a generating, conducting porous medium characterized by its uniform pebble diameter, the core diameter ratio, and its void fraction distribution. In a PBR the bed volume and diameter ratio are both sufficiently large to allow characterization by a volume-averaged void fraction distribution, which allows calculation of local macroscopic values of the thermal-hydraulic variables.

The predominate assumption made in formulating the hydraulic model is that the coolant flow in a PBR core can be described adequately by a Forchheimer-type equation, relating the pressure, P (Pa), and the superficial velocity, V (m/s), such that

$$\vec{\nabla}P = -\vec{V}\,(f_1 + f_2\,|\vec{V}|), \tag{10}$$

where the products f_1V and f_2V^2 represent the linear and quadratic resistance terms, respectively.

Koida [25] has developed expressions for f_1 and f_2 so that

$$f_1 = \frac{A\,\mu}{\varepsilon\,R_h^{\,2}}\,, \tag{11}$$

$$f_2 = \frac{B\,\rho}{\varepsilon^2\,R_h}\,, \tag{12}$$

where

A and B = empirical coefficients that are constant for a given particle shape,

R_h = effective hydraulic radius for the flow within the packed bed (m),

ε = bed void fraction,

μ = fluid dynamic viscosity (Pa·s), and

ρ = fluid density (kg/m^3).

R_h for a randomly packed bed of spheres is given by [26]

$$R_h = \left(\frac{d_p}{6}\right)\frac{\varepsilon}{1-\varepsilon} \quad , \tag{13}$$

where d_p = pebble diameter (m). Equation (10) clearly neglects body forces (gravity) and does not explicitly include the inertial terms. The body forces may be safely ignored, as their effect is negligible for the high gas velocities considered here. It is assumed that the inertial terms can be safely ignored following the study of Choudhary, et al. [19] discussed in the previous chapter.

Numerical values for the constants A and B in Eqs. (11) and (12) of 24.5 and 0.1754, respectively, were calculated using Barthels [27] friction factor correlation for high Reynolds number gas flows in packed sphere beds. Equations (10), (11) and (12) and Barthels correlation can now be expressed as the friction factor defined by Eq. (8). Figure 4 shows the comparison of these friction factors versus Reynolds number with the information previously displayed in Fig. 2. This model should not be applied outside the range $10^3 \leq N_{Re} \leq 4 \times 10^4$.

If the fluid pressure drop and temperature rise across the bed result in an appreciable change in fluid density, it is more convenient to

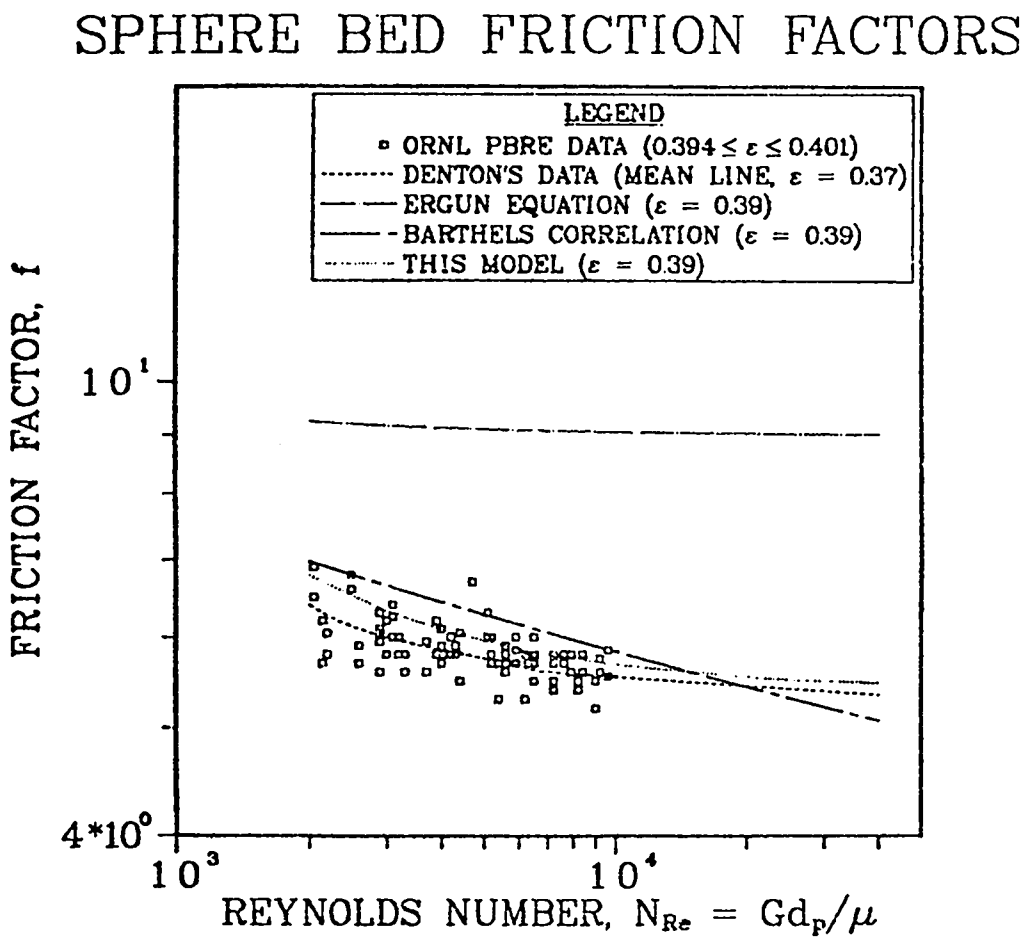

Fig. 4. Comparison of the new flow model with other models and experimental data. The ORNL PBRE data was taken on a series of beds assembled by different methods in the same vessel.

calculate the mass flux, $G = \rho V$, rather than the fluid velocity. Using G, Eq. (10) becomes

$$\vec{\nabla}P = - \vec{G} (g_1 + g_2 |\vec{G}|) , \tag{14}$$

where

$$g_1 = f_1/\rho , \tag{15}$$

$$g_2 = f_2/\rho^2 , \tag{16}$$

Since curl grad = 0, the pressure variable can be eliminated from Eq. (14); thus

$$\vec{\nabla} \times [- \vec{G} (g_1 + g_2 |\vec{G}|)] = 0. \tag{17}$$

The model's equations have been formulated in axisymmetric cylindrical coordinates because they allow a realistic representation of actual physical conditions, and facilitate coupling of this model to the current neutronics model. Manipulation of Eq. (17) yields the following scalar equation

$$\frac{\partial}{\partial z'} \left[- (g_1 + g_2 |\vec{G}|) G_r \right] - \frac{\partial}{\partial r'} \left[- (g_1 + g_2 |\vec{G}|) G_z \right] = 0, \tag{18}$$

were z' and r' are the axial and radial coordinates.

The equation is made nondimensional by the appplication of the following definitions:

$$\xi = \frac{g_1}{g_2 G_{IN}} , \quad G^* = \frac{|\vec{G}|}{G_{IN}} , \quad g_2^* = \frac{g_2}{g_{2IN}} , \tag{19}$$

$$r = \frac{r'}{R} , \quad z = \frac{z'}{L} , \quad \text{and} \quad a = \frac{R}{L} ,$$

where

R = bed radius (m),

L = bed height (m), and

IN = inlet plenum values.

Introducing the above definitions into Eq. (18) gives a nondimensional scalar equation in terms of G_r^* and G_z^*, the unknown radial and axial components of $\vec{G}^*$,

$$\frac{\partial}{\partial z}\left[(\xi + G^*)\, g_2^*\, G_r^*\right] - \frac{1}{a}\,\frac{\partial}{\partial r}\left[(\xi + G^*)\, g_2^*\, G_z^*\right] = 0. \qquad (20)$$

The continuity equation, $\vec{\nabla} \cdot \vec{G} = 0$, in nondimensional form and axisymmetric cylindrical coordinates is

$$\frac{1}{r}\,\frac{\partial}{\partial r}\left(r\, G_r^*\right) + a\,\frac{\partial}{\partial z}\, G_z^* = 0. \qquad (21)$$

For the purposes of computation, the coupled system of Eqs. (20) and (21) are replaced by a single equation of higher order for the nondimensional stream function, ψ, defined by

$$G_r^* = -\frac{a}{r}\,\frac{\partial \psi}{\partial z}, \qquad G_z^* = \frac{1}{r}\,\frac{\partial \psi}{\partial r}. \qquad (22)$$

When so defined, the stream function inherently satisfies the continuity equation. Combining Eqs. (20) and (22) gives a nonlinear, elliptical partial differential equation:

$$-\frac{\partial}{\partial z}\left[\frac{1}{r}\,(\xi + G^*)\, g_2^*\,\frac{\partial \psi}{\partial z}\right] - \frac{\partial}{\partial r}\left[\frac{1}{ra^2}\,(\xi + G^*)\, g_2^*\,\frac{\partial \psi}{\partial r}\right] = 0. \qquad (23)$$

Because the coefficients are a function of temperature, and the temperatures in turn depend on the mass flux, a complete thermal-hydraulic description results in a set of coupled elliptic partial differential equations like Eq. (23). The numerical solution method selected [28] requires that the equations be expressed in terms of the nondimensional variables in the following form (See Appendix A):

$$a_\phi \left[\frac{\partial}{\partial z}\left(\phi \frac{\partial \psi}{\partial r}\right) - \frac{\partial}{\partial r}\left(\phi \frac{\partial \psi}{\partial z}\right)\right] - \frac{\partial}{\partial z}\left[b_\phi\, r \frac{\partial}{\partial z}\left(c_\phi\, \phi\right)\right]$$

$$- \frac{\partial}{\partial r}\left[b_\phi \frac{r}{a^2} \frac{\partial}{\partial r}\left(c_\phi\, \phi\right)\right] + r d_\phi = 0 , \qquad (24)$$

where ϕ is the dependent variable,

ψ is the stream function, and

a_ϕ, b_ϕ, c_ϕ, and d_ϕ are functions used as required to make Eq. (24) and the equation transformed identical.

For Eq. (23), the following functions are used:

$$\phi = \psi, \quad a_\phi = 0, \quad b_\phi = (\xi + G^*)g_2^*, \text{ and } c_\phi = 1. \qquad (25)$$

Equations (23) and (24) are expanded and set equal to each other to obtain the expression for d_ϕ. The resulting general nondimensional form of Eq. (23) becomes

$$- \frac{\partial}{\partial z}\left[r\,(\xi + G^*)\, g_2^* \frac{\partial \psi}{\partial z}\right] - \frac{\partial}{\partial r}\left[\frac{r}{a^2}(\xi + G^*)\, g_2^* \frac{\partial \psi}{\partial r}\right]$$

$$+ \frac{2}{a^2}(\xi + G^*)\, g_2^* \frac{\partial \psi}{\partial r} = 0. \qquad (26)$$

Once the stream function field is obtained, the pressure distribution follows. Computing the divergence of Eq. (14), with application of the continuity equation, and applying the nondimensional definitions yields the following scalar equation:

$$-\frac{\partial}{\partial r}\left(\frac{r}{a^2}\frac{\partial P^*}{\partial r}\right) - \frac{\partial}{\partial z}\left(r\frac{\partial P^*}{\partial z}\right)$$

$$-\left[\frac{G_{IN}^{\ 2}\, g_{2IN}\, L}{P_{ref}}\right]\left\{\frac{\partial \psi}{\partial r}\frac{\partial}{\partial z}\left[(\xi + G^*)\, g_2^*\right] - \frac{\partial \psi}{\partial z}\frac{\partial}{\partial r}\left[(\xi + G^*)\, g_2^*\right]\right\} = 0, \tag{27}$$

were $P^* = P/P_{ref}$, the nondimensional pressure. Equation (27) is in the form of Eq. (24) where

$$\phi = P^*,\ a_\phi = 0,\ b_\phi = c_\phi = 1, \text{ and}$$

$$d_\phi = -\left[\frac{G_{IN}^{\ 2}\, g_{2IN}\, L}{r\, P_{ref}}\right]\left\{\frac{\partial \psi}{\partial r}\frac{\partial}{\partial z}\left[(\xi + G^*)\, g_2^*\right] - \frac{\partial \psi}{\partial z}\frac{\partial}{\partial r}\left[(\xi + G^*)\, g_2^*\right]\right\}. \tag{28}$$

Using the coupled set of Eqs. (26) and (27), one can solve for the pressure and velocity distributions within the confines of the bed.

B. Thermal Model

The rate of heat transfer in a generating, conducting porous medium with a flowing fluid phase is controlled by a number of mechanisms, including bulk movement of the fluid, conduction in both the solid and fluid phases, convective transfer between phases, dispersion of the fluid in the interstices of the porous medium, and radiant exchange. When different mechanisms have a common driving potential, they may be combined by applying an effective heat transfer coefficient.

The macroscopic temperature gradient in the solid phase drives a complex group of heat transfer mechanisms, which operate both in parallel and in series. These include thermal conduction through the solid pebbles, conduction through the stagnant fluid film near the contact point of two adjacent pebbles, thermal conduction by contact between pebbles and for a gaseous fluid, radiant heat exchange. The net effect of these mechanisms can be expressed by an effective thermal conductivity coefficient for the solid phase, k_{se}. The static term, k_e^o, derived by Kunni and Smith [29] is used in the model, given by:

$$k_e^o/k_f = \varepsilon\,(1 + \beta\,Nu_{rv}) + \beta\,(1 - \varepsilon)/\left[1/\left(\frac{1}{\phi} + Nu_{rs}\right) + \gamma\,\frac{k_f}{k_s}\right], \quad (29)$$

where

k_f = fluid molecular thermal conductivity (W/m·K),

k_s = solid thermal conductivity (W/m·K)

β = geometry factor, here equal to 0.95, and

γ = geometry factor, equal to 2/3 for spheres.

Nu_{rv} and Nu_{rs} are Nusselt numbers for radiant heat exchange between void spaces and between solid surfaces:

$$Nu_{rv} = h_{rv}\,d_p/k_f; \quad h_{rv} = 4\sigma t_s^3 \Big/ \left[1 + \frac{\varepsilon}{2(1-\varepsilon)}\left(\frac{1-\varepsilon_r}{\varepsilon_r}\right)\right], \quad (30)$$

$$Nu_{rs} = h_{rs}\,d_p/k_f; \quad h_{rs} = 4\sigma t_s^3 \left(\frac{\varepsilon_r}{2-\varepsilon_r}\right) \quad (31)$$

where ε_r is the solid surface emissivity and σ is the Stephan-Boltzmann constant, and t_s is the pebble average surface temperature (K).

The empirical factor, ϕ, is calculated from:

$$\phi = \phi_2 + (\phi_1 - \phi_2)\ (\varepsilon - 0.260)/0.216. \tag{32}$$

When $\varepsilon \leq 0.260$, $\phi = \phi_2$. When $\varepsilon \geq 0.476$, $\phi = \phi_1$. ϕ_1 and ϕ_2 are given graphically in [29]. Curve fits of these parameters [30] are used here. For the range

$$10 \leq \frac{k_s}{k_f} \leq 300,$$

$$\phi_1 = 0.2770 \left(\frac{k_f}{k_s}\right)^{0.2426}, \tag{33}$$

$$\phi_2 = 0.1293 \left(\frac{k_f}{k_s}\right)^{0.3292}.$$

In the fluid phase, heat is transferred between fluid regions at different temperatures by two mechanisms: molecular conduction and turbulent dispersion in the interconnected interstitial voids of the solid phase. These combined effects are approximated by a single effective thermal conductivity coefficient for the fluid phase [23] given by

$$k_{fe} = \varepsilon\, k_f + \rho\, cE\ , \tag{34}$$

where

c = fluid specific heat capacity at constant pressure (J/kg·K), and

E = turbulent thermal diffusivity of the flowing fluid phase (m^2/s).

Because the turbulent thermal diffusivity is anisotropic, the fluid effective thermal conductivity is also anisotropic. The axes of interest (r,z) coincide with the axes of the principal effective thermal conductivities.

The numerical values of E are calculated using the method suggested by Finlayson [31]. The turbulent Peclet number is defined as

$$N_{Pe} = \frac{V\, d_p}{E} \tag{35}$$

Finlayson suggests that the radial and axial variations in the local value of E can be correlated with variations in the axial fluid velocity, V_z, such that

$$\left.\frac{E_r}{V_z}\right|_{r=r} = \frac{d_p}{N_{Pe,r}},$$

and

$$\left.\frac{E_z}{V_z}\right|_{z=z} = \frac{d_p}{N_{Pe,z}}. \tag{36}$$

The radial and axial turbulent Peclet numbers can be easily changed in the code. At present the radial and axial values are 10 and 2, respectively. These values assume the turbulent thermal diffusivity is numerically equal to the turbulent mass diffusivity. The turbulent Peclet numbers above correspond to "consensus" values reported by Deans and Lapidus [7].

The distributions of local fluid bulk temperature and pebble average surface temperature can be obtained by the solution of equations derived from thermal energy balances on the two phases. These balances are based on the fluid superficial velocity and the total cross-sectional area. Convective coefficients, generation rates, and thermal conductivities are corrected for the proper fraction of the bed. A thermal energy balance on the solid phase results in the following equation:

$$\vec{\nabla} \cdot (-k_{se}\, \vec{\nabla}\, t_s) + h\, a_v\, (t_s - t_f) - q = 0, \tag{37}$$

where

h = convective heat transfer coefficient ($W/m^2 \cdot K$),

a_v = pebble surface area per unit volume of the bed (m^{-1}),

t_f = local value of the bulk temperature of the interstitial fluid (K),

t_s = local value of the pebble average surface temperature (K), and

q = energy release rate per unit volume of the bed (W/m^3).

The terms in Eq. (37) represent, from left to right, effective conduction in the solid phase, convective transfer between the phases, and internal generation from fission and decay. Introducing the following nondimensional variables

$$T_s = \frac{t_s}{t_{fIN}}, \quad T_f = \frac{t_f}{t_{fIN}}, \quad c^* = \frac{cG_{IN}L}{k_{fIN}}, \quad K_f = \frac{k_{fe}}{k_{fIN}},$$

$$K_s = \frac{k_{se}}{k_{fIN}}, \quad a_v^* = a_v L, \quad h^* = \frac{hL}{k_{fIN}}, \text{ and } q^* = \frac{q L^2}{k_{fIN}\, t_{fIN}} \tag{38}$$

allows Eq. (37) to be transformed by the same methods and definitions used to obtain Eq. (26). The result, in axisymmetric cylindrical coordinates is

$$-\frac{\partial}{\partial z}\left[r K_s \frac{\partial T_s}{\partial z}\right] - \frac{\partial}{\partial r}\left[\frac{r}{a^2} K_s \frac{\partial T_s}{\partial r}\right] + r\left[h^* a_v^* (T_s - T_f) - q^*\right] = 0, \tag{39}$$

which is in the appropriate general nondimensional elliptic form required by the numerical solution technique.

Peterson [32] has shown that for helium, the specific heat at constant pressure, c, can be assumed constant for engineering purposes.

Assuming c constant, a similar treatment of the thermal energy balance for the fluid phase yields

$$c^* \left[\frac{\partial}{\partial z} \left(T_f \frac{\partial \psi}{\partial r} \right) - \frac{\partial}{\partial r} \left(T_f \frac{\partial \psi}{\partial z} \right) \right]$$

$$- \frac{\partial}{\partial z} \left[r K_{fz} \frac{\partial T_f}{\partial z} \right] - \frac{\partial}{\partial r} \left[\frac{r}{a^2} K_{fr} \frac{\partial T_f}{\partial r} \right] - rh^* a_v^* (T_s - T_f) = 0, \qquad (40)$$

where it should be noted that the effective thermal conductivity coefficients are anisotropic.

Values for the convective heat transfer coefficient, h, are obtained from the Jeschar correlation [33] for the Nusselt number, which is applied locally:

$$N_{Nu} = \frac{h d_p}{k_f} = 2.0 + \left[\frac{(1 - \varepsilon)}{\varepsilon^2} N_{Re} \right]^{0.5} + 0.005 \frac{N_{Re}}{\varepsilon}, \qquad (41)$$

where the Reynolds number, based on the superficial velocity and the particle diameter, d_p, is given by

$$N_{Re} = \frac{G d_p}{\mu}. \qquad (42)$$

The Nusselt number correlation is reported to be valid for Reynolds numbers between 250 and 5.5×10^4.

The effective thermal conductivities of the solid and fluid phases are functionally related to the local film temperature, usually the arithmetic average of t_s and t_f. This dependence of the coefficients on the dependent variables makes Eqs. (39) and (40) nonlinear.

The computer code based on this model solves Eqs. (26), (27), (39), and (40) as a coupled system of nonlinear elliptic partial differential equations. Boundary conditions for the solution of a selected physical system are specified at r = 0, r = 1, and both z limits (inlet and outlet) which need not be parallel.

Once the numerical solution has converged and the pebble average surface temperatures have been obtained, the internal temperatures and temperature gradients can be calculated. Referring to Fig. 2, let

r_1 = radius of inner fueled/unfueled interface (equal to zero for the conventional ball),

r_2 = radius of outer fueled/unfueled interface (m),

r_3 = pebble radius (m), and

Q = power per ball (W/ball).

For the conventional element, the temperatures at r_1 and r_2 are given by

$$t_1 = \frac{Q}{8\pi k_s r_2} + t_2 , \tag{43}$$

and

$$t_2 = \frac{Q}{4\pi k_s}\left(\frac{1}{r_2} - \frac{1}{r_3}\right) + t_s . \tag{44}$$

The temperature gradient at the fueled/unfueled interface is given by

$$\frac{dt}{dr} = \frac{-Q}{4\pi k_s r_2^2} . \tag{45}$$

For the shell ball

$$t_1 = \frac{Q}{4\pi k_s}\frac{1}{(r_2^3 - r_1^3)}\left[\left(\frac{r_2^2 - r_1^2}{2}\right) - r_1^3\left(\frac{1}{r_1} - \frac{1}{r_2}\right)\right] + t_2, \tag{46}$$

with t_2 given by Eq. (44). The temperature gradient at the outer fueled/unfueled interface is given by Eq. (45).

The thermal conductivity of the pebble is a function of temperature and integrated fast neutron flux. Lacking a thermal conductivity model, a curve fit to an axial distribution corresponding to an idealized OTTO fuel cycle [34] is used in the code. It is assumed that the thermal conductivity of the fueled matrix and unfueled graphite are equal. The function used to fit the data is

$$k_s(z) = 17. + 20.5\, e^{-15.37z} \tag{47}$$

The resulting distribution is shown in Fig. 5.

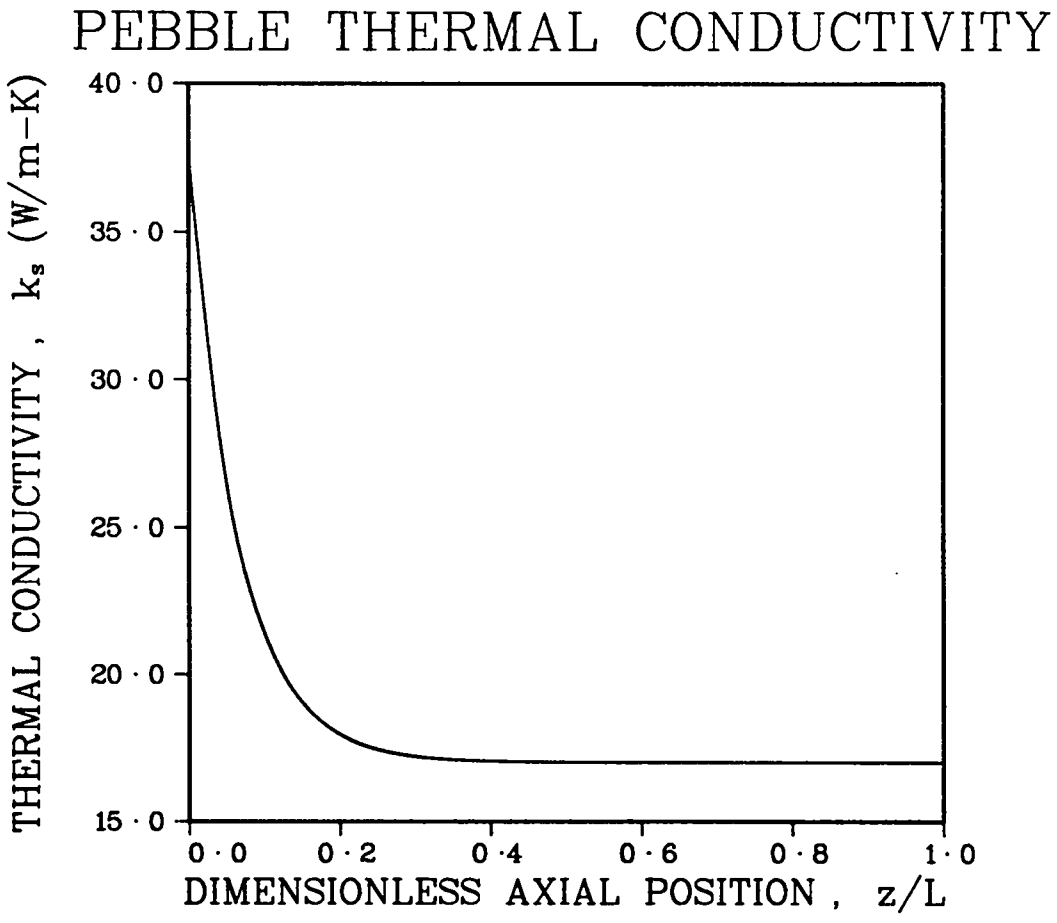

Fig. 5. Distribution of pebble thermal conductivity corresponding to an idealized OTTO fuel cycle.

IV. COMPUTER CODE PEBBLE

A. Solution Technique

The finite difference equations used in program PEBBLE were derived from the differential equations of the mathematical model by integrating over finite areas, based on assumed distributions of the variables between the nodes of the grid [28,35]. This approach ensures that conservation laws are obeyed over arbitrarily large or small portions of the field. In addition, this approach is most appropriate for the macroscopic porous medium model of a packed sphere bed, which already includes the assumption that the variables in a given bed volume are well characterized by macroscopic average values.

The coupled system of nonlinear algebraic equations is solved by a point iterative method, with the option of under or over-relaxing the dependent variables as necessary. A Gauss-Seidel method is used, in which the new values are used in each iteration cycle as soon as they become available. This method is known to yield rapid convergence and places low demands on computer storage. Details of the derivation of the finite difference equations from their differential counterparts, along with details of the successive substitution formulae can be found in Appendix A. This method is a modification of the techniques developed by Gosman, et al. [28]. The code is written in modular form, with the finite differencing being done by the code. This allows great flexibility, in that equations can be easily changed or added.

The user has the option of using either upwind or central differences for the advective terms (those terms multiplied by a_ϕ in Eq. 24). Central differences are more accurate, but upwind differences may be required to ensure the convergence of some equations. This will be

discussed further in Chapter VI. Properties are updated at the end of major iteration cycles, and the mesh can be swept for an equation as many times as desired within each major iteration cycle. References are given in the code for property models. A subroutine solves the Beattie-Bridgeman equation of state to recover the coolant density at each property update.

The convergence criterion used dictates that the maximum fractional change in a dependent variable, ϕ, in the field must not exceed a prescribed value, that is

$$\left[\left(\phi^{(N)} - \phi^{(N-1)}\right) \Big/ \phi^{(N)}\right]_{max} \leq cc, \tag{48}$$

where the bracketed superscripts denote the values for the Nth and Nth-1 iterations, respectively. Tests with PEBBLE have shown that changes in calculated values are insignificant for $cc < 0.005$.

To recover the mass flux at the axis of symmetry, we note that for a finite mass flux, the radial derivative of the stream function, ψ, must approach zero at the same rate as r near the axis. It follows that the $\psi \sim r$ distribution is parabolic near the axis. The program assumes this relationship holds at grid points once and twice removed from the axis, allowing the mass flux, G*, to be calculated at $r = 0$. The mass flux, G*, is set equal to zero at the impervious wall to approximate the no-slip condition. The presence of G* in the resistance coefficient, however, then incorrectly leads to a reduced resistance to flow adjacent to the wall. In the code, therefore, it is assumed that the flow resistance at the radial boundary node is the same as the resistance at the adjacent interior node.

The code does not require rectangular boundaries at the z limits of the bed (inlet and exit). The boundaries are set with the arrays IINLET, IMIN, IMAX and IEXIT. The successive substitution formula is only applied from IMIN to IMAX. The code does assume that the grid is defined so that grid points lie on the boundaries. If the user wants to incorporate non-rectangular boundaries, changes will need to be made in subroutines GRID and BOUND, and MFLUX should be checked.

The code is heavily commented and referenced, and was written to be used by others. A listing of the code, as set up for a coupled thermal-hydrualic test problem, is provided as Appendix B. The thermal-hydraulic test problem is discussed in Chapter VI.

V. ORNL PBRE ANALYSIS

A. Pebble Bed Reactor Experiment

Though the ORNL PBRE was never built, a full-scale mockup was constructed and extensive velocity and mass-diffusion measurements were made [21]. The PBRE was designed to be a 5 MW(t) all ceramic, helium-cooled pebble bed reactor system, with the core volume containing approximately 11700 spherical fuel-moderator elements [36].

The mockup used unfueled graphite spheres, 0.0381 m in diameter, loaded in a Plexiglas core model. The cylindrical core had an inverted conical core support plate with an included solid angle of 120^{o}, which had a central 120^{o} conical ball discharge dome. A free-surface fill cone at the angle of repose topped the bed. The basic geometry is shown in Fig. 6. The core had a diameter of 0.762 m, giving a bed to ball diameter ratio of 20. For experimental Bed 13 (modeled in this paper), the height from the lowest point of the core support plate to the peak of the fill cone was 1.35 m. Air was supplied to a plenum structure below the slotted core support plate, flowed upward through the interstitial voids in the bed, and exhausted to atmospheric pressure above the fill cone.

Point velocities were measured above the bed with a hot-wire anemometer, and averaged over all angular measurements at each radial position to give the mean radial velocity profile. The velocities measured correspond to superficial velocities, and the angular averaging makes comparison of measurements with an axisymmetric cylindrical coordinate prediction reasonable.

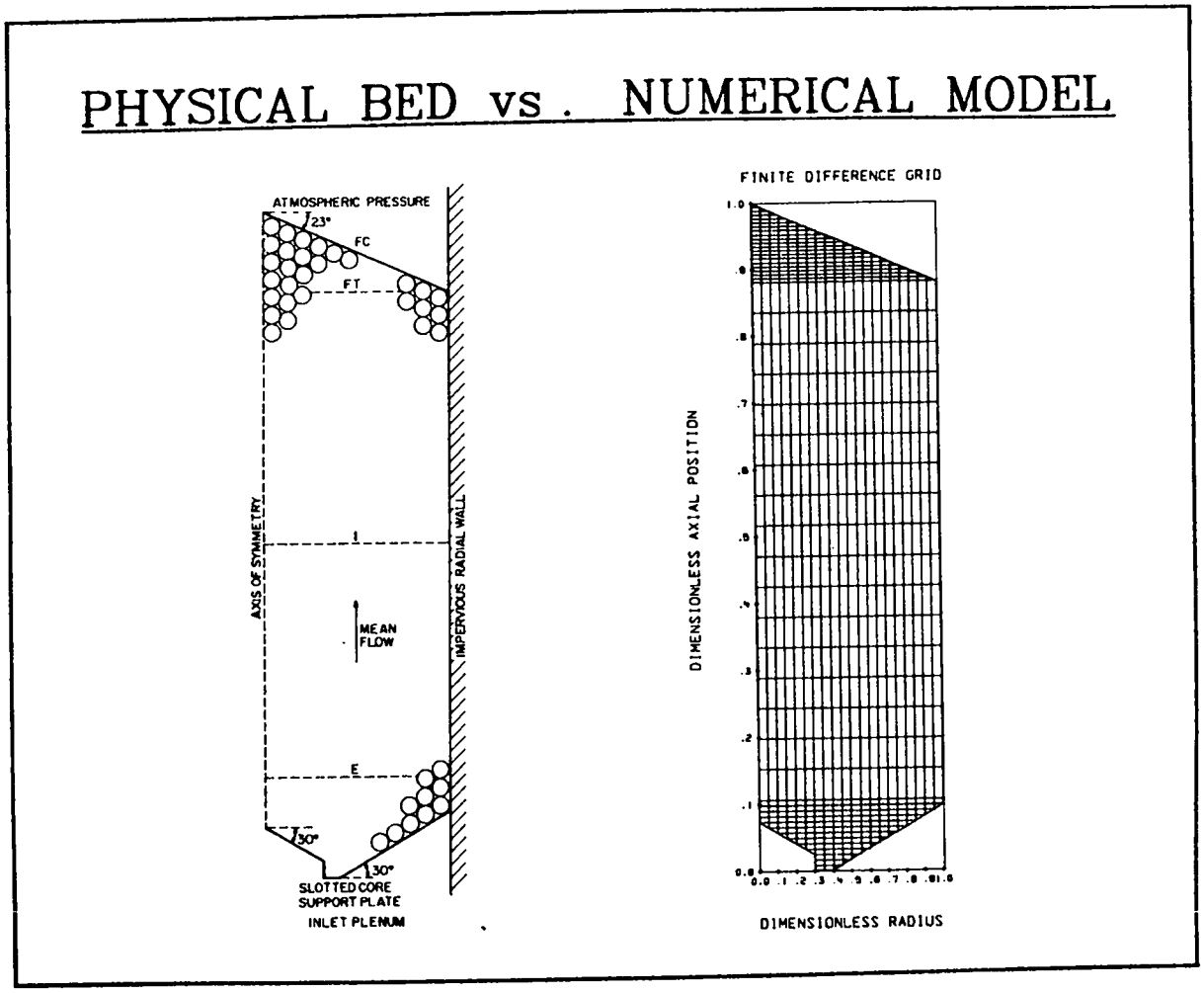

Fig. 6. The basic geometry of the ORNL PBRE is shown at the left. The letters E, I, FT and FC denote the location of the exit faces above which measurements were made. The corresponding finite difference grid is shown at the right.

Once a bed was constructed and measurements had been made above the fill cone, graphite spheres were removed to form flat-topped beds at three axial positions. Referring to Fig. 6, FC denotes the location of measurements taken above the fill cone, FT denotes the flat top configuration with the fill cone removed, I denotes the intermediate configuration with the upper half of the bed removed, and E denotes the bed configuration where only the entrance region was filled with spheres. For each bed, the flow rate was varied to give Reynolds numbers, based on the pebble diameter and superficial velocity, between 1150 and 9400. The small bed to ball diameter ratio, and complicated inlet geometry caused some modeling difficulties, but the PBRE mockup measurements offer the only experimental data available for relatively large packed beds of large, uniform-diameter spheres with an interstitial fluid flowing at high Reynolds numbers.

B. Code Validation Concerns

Normally, code validation relies on analytical solutions, or data from geometrically simple experiments; in this case, no two-dimensional analytical solution could be obtained, and no simple experiment was available. The only comparison that has been made with a known solution involved modeling an isothermal, uniform-property bed. With constant pressure conditions at the inlet and outlet, this configuration should yield a uniform velocity profile (plugflow). The plugflow calculation uses a rectangular grid, modeling an axisymmetric cylinder with flat, constant-z inlet and outlet faces, having a uniform void fraction of 0.39. The pressure boundary conditions are based on symmetry at $r = 0$ and $r = 1$, and constant pressure at the inlet and outlet, with the inlet

face value specified at 1.0. Boundary conditions on ψ at both the inlet and outlet correspond to parallel, axial flow (i.e. $\partial\psi/\partial z = 0$). The axis of symmetry and impervious radial wall must both be lines of constant ψ. Because the introduction of ψ increased the order of the original differential equation, one of the ψ boundary conditions is arbitrary. For numerical simplicity, we chose the value of $\psi = 0$ at $r = 0$ for all z. Once the value of ψ has been set at $r = 0$, the ψ distribution for plugflow can be determined from Eq. (22), by setting $G_z^* = 1$ and integrating from $r = 0$ to $r = r$. Thus for plugflow, $\psi = 0.5\ r^2$. This function is shown in Fig. 7. The wall values of ψ can then be set at 0.5, which ensures that the area-averaged dimensionless mass flux across each bed cross-section equals unity [16]. For this configuration, program PEBBLE calculated uniform velocity flow. The calculated pressure distribution was consistent with a one-dimensional form of the governing equation. The solution is well behaved, converging in a stable manner regardless of the initial guess.

With confidence in the numerical technique gained from the plugflow calculation, the ORNL PBRE mockup was modeled with PEBBLE. The radial boundary conditions on ψ and pressure are the same as for the plugflow case. The boundary conditions on ψ at the inlet and outlet correspond to flow perpendicular to the face; the condition being that the normal derivative of ψ is zero. The boundary condition on pressure at the outlet specifies the value of 1.0, the reference value. In the solution reported previously [37], the boundary values of pressure at the inlet were computed using the calculated normal pressure gradient at the inlet, the appropriate area-averaged value of the pressure for the adjacent internal nodes, and the appropriate distance normal to the inlet

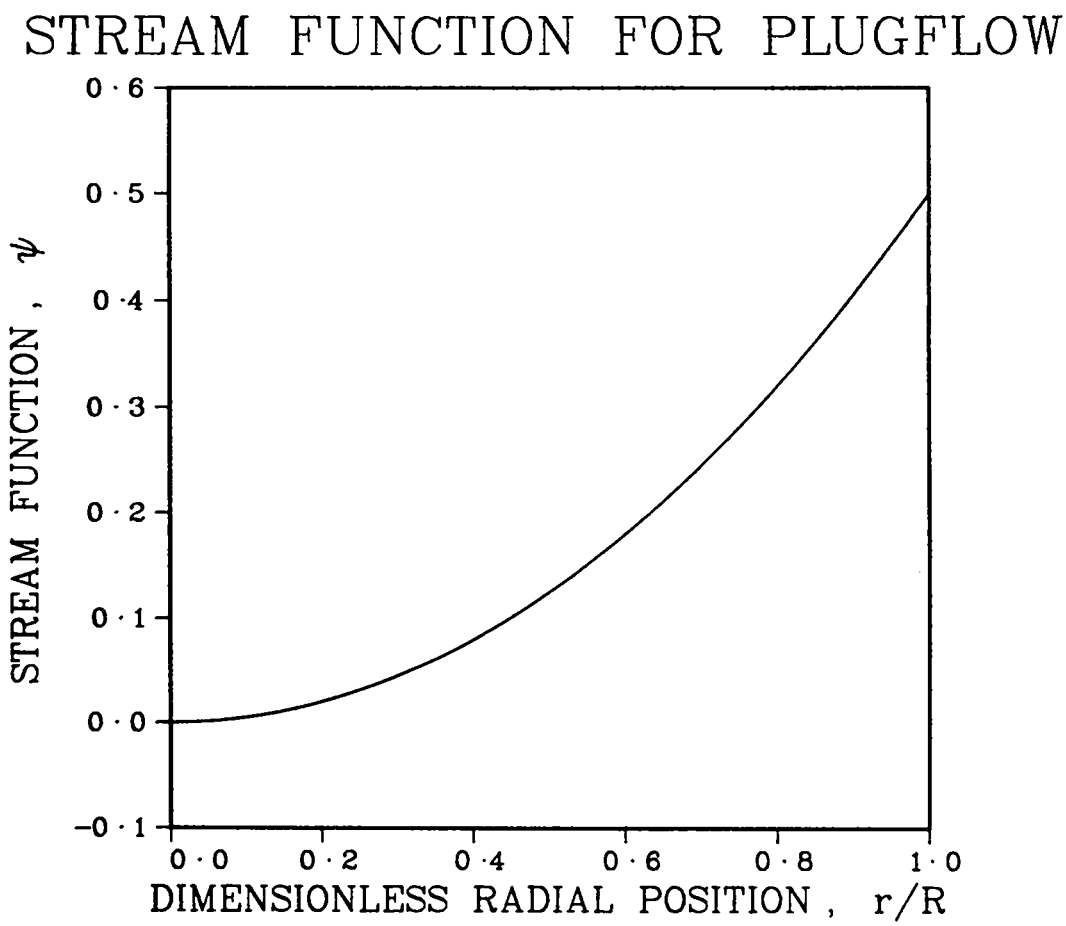

Fig. 7. The radial distribution of ψ for plugflow.

face. As reported earlier, for Bed 13FCa this resulted in an apparent error in the calculated core pressure drop of 5.5%, and the calculated pressure distribution near the inlet did not vary smoothly. Application of this boundary condition later yielded an obviously incorrect solution for the coupled thermal-hydraulic problem. It was found in the literature [35] that this plausible (and physically correct) technique is known to cause numerical problems. Since the inlet boundary condition on ψ assumed flow normal to the face, the pressure had to be constant along the face for a physically correct solution. The new boundary technique involves applying the above condition at one point, and then setting the pressure at all inlet boundary points to that value.

The finite difference grid was set up with a constant Δr and a variable Δz, so that grid points fell on the inlet and outlet boundaries. Bed 13FC was calculated on a 21 x 51 grid. The grid definition and outlet boundary conditions were then adjusted to model Beds 13FT, I, and E. Bed 13E was calculated on a 21 x 16 grid. The grid for Bed 13FC is shown in Fig. 6.

A relaxation parameter of 1.285 was used for the calculation of ψ; a value of 1.0 was used for the pressure recovery calculation. Calculation of Bed 13FCa for cc = 0.005 required 31 s of CP time using a CDC 6600 computer, the interactive NOS operating system, and the LASL FUN compiler.

C. Void Fraction Distribution in the PBRE

The void fraction, ε, in a cylindrical packed bed only achieves the random packed bed value of 0.39 for very large beds. Since a sphere makes only point contact with the wall, the void fraction varies from 1.0 at the wall to a minimum at one-half ball diameter from the wall. Its

value then oscillates before approaching a constant value 5 to 10 ball diameters from the wall [38-40]. Bundy [21] measured the total void fraction of Beds 13FT and 13E, reporting values of 0.401 for Bed 13FT, and 0.366 for Bed 13E. The void fraction distribution used by PEBBLE for the cylindrical portion of the bed is shown in Fig. 8. This distribution is based on the D_{Bed}/d_p = 14.1 data of Benenati and Brosilow [38], modified by data from measurements on one-fourth scale PBRE models by Thadani and Peebles [39]. The fill cone void fraction was set to the nominal value of 0.401, as no data are available for free-surface fill cones.

The porous medium model is difficult to apply in the entrance region, which has numerous structural surfaces and contains a relatively small number of spheres. Bundy [21] measured a large void fraction in the lowest part of the entrance region, a low value higher in the region, and a mean value of only 0.366 for Bed 13E. It was believed that the large value was a result of the wall effect, with spheres in only point contact with the structure, while the low value was a result of rhombohedral close-packing (ε = 0.26) at the bottom of the cylindrical bed. Wadsworth [41] had previously observed rhombohedral packing near the bottom of flat-bottomed beds.

In the absence of detailed information on the distribution of ε in the entrance region, the void fraction distribution assigned to this region in PEBBLE was manipulated to give the approximate shape of the reported velocity profile, causing the flow to enter the calculational bed in approximately the same manner as it had entered the experimental bed. The resulting distribution used the area void fraction of the core

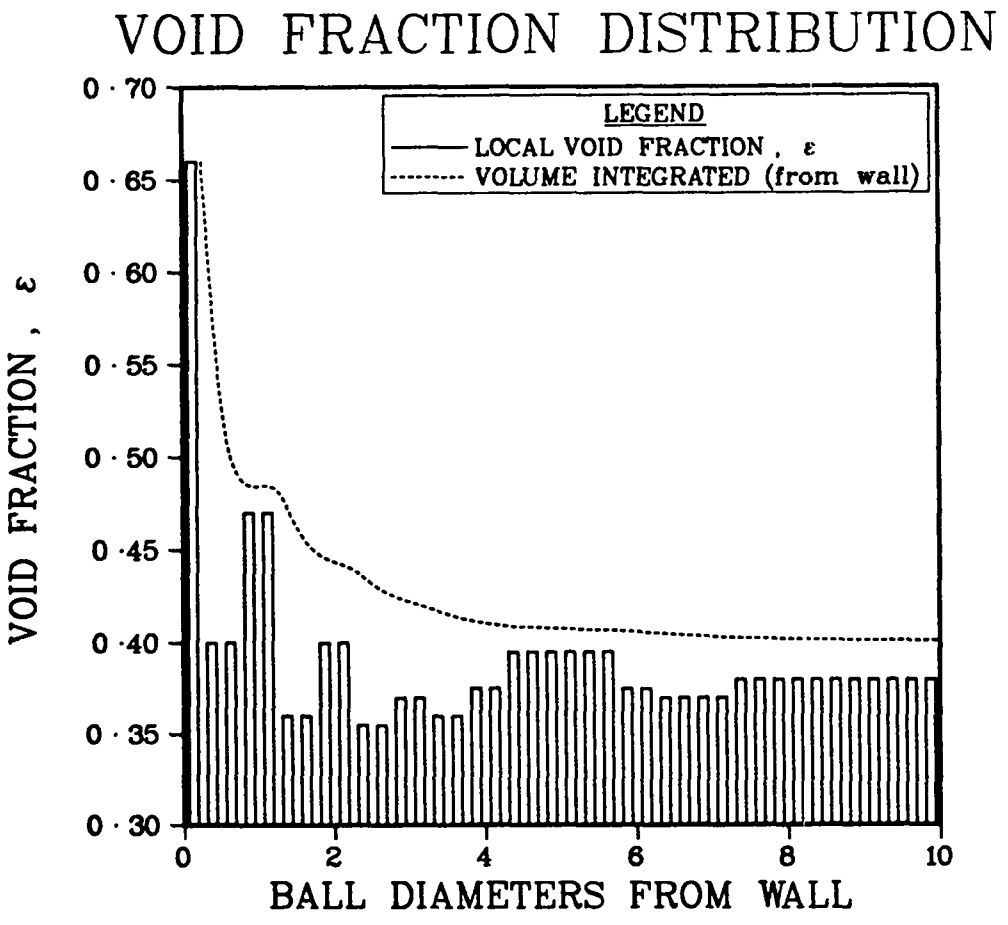

Fig. 8. Void fraction distribution used in PEBBLE to model the cylindrical portion of PBRE Bed 13.

support plate (including no-flow regions) for the value of ϵ at the boundary and the first two internal grid points (about one-half ball diameter). Next, a layer of rhombohedral close-packing, one ball diameter thick, was assumed for the regions above the discharge dome and the slanted core bottom. The void fraction of the remainder of the entrance region was set to the measured mean value of 0.366.

D. Comparison of Predictions with Measured Values

Figures 9 and 10 display predictions by PEBBLE for the distribution of stream function, pressure and velocity in Bed 13FCa of the PBRE mockup series. Some general observations can be made concerning these figures. The streamlines are perpendicular to the isobars. When bed properties change, such as in the entrance region or the fill cone, the flow redistributes in very short distances. In the cylindrical portion of the bed, where the void fraction in the model varies only radially, the streamlines are parallel and the flow is purely axial. The pressure gradient is steeper in the entrance region, where there is denser packing, than in the remainder of the bed.

Pressure data for the PBRE mockups were reported in the form of friction factors. For Bed 13FCa, with an inlet Reynolds number of 6275, the reported value was 5.59. With the inlet boundary technique discussed in Section B of this chapter, PEBBLE calculated a value of 5.607. The print output for the analysis of Bed 13FCa is provided as Appendix D.

Figures 11 through 14 compare predictions by PEBBLE for the exit velocity profiles of Beds 13E-FC with those measured on the full-scale mockups. The calculated velocity profile at the exit face of the entrance region of Bed 13E, resulting from the void fraction distribution

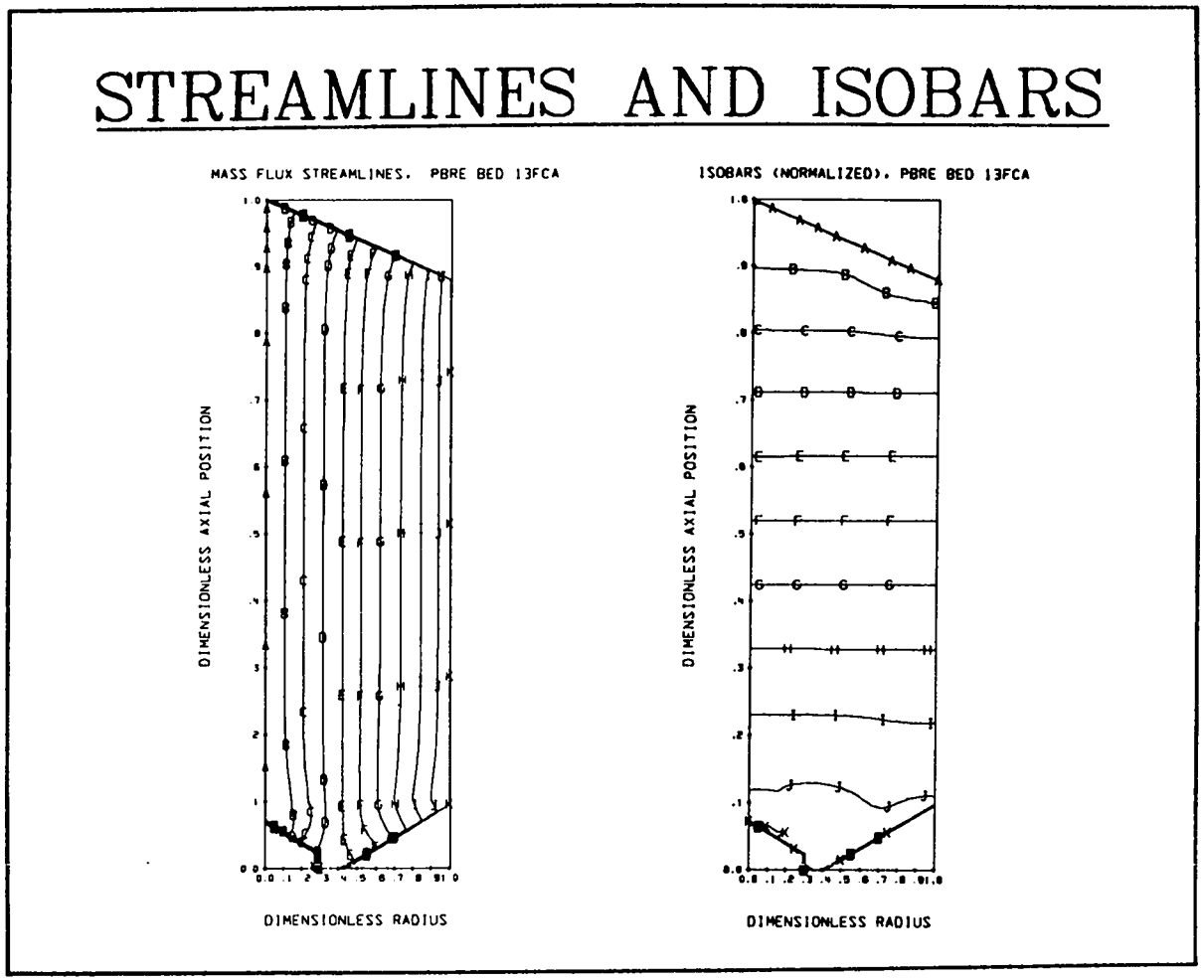

Fig. 9. Calculated mass flux streamlines and isobars for PBRE Bed 13FCa. Contour values correspond to $\psi = 0.5\ r^2$ in steps of 0.1, where contour A is zero. Pressure contour values range from A = 1.0 to K = 1.031 and are equally spaced.

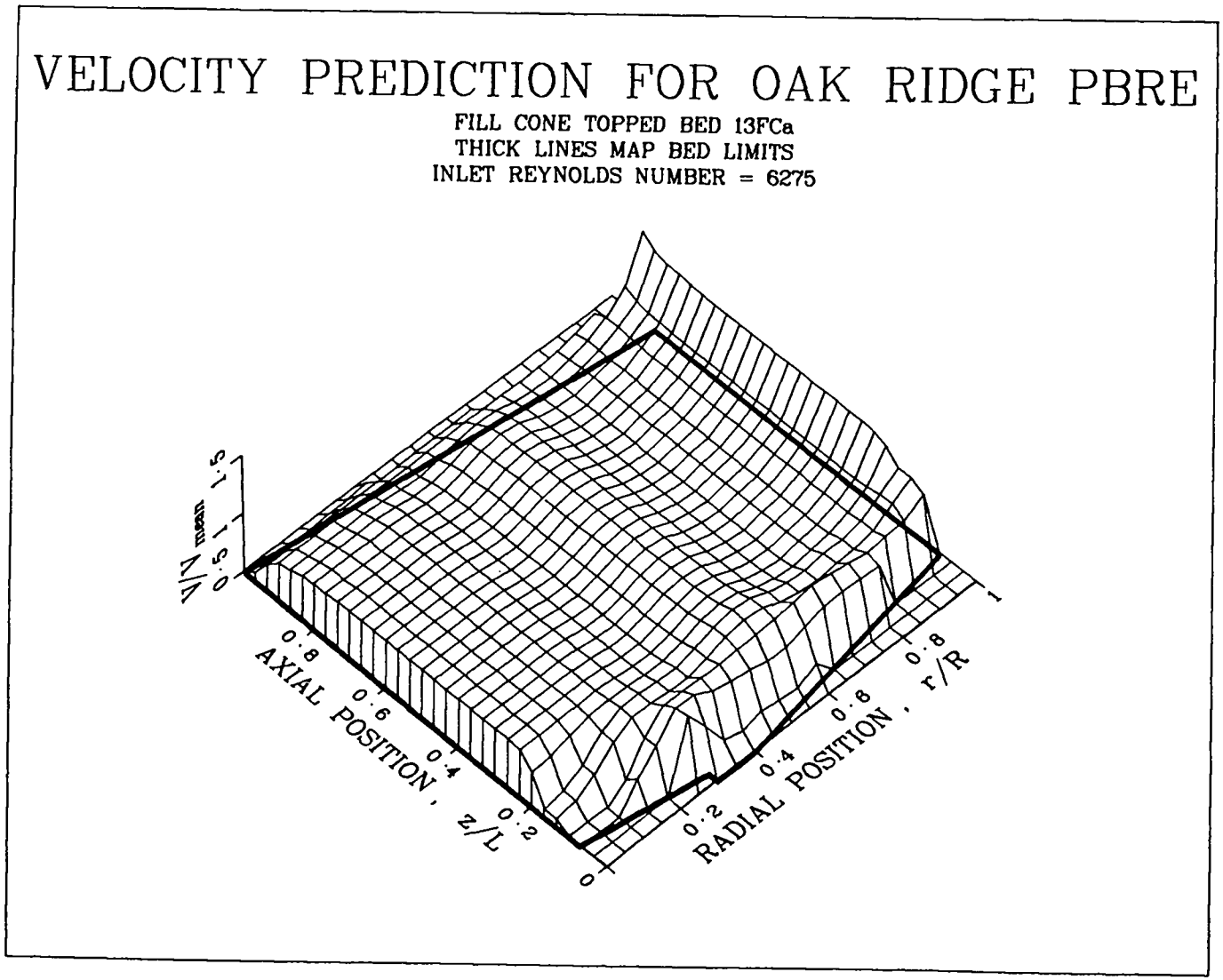

Fig. 10. Calculated distribution of normalized velocity for PBRE Bed 13FCa.

and inlet boundary conditions discussed in the previous sections, is shown in Fig. 11 with the corresponding experimental data. Figures 12 and 13 demonstrate that the calculated velocity profiles for Beds I and FT are essentially the same, which is consistent with Fig. 9. The different shape of the experimental velocity profiles at the two locations may be caused by axial variations in the bed packing. Wadsworth [41] has noted that axial variations in the void fraction distribution can exist, but none were modeled here because no data are available. The agreement between predicted and measured velocities for Bed 13FT, shown in Fig. 13, appears excellent, at least for an inlet N_{Re} of 8555 (see also Fig. 17). Note, however, that other choices could have been made in assigning the distribution of ε in the cylindrical portion of the bed; a different distribution would change the shape of the calculated velocity profile. The void fraction distribution shown previously in Fig. 8, while having the correct characteristics in an overall sense, may be locally inaccurate. Differences probably exist between PBRE Bed 13, formed from the previous bed by through-cycling 12710 spheres [21], and the very small scale beds used for the measurement of void fraction distribution. These small scale beds were formed by simply dumping spheres into a cylindrical volume [38-40].

Calculated and measured velocities above the fill cone are compared in Fig. 14. The calculated velocity profile is in good agreement with the experimental measurements. Since the entire fill cone region was assigned a uniform void fraction of 0.401 in the numerical model, the good agreement between the measured and calculated FC velocity profiles is probably not the result of a fortunate choice of void fraction distribution. The results shown in Fig. 14, therefore, indicate that the

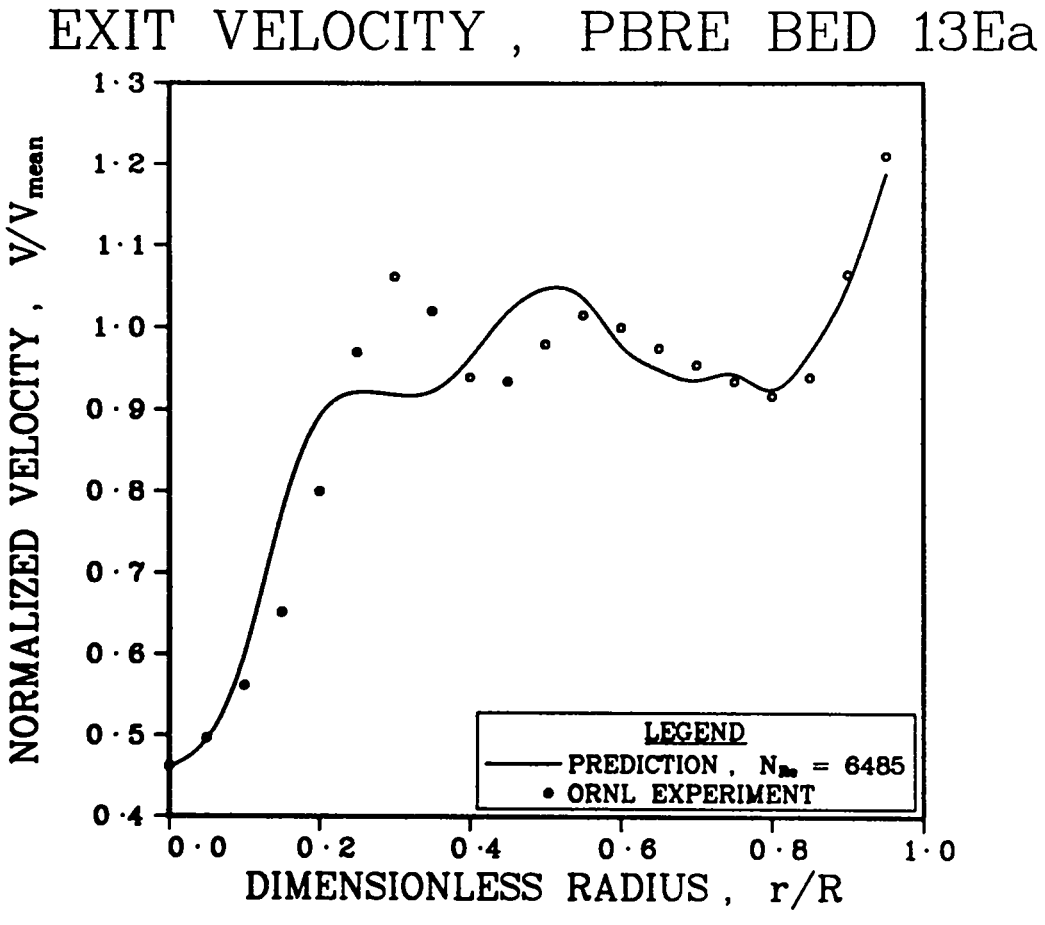

Fig. 11. Comparison of predicted and measured exit velocity profiles above PBRE Bed 13Ea (entrance region).

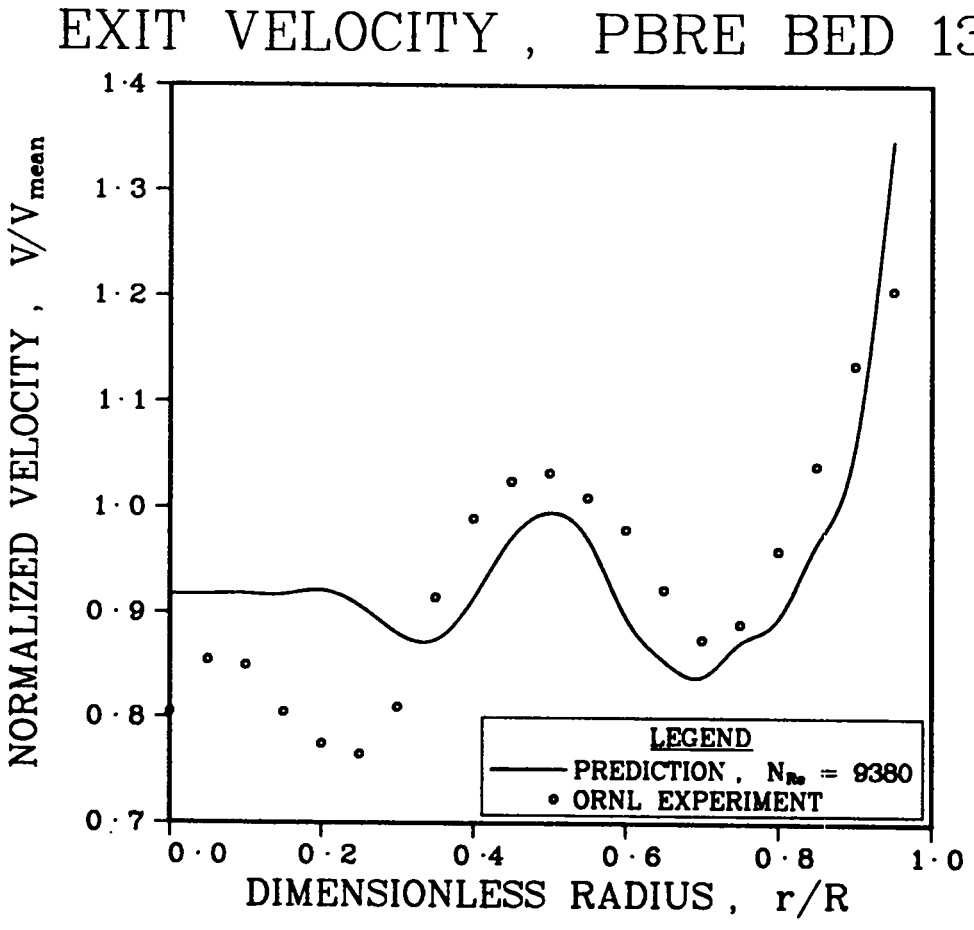

Fig. 12. Comparison of predicted and measured exit velocity profiles above PBRE Bed 13Ia (lower half of the bed).

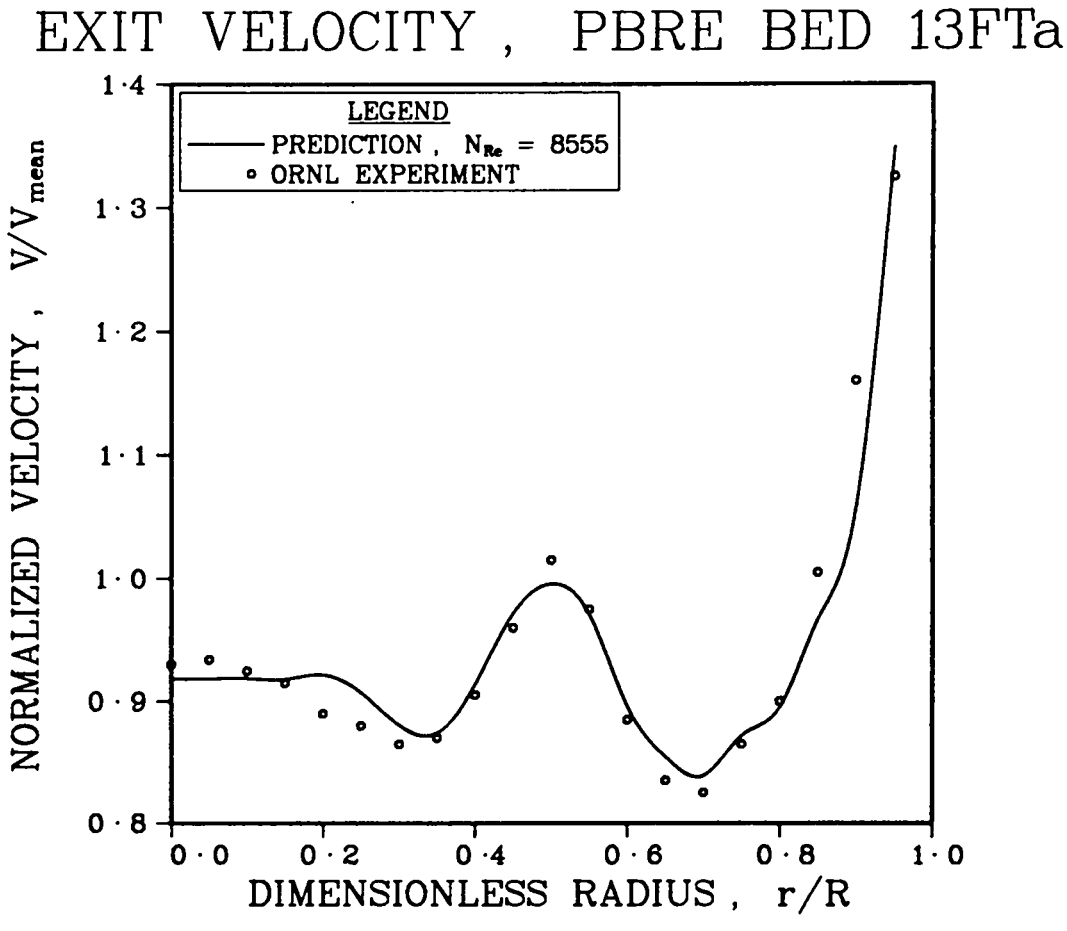

Fig. 13. Comparison of predicted and measured exit velocity profiles above PBRE Bed 13 FTa (flat-top bed, fill cone removed).

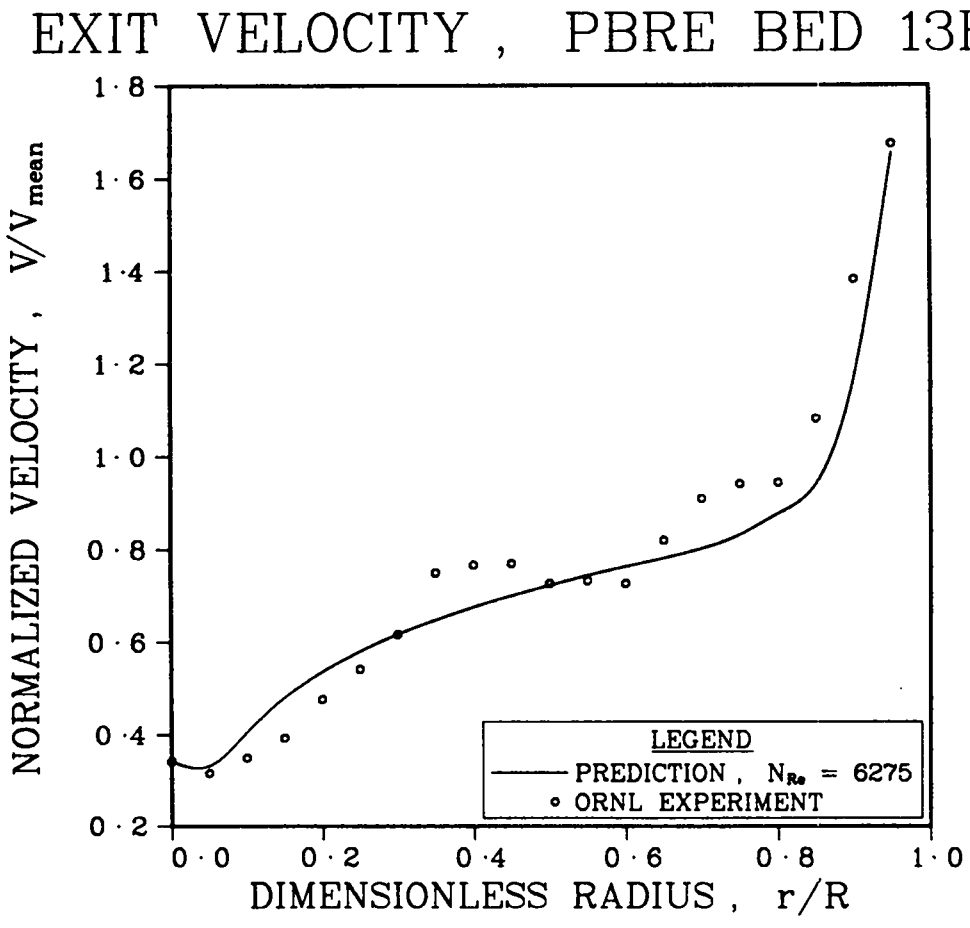

Fig. 14. Comparison of predicted and measured exit velocity profiles above PBRE Bed 13FCa (entire bed topped by fill cone).

mathematical model and numerical technique used by PEBBLE are appropriate for the analysis of high Reynolds number flows in packed sphere beds.

Figures 15 through 18 show the effect of inlet Reynolds number on both prediction and experiment for Beds 13E-FC. Again, the results for the Bed 13FC are encouraging, but the results for Beds 13E-FT require further comment. The response of the prediction with respect to Reynolds number is consistent with the mathematical model. It has been previously noted by Szekely and Povermo [17] that the profiles should be similar as long as the quadratic term dominates the resistance to flow. In reporting the PBRE mockup measurements, Bundy [21] questioned the apparent Reynolds number effect shown in the data, stating

> "...an effect of the flow rate on the shape of the velocity profile cannot be clearly deduced from the present data, and such an effect of the flow rate, if it exists, must certainly be small. The differences observed in the normalized velocity profiles measured at the same point above a bed at different mean velocities might have resulted from changes in the velocity profile between the exit face of the bed and the measurement height, which was 9 in. above the bed."

E. Discussion of PBRE Results

A mathematical model and numerical solution technique have been developed that allow calculation of macroscopic values of the hydraulic variables in an isothermal axisymmetric pebble bed under steady-state conditions. The computer code PEBBLE has been shown to predict distributions of coolant velocity and pressure, limited only by knowledge of the geometry of the bed.

The lack of detailed knowledge of the local void fraction does not limit the ability of PEBBLE to perform an accurate thermal-hydraulic

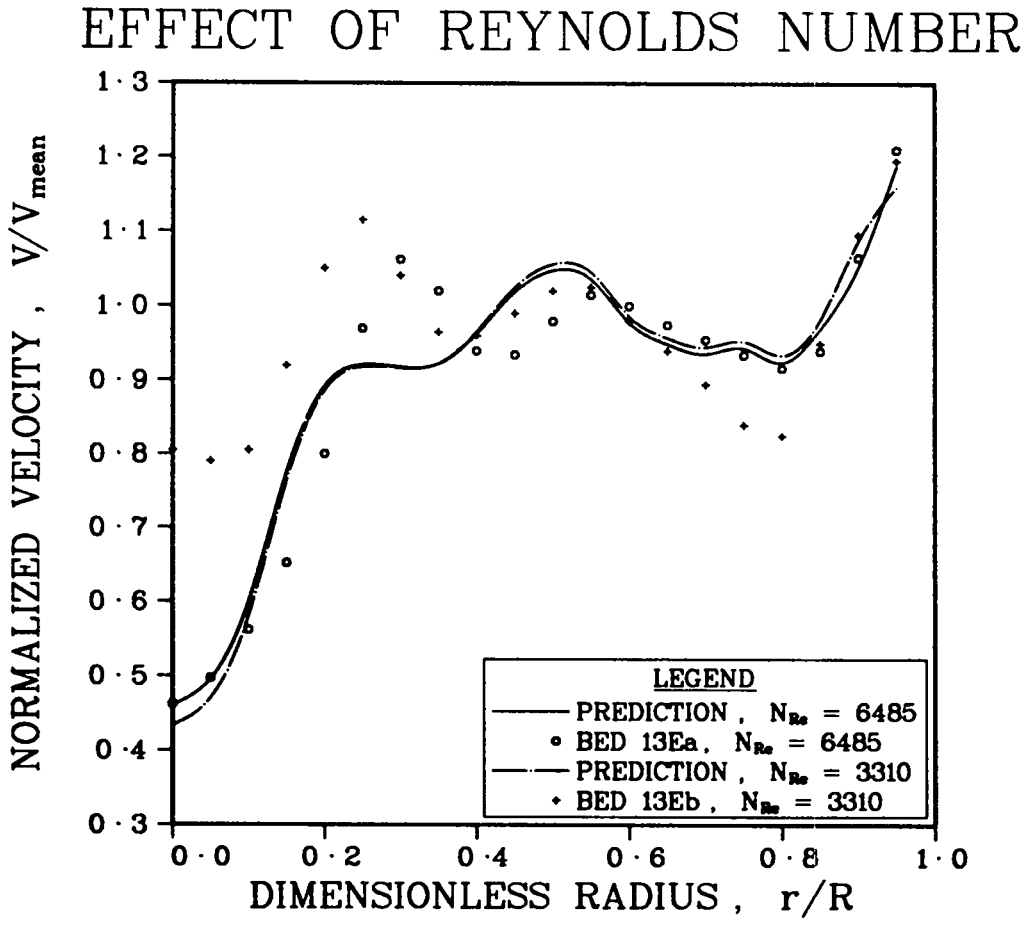

Fig. 15. Comparison of predicted and measured exit velocity profiles above PBRE Bed 13E for two different inlet Reynolds numbers.

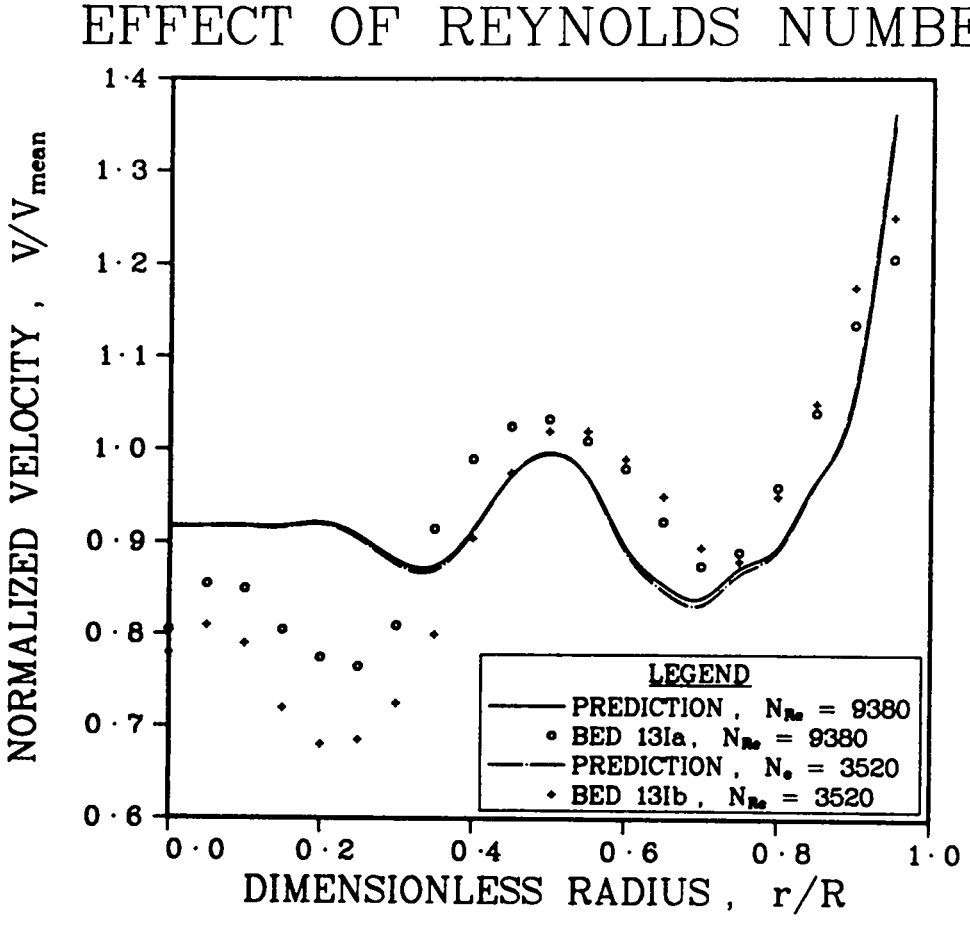

Fig. 16. Comparison of predicted and measured exit velocity profiles above PBRE Bed 13I for two different inlet Reynolds numbers.

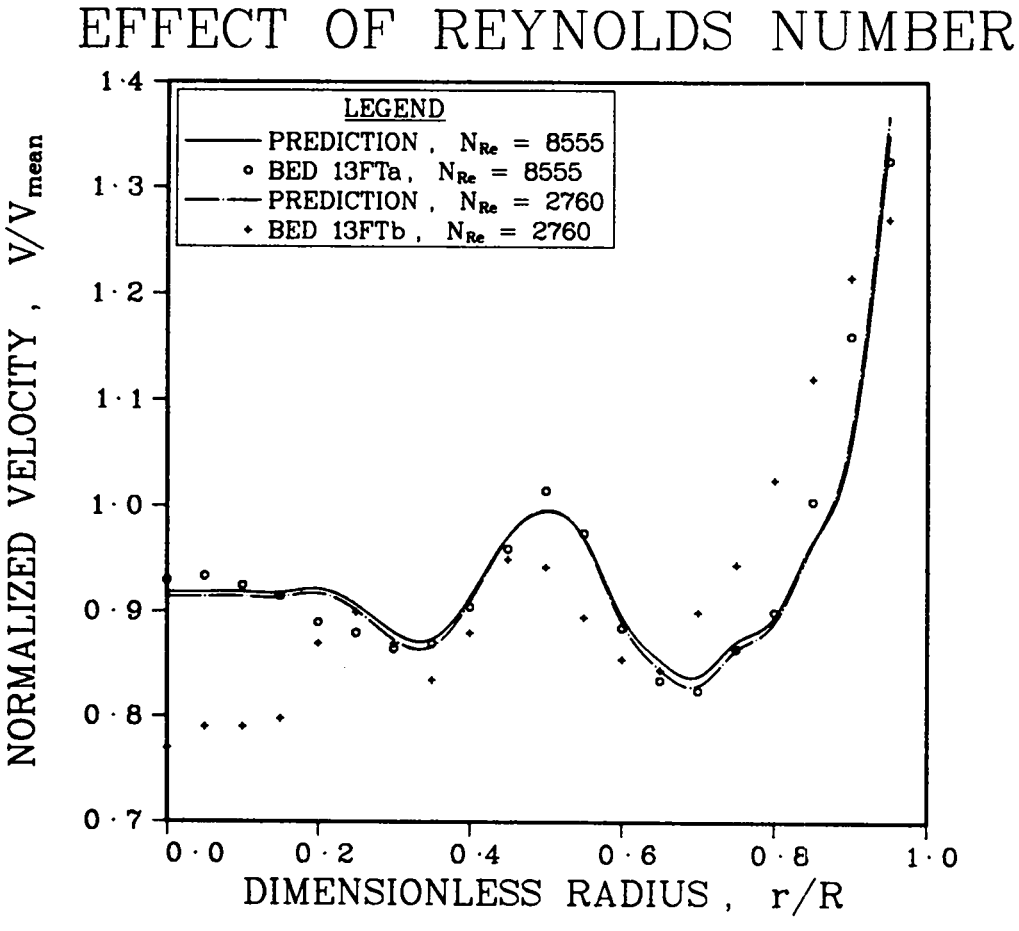

Fig. 17. Comparison of predicted and measured exit velocity profiles above PBRE Bed 13FT for two different inlet Reynolds numbers.

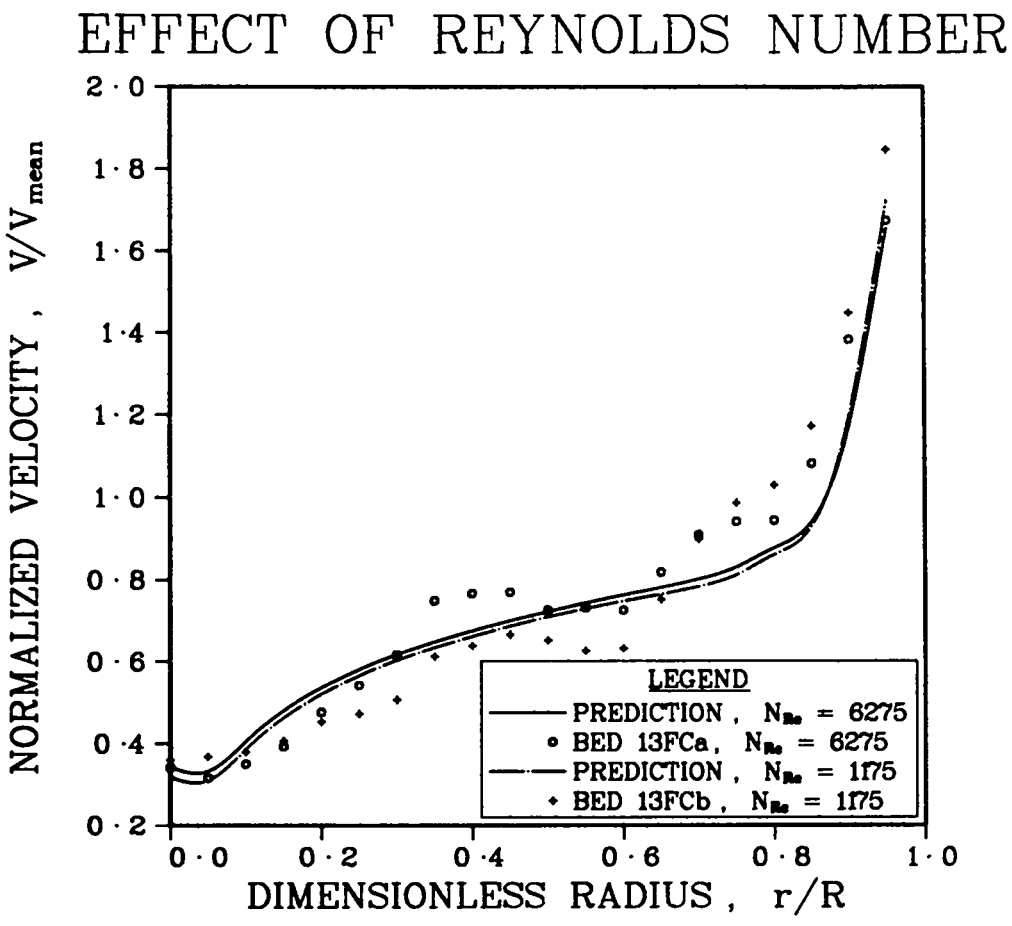

Fig. 18. Comparison of predicted and measured exit velocity profiles above PBRE Bed 13FC for two different inlet Reynolds numbers.

analysis of large pebble bed power reactors, such as those being designed by the Institut fur Reaktorentwicklung, Kernforschungsanlage, Julich (KFA). These large power reactors have bed-to-ball diameter ratios of about 200, and even have an array of structural depressions in the radial reflector to minimize, or eliminate, the wall effect. These beds can be modeled accurately (on a macroscopic scale) by assuming the entire bed to be characterized by a nominal void fraction of 0.39. In addition, the combination of the continuous OTTO fuel cycle and coolant downflow ensures that very little heat is generated in the portion of the core adjacent to the ball discharge structure, resulting in nearly isothermal conditions in this region [42]. Thus, the thermal-hydraulic calculation is not of critical importance in those regions where its accuracy may be in question.

Further validation of the flow model will require data from a geometrically simple flow experiment. The experimental bed should have a large bed to ball diameter ratio and parallel, constant-z inlet and outlet faces. Its void fraction distribution should be measured in both the radial and axial directions. Annular flow dividers should be used beyond the exit face to minimize the tendency of the flow to return to an empty tube velocity profile, ensuring that the anemometer measures the proper velocity. The possibility of using a circular hot-wire in these annular regions should be investigated.

VI. COUPLED THERMAL-HYDRAULIC TEST PROBLEM

A. KFA Power Reactor Design

The design chosen for the test case is the KFA PR3000 Design Case 1013. This design was chosen because the axisymmetric power distribution is available in the literature [34]. Case 1013 is a 3000 MW(t) PBR operating on a low-enriched uranium (LEU) OTTO fuel cycle The bed contains approximately 1.8×10^6 shell type fuel-moderator elements, and has a core-average power density of 9 MW(t)/m^3. Helium is supplied to the upper void space at a pressure of 4 MPa, with a mixed-mean temperature of 523 K at the rate of 785 kg/s. All input values for geometry and design parameters can be found on the third page of the code listing supplied as Appendix B. The axisymmetric thermal power distribution is entered in the Block Data Subprogram POWER. Input values, including the power distribution, can also be found in the print output from program PEBBLE for this test case, which is supplied as Appendix C.

B. Numerical Model

The physical reactor is assumed to be axisymmetric, and the effects of the many small fill cones on the upper free surface, and the ball discharge structures, are ignored. The bed is characterized by an average height in the design information. A comparison of the physical reactor and the numerical model is shown in Fig. 19. These approximations are the same as those used for the neutronics calculation which supplies the axisymmetric thermal power distribution.

The KFA neutronics code VSOP provides power per ball (kW/ball) at the volumetric centers of N equal annular volumes. Design Case 1013 was

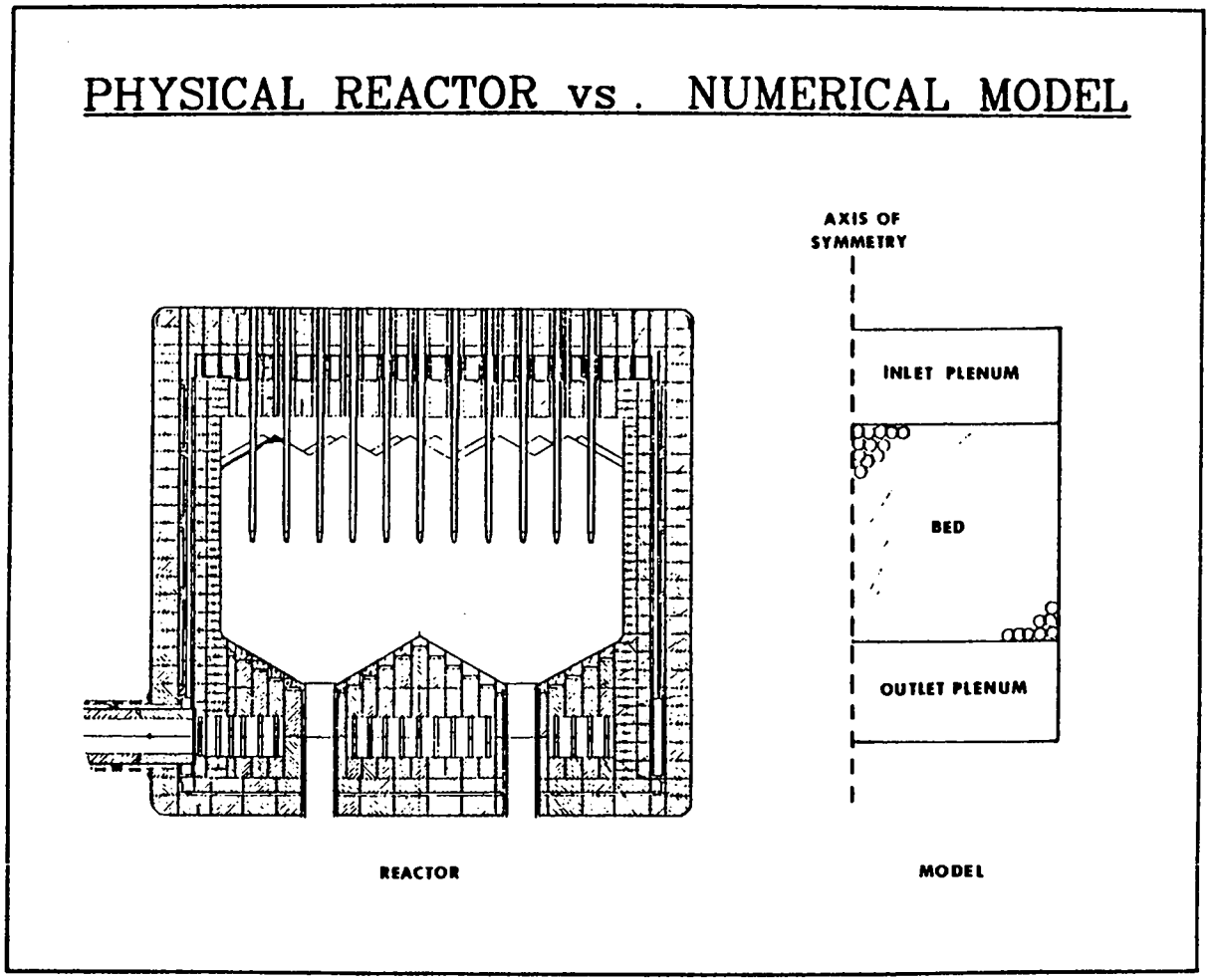

Fig. 19. A comparison of the physical reactor and the axisymmetric model used in the analysis.

calculated on 18 equal radial volumes. The resulting radial grid spacing can be seen in Fig. 20. Power per ball values are available for radial locations 4-21 (22 total radial points). PEBBLE was originally set up using the finite difference grid shown in Fig. 20, where the extra grid lines near the axis of symmetry were added to aid in the calculation of G* at r = 0 (See Chapter IV). This grid resulted in a false flow maldistribution being calculated in the region of radial lines 4 through 7 (verified by another plugflow test). The grid spacing need not be uniform, but neither can it be too coarse. It is noted that the calculation of G_z* requires the radial derivative of a function something like that shown in Fig. 7. PEBBLE now includes the subroutine INTERP which interpolates the VSOP input to equally spaced radial grid points for the thermal-hydraulic calculations. It would be possible to use INTERP to interpolate the thermal-hydraulic variables back to the VSOP spacing if required, though this capability is not inlcuded in the present version of PEBBLE. The new finite difference grid is shown in Fig. 21.

C. Boundary Conditions

The boundary conditions for ψ and P* are the same as for the ORNL PBRE analysis reported in Section B of Chapter V, except here P* = 1 at the inlet face. The radial boundary conditions for temperature are based on symmetry at r = 0, and the assumption of an adiabatic wall at r = 1, or stated mathematically,

$$\frac{\partial T_s}{\partial r} = \frac{\partial T_f}{\partial r} = 0. \qquad (49)$$

The temperature boundary conditions at the inlet face are based on thermal energy balances between the incoming gas stream and the solid front

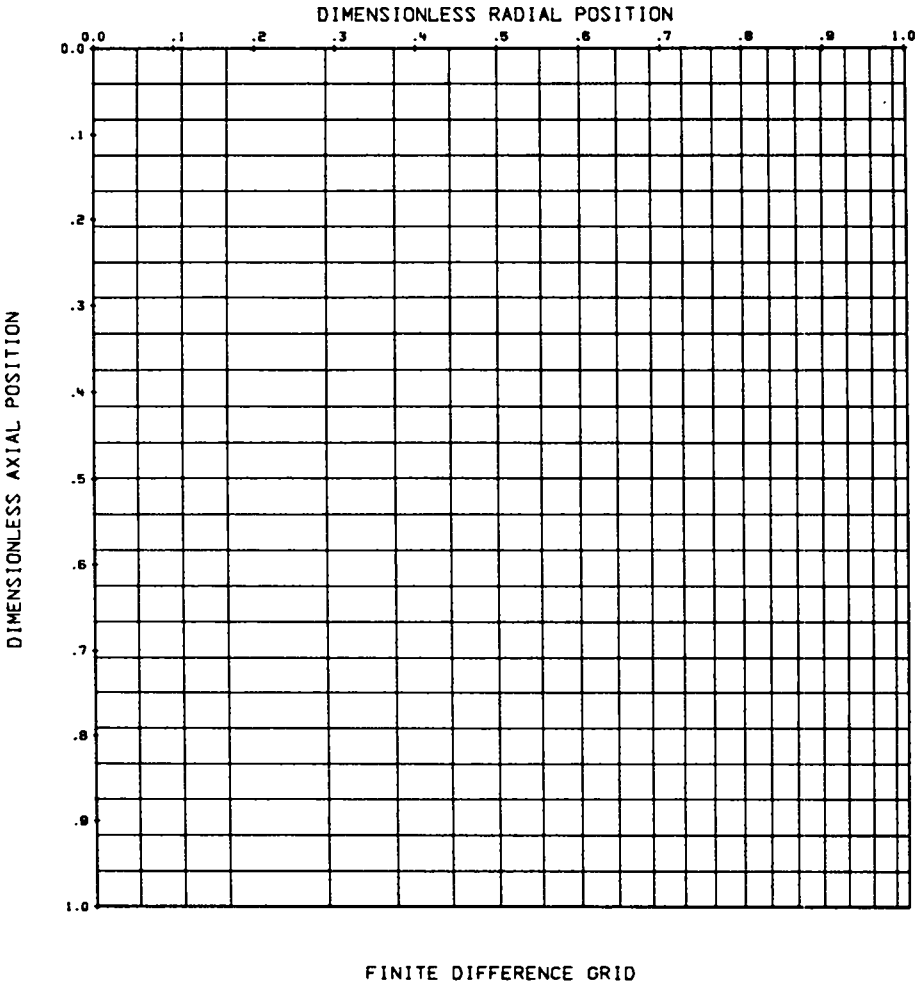

Fig. 20. Original grid used by PEBBLE, where radial grid lines 4-21 (of 22 total) correspond to those locations where VSOP supplies power per ball values for KFA Design Case 1013.

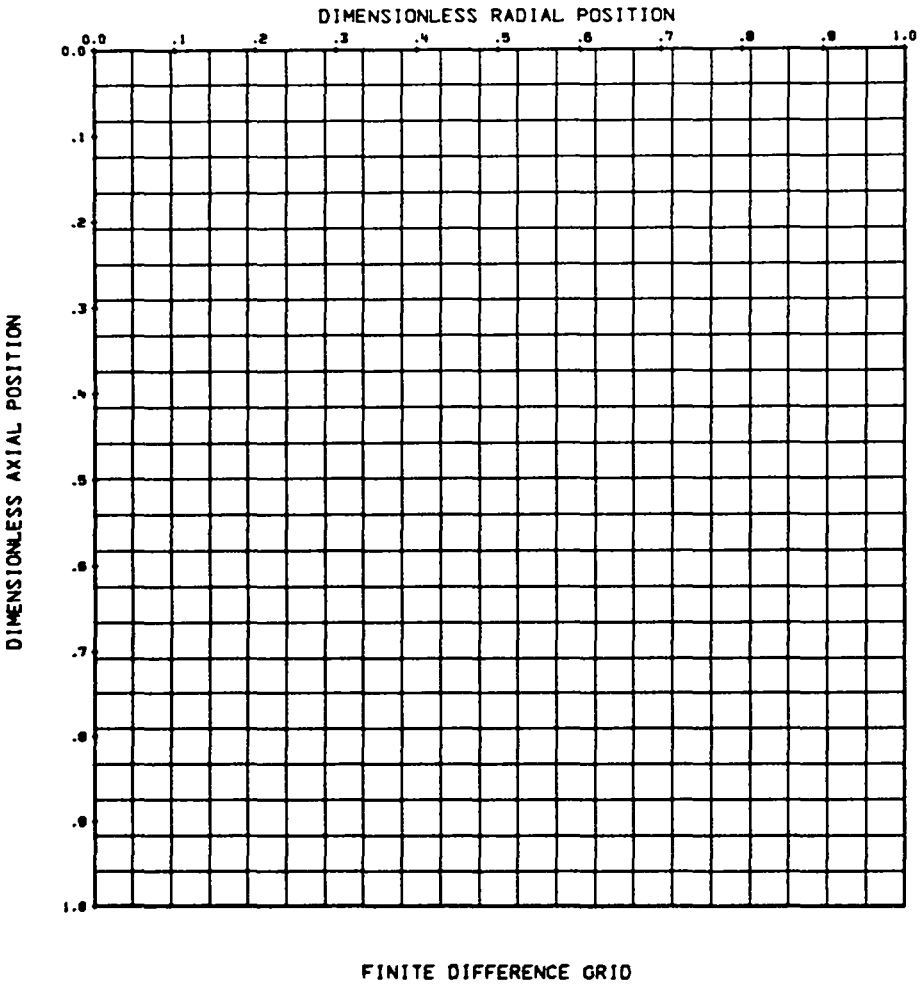

Fig. 21. Finite difference grid used for the thermal-hydraulic calculations.

surface after the work of Vortmeyer and Schaefer [43]. If we assume the mixed-mean inlet gas temperature, T_{IN} (nondimensional value = 1.0), corresponds to a temperature away from the bed, the temperatures at z = 0 can be calculated from

$$T_{FI} = \frac{1}{G^*c^*}\left[h^* (1-\varepsilon)(T_{SI} - 1) + K_{fz} \frac{\partial T_F}{\partial z} \right] + 1, \qquad (50)$$

and

$$T_{SI} = \frac{1}{h^*(1-\varepsilon)}\left[\frac{q^*}{a_v^*}(1-\varepsilon) + K_s \frac{\partial T_s}{\partial z} \right] + 1. \qquad (51)$$

where T_{FI} and T_{SI} represent the nondimensional fluid and solids temperature at the inlet face.

PEBBLE was originally set up with the temperatures at the outlet face being calculated from one-dimensional thermal energy balances, but it was found that a constant thermal flux condition, or

$$\left.\frac{\partial^2 T_s}{\partial z^2}\right|_{z=1} = \left.\frac{\partial^2 T_f}{\partial z^2}\right|_{z=1} = 0, \qquad (52)$$

gave essentially the same answers and enhanced the rate of convergence. Considering the structure supporting the bed, balances based on gas exiting from a generating, conducting bed directly to an empty plenum are not physically correct anyway. The reference design for the core bottom structure is shown in Fig. 22.

D. Lessons Learned in Debugging the Problem

The only value of any of the four dependent variables that can be calculated analytically is the mixed-mean outlet temperature of the

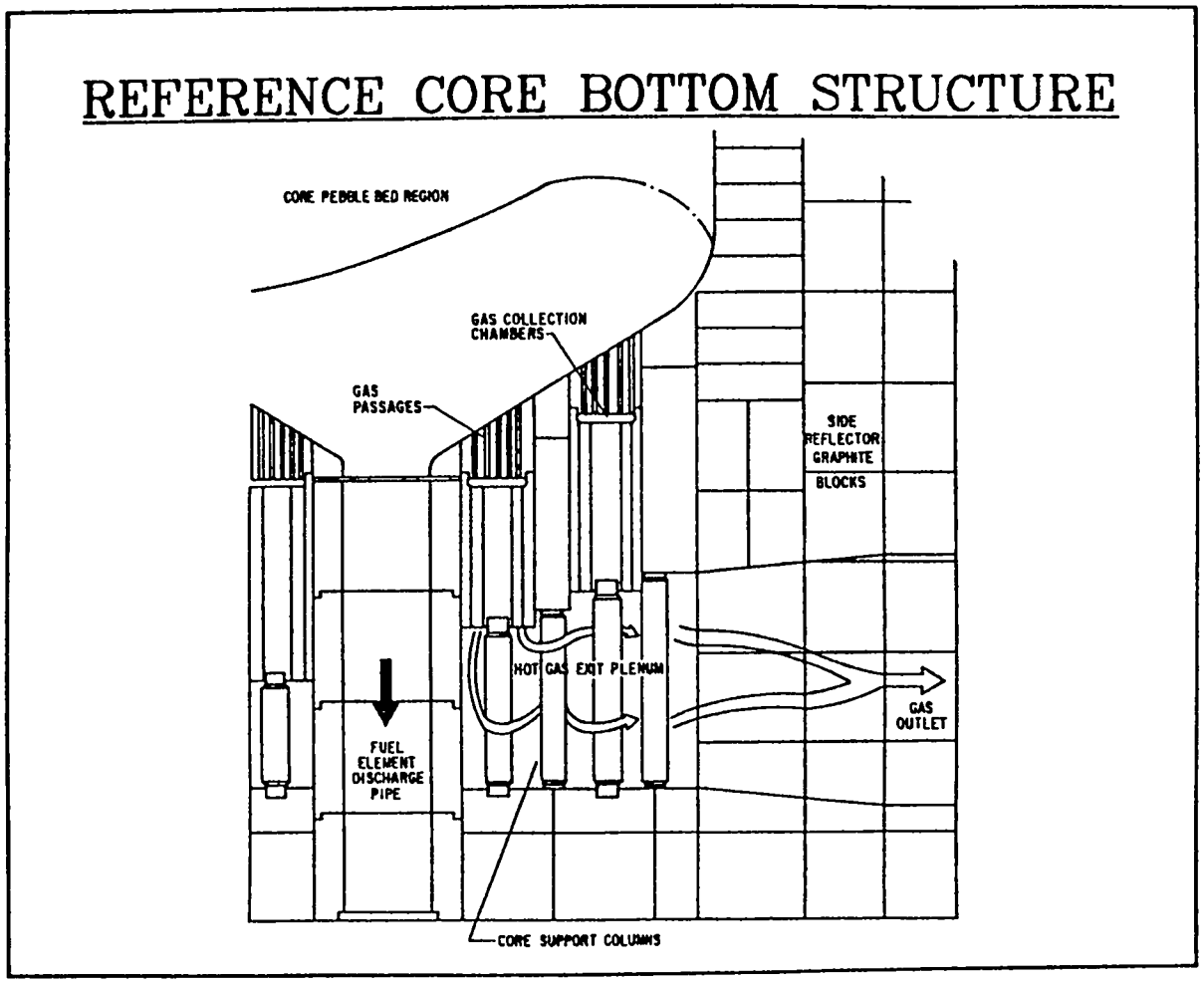

Fig. 22. Design for the core bottom structure showing the complicated gas exit path [4].

coolant. The code calculates the bed power from the VSOP input, and the coolant mass flow rate, specific heat and inlet temperature are known. For the Design Case 1013 input, PEBBLE calculated at total power of 3006 MW(t) (design 3000 MW(t)) which indicates the mixed-mean outlet temperature of the coolant should be 1260 K.

As originally set up, PEBBLE calculated a mixed-mean outlet helium temperature of 1232 K, an error of -28 K or -3.8%. Analysis of the numerical model indicated that this error was probably due to the use of upwind differences for the term multiplied by c* in Eq. 40. This is the only equation of the four in which the so-called advective terms appear. The code was rewritten to allow the user the option of using either central or upwind differences on these terms, as upwind differences are known to be necessary to ensure convergence for some equations [28,35]. With central differencing of the advective terms, the fluid temperature equation requires under-relaxation and the convergence rate is slower, but the calculated mixed-mean outlet temperature is now 1259 K; an error of only -0.2%.

The equation for the pebble average surface temperature is numerically unstable, possibly because the source terms (bracketed terms multiplied by r in Eq. 39) are very large while the effective conductivity, K_s, is relatively small. It can also be noted that the dependent variable appears in the source term. Convergence is obtained by over-riding the successive substitution when unreasonable values are calculated and by strongly under-relaxing the successive substitution. The substitution over-ride is controlled by an IF statement, and is only called upon during the first few iterations.

The relaxation parameters, and number of sweeps of the mesh for each equation, have not been optimized for this problem. The values of these parameters and the numerical convergence information for this problem can be found on the first few pages of the print output in Appendix C. With the parameters listed, the solution of the basic equations required 46 s of CP time (exclusive of compilation time) on a CDC 6600, using the NOS interactive operating system and the LASL FUN compiler. Execution time could probably be reduced by using the FTN compiler under OPT = 2. The reduction in execution time which could be realized by optimizing relaxation parameters and number of sweeps is not known.

E. Discussion of Results

The results of this calculation are presented graphically in Figs. 23 through 37, and in the print output presented in Appendix C. As mentioned previously, the only analytical check available is the mixed-mean outlet coolant temperature, for which the calculated value is within one degree K of the analytic value. The error in the calculated coolant temperature rise is only -0.2%.

Figures 23 and 32 show the thermal power per ball calculated by the neutronics code VSOP [34]. Two things to note are the characteristic OTTO cycle axial profile, with approximately 90% of the thermal power being generated in the upper half of the core, and the power peaks at dimensionless radii of 0.833 and 1.0. The peak at r = 0.833 is caused by the two-zone fuel loading used in Design Case 1013. The pebbles loaded in the region from r = 0.833 to the wall have a higher heavy metal loading than the pebbles in the center of the core. This strategy flattens the radial power profile, but a power peak results near the inner edge of

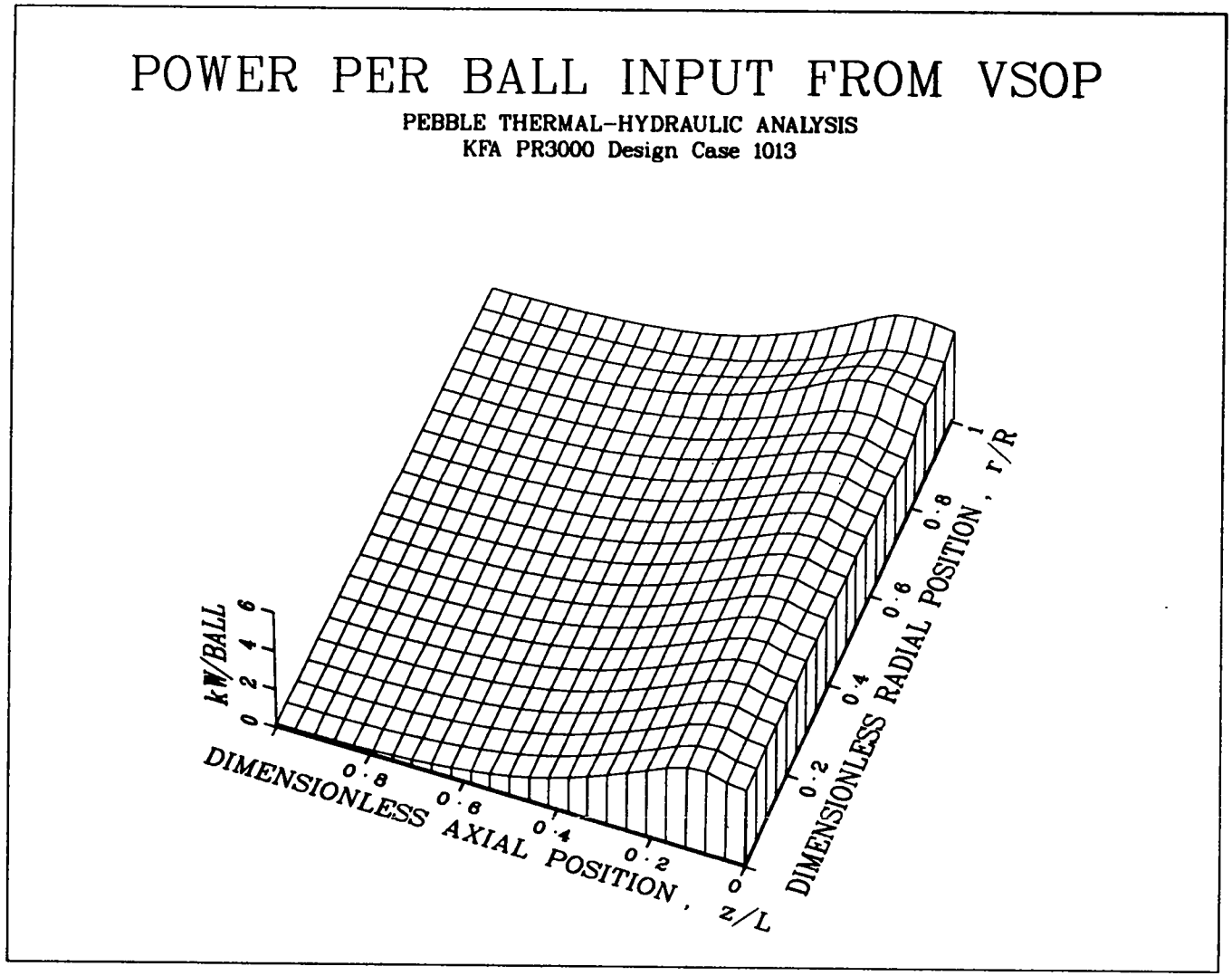

Fig. 23. Distribution of thermal power per ball for KFA PR3000 Design Case 1013. The coordinates (0,0) correspond to the core centerline at the top of the bed.

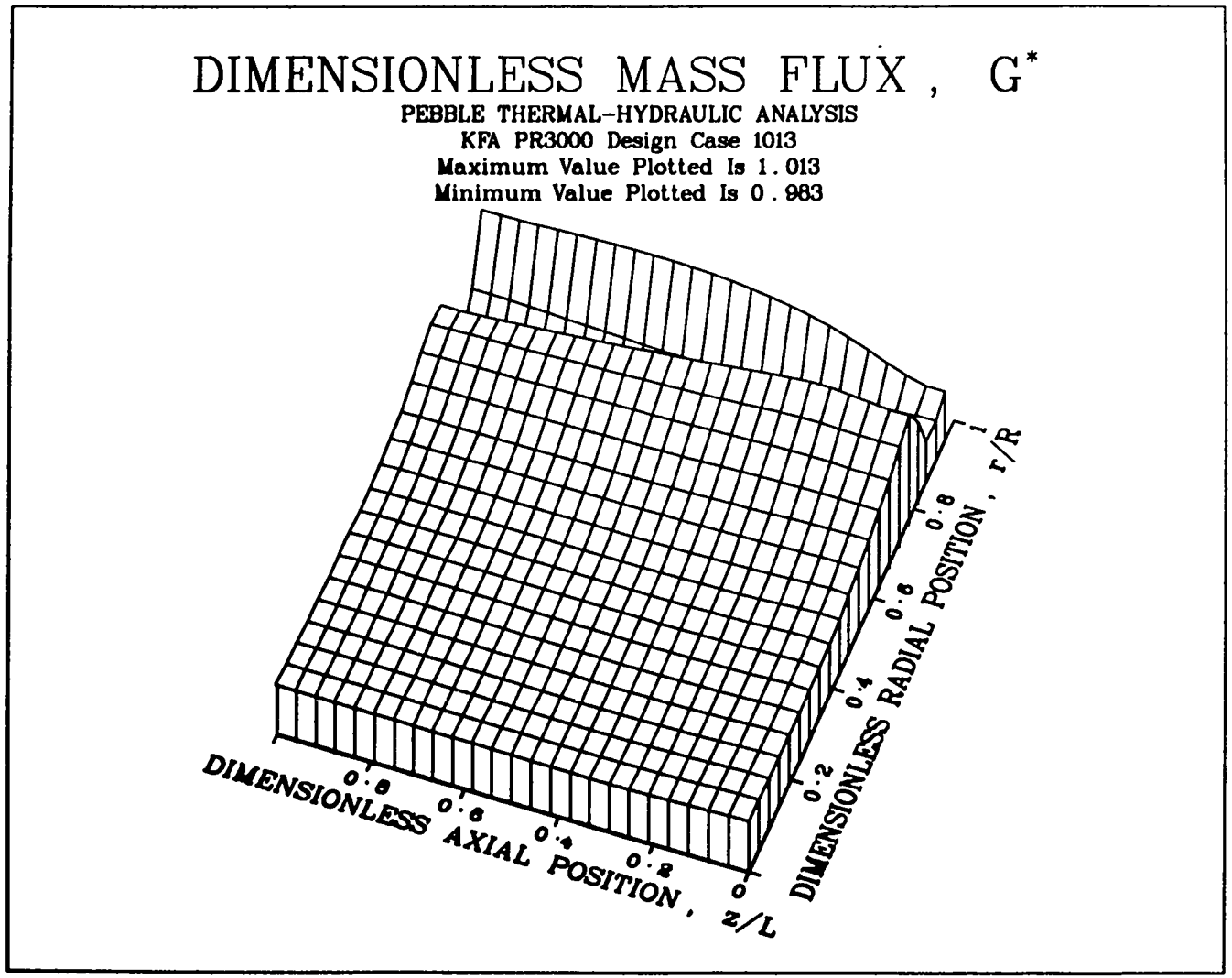

Fig. 24. Calculated distribution of the dimensionless mass flux, G*. The wall value of G* = 0 was not plotted to allow expansion of the vertical scale.

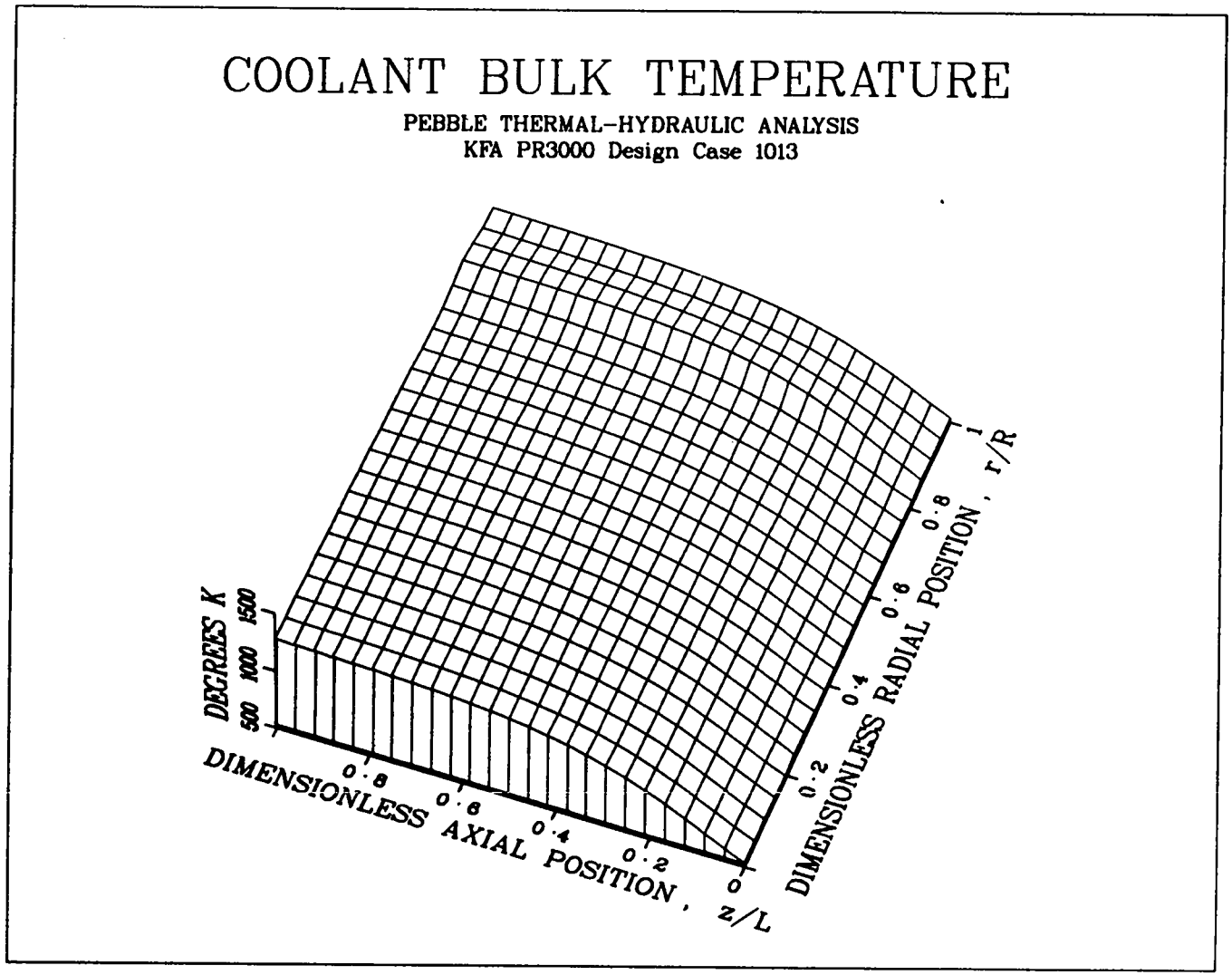

Fig. 25. Calculated distribution of the coolant bulk temperature for KFA PR3000 Design Case 1013.

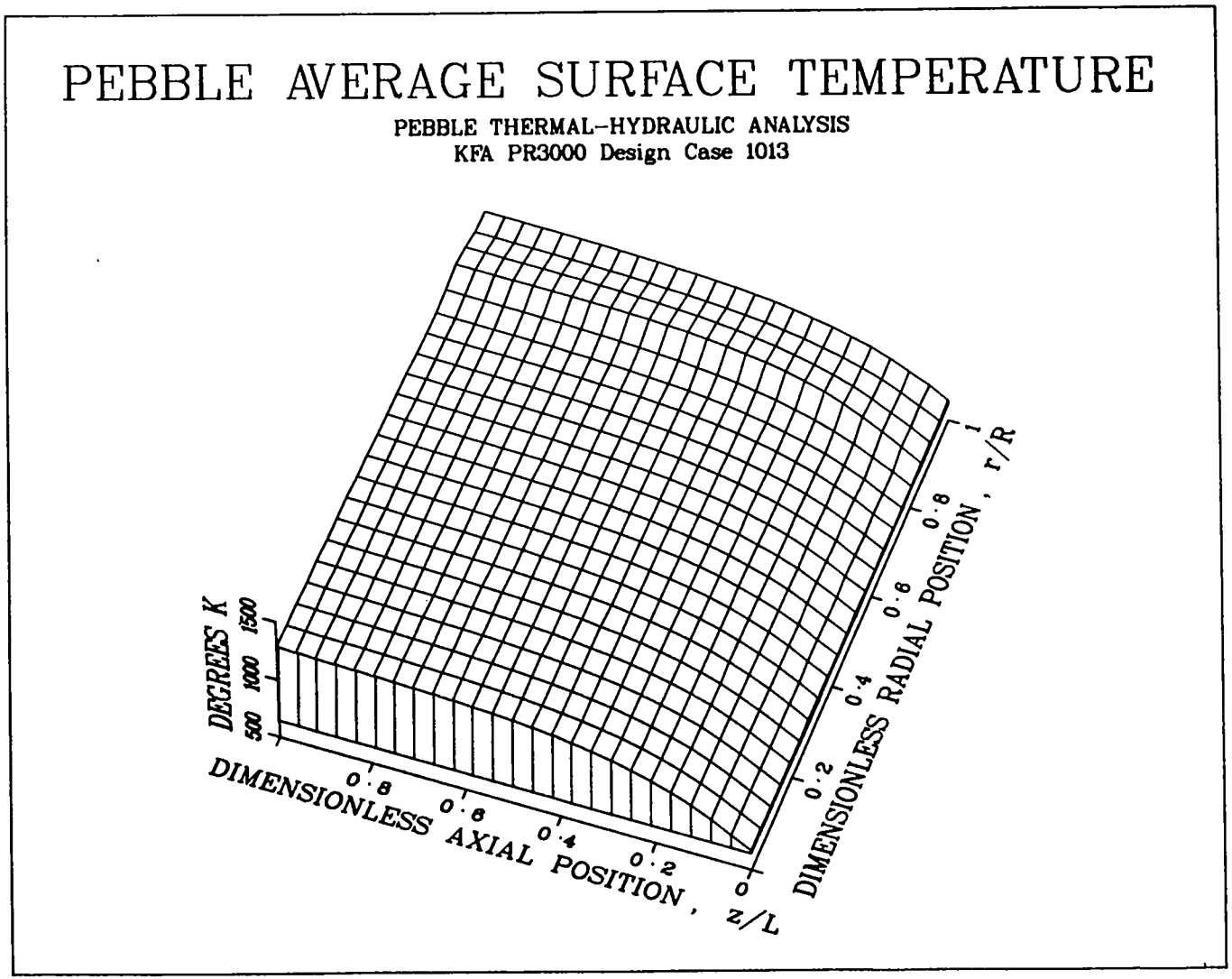

Fig. 26. Calculated distribution of the pebble average surface temperature for KFA PR3000 Design Case 1013.

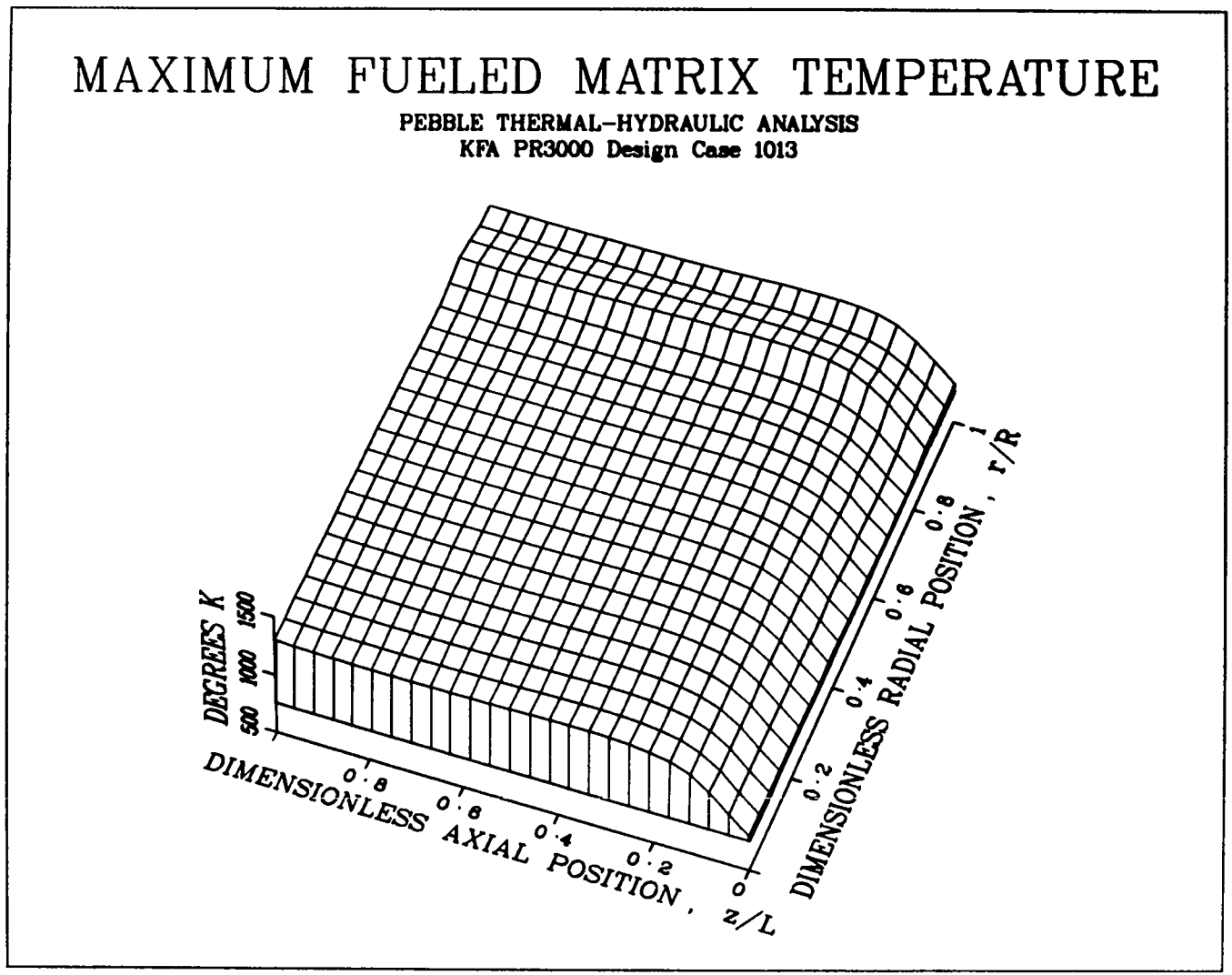

Fig. 27. Calculated distribution of the maximum internal fueled matrix temperature for KFA PR3000 Design Case 1013.

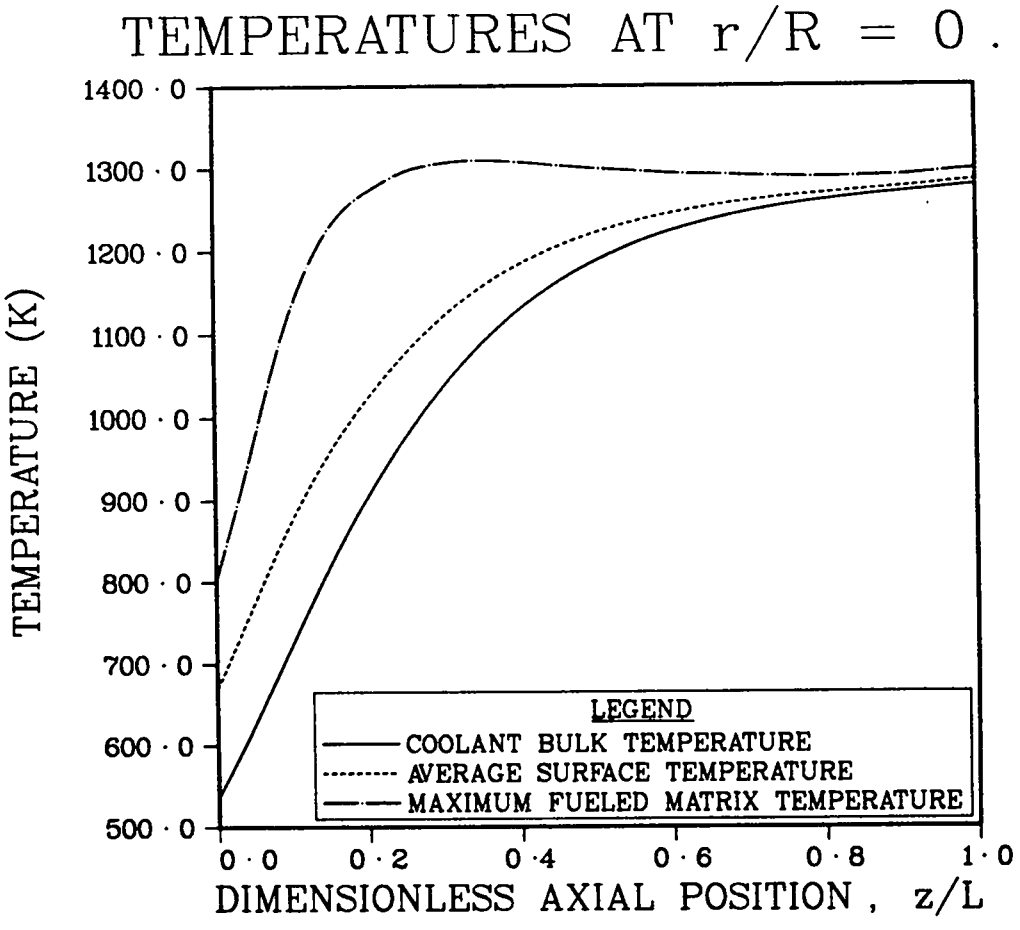

Fig. 28. Calculated axial distribution of temperatures at the core centerline for KFA PR3000 Design Case 1013.

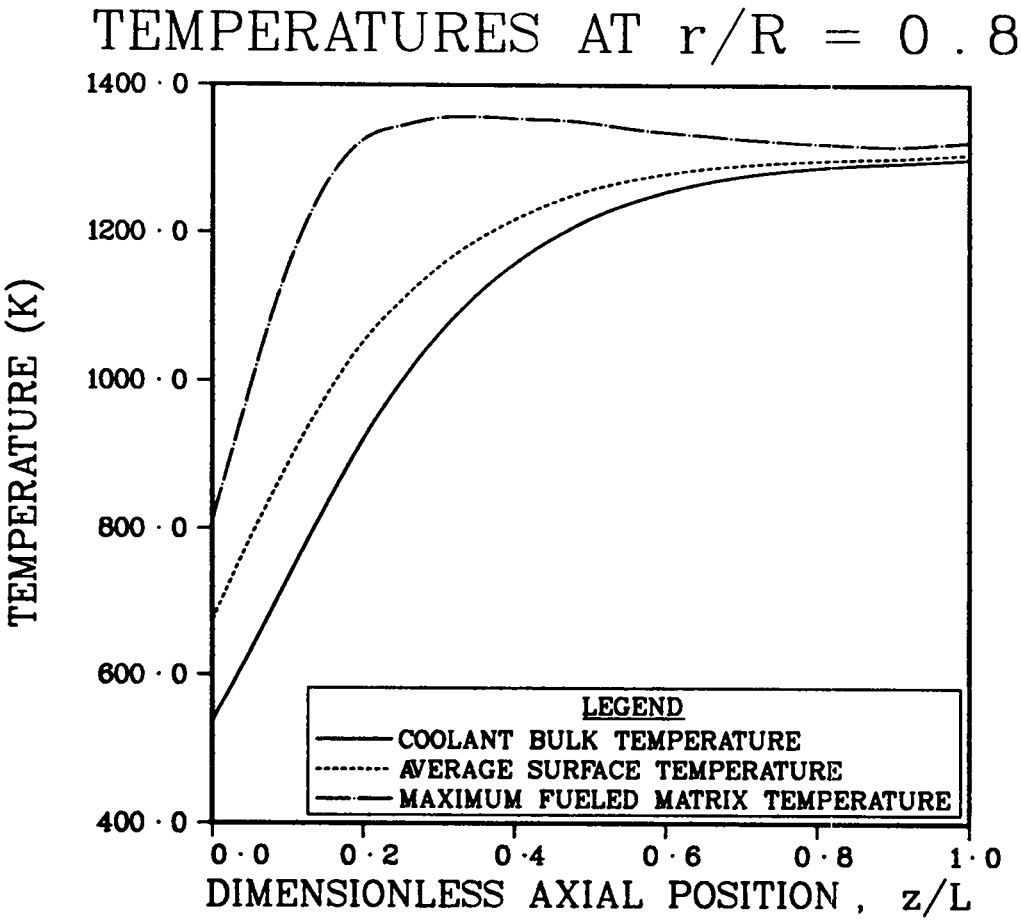

Fig. 29. Calculated axial distribution of temperatures at the hot radius for KFA PR3000 Design Case 1013.

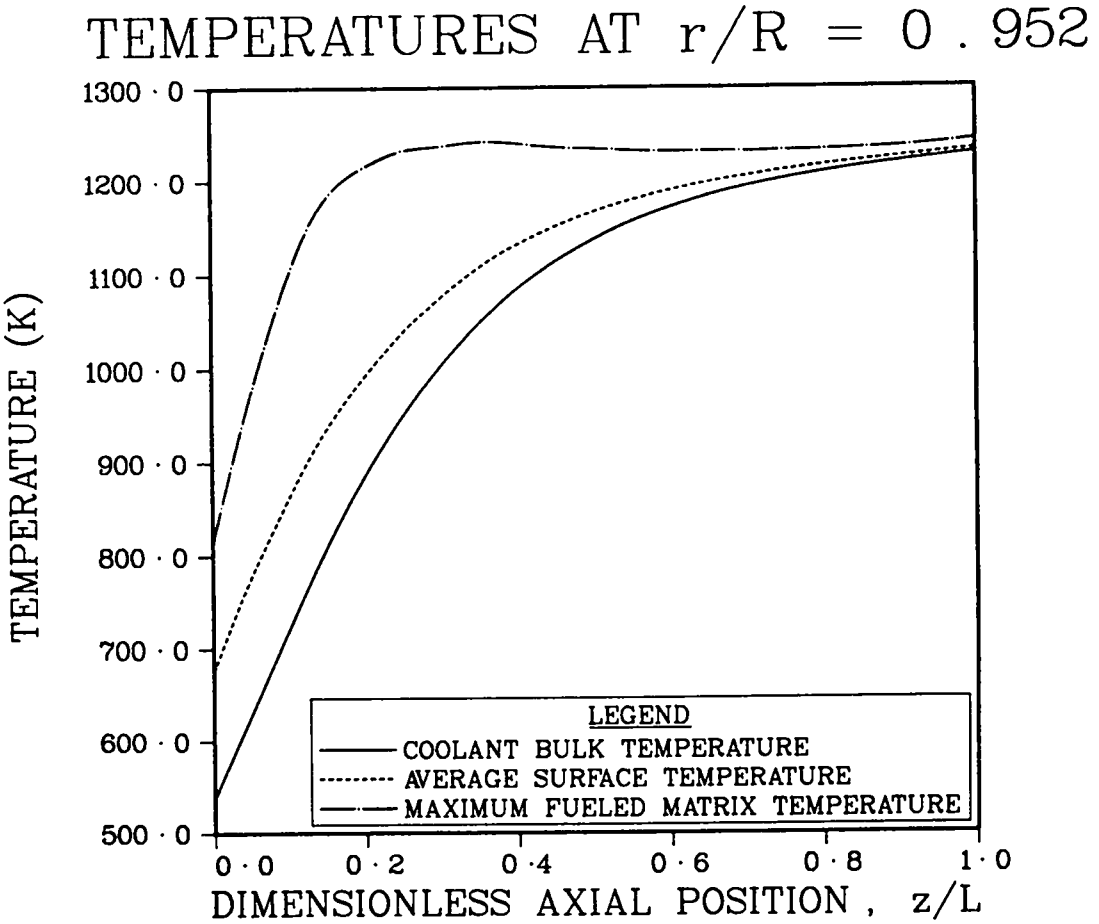

Fig. 30. Calculated axial distribution of temperatures at the cold radius for KFA PR3000 Design Case 1013.

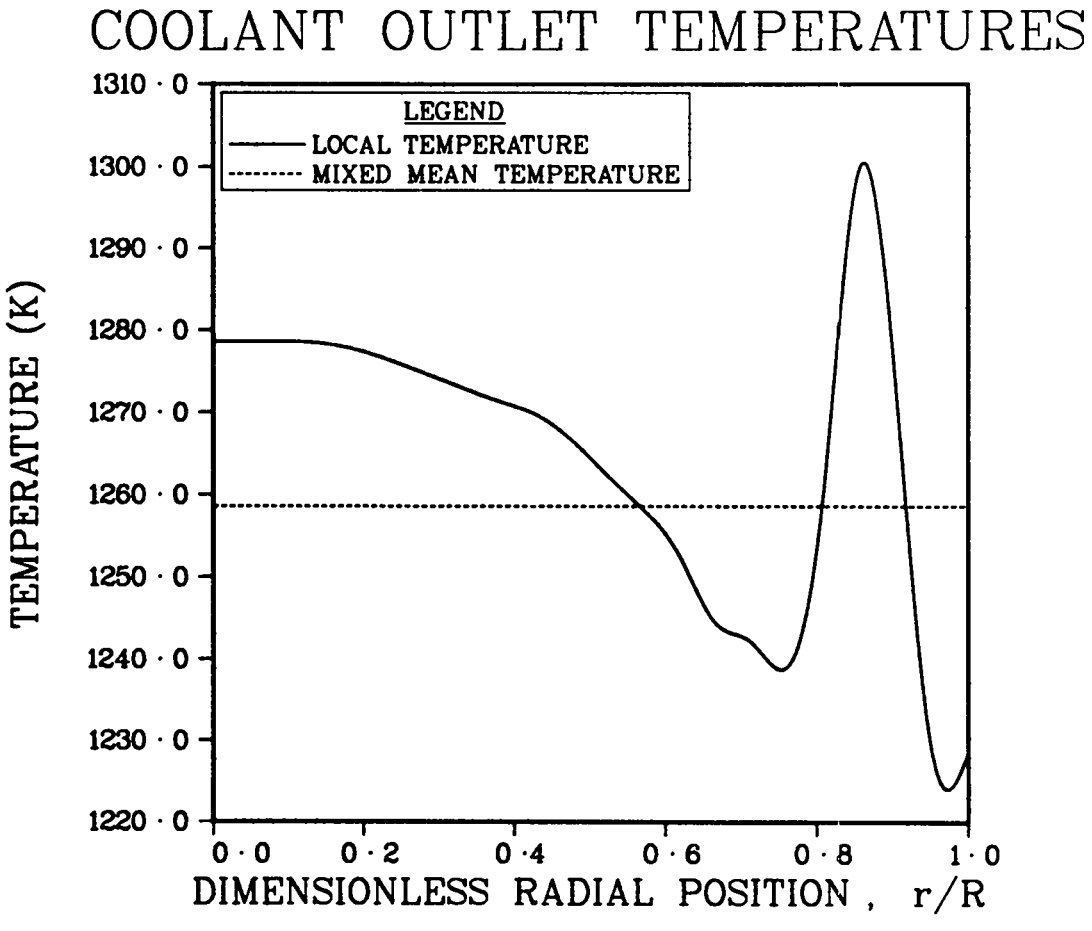

Fig. 31. Calculated coolant outlet temperatures for KFA PR3000 Design Case 1013.

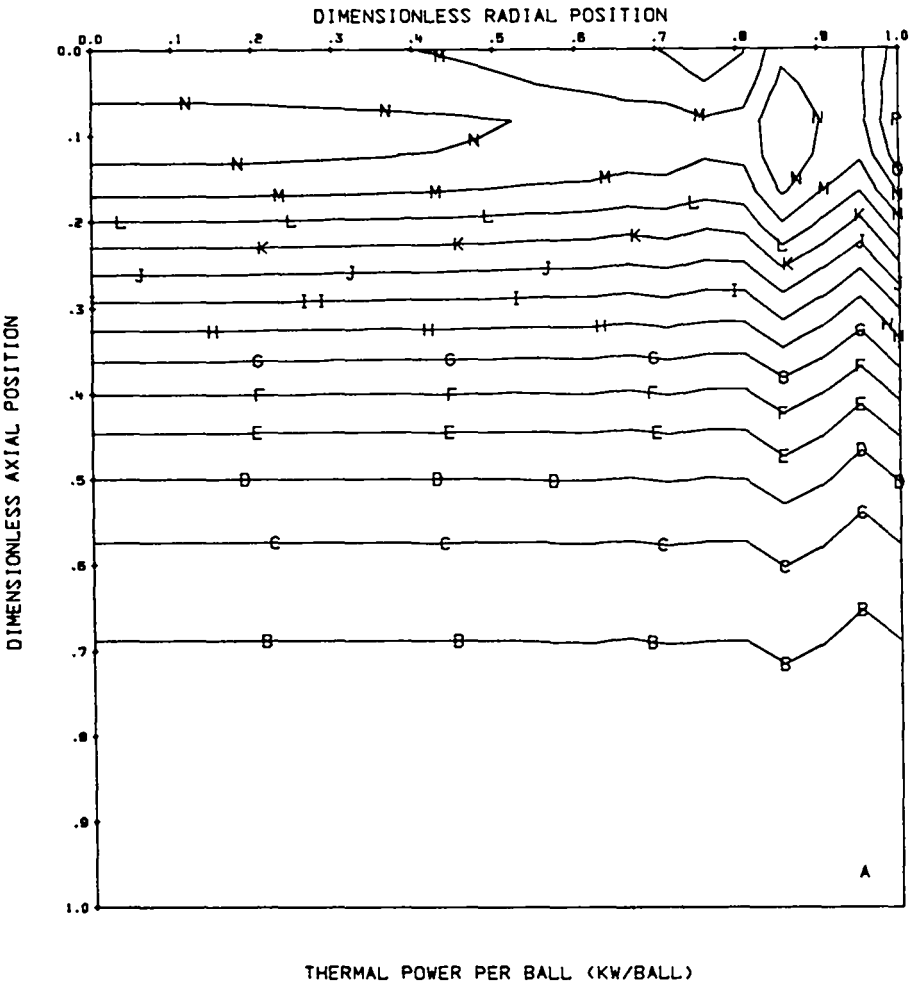

Fig. 32. Contour plot of thermal power per ball values from VSOP. The contours are evenly spaced, from A = 0.140 kw/ball to P = 4.850 kw/ball.

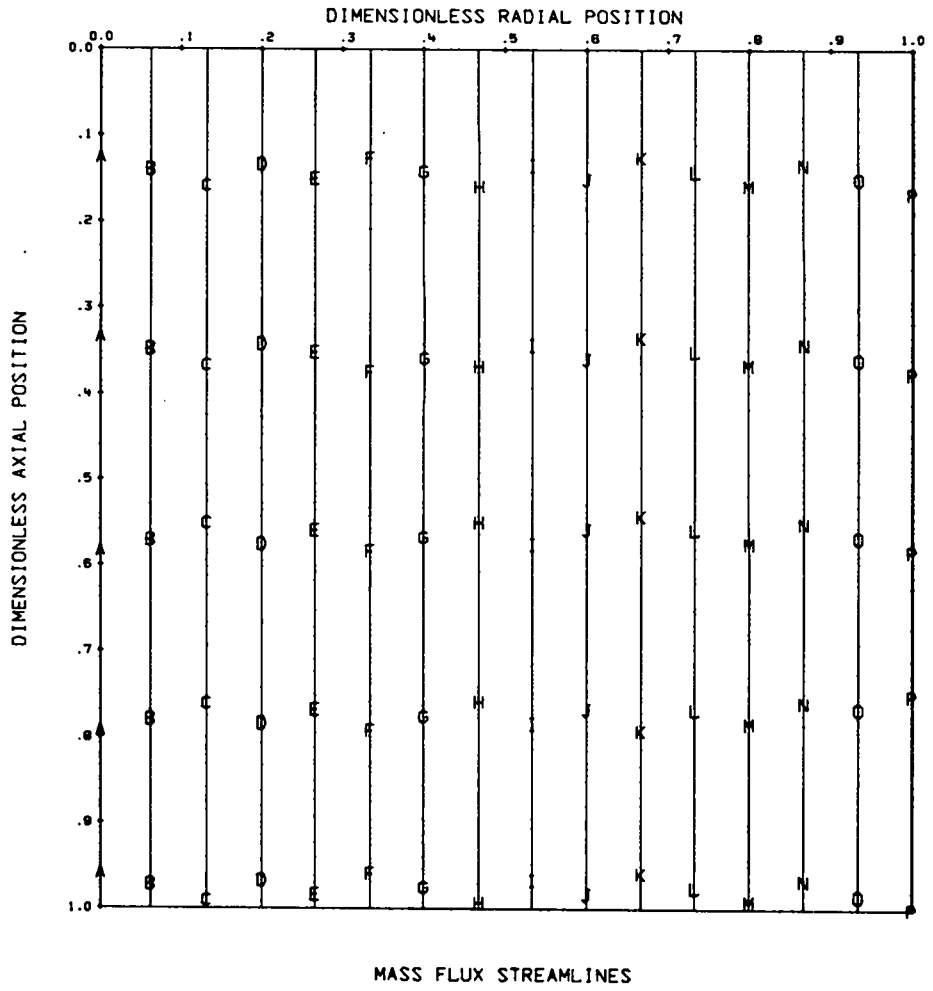

Fig. 33. Calculated mass flux streamlines. Contours are spaced at 0.5 r^2, where r = 0 for contour A and r = 1 for contour P, with r increasing in steps of 1/15.

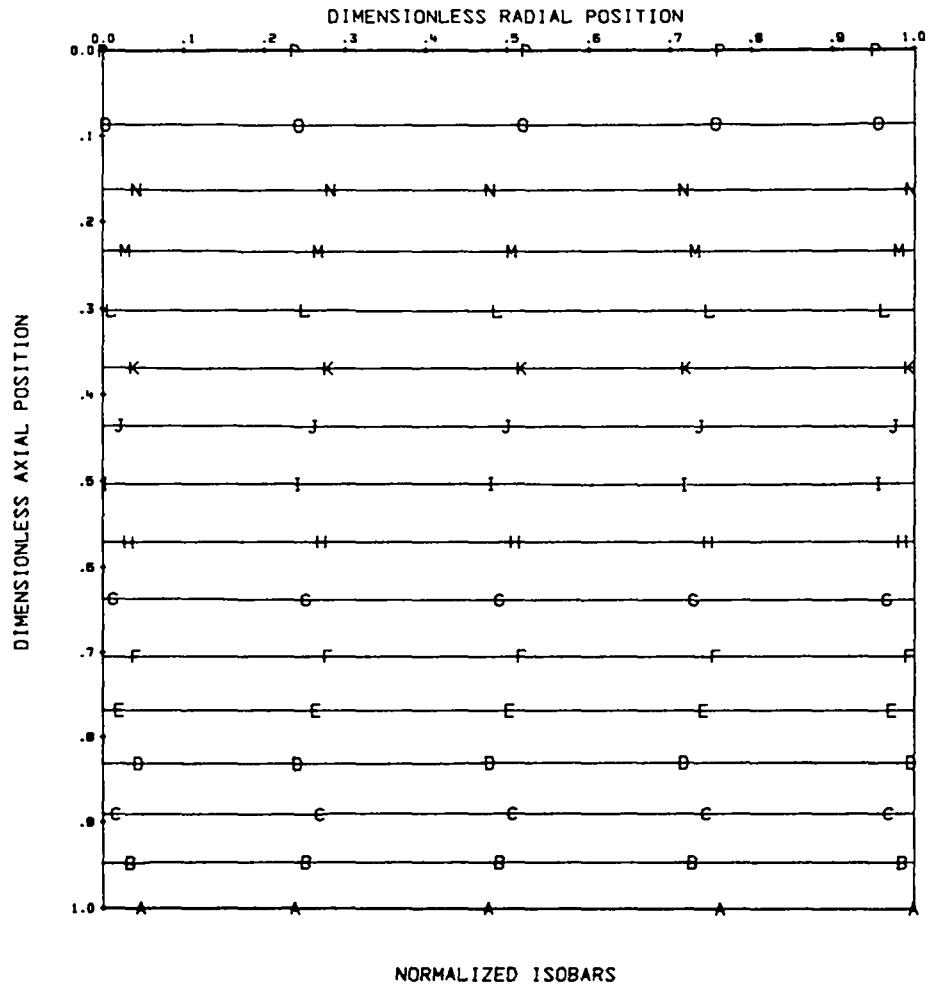

Fig. 34. Calculated equipressure lines. The contours are evenly spaced, from A = 0.982 to P = 1.0.

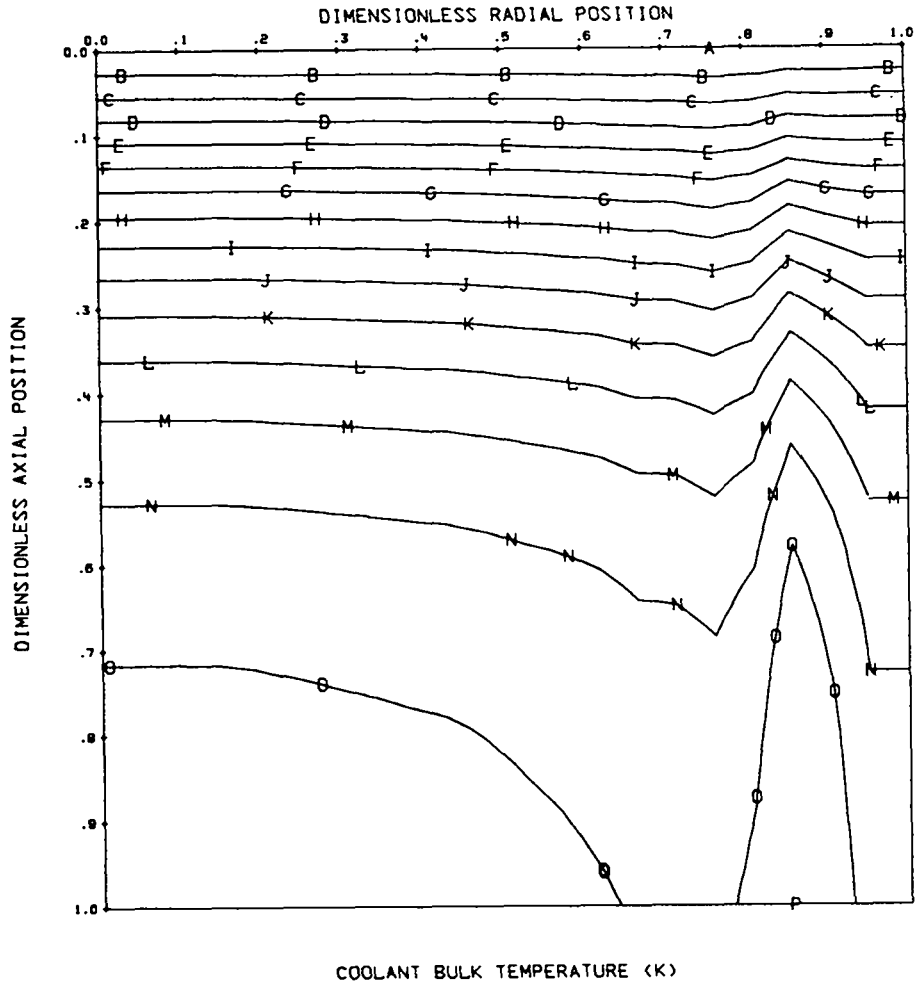

Fig. 35. Contour plot of calculated coolant bulk temperatures. The contours are evenly spaced, from A = 535 K to P = 1300 K.

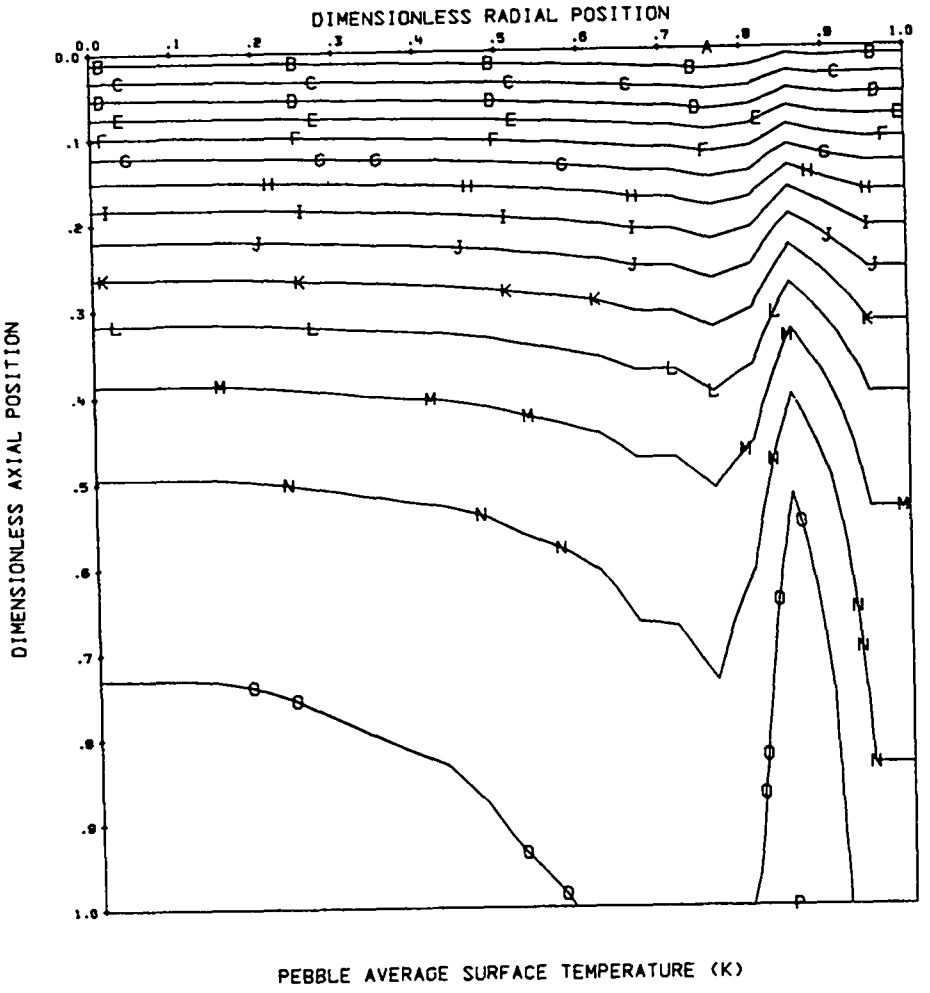

Fig. 36. Contour plot of calculated pebble average surface temperatures. The contours are evenly spaced from A = 648 K to P = 1307 K.

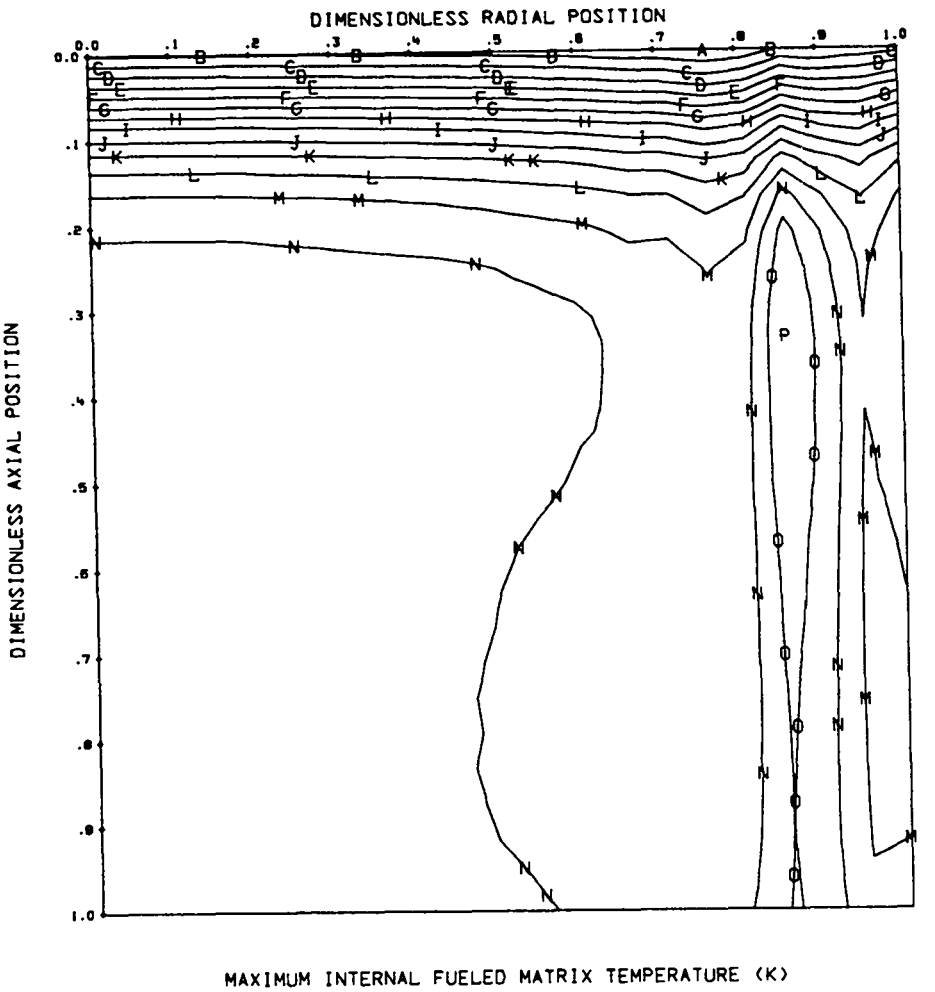

Fig. 37. Contour plot of calculated maximum internal fueled matrix temperatures. The contours are evenly spaced from A = 763 K to P = 1357 K.

the region with the higher heavy metal loading. The peak at r = 1.0 results from the graphite reflector, which acts as a source of thermal neutrons. These power peaks cause a maldistribution in the coolant velocity radial profile.

Referring to Eq. 26, ξ varies as μ and g_2^* varies as $1/\rho$. For helium, μ increases and ρ decreases with increasing temperature. Thus, the resistance to flow through the bed increases with temperature. Since the convective heat transfer coefficient decreases with decreasing gas velocity, the problem compounds itself. The distribution of the dimensionless mass flux, G*, is shown in Fig. 24. In this figure the wall value of G* = 0 is not plotted so the scale can be expanded to show the detail. The flow maldistribution is not large, +1.3% and -1.7% from the mean. Streamlines and isobars are shown in Figs. 33 and 34. The mass flux distribution can be quantified from the print output, but the flow is seen to be mostly axial and parallel. The maximum radial mass flux within the bed is about 0.4% of the mean axial mass flux. The isobar plot in Fig. 34 clearly shows that the pressure gradient becomes steeper towards the outlet where the film temperature is higher. The overall calculated core pressure drop is 0.7 MPa.

The remaining figures show the distributions of coolant bulk temperature, pebble average surface temperature and maximum internal fueled matrix temperature. Examination of the plots will show a radial maldistribution of all three temperatures. This maldistribution is primarily caused by radial differences in the axially integrated thermal power, compounded by the flow maldistribution discussed above. For example, the neutronic calculation for Design Case 1013 used 18 equal

radial volumes: the axially integrated power at r = 0.799 is 148.1 MW(t) while for the adjacent volume, centered at r = 0.833, the axially integrated power is 192.9 MW(t).

Figures 28, 29 and 30 show the axial distributions of the three temperatures at the core centerline, the hot radius and the cold radius, respectively. This type of temperature distribution is characteristic of OTTO fuel cycles. Figure 31 shows the radial distribution of coolant temperature at the outlet, and the mixed-mean outlet coolant temperature. Temperature streaking in the coolant is important to the designers of the core support structure, because the materials problems at these temperatures are very significant. Other maxima and quantitative values can be found in the print output in Appendix C.

As with the isothermal flow model, further validation of the coupled thermal-hydraulic modeling of packed beds will require data from well-characterized experiments. The heating of spheres in the experimental bed should be non-uniform, to test the modeling completely.

VII. CONCLUSIONS

A mathematical model and numerical solution technique have been developed that allow calculation of macroscopic values of thermal-hydraulic variables in an axisymmetric pebble bed nuclear reactor core under steady-state conditions. The nonlinear fluid flow model and numerical solution technique have been validated by comparing predictions with data from the ORNL PBRE full-scale mockup. The computer code PEBBLE has been shown to predict distributions of coolant velocity and pressure adequately, limited only by knowledge of the geometry of the bed. A fully coupled thermal-hydraulic analysis of a large power reactor design, KFA Design Case 1013, has been completed using calculated fission power profiles. The code PEBBLE calculated a mixed-mean outlet coolant temperature which is within one degree K of the analytic value.

The pebble bed has been treated macroscopically as a generating, conducting porous medium. The model uses a nonlinear Forchheimer-type relation between the coolant pressure gradient and mass flux, with newly derived coefficients for the linear and quadratic resistance terms. These coefficients, together with the dimensionless form of Eq. 28 and the numerical solution method, represent an apparent advance in the techniques for calculation of flow maldistribution in packed sphere beds. The complete mathematical model and computer code PEBBLE provide a more complete description of the coupled thermal-hydraulic phenomena in a generating, conducting packed bed than any found in the literature.

The numerical technique uses finite difference forms of the coupled system of nonlinear elliptic partial differential equations, derived by

integrating over finite areas, based on assumptions about the distributions of the variables between the nodes of the grid. This method is most appropriate for a porous medium model of a packed sphere bed, which already includes the assumption that the thermal-hydraulic variables in a sub-volume of the bed can be well characterized by average values. The result is a code which places rather modest requirements on such computer resources as CP time and storage.

The computer code is very flexible, as demonstrated by the complex geometry modeled for the ORNL PBRE, and the variable properties, including an anisotropic thermal conductivity, used in the thermal model. This flexibility, and the modular form of the subroutines which solve the elliptic equations should allow PEBBLE to be applied in the analysis of other packed bed (or porous media) systems, such as chemical catalytic reactors.

The goal of this effort has been the development of analysis techniques. Now that the code PEBBLE exists, further refinement of the model is possible. As experimental data becomes available, the appropriateness of the property models for the solid phase effective thermal conductivity, and turbulent thermal diffusivity, can be examined. There is room for improvement in the boundary conditions applied to model a selected physical system. The modular form of PEBBLE facilities changing the code as the modeling of pebble bed nuclear reactors is refined.

ACKNOWLEDGMENTS

The author wishes to express his gratitude to his advisor, H. G. Olson, and his LASL site supervisors, C. A. Anderson and R. J. Jiacoletti for their guidance and counseling, and to his committee, R. D. Haberstroh, D. A. Krueger, and P. J. Wilbur. The author also wishes to express his gratitude to Elsie Trujillo and Sally Sullivan for their careful preparation of the final draft.

This study was supported by the United States Department of Energy through funds administered by the Associated Western Universities, Inc., and the Reactor and Advanced Heat Transfer Technology Group, Energy Division, of the Los Alamos Scientific Laboratory.

LIST OF REFERENCES

1 F. Daniels, Daniels Pebble Pile, U.S. Patent 2,809,931, October 15, 1957 (filed October 11, 1945).

2 H. Knüfer, Preliminary Operating Experiences with the AVR at an Average Hot-Gas Temperature of 950 C, Nucl. Eng. Des., 34, 1975, p. 33.

3 C. F. Bonilla and T. A. Jaeger, eds., Special Issue: High Temperature Reactor for Process Heat Applications, Nucl. Eng. Des., 34, 1975.

4 Staff, General Electric Energy Systems Programs Dept., Gas Reactor International Cooperative Program Fiscal Year 1977 Annual Report, Topical Report 4: German Pebble Bed Reactor Design and Technology Review, DoE Rept. COO-4057-2, December, 1977.

5 A. Badur and C. Giersch, Thermo-Und Fluiddynamik In Kugelschuttüngen: Literatürubersicht, Interner Bericht, KFA-ISF-IB-8175.

6 A. E. Scheidegger, The Physics of Flow Through Porous Media, Macmillan, N.Y. 1960.

7 H. A. Deans and L. Lapidus, A Computational Model for Predicting and Correlating the Behavior of Fixed-Bed Reactors, AIChE J., 6, 1960, p. 656.

8 R. E. Haring and R. A. Greenkorn, A Statistical Model of a Porous Medium with Non-Uniform Pores, AIChE J., 16, 1970, p. 477.

9 S. Irmay, On the Theoretical Derivation of Darcy and Forchheimer Formulas, Trans. Am. Geo. Union, 39, 1958, p. 702.

10 N. Ahmed, Physical Properties of Porous Medium Affecting Laminar and Turbulent Flow of Water, dissertation, Dept of Civil Engineering, Colorado State University, Fort Collins, CO, 1967.

11 S. Ergun, Fluid Flow Through Packed Columns, Chem. Eng. Prog., 48, 1957, p. 89.

12 J. Radestock and R. Jeschar, Study of the Flow Through the Column of Charges in the Blast Furnace, Stahl u. Eisen, 90, 1970, p. 1249.

13 J. Radestock and R. Jeschar, Theoretical Untersuchung der gegenseitigen Beeinflussung von Temperatur-und Strömungsfeldern in Schüttungen, Chemie-Ing.-Techn., 43, 1971, p. 1304.

LIST OF REFERENCES (continued)

14 V. Stanek and J. Szekely, The Effect of Non-Uniform Porosity in Causing Flow Maldistributions in Isothermal Packed Beds., Can. J. Chem. Eng., 50, 1972, p. 9.

15 V. Stanek and J. Szekely, Flow Maldistribution in Two Dimensional Packed Beds, Part II: The Behavior of Non-Isothermal Systems, Can. J. Chem. Eng., 51, 1973, p. 22.

16 V. Stanek and J. Szekely, Three-Dimensional Flow of Fluids Through Non-Uniform Packed Beds, AIChE J., 20, 1974, p. 974.

17 J. Szekely and J. J. Povermo, Flow Maldistribution in Packed Beds: A Comparison of Measurements with Predictions, AIChE J., 21, 1975, p. 769.

18 V. S. Shvydikii, U. M. Gordon, Y. G. Yaroshenko, and V. B. Shcherbatskii, Gas Distribution Given by a Non-Linear Resistance Pattern in Shaft Furnaces, Steel in the USSR, 4, 1974, p. 662.

19 M. Choudhary, M. Propster, and J. Szekely, On the Importance of the Inertial Terms in the Modeling of Flow Maldistribution in Packed Beds, AIChE J., 22, 1976, p. 600.

20 W. H. Denton, C. H. Robinson, and R. S. Tibbs, The Heat Transfer and Pressure Loss in Fluid Flow Through Randomly Packed Spheres, AERE-R4346, 1963.

21 R. D. Bundy, Velocity and Mass-Diffusion Measurements for Beds of Large, Uniform-Diameter Spheres Randomly Packed in a Full-Scale Model of a Pebble-Bed Nuclear Reactor Core (Thesis), ORNL-TM-1075, 1966.

22 W. U. Choudhury, Heat Transfer and Flow Characteristics in Conductive Porous Media with Energy Generation, dissertation, Department of Mechanical Engineering, University of Wisconsin, 1969.

23 E. Singer and R. H. Wilhelm, Heat Transfer in Packed Beds: Analytical Solution and Design Method, Chem. Eng. Prog., 46, 1950, p. 343.

24 J. J. Barker, Heat Transfer in Packed Beds, Ind. and Eng. Chem., 57, 1965, p. 43.

25 N. U. Koida, The Application of the Similarity Principle to the Filtration of Liquids, Russ. J. Phy. Chem., 34, 1960, p. 375.

26 S. Debbas and H. Rumpf, On the Randomness of Beds Packed with Spheres or Irregular Shaped Particles, Chem. Eng. Sci., 21, 1966, p. 583.

LIST OF REFERENCES (continued)

27 H. Barthels, Druckverlust in Kugelschüttungen, Brennstoff-Warme-Kraft, 24, 1972.

28 A. D. Gosman, W. M. Pun, A. K. Runchal, D. B. Spalding, and M. Wolfshtein, Heat and Mass Transfer in Recirculating Flows, Academic Press, London, 1969.

29 D. Kunii and J. M. Smith, Heat Transfer Characteristics of Porous Rocks, AIChE J., 6, 1960, p. 71.

30 R. D. McFarland, Office Memorandum to R. Jiacoletti, LASL Q-23, April 5, 1976.

31 B. A. Finlayson, Packed Bed Reactor Analysis by Orthogonal Collocation, Chem. Eng. Sci., 26, 1971, p. 1081.

32 H. Petersen, The Properties of Helium: Density, Specific Heats, Viscosity, and Thermal Conductivity at Pressures from 1 to 100 bar and from Room Temperature to About 1800 K, Danish AEC Rept. RISO-224, 1970.

33 R. Jeschar, Wärmeübergang in Mehrkornschüttungen aus Kugeln, Archiv für das Eisenhüttenwesen, 35, 1964.

34 E. Teuchert, L. Bohl, H. J. Rütten and K. A. Haas, The Pebble Bed High Temperature Reactor as a Source of Nuclear Process Heat, Volume 2: Core Physics Studies, Jül-1114-RG, Oktober 1974.

35 P. J. Roache, Computational Fluid Dynamics, Hermosa Publishers, Albuquerque, New Mexico, 1976.

36 Staff, Oak Ridge National Laboratory, Conceptual Design of the Pebble Bed Reactor Experiment, ORNL-TM-201, 1962.

37 K. R. Stroh, H. G. Olson and R. J. Jiacoletti, Comparison of Coolant Flow Predictions with Those Measured on a Full-Scale Mockup of a Pebble Bed Reactor Core, LA-UR-78-1766, Submitted to Nucl. Eng. Des., June 1978.

38 R. F. Benenati and C. B. Brosilow, Void Fraction Distribution in Beds of Spheres, AIChE J., 8, 1962, p. 359.

39 M. C. Thadani and F. N. Peebles, Variation of Local Void Fraction in a Randomly Packed Bed of Equal Spheres, by the Techniques of Radiography and Microphotometry, Rept, EM64-8-1, University of Tennessee, 1964.

LIST OF REFERENCES (continued)

40 L. H. S. Roblee, R. M. Baird and J. W. Tierney, Radial Porosity Variations in Packed Beds, AIChE J., 4, 1958, p. 460.

41 J. Wadsworth, An Experimental Investigation of the Local Packing and Heat Transfer Processes in Packed Beds of Homogeneous Spheres, pp. 760-769 in International Developments in Heat Transfer, Part IV, ASME, 1961.

42 R. Schulten, K. Kugeler, M. Kugeler, H. NieBen, H. Hohn, O. Woike and J. H. Germer, The Pebble Bed High Temperature Reactor as a Source of Nuclear Process Heat, Vol. 1 Conceptual Design, Jül-1113-RG, Oktober 1974.

43 D. Vortmeyer and R. J. Schaefer, Equivalence of One and Two-Phase Models for Heat Transfer Processes in Packed Beds: One-Dimensional Theory, Chem. Eng. Sci., 29, 1974, p. 485.

APPENDIX A: NUMERICAL SOLUTION TECHNIQUE

A.1 The Domain of Integration

For the purpose of the derivation of the finite difference equations, we assume the field of interest has been covered by an orthogonal grid network, and that the nodes of the finite difference grid coincide with the intersections of the grid lines. These grid lines need not be equally spaced. Figure 38 displays a portion of a grid showing a typical node P, and the four surrounding nodes N, S, E, and W. The finite difference equation will eventually be expressed primarily in terms of the values of the variables at these nodes, and to a lesser extent in terms of the values at the nodes labelled NE, NW, SE, and SW.

The integration of the differential equation will be performed over the volume formed by the rotation of the small dotted rectangle, which encloses the point P, through an angle of one radian about the axis of symmetry. The sides of this rectangle lie midway between the adjacent grid lines. The differential equations to be solved are summarized in Table 1.

A.2 Integration of the Equation

The double integral which we wish to evaluate is

$$\int_{r,s}^{r,n} \int_{z,w}^{z,e} \left\{ a_\phi \frac{\partial}{\partial z}\left(\phi \frac{\partial \psi}{\partial r}\right) - \frac{\partial}{\partial r}\left(\phi \frac{\partial \psi}{\partial z}\right)\right\} \, dzdr$$

$$- \int_{r,s}^{r,n} \int_{z,w}^{z,e} \left\{ \frac{\partial}{\partial z}\left(r b_\phi \frac{\partial}{\partial z}\left(c_\phi \phi\right)\right) + \frac{\partial}{\partial r}\left(\frac{r}{a^2} b_\phi \frac{\partial}{\partial r}\left(c_\phi \phi\right)\right)\right\} \, dzdr$$

$$+ \int_{r,s}^{r,n} \int_{z,w}^{z,e} r d_\phi \, dzdr = 0, \qquad \text{(A-1)}$$

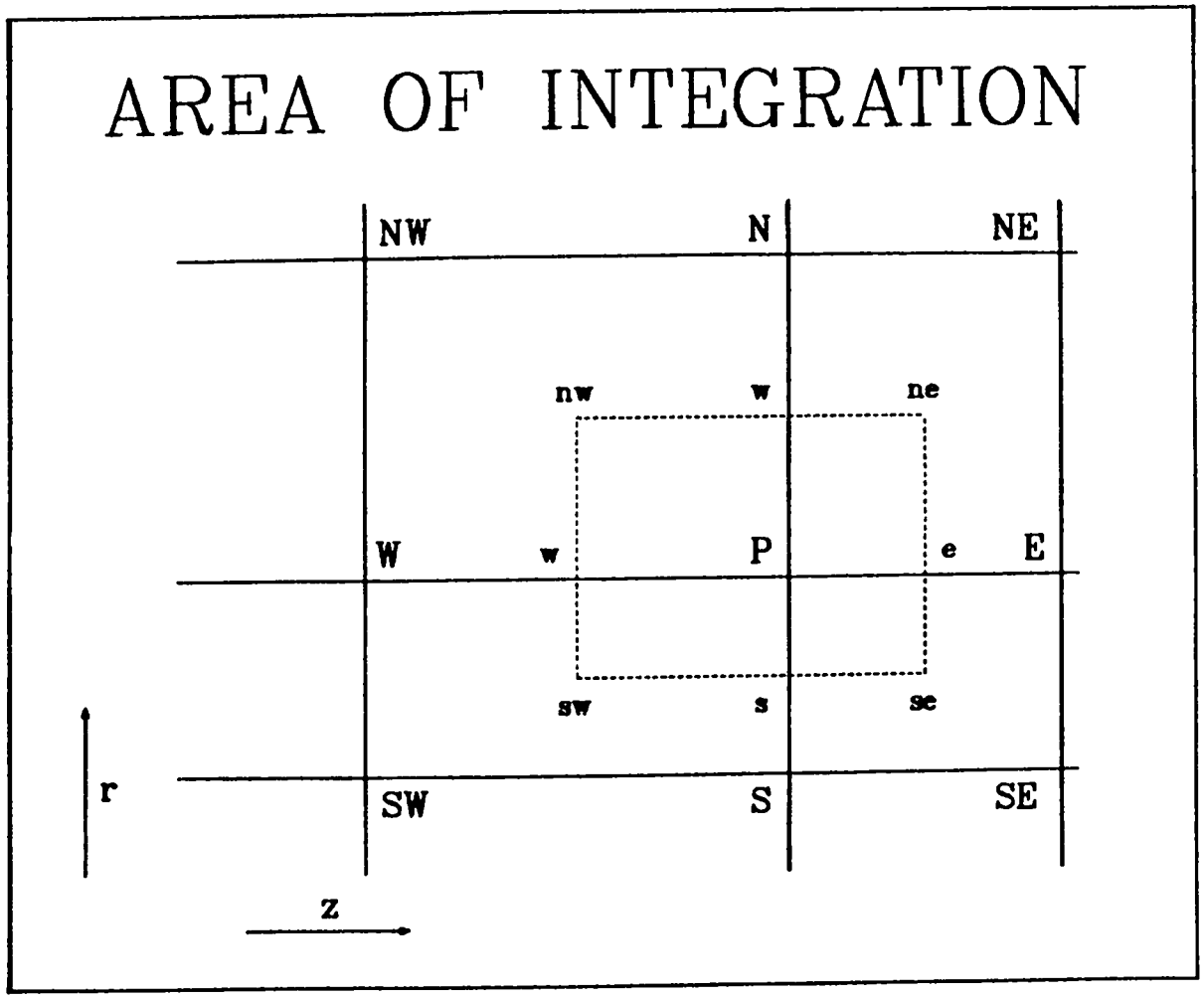

Fig. 38. Illustration of a portion of the finite difference grid showing the area of integration for the differential equations.

Table 1. Model elliptic partial differential equations in standard non-dimensional form.

$$a_\phi \left[\frac{\partial}{\partial z}\left(\phi \frac{\partial \psi}{\partial r}\right) - \frac{\partial}{\partial r}\left(\phi \frac{\partial \psi}{\partial z}\right)\right] - \frac{\partial}{\partial z}\left[b_\phi\, r \frac{\partial}{\partial z}\left(c_\phi \phi\right)\right] - \frac{\partial}{\partial r}\left[b_\phi \frac{r}{a^2} \frac{\partial}{\partial r}\left(c_\phi \phi\right)\right] + r d_\phi = 0$$

EQUATION	DEPENDENT VARIABLE ϕ	a_ϕ	b_ϕ	c_ϕ	d_ϕ
STREAM FUNCTION	ψ	0	$(\xi + G^*) g_2^*$ (1)	+ 1	$+ \frac{2}{ra^2} (\xi + G^*)\, g_2^* \frac{\partial \psi}{\partial r}$
FLUID THERMAL ENERGY BALANCE	T_f	$+c^*$	$+ K_f$ (2)	+ 1	$-h^*\, a_v^*\, (T_s - T_f)$
SOLID THERMAL ENERGY BALANCE	T_s	0	$+ K_s$	+ 1	$+ h^*\, a_v^*\, (T_s - T_f) - q^*$
PRESSURE RECOVERY	p^*	0	+ 1	+ 1	$-\left[\frac{G_{IN}^2\, g_{2IN}\, L}{r\, p_{ref}}\right] \left\{\frac{\partial \psi}{\partial r} \frac{\partial}{\partial z}\left[(\xi + G^*)\, g_2^*\right] - \frac{\partial \psi}{\partial z} \frac{\partial}{\partial r}\left[(\xi + G^*)\, g_2^*\right]\right\}$

(1) $G^* = \frac{1}{r}\, a^2 \left[\left(\frac{\partial \psi}{\partial z}\right)^2 + \left(\frac{\partial \psi}{\partial r}\right)^2\right]^{0.5}$

(2) K_f is anisotropic and requires special treatment in the code.

where the integration limits are the coordinates of the sides of the rectangle.

Inspection of the above equation reveals that all the terms but the last could be formally integrated once if a_ϕ were a constant. Examination of Table 1 shows that a_ϕ is zero for all equations except the fluid phase thermal energy balance, and c* can be assumed constant for engineering purposes. We denote a suitable local average value of a_ϕ near the point P as $a_{\phi,p}$.

$$a_{\phi,p}\left\{\int_{r,s}^{r,n}\left[\phi_e\left(\frac{\partial\psi}{\partial r}\right)_e-\phi_w\left(\frac{\partial\psi}{\partial r}\right)_w\right]dr-\int_{z,w}^{z,e}\left[\phi_n\left(\frac{\partial\psi}{\partial z}\right)_n-\phi_s\left(\frac{\partial\psi}{\partial z}\right)_s\right]dz\right\}$$

ADVECTION TERMS

$$-\int_{r,s}^{r,n}\left\{\left[rb_\phi\right]_e\left[\frac{\partial}{\partial z}\left(c_\phi\phi\right)\right]_e-\left[rb_\phi\right]_w\left[\frac{\partial}{\partial z}\left(c_\phi\phi\right)\right]_w\right\}dr$$

DIFFUSION TERMS

$$-\frac{1}{a^2}\int_{z,w}^{z,e}\left\{\left[rb_\phi\right]_n\left[\frac{\partial}{\partial r}\left(c_\phi\phi\right)\right]_n-\left[rb_\phi\right]_s\left[\frac{\partial}{\partial r}\left(c_\phi\phi\right)\right]_s\right\}dz$$

$$+\int_{r,s}^{r,n}\int_{z,w}^{z,e}rd_\phi\,drdz=0, \qquad \text{(A-2)}$$

SOURCE TERM

where those quantities which appear with the subscripts n, s, e, or w are to be evaluated along the side of the rectangle denoted by the subscript.

In the above equation, various groups of terms have been assigned the names advection, diffusion, and source. In order to proceed further, assumptions must be made about the distributions of the variables according to the nature of the terms.

a. Advection Terms

There are four integrals to be evaluated in the advection terms. It will be sufficient to outline the procedure for only one of these in detail, for the treatment of the others will follow similar lines. If we denote the first integral by the symbol I_a,

$$I_a = a_{\phi,p} \int_{r,s}^{r,n} \phi_e \left(\frac{\partial \psi}{\partial r}\right)_e dr. \tag{A-3}$$

If both ϕ and ψ are well behaved functions, there exists an average value of ϕ_e, which is denoted $\overline{\phi}_e$, such that

$$\overline{\phi}_e \equiv \frac{\int_{r,s}^{r,n} \phi_e \left(\frac{\partial \psi}{\partial r}\right)_e dr}{\int_{r,s}^{r,n} \left(\frac{\partial \psi}{\partial r}\right)_e dr} \approx \frac{I_a}{a_{\phi,p}\left(\psi_{ne} - \psi_{se}\right)} \tag{A-4}$$

where the subscripts ne and se refer to the relevant corners of the rectangle shown in Fig. 38. The equation can now be rewritten as

$$I_a = a_{\phi,p}\, \overline{\phi}_e \left(\psi_{ne} - \psi_{se}\right) . \tag{A-5}$$

The next task is to express $\overline{\phi}_e$, ψ_{ne} and ψ_{se} in terms of values of the variables at the nodes of the grid. We assume that ϕ is uniform

within each rectangle, and has the value which prevails at the particular node which the rectangle encloses. At this point, we develop two alternate formulations for $\overline{\phi}_e$. We will allow the user the option of using either upwind differences or central differences on the advection terms. Central differences are more accurate, but upwind differences may be required to ensure convergence with certain equations. For upwind differences it is assumed that $\overline{\phi}_e$ takes on the ϕ value possessed by the fluid upstream of the e-face of the rectangle. For central differences we assume that

$$\overline{\phi}_e \approx \frac{\phi_p + \phi_E}{2} \quad . \tag{A-6}$$

For upwind differences

$$I_a \approx a_{\phi,p} \left\{ \phi_E \left[\frac{(\psi_{ne} - \psi_{se}) - |\psi_{ne} - \psi_{se}|}{2} \right] + \phi_p \left[\frac{(\psi_{ne} - \psi_{se}) + |\psi_{ne} - \psi_{se}|}{2} \right] \right\} . \tag{A-7}$$

In this equation, the presence of the ψ-difference, first within a bracket and then within a modulus sign, ensures that one of the terms in the square brackets in the equation will be zero. The term which remains will represent the contribution from the node upstream from the e-face of the rectangle. In this way upwind differences are introduced into the finite-difference scheme.

We now assume that the value of the stream function at a particular corner of the rectangle is equal to the average of the values at the four neighboring nodes, such that

$$\psi_{se} = \frac{\psi_{SE} + \psi_E + \psi_P + \psi_S}{4} \quad . \tag{A-8}$$

Assembling the expression for I_{adv}, the sum of all the advection terms yields

$$I_{adv} = AE\ (\phi_P - \phi_E) + AW\ (\phi_P - \phi_W)$$

$$+ AN\ (\phi_P - \phi_N) + AS\ (\phi_P - \phi_S),$$

where

$$AE = \frac{a_{\phi,P}}{8} \left[(\psi_{SE} + \psi_S - \psi_{NE} - \psi_N) + |\psi_{SE} + \psi_S - \psi_{NE} - \psi_N|\right] ,$$

$$AW = \frac{a_{\phi,P}}{8} \left[(\psi_{NW} + \psi_N - \psi_{SW} - \psi_S) + |\psi_{NW} + \psi_N - \psi_{SW} - \psi_S|\right] ,$$

$$AW = \frac{a_{\phi,P}}{8} \left[(\psi_{NE} + \psi_E - \psi_{NW} - \psi_W) + |\psi_{NE} + \psi_E - \psi_{NW} - \psi_W|\right] , \tag{A-9}$$

and

$$AS = \frac{a_{\phi,P}}{8} \left[(\psi_{SW} + \psi_W - \psi_{SE} - \psi_E) + |\psi_{SW} + \psi_W - \psi_{SE} - \psi_E|\right] ,$$

For central differences

$$I_a \approx a_{\phi,P} \left[\left(\frac{\phi_P + \phi_E}{2}\right)(\psi_{ne} - \psi_{se})\right] , \tag{A-10}$$

and

$$I_{adv} = AE^* (\phi_P + \phi_E) + AW^* (\phi_P + \phi_N)$$

$$+ AN^* (\phi_P + \phi_N) + AS^* (\phi_P + \phi_S), \tag{A-11}$$

where

$$AE^* = \frac{a_{\phi,P}}{8} \left(\psi_{NE} + \psi_N - \psi_S - \psi_{SE}\right) ,$$

$$AW^* = \frac{a_{\phi,P}}{8} \left(\psi_S + \psi_{SW} - \psi_{NW} - \psi_N\right) ,$$

$$AN^* = \frac{a_{\phi,P}}{8} \left(\psi_{NW} + \psi_W - \psi_{NE} - \psi_E\right) ,$$

$$AS^* = \frac{a_{\phi,P}}{8} \left(\psi_E + \psi_{SE} - \psi_W - \psi_{SW}\right) .$$

b. Diffusion Terms

As before, to consider one integral is to consider all, so we will evaluate the integral

$$I_d = \int_{z,s}^{z,n} \left[rb_\phi\right]_e \left[\frac{\partial}{\partial z} \left(c_\phi \phi\right)\right]_e dr. \tag{A-12}$$

Assuming that

$$r_e \approx \frac{(r_E + r_P)}{2} ,$$

$$b_{\phi,e} \approx \frac{(b_{\phi,E} + b_{\phi,P})}{2} , \tag{A-13}$$

and

$$\left[\frac{\partial}{\partial z} \left(c_\phi \phi\right)\right]_e \approx \frac{c_{\phi,E}\, \phi_E - c_{\phi,P}\, \phi_P}{z_E - z_P} ,$$

Equation (A-12) can be integrated to yield

$$I_d = \frac{b_{\phi,E} + b_{\phi,P}}{2} \cdot \frac{r_E + r_P}{2} \cdot \frac{c_{\phi,E}\, \phi_E - c_{\phi,P} \phi_P}{z_E - z_P} \cdot \frac{r_N - r_S}{2} . \tag{A-14}$$

The other diffusion terms may be evaluated by similar arguments, yielding I_{diff}, the sum of the integrals of all four terms:

$$I_{diff} = BE\ (c_{\phi,E}\phi_E - c_{\phi,P}\phi_P) + BW\ (c_{\phi,W}\phi_W - c_{\phi,P}\phi_P)$$

$$+ BN\ (c_{\phi,N}\phi_N - c_{\phi,P}\phi_P) + BS\ (c_{\phi,S}\phi_S - c_{\phi,P}\phi_P),$$

where

$$BE = \frac{b_{\phi,E} + b_{\phi,P}}{8} \left(\frac{r_N - r_S}{z_E - z_P}\right)(r_E + r_P),$$

$$BW = \frac{b_{\phi,W} + b_{\phi,P}}{8} \left(\frac{r_N - r_S}{z_P - z_W}\right)(r_W + r_P),$$

$$BN = \frac{b_{\phi,N} + b_{\phi,P}}{8a^2} \left(\frac{z_E - z_W}{r_N - r_P}\right)(r_N + r_P), \qquad \text{(A-15)}$$

and

$$BS = \frac{b_{\phi,S} + b_{\phi,P}}{8a^2} \left(\frac{z_E - z_W}{r_P - r_S}\right)(r_S + r_P).$$

c. Source Terms

The final integral we must evaluate is

$$I_{sor} = \int_{r,s}^{r,n} \int_{z,w}^{z,e} r d_\phi\, dz dr. \qquad \text{(A-16)}$$

Here we note that there is a double integral to evaluate, since d_ϕ may assume various forms, according to the particular variable under consideration, making it impossible to perform the first integration immediately as was done with the other terms. This problem can be avoided by assuming that d_ϕ is uniform over the area of integration and takes on the value at point P. Then, if it is further assumed that r_P

is a close approximation to the space-average value of r, Eq. (A-16) may be integrated to yield

$$I_{sor} \approx d_{\phi,P} \cdot V_P, \tag{A-17}$$

where

$$V_P = r_P \left(\frac{z_E - z_W}{2}\right) \left(\frac{r_N - r_S}{2}\right), \tag{A-18}$$

which represents the approximate volume swept out by the rotation of the rectangle through an angle of one radian about the axis of symmetry.

It is now a relatively simple matter to express the $d_{\phi,P}$ term for each variable in finite difference form. If, for example, this term contains first-order differential coefficients, these may be expressed in terms of central differences. When the grid spacing is non-uniform

$$\left(\frac{\partial \phi}{\partial r}\right)_P = \frac{(\phi_N - \phi_P)\left(\frac{r_P - r_S}{r_N - r_P}\right) + (\phi_P - \phi_S)\left(\frac{r_N - r_P}{r_P - r_S}\right)}{r_N - r_S} \tag{A-19}$$

with a similar expression describing the axial derivitive.

d. The Complete Finite Difference Equation

The integration of the general differential equation over the small control volume has been completed. We may now assemble the expressions for the various terms. For upwind differencing of the advection terms

$$\begin{aligned} &AE\,(\phi_P - \phi_E) + AW\,(\phi_P - \phi_W) + AN\,(\phi_P - \phi_N) + AS\,(\phi_P - \phi_S) \\ &-BE\,(c_{\phi,E}\,\phi_E - c_{\phi,P}\,\phi_P) - BW\,(c_{\phi,W}\,\phi_W - c_{\phi,P}\,\phi_P) \\ &-BN\,(c_{\phi,N}\,\phi_N - c_{\phi,P}\,\phi_P) - BS\,(c_{\phi,S}\,\phi_S - c_{\phi,P}\,\phi_P) \end{aligned} \tag{A-20}$$

For central differencing of the advection terms

$$AE^* (\phi_P + \phi_E) + AW^* (\phi_P + \phi_W) + AN^* (\phi_P + \phi_N)$$

$$+ AS^* (\phi_P + \phi_S) - BE \ (c_{\phi,W}\phi_W - c_{\phi,P}\phi_P)$$

$$- BW \ (c_{\phi,W}\phi_W - c_{\phi,P}\phi_P) - BN \ (c_{\phi,N}\phi_N - c_{\phi,P}\phi_P)$$

$$- BS \ (c_{\phi,S}\phi_S - c_{\phi,P}\phi_P) + d_{\phi,P} V_P = 0. \qquad \text{(A-21)}$$

Equations (A-20) and (A-21) are the major outcome of the effort so far; they provide an algebraic relation between the value of ϕ at a particular node and the values at the surrounding nodes. There will be one such equation for each variable at every interior node in the field. Together with equations for the boundary nodes, there are as many equations as unknowns.

A.3 The Successive-Substitution Formula

It is now possible to recast Eqs. (A-20) and (A-21) as successive-substitution formulae. Removing ϕ_P to the left-hand side

$$\phi_P = CE\phi_E + CW\phi_W + CN\phi_N + CS\phi_S + D, \qquad \text{(A-22)}$$

where, for upwind differences on the advection terms,

$$\begin{aligned} CE &= (AE + BE \ c_{\phi,E})/\Sigma AB, \\ CW &= (AW + BW \ c_{\phi,W})/\Sigma AB, \\ CN &= (AN + BN \ c_{\phi,N})/\Sigma AB, \\ CS &= (AS + BS \ c_{\phi,S})/\Sigma AB, \\ D &= -d_{\phi,P} \ V_P/\Sigma AB, \end{aligned} \qquad \text{(A-23)}$$

and

$$\Sigma_{AB} = AE + AW + AN + AS + c_{\phi,P}\,(BE + BW + BN + BS).$$

For central differencing of the advection terms

$$\begin{aligned} CE &= (-AE^* + BE\ c_{\phi,E})/\Sigma AB^*, \\ CW &= (-AW^* + BW\ c_{\phi,W})/\Sigma AB^*, \\ CN &= (-AN^* + BN\ c_{\phi,N})/\Sigma AB^*, \\ CS &= (-AS^* + BS\ c_{\phi,S})/\Sigma AB^*, \\ D &= -d_{\phi,p}\ V_P/\Sigma AB^*, \end{aligned} \tag{A-24}$$

and

$$\Sigma AB^* = -(AE^* + AW^* + AN^* + AS^*) + c_{\phi,P}\,(BE + BW + BN + BS).$$

It is useful to now recast Eq. (A-22) in a form more suitable for programming. Writing the formula in terms of the A's and B's

$$\phi_P = \frac{\sum_{j\,=\,N,\,S,\,E,\,W} \left\{(A_j + c_{\phi,j}\,B_j)\,\phi_j\right\} - d_{\phi P}\,V_P}{\sum_{j\,=\,N,\,S,\,E,\,W} (A_j + c_{\phi,P}\,B_j)}, \tag{A-25}$$

where $\sum_{j\,=\,N,\,S,\,E,\,W}$ denotes summation over nodes N,S,E, and W.

Dividing both the numerator and denominator by V_P

$$\phi_P = \frac{\sum_{j\,=\,N,\,S,\,E,\,W} \left[\left\{A_j' + c_{\phi,j}\,(b_{\phi,j} + b_{\phi,P})\,B_j'\right\}\,\phi_j\right] - d_{\phi,P}}{\sum_{j\,=\,N,\,S,\,E,\,W} \left\{A_j' + c_{\phi,P}\,(b_{\phi,j} + b_{\phi,P})\,B_j'\right\}}, \tag{A-26}$$

where A_j' and B_j' are related to A_j and B_j by

$$A_j' = A_j/V_P,$$

and

$$B_j' = B_j/V_P\ (b_{\phi,j} + b_{\phi,P}). \tag{A-27}$$

Equation (A-26) expresses the substitution formula in the form used by PEBBLE. A similar formula is derived for the situation where central differences are used for the advection terms, with

$$A_j' = -\ A_j^*/V_P. \tag{A-28}$$

The rate of convergence of an iterative solution procedure can sometimes be improved by over-relaxation: for this, the variation of the ϕ's from one iteration to another is caused to be greater than that which would be obtained in the normal iteration process. Alternately, some equations may require under-relaxation to ensure convergence. Both of these techniques can be applied in the code through the formula

$$\phi_P = RP\phi_P^{(N)} + (1 - RP)\,\phi_P^{(N-1)}, \tag{A-29}$$

where RP is the relaxation parameter specified for the variable ϕ, and the bracketed superscripts denote the new value from iteration N and the previous value from iteration N-1. If very slow variations in ϕ are necessary for stability, RP can be set equal to an arbitrarily small number. Care must be taken when over-relaxing, as ill-chosen values of RP can slow the rate of convergence, or even provoke divergence.

The numerical method reported here is a modified form of the techniques developed by Gosman, et al. [28]. Modifications include the

non-dimensionalization of the general elliptic equation form and the resulting successive substitution formulae, and the addition of the ability to use central differences for the advection terms.

APPENDIX B. LISTING OF PROGRAM PEBBLE AND ITS SUBROUTINES

The program as listed is set up for the coupled thermal-hydrualic test problem: KFA Design Case 1013.

LASL Identification No.: LP-1046

```
      PROGRAM PEBBLE (OUTPUT,TAPE2,TAPE3,TAPE4,TAPE5,TAPE6,TAPE7,TAPE8
     1 ,TAPE9,TAPE10,FILM)
C
C     ***  SET UP TO ANALYZE KFA POWER REACTOR PR3000, CASE 1013  ***
C          REF:  E. TEUCHERT, L. BOHL, H.J. RUTTEN AND K.A. HASS,
C                JUL-1114-RG, OCTOBER 1974
C
C     C**********************************************************C
C     C**********************************************************C
C     C                                                          C
C     C     PEBBLE - A PROGRAM FOR THE THERMAL/HYDRAULIC ANALYSIS C
C     C                                                          C
C     C       OF A STEADY-STATE PEBBLE BED NUCLEAR REACTOR CORE  C
C     C                                                          C
C     C         (AXISYMMETRIC CYLINDRICAL COORDINATE GEOMETRY)   C
C     C                                                          C
C     C                                                          C
C     C                          K.R. STROH                      C
C     C                          GROUP Q-13                      C
C     C          REACTOR AND ADVANCED HEAT TRANSFER TECHNOLOGY   C
C     C                LOS ALAMOS SCIENTIFIC LABORATORY          C
C     C                                                          C
C     C             PROGRAM IS DOCUMENTED IN A DISSERTATION      C
C     C          FOR THE DEPARTMENT OF MECHANICAL ENGINEERING    C
C     C                     COLORADO STATE UNIVERSITY            C
C     C                                                          C
C     C                  - VERSION AS OF JULY 15, 1978 -         C
C     C                                                          C
C     C**********************************************************C
C     C**********************************************************C
C
C     C**********************************************************C
C     C                                                          C
C     C                                                          C
C     C              VARIABLES STORED IN THE ARRAY A(I,J,K)      C
C     C                                                          C
C     C      K            CORRESPONDING DIMENSIONLESS VARIABLE   C
C     C     ---           ------------------------------------   C
C     C                                                          C
C     C      1            STREAM FUNCTION, PSI                  C
C     C                                                          C
C     C      2            FLUID BULK TEMPERATURE, TF            C
C     C                                                          C
C     C      3            AVERAGE PEBBLE SURFACE TEMPERATURE, TS C
C     C                                                          C
C     C      4            PRESSURE, PSTAR                       C
C     C                                                          C
C     C      5            MASS FLUX, GSTAR                      C
C     C                                                          C
C     C      6            (XI + GSTAR)*G2STAR                   C
C     C                                                          C
C     C      7            RADIAL DERIVITIVE OF PSI              C
C     C                                                          C
C     C      8            AXIAL DERIVITIVE OF PSI               C
C     C                                                          C
C     C      9            AXIAL COMPONENT OF MASS FLUX, GZSTAR  C
C     C                                                          C
C     C     10            RADIAL COMPONENT OF MASS FLUX, GRSTAR C
C     C                                                          C
C     C                                                          C
C     C**********************************************************C
C
```

```
C
C     C*****************************************************************C
C     C                                                                 C
C     C                                                                 C
C     C          VARIABLES STORED IN THE ARRAY PROPTY(I,J,K)            C
C     C                                                                 C
C     C     K                CORRESPONDING VARIABLE                     C
C     C    ---    ------------------------------------------            C
C     C                                                                 C
C     C     1     COOLANT DENSITY, RHO (DIMENSIONAL, KG/M**3)           C
C     C                                                                 C
C     C     2     FRICTION PARAMETER RATIO, XI                          C
C     C                                                                 C
C     C     3     FRICTION PARAMETER, G2STAR                            C
C     C                                                                 C
C     C     4     VOID FRACTION, EPSILON                                C
C     C                                                                 C
C     C     5     DIMENSIONLESS SPECIFIC SURFACE, AVSTAR                C
C     C                                                                 C
C     C     6     XI/COOLANT DYNAMIC VISCOSITY ((PA-S)**-1)             C
C     C                                                                 C
C     C     7     G2STAR*RHO (KG/M**3)                                  C
C     C                                                                 C
C     C     8     DIMENSIONLESS CONVECTIVE COEFFICIENT, HSTAR            C
C     C                                                                 C
C     C     9     DIMENSIONLESS VOLUMETRIC GENERATION                   C
C     C            RATE, QSTAR                                          C
C     C                                                                 C
C     C    10     DIMENSIONLESS EFFECTIVE SOLID PHASE                   C
C     C            THERMAL CONDUCTIVITY, KS                             C
C     C                                                                 C
C     C    11     DIMENSIONLESS EFFECTIVE FLUID PHASE                   C
C     C            THERMAL CONDUCTIVITY (RADIAL), KFR                   C
C     C                                                                 C
C     C    12     DIMENSIONLESS EFFECTIVE FLUID PHASE                   C
C     C            THERMAL CONDUCTIVITY (AXIAL), KFZ                    C
C     C                                                                 C
C     C*****************************************************************C
C     C                                                                 C
C     C                                                                 C
C     C          VARIABLES STORED IN THE ARRAY TEMPIN(I,J,K)            C
C     C                                                                 C
C     C     K                CORRESPONDING VARIABLE                     C
C     C    ---    ------------------------------------------            C
C     C                                                                 C
C     C     1     PEBBLE INTERNAL FUELED/UNFUELED                       C
C     C            INTERFACE TEMPERATURE (K)                            C
C     C                                                                 C
C     C     2     FUELED/UNFUELED INTERFACE TEMPERATURE                 C
C     C            GRADIENT (K/CM)                                      C
C     C                                                                 C
C     C     3     MAXIMUM FUEL TEMPERATURE (K)                          C
C     C                                                                 C
C     C*****************************************************************C
C
```

```
      COMMON /REACTR/ HEIGHT, RADIUS, DKUGEL, FMDOT, QTOT, TINLET,
     1 PINLET, GINLET, REYNIN, ARL, ASQ, AFRIC, BFRIC, VFNOM
C
      COMMON /PROP/ PROPTY(25,22,12), PCOND(25), CP, CSTAR, DSUBPC, EDVR
     1 , EDVA, FKC, SIGMA4, TFILMC, BETAK, GAMMAK, HENTC
C
      COMMON /GEOM/ IN, INM, JN, JNM, Z(25), R(22), IINLET(22), IMIN(22)
     1 , IMAX(22), IEXIT(22), PI, VOLS, RVSOP(22), NDEG
C
      COMMON /NUMER/ RP(4), RSDU(4), LOCI(4), LOCJ(4), REDUCE, IOVER
C
      COMMON /EQN/ AE, AW, AN, AS, ASUM, BE(25), BW(25), BN(22), BS(22),
     1 BBE, BBW, BBN, BBS, NSWP1, NSWP2, NSWP3, NSWP4, IUPWND
C
      COMMON /BALL/ TEMPIN(25,22,3), IBALL, R1, R2
C
      COMMON /RESULT/ IOUTP(12), IFILM1, IFILM2, IFILM3, JLOCTP, ID,
     1 INDEX, KOA, NC
C
      CALL SECOND (STIME)
      PRINT 80, STIME
C
C     SPECIFY BED GEOMETRY AND INLET VALUES FOR REACTOR
C     -------------------------------------------------
C     FMDOT = COOLANT MASS FLOW (KG/S)
C     PINLET = INLET PLENUM COOLANT PRESSURE (PA)
C     TINLET = MIXED MEAN INLET PLENUM COOLANT TEMPERATURE (K)
C     RADIUS, HEIGHT = BED DIMENSIONS (M)
C     VFNOM = NOMINAL BED VOID FRACTION
C     KW/BALL INPUT IS ENTERED IN POWER BLOCK-DATA SUBPROGRAM
C     REF:  JUL-1114-RG, 1974, PP. 16,17
C
      FMDOT=785.
      PINLET=40.E05
      TINLET=523.
      RADIUS=4.61
      HEIGHT=5.0
      VFNOM=0.39
C
C     SPECIFY FUEL/MODERATOR ELEMENT (PEBBLE) GEOMETRY
C     ------------------------------------------------
C     IBALL = 1 FOR CONVENTIONAL BALL
C     IBALL = 2 FOR SHELL BALL
C     DKUGEL = PEBBLE DIAMETER (M)
C     R1 = INNER RADIUS OF FUELED/UNFUELED INTERFACE (M)
C          (IGNORED IF IBALL = 1)
C     R2 = OUTER RADIUS OF FUELED/UNFUELED INTERFACE (M)
C     REF:  JUL-1114-RG, 1974, P.17
C
      IBALL=2
      DKUGEL=0.06
      R1=0.015
      R2=0.025
C
```

```
C     SET OPTIONS FOR PROGRAM CONTROL
C     -------------------------------
C     NMAX = MAXIMUM NUMBER OF MAJOR ITERATIONS
C     IN = NUMBER OF AXIAL GRID POINTS
C     JN = NUMBER OF RADIAL GRID POINTS (=VOLS+4.)
C     VOLS = NUMBER OF EQUAL RADIAL VOLUMES FOR VSOP INPUT DATA
C     NDEG = DEGREE OF NEWTONS DIVIDED-DIFFERENCE POLYNOMIAL
C            USED TO INTERPOLATE VSOP THERMAL POWER DATA TO
C            EVENLY SPACED RADIAL GRID POINTS (NDEG.LE.2)
C     NE = NUMBER OF EQUATIONS
C     CC = CONVERGENCE CRITERION
C     NSWP1 THROUGH NSWP4 = NUMBER OF SWEEPS OF MESH FOR EQUATIONS
C                           ONE THROUGH FOUR FOR EACH MAJOR ITERATION
C     IUPWND = FLAG FOR DIFFERENCING OF ADVECTION TERMS
C              1 = UPWIND DIFFERENCES
C              OTHER = CENTRAL DIFFERENCES
C     RP(1) THROUGH RP(4) = RELAXATION PARAMETERS FOR EQUATIONS
C                           ONE THROUGH FOUR
C     REDUCE = REDUCTION FACTOR USED IF SUBSTITUTION OVERRIDE
C              IS NECESSARY FOR TEMPERATURE EQUATIONS
C     IOVER = FLAG TO PRINT SUBSTITUTION OVERRIDE INFORMATION
C             1 = PRINT
C             OTHER = NO PRINT
C     ICTRL = FLAG TO PRINT PROGRAM CONTROL INFORMATION
C     CPTMAX = MAXIMUM CP TIME
C
      NMAX=50
      IN=25
      JN=22
      VOLS=18.
      NDEG=1
      NE=4
      CC=0.005000
      NSWP1=1
      NSWP2=2
      NSWP3=5
      NSWP4=1
      IUPWND=0
      RP(1)=1.
      RP(2)=0.25
      RP(3)=0.0025
      RP(4)=1.0
      REDUCE=0.995
      IOVER=0
      ICTRL=1
      CPTMAX=100.
      IF (ICTRL.NE.1) GO TO 10
      PRINT 90, IN,JN,VOLS,NSWP1,NSWP2,NSWP3
      PRINT 100, NSWP4,CC,RP(1),RP(2),RP(3),RP(4)
   10 CONTINUE
C
```

```
C     SET OPTIONS FOR OUTPUT CONTROL
C     ------------------------------
C     IOUTP = FLAGS TO SELECT VARIABLES FOR PRINTOUT
C       VARIABLE 1 = DIMENSIONLESS STREAM FUNCTION
C                2 = DIMENSIONLESS MASS FLUX, GSTAR
C                3 = RADIAL COMPONENT OF DIMENSIONLESS MASS
C                    FLUX, GRSTAR
C                4 = AXIAL COMPONENT OF DIMENSIONLESS MASS
C                    FLUX, GZSTAR
C                5 = DIMENSIONLESS COOLANT PRESSURE, PSTAR
C                6 = COOLANT BULK TEMPERATURE, TF (K)
C                7 = PEBBLE AVERAGE SURFACE TEMPERATURE, TS (K)
C                8 = MAXIMUM INTERNAL FUELED MATRIX TEMPERATURE (K)
C                9 = PEBBLE INTERNAL SHELL/MATRIX INTERFACE
C                    TEMPERATURE (K)
C               10 = PEBBLE INTERNAL SHELL/MATRIX INTERFACE
C                    TEMPERATURE GRADIENT (K/CM)
C               11 = POWER PER BALL INPUT FROM VSOP (KW/BALL)
C               12 = AUXILIARY OUTPUT (CONTROLLED BY KOA AND INDEX)
C                    INDEX = 1 FOR A(I,J,KOA)
C                    INDEX = OTHER FOR PROPTY(I,J,KOA)
C     IFILM1 = FLAG FOR CREATION OF PLOT FILES FOR TGAS/TSURFACE/TMAX
C              VERSUS AXIAL POSITION AT CENTERLINE, HOT RADIUS AND
C              USER DESIGNATED RADIUS SET BY JLOCTP
C              ALSO PLOT OF TGAS AND MIXED MEAN COOLANT TEMPERATURE
C              AT OUTLET VERSUS RADIUS (TAPE2 THROUGH TAPE5)
C     IFILM2 = FLAG FOR CREATION OF 3-D PLOT FILE FOR THERMAL POWER,
C              TEMPERATURES AND DIMENSIONLESS MASS FLUX VERSUS
C              2-D POSITION (TAPE6 THROUGH TAPE10)
C     IFILM3 = FLAG FOR CREATION OF CONTOUR PLOT FILM FILE FOR
C              POWER, TEMPERATURES, STREAM FUNCTION AND PRESSURE
C              NUMBER OF CONTOURS IS SET BY NC (NC.LE.21)
C     ID = FOUR DIGIT IDENTIFYING CODE FOR CALCULATION
C     INUM = FLAG FOR OUTPUT OF NUMERICAL CONVERGENCE INFORMATION
C
      DATA IOUTP /1,1,1,1,1,1,1,1,1,1,1,0/
C
      IFILM1=1
      IFILM2=1
      IFILM3=1
      NC=16
      JLOCTP=21
      INDEX=2
      KOA=1
      ID=1013
      INUM=1
C
C     SPECIFY CONSTANTS FOR FRICTION PARAMETERS
C     -----------------------------------------
C     AFRIC AND BFRIC = CONSTANTS A AND B IN FORCHHEIMER COEFFICIENTS
C
      AFRIC=24.5
      BFRIC=0.1754
C
      INM=IN-1
      JNM=JN-1
C
C     CREATE FINITE-DIFFERENCE GRID AND INITIALIZE VARIABLES
C
      CALL GRID
      CALL INIT
C
```

```
C     BEGIN ITERATION CYCLE
C
      IF (INUM.NE.1) GO TO 20
      PRINT 110
      PRINT 120
   20 ITER=0
   30 CONTINUE
      ITER=ITER+1
C
C     CALL SOLVER FOR ELLIPTIC PARTIAL DIFFERENTIAL EQUATIONS
C
      CALL PDE
C
      CALL SECOND (TIME)
      RTIME=TIME-STIME
      IF (INUM.NE.1) GO TO 40
      PRINT 130, ITER,RTIME, (L,RSDU(L),LOCI(L),LOCJ(L),L=1,NE)
   40 IF (RTIME.GE.CPTMAX) GO TO 60
      IF (ITER.EQ.NMAX) GO TO 60
C
C     CHECK FOR CONVERGENCE
C
      RES=0.
      DO 50 K=1,NE
   50 IF (ABS(RES).LT.ABS(RSDU(K))) RES=RSDU(K)
      IF (ABS(RES).GT.CC) GO TO 30
      GO TO 70
   60 PRINT 140, ITER
   70 CONTINUE
C
C     COMPUTE PEBBLE INTERNAL TEMPERATURES AND GRADIENTS
C
      CALL TEMPS
C
C     OUTPUT CALCULATIONAL RESULTS
C
      CALL RESULT
C
      STOP
C
   80 FORMAT (//,2X,*STARTING TIME AFTER COMPILATION = *,F6.3)
   90 FORMAT (//,28X,*PROGRAM CONTROL VARIABLES*,/,5X,70(*-*),/,5X,70(*-
     1*),///,9X,*IN*,10X,*JN*,9X,*VOLS*,7X,*NSWP1*,7X,*NSWP2*,7X,*NSWP3*,
     2 /,6X,8(*--*),4X,8(*--*),4X,8(*--*),4X,8(*--*),4X,8(*--*),4X,8(*--*),/,9
     3 X,I2,10X,I2,9X,F3.0,10X,I1,11X,I1,10X,I2)
  100 FORMAT (/,7X,*NSWP4*,9X,*CC*,8X,*RP(1)*,7X,*RP(2)*,7X,*RP(3)*,7X,*
     1RP(4)*,/,6X,8(*--*),4X,8(*--*),4X,8(*--*),4X,8(*--*),4X,8(*--*),4X,8(*--
     2*),/,9X,I1,8X,F7.5,6X,F5.3,7X,F5.3,6X,F6.4,7X,F5.3,/)
  110 FORMAT (///,23X,*NUMERICAL CONVERGENCE INFORMATION*,/,5X,70(*--*),/
     1 ,5X,70(*--*),/)
  120 FORMAT (/,7X,*MAJOR*,6X,*EXECUTION*,3X,*EQUATION*,4X,*MAXIMUM*,5X,
     1 *LOCATION*,4X,*LOCATION*,/,5X,*ITERATION*,5X,*CP TIME*,5X,*NUMBER
     2*,5X,*RESIDUAL*,5X,*I INDEX*,5X,*J INDEX*,/,5X,9(*--*),4X,9(*--*),3X
     3 ,8(*--*),4X,8(*--*),4X,8(*--*),4X,8(*--*),/)
  130 FORMAT (/,8X,I2,7X,F6.3,* SEC*,7X,I1,6X,F10.6,6X,I2,10X,I2,/,3(34X
     1 ,I1,4X,F12.6,6X,I2,10X,I2,/))
  140 FORMAT (//,2X,*DID NOT CONVERGE IN *,I2,* MAJOR ITERATIONS*,/)
      END
```

```
      BLOCK DATA POWER
C
      COMMON /FPOWER/ PBALL(25,22)
C
C     READ KW/BALL DATA FROM VSOP CALCULATION INTO PBALL(I,J)
C     J INDEX RUNS FROM 4 TO VOLS+3
C     KFA CASE 1013 WAS CALCULATED ON 18 EQUAL RADIAL VOLUMES
C     REF:  JUL-1114-RG, 1974, P. 22
C
C     CDC DATA STATEMENTS ALLOW ONLY SINGLE-SUBSCRIPT, DO-LOOP-IMPLYING
C     NOTATION
C     THIS BLOCK DATA SUBPROGRAM IS EQUIVALENT TO
C
C          DO 10 J=4,JNM
C          DO 10 I=1,IN
C          READ PBALL(I,J)
C       10 CONTINUE
C
      DATA (PBALL(L),L=76,100) /4.00,4.10,4.36,4.28,3.95,3.50,3.08,2.66,
     1 2.27,1.91,1.59,1.31,1.08,0.89,0.73,0.60,0.50,0.41,0.34,0.28,0.24,
     2 0.21,0.19,0.19,0.18/
      DATA (PBALL(L),L=101,125) /3.97,4.06,4.33,4.25,3.93,3.48,3.06,2.65
     1 ,2.26,1.90,1.58,1.31,1.08,0.89,0.73,0.60,0.50,0.41,0.34,0.28,0.24
     2 ,0.21,0.19,0.19,0.18/
      DATA (PBALL(L),L=126,150) /3.93,4.03,4.30,4.22,3.91,3.47,3.05,2.64
     1 ,2.25,1.89,1.58,1.31,1.08,0.89,0.73,0.60,0.50,0.41,0.34,0.28,0.24
     2 ,0.21,0.19,0.19,0.18/
      DATA (PBALL(L),L=151,175) /3.89,3.99,4.28,4.21,3.90,3.47,3.05,2.64
     1 ,2.26,1.90,1.59,1.31,1.08,0.89,0.74,0.61,0.50,0.41,0.34,0.29,0.24
     2 ,0.21,0.19,0.19,0.18/
      DATA (PBALL(L),L=176,200) /3.85,3.96,4.24,4.18,3.87,3.44,3.04,2.63
     1 ,2.25,1.89,1.58,1.31,1.08,0.89,0.73,0.60,0.50,0.41,0.34,0.29,0.24
     2 ,0.21,0.19,0.19,0.18/
      DATA (PBALL(L),L=201,225) /3.80,3.91,4.20,4.14,3.84,3.42,3.01,2.61
     1 ,2.23,1.88,1.57,1.30,1.08,0.89,0.73,0.60,0.50,0.41,0.34,0.28,0.24
     2 ,0.21,0.19.0.19,0.18/
      DATA (PBALL(L),L=226,250) /3.74,3.87,4.16,4.12,3.84,3.42,3.03,2.63
     1 ,2.26,1.91,1.60,1.32,1.10,0.90,0.74,0.61,0.51,0.42,0.35,0.29,0.24
     2 ,0.21,0.19,0.19,0.18/
      DATA (PBALL(L),L=251,275) /3.69,3.81,4.11,4.07,3.79,3.38,2.99,2.60
     1 ,2.23,1.88,1.58,1.31,1.08,0.89,0.74,0.61,0.50,0.41,0.34,0.29,0.24
     2 ,0.21,0.19,0.19,0.18/
      DATA (PBALL(L),L=276,300) /3.63,3.75,4.05,4.00,3.73,3.32,2.94,2.55
     1 ,2.18,1.85,1.54,1.28,1.06,0.87,0.72,0.59,0.49,0:40,0.34,0.28,0.23
     2 ,0.20,0.18,0.18,0.17/
      DATA (PBALL(L),L=301,325) /3.55,3.72,4.07,4.06,3.81,3.43,3.05,2.66
     1 ,2.28,1.94,1.63,1.35,1.12,0.93,0.76,0.63,0.52,0.43,0.36,0.30,0.25
     2 ,0.21,0.20,0.20,0.19/
      DATA (PBALL(L),L=326,350) /3.45,3.60,3.93,3.92,3.67,3.29,2.92,2.54
     1 ,2.19,1.85,1.55,1.29,1.07,0.88,0.73,0.60,0.50,0.41,0.34,0.28,0.24
     2 ,0.20,0.19,0.19,0.18/
      DATA (PBALL(L),L=351,375) /3.28,3.40,3.68,3.65,3.41,3.05,2.71,2.35
     1 ,2.02,1.71,1.43,1.19,0.99,0.82,0.67,0.56,0.46,0.38,0.31,0.26,0.22
     2 ,0.19,0.17,0.17,0.17/
      DATA (PBALL(L),L=376,400) /4.26,4.48,4.74,4.73,4.49,4.05,3.50,3.03
     1 ,2.59,2.19,1.85,1.57,1.31,1.07,0.88,0.73,0.60,0.49,0.41,0.34,0.29
     2 ,0.24,0.22,0.23,0.23/
      DATA (PBALL(L),L=401,425) /4.08,4.25,4.44,4.41,4.18,3.77,3.26,2.82
     1 ,2.41,2.04,1.72,1.46,1.22,1.00,0.82,0.68,0.56,0.46,0.38,0.32,0.27
     2 ,0.23,0.21,0.21,0.22/
      DATA (PBALL(L),L=426,450) /4.01,4.15,4.31,4.27,4.06,3.67,3.18,2.76
     1 ,2.36,2.00,1.69,1.44,1.20,0.98,0.81,0.67,0.55,0.45,0.38,0.31,0.26
     2 ,0.22,0.20,0.20,0.21/
      DATA (PBALL(L),L=451,475) /4.01,3.97,3.92,3.76,3.40,2.96,2.56,2.17
     1 ,1.85,1.56,1.28,1.05,0.87,0.71,0.58,0.48,0.39,0.32,0.27,0.22,0.19
     2 ,0.16,0.14,0.14,0.15/
      DATA (PBALL(L),L=476,500) /4.20,4.18,4.15,4.00,3.63,3.17,2.75,2.34
     1 ,2.00,1.69,1.39,1.14,0.94,0.77,0.63,0.52,0.43,0.35,0.29,0.24,0.20
     2 ,0.17,0.15,0.14,0.14/
      DATA (PBALL(L),L=501,525) /4.68,4.80,4.85,4.70,4.27,3.72,3.24,2.75
     1 ,2.35,1.98,1.63,1.34,1.10,0.90,0.74,0.61,0.50,0.41,0.34,0.28,0.23
     2 ,0.20,0.17,0.15,0.15/
C
      END
```

```
      SUBROUTINE GRID
C
C     C*********************************************************************C
C     C                                                                     C
C     C  COMPUTES GRID POINTS, GEOMETRY FACTORS, AND B-PRIME FACTORS        C
C     C        REQUIRED FOR THE SUCCESSIVE SUBSTITUTION FORMULA             C
C     C                GRID SPACING NEED NOT BE UNIFORM                     C
C     C                                                                     C
C     C*********************************************************************C
C
      COMMON /REACTR/ HEIGHT, RADIUS, DKUGEL, FMDOT, QTOT, TINLET,
     1 PINLET, GINLET, REYNIN, ARL, ASQ, AFRIC, BFRIC, VFNOM
C
      COMMON /GEOM/ IN, INM, JN, JNM, Z(25), R(22), IINLET(22), IMIN(22)
     1 , IMAX(22), IEXIT(22), PI, VOLS, RVSOP(22), NDEG
C
      COMMON /DERIV/ H1(25), H1D(25), H2(22), H2D(22)
C
      COMMON /EQN/ AE, AW, AN, AS, ASUM, BE(25), BW(25), BN(22), BS(22),
     1 BBE, BBW, BBN, BBS, NSWP1, NSWP2, NSWP3, NSWP4, IUPWND
C
      COMMON /BDY/ DELZIN(22), DELZO(22), SFRACI(22), AXIS, AXISM
C
C     SET NON-RECTANGULAR BOUNDARIES AS NEEDED
C
      DATA IINLET /22(1)/
      DATA IMIN /22(2)/
      DATA IMAX /22(24)/
      DATA IEXIT /22(25)/
      ARL=RADIUS/HEIGHT
C
C     COMPUTE THE AXIAL COORDINATES
C     FOR THIS PROBLEM THE AXIAL GRID SPACING IS UNIFORM
C
      ZSTEP=1./FLOAT(INM)
      DO 10 I=1,IN
   10 Z(I)=FLOAT(I-1)*ZSTEP
C
C     COMPUTE THE RADIAL COORDINATES
C     RADIAL GRID POINTS FOR POWER INPUT LIE AT THE VOLUMETRIC
C     CENTER OF VOLS EQUAL RADIAL VOLUMES (FOR VSOP INPUT), PLUS
C     THREE EXTRA GRID POINTS NEAR THE AXIS OF SYMMETRY AND A GRID
C     POINT ON THE RADIAL REFLECTOR
C
      XAREA=RADIUS*RADIUS/VOLS
      NVOLS=VOLS
      JV=NVOLS+3
      EVOL1=0.
      EVOL2=XAREA+EVOL1
      STEP1=SQRT(0.5*EVOL2)/RADIUS
      DELRA=STEP1/3.
      RVSOP(1)=0.
      RVSOP(2)=RVSOP(1)+DELRA
      RVSOP(3)=RVSOP(2)+DELRA
      RVSOP(4)=STEP1
      DO 20 J=5,JV
      EVOL1=EVOL2
      EVOL2=XAREA+EVOL1
   20 RVSOP(J)=SQRT(0.5*(EVOL2+EVOL1))/RADIUS
      RVSOP(JV+1)=1.0
C
C     COMPUTE THE EQUALLY SPACED RADIAL GRID POINTS
C
      R(1)=0.
      DELR=1./FLOAT(JNM)
      DO 30 J=2,JN
   30 R(J)=R(J-1)+DELR
C
```

```
C     COMPUTE THE FACTORS NEEDED FOR THE SPATIAL DERIVITIVES
C
      DO 40 I=2,INM
      H1(I)=(Z(I)-Z(I-1))/(Z(I+1)-Z(I))
   40 H1D(I)=1./(Z(I+1)-Z(I-1))
      DO 50 J=2,JNM
      H2(J)=(R(J)-R(J-1))/(R(J+1)-R(J))
   50 H2D(J)=1./(R(J+1)-R(J-1))
      DO 60 J=1,JN
      I1=IINLET(J)
      I2=IMIN(J)
      I3=IMAX(J)
      I4=IEXIT(J)
      DELZIN(J)=Z(I2)-Z(I1)
   60 DELZO(J)=Z(I4)-Z(I3)
      AXIS=1./(1.-((R(2)-R(1))/(R(3)-R(1)))**2)
      AXISM=AXIS-1.
C
C     COMPUTE THE B-PRIME FACTORS
C
      ASQ=ARL*ARL
      DO 70 I=2,INM
      BW(I)=H1D(I)/(Z(I)-Z(I-1))
   70 BE(I)=H1D(I)/(Z(I+1)-Z(I))
      DO 80 J=2,JNM
      DR=0.5*H2D(J)
      BS(J)=(1.+R(J-1)/R(J))/(R(J)-R(J-1))*DR/ASQ
   80 BN(J)=(1.+R(J+1)/R(J))/(R(J+1)-R(J))*DR/ASQ
C
      RETURN
      END
```

```
      SUBROUTINE INIT
C
C     C*********************************************************************C
C     C                                                                     C
C     C              INITIALIZES ALL DEPENDENT VARIABLES                    C
C     C           ALSO SETS FIXED-VALUE BOUNDARY CONDITIONS                 C
C     C            AND PERFORMS ONE-TIME-ONLY CALCULATIONS                  C
C     C                                                                     C
C     C*********************************************************************C
C
      COMMON /REACTR/ HEIGHT, RADIUS, DKUGEL, FMDOT, QTOT, TINLET,
     1 PINLET, GINLET, REYNIN, ARL, ASQ, AFRIC, BFRIC, VFNOM
C
      COMMON /FPOWER/ PBALL(25,22)
C
      COMMON /GAS/ AZERO, RGAS, WMOL, BBC1, BBC2, BBC3, BBC4, BBC5, BBC6
C
      COMMON /PROP/ PROPTY(25,22,12), PCOND(25), CP, CSTAR, DSUBPC, EOVR
     1 , EOVA, FKC, SIGMA4, TFILMC, BETAK, GAMMAK, HENTC
C
      COMMON /GEOM/ IN, INM, JN, JNM, Z(25), R(22), IINLET(22), IMIN(22)
     1 , IMAX(22), IEXIT(22), PI, VOLS, RVSOP(22), NDEG
C
      COMMON /BDY/ DELZIN(22), DELZO(22), SFRACI(22), AXIS, AXISM
C
      COMMON /ANSWER/ A(25,22,10)
C
      PI=3.1415927
      SIGMA4=4.*5.6697E-08
C
C     ASSIGN COEFFICIENTS FOR SOLID PHASE EFFECTIVE THERMAL
C     CONDUCTIVITY MODEL
C     (SEE SUBROUTINE SOLIDK FOR REFERENCE)
C
      BETAK=0.95
      GAMMAK=2./3.
C
C     ASSIGN CONVECTIVE COEFFICIENT ENTRANCE REGION CORRECTION FACTOR
C     (THIS NUMBER IS NOT WELL KNOWN)
C
      HENTC=1.0
C
C     SPECIFY CONSTANTS FOR REACTOR COOLANT
C     AGAS, AZERO, B, BZERO, C = BEATTIE-BRIDGEMAN COEFFICIENTS
C                                (P ATM, V LITERS, T KELVIN)
C     RGAS = UNIVERSAL GAS CONSTANT (LITER-ATM/GMOLE-K)
C     CP = SPECIFIC HEAT AT CONSTANT PRESSURE (J/KG-K)
C     WMOL = MOLECULAR WEIGHT OF COOLANT GAS (G/GMOLE)
C     HELIUM REFS:  M.P. WILSON, JR., GA-1355, 1960
C                   H. PETERSEN, DANISH AEC REPT., RISO-224, 1970
C                   D.P. SHOEMAKER AND C.W. GARLAND, EXPERIMENTS IN
C                   PHYSICAL CHEMISTRY, MCGRAW-HILL, NY, 1962, P. 57
C
      DATA AGAS, AZERO, B, BZERO, C, RGAS /0.05984,0.0216,0.0,0.01400,0.
     1 004E04,0.08206/
      CP=5195.
      WMOL=4.00260
C
C     COMPUTE CONSTANTS FOR STATE SUBROUTINE
C
      BBC1=RGAS*BZERO
      BBC2=RGAS*C
      BBC3=-BBC1*B
      BBC4=AZERO*AGAS
      BBC5=BBC1*C
      BBC6=BBC5*B
C
```

```
C     CALL SUBROUTINE TO CALCULATE INLET COOLANT DENSITY
C
      PINATM=PINLET/1.013E05
      CALL STATE (PINATM,TINLET,RHOIN)
C
C     COMPUTE INLET PLENUM VALUES FOR SELECTED VARIABLES
C     SEE SUBROUTINE PROPS FOR REFERENCES
C
      FMUIN=3.674E-07*TINLET**0.7
      TEMP=TINLET**(0.71*(1.-2.E-09*PINLET))
      FKIN=2.662E-03*(1.-1.123E-08*PINLET)*TEMP
      FKC=1./FKIN
C
      COEFF1=6.*AFRIC/(BFRIC*DKUGEL)
      COEFF2=6.*BFRIC/DKUGEL
      HTODK=HEIGHT/DKUGEL
      TFILMC=TINLET*0.5
C
      GINLET=FMDOT/(RADIUS*RADIUS*PI)
      REYNIN=GINLET*DKUGEL/FMUIN
      VCG=(1.-VFNOM)/VFNOM**3
      G1IN=36.*AFRIC*FMUIN*(1.-VFNOM)*VCG/(RHOIN*DKUGEL*DKUGEL)
      G2IN=COEFF2*VCG/RHOIN
      CSTAR=CP*GINLET*HEIGHT*FKC
C
C     ASSUME PLUG FLOW FOR STREAM FUNCTION INITIAL GUESS
C
      DO 10 J=2,JNM
      IL=IINLET(J)
      IH=IEXIT(J)
      DO 10 I=IL,IH
   10 A(I,J,1)=R(J)*R(J)*0.5
C
C     THE INLET COOLANT PRESSURE IS SPECIFIED
C     INITIAL GUESS FOR PRESSURE CORRESPONDS TO A ONE-DIMENSIONAL
C     UNIFORM PRESSURE DROP, ASSUMING THE OVERALL CORE DELTA P IS
C     190 PERCENT OF THAT CALCULATED USING INLET CONDITIONS
C
      PERCNT=1.90
      CDELP=PERCNT*GINLET*(G1IN+G2IN*GINLET)*HEIGHT
      DO 20 J=1,JN
      IL=IMIN(J)
      IH=IEXIT(J)
      DO 20 I=IL,IH
   20 A(I,J,4)=(PINLET-CDELP*Z(I))/PINLET
      DSUBPC=GINLET*GINLET*G2IN*HEIGHT/PINLET
C
C     ASSIGN APPROXIMATE DISTRIBUTION OF PEBBLE THERMAL CONDUCTIVITY
C     CONSISTENT WITH THE AXIAL GRID SPACING
C     PEBBLE THERMAL CONDUCTIVITY IS A FUNCTION OF FAST NEUTRON
C     FLUENCE AND TEMPERATURE
C     THE THERMAL CONDUCTIVITY OF THE FUELED MATRIX AND UNFUELED
C     SHELL ARE ASSUMED EQUAL
C     THIS DISTRIBUTION CORRESPONDS TO AN IDEALIZED OTTO FUEL CYCLE
C     REF:  JUL-1114-RG, 1974, FIG. 25, P. 63
C
      DO 30 I=1,IN
   30 PCOND(I)=17.+20.5*EXP(-15.37*Z(I))
C
C     ASSIGN CONSTANT VALUES OF RADIAL AND AXIAL TURBULENT
C     PECLET NUMBERS
C     COMPUTE RATIO OF TURBULENT THERMAL DIFFUSIVITY DIVIDED BY
C     AXIAL VELOCITY
C     REFS:  B. FINLAYSON, CHEM. ENG. SCI., 26, 1971, P. 1081
C            H. DEANS AND L. LAPIDUS, AICHE J., 6, 1960, P. 656
C
      PECLTR=10.
      EDVR=DKUGEL/PECLTR
      PECLTA=2.
      EDVA=DKUGEL/PECLTA
C
```

```
C     SET THE BED VOID FRACTION DISTRIBUTION
C     FOR KFA DESIGNS THE ENTIRE BED CAN BE ASSIGNED THE NOMINAL
C     VALUE OF 0.39
C
      DO 40 J=1,JN
      IL=IINLET(J)
      IH=IEXIT(J)
      DO 40 I=IL,IH
   40 PROPTY(I,J,4)=VFNOM
C
C     CALCULATE THE NON-DIMENSIONAL SPECIFIC SURFACE
C
      CAV=6.*HTODK
      DO 50 J=1,JN
      IL=IINLET(J)
      IH=IEXIT(J)
      DO 50 I=IL,IH
   50 PROPTY(I,J,5)=(1.-PROPTY(I,J,4))*CAV
C
C     ASSIGN KW/BALL DATA TO EXTRA GRID POINTS NOT USED BY VSOP
C
      DO 60 J=1,3
      IL=IINLET(J)
      IH=IEXIT(J)
      DO 60 I=IL,IH
   60 PBALL(I,J)=PBALL(I,4)
      IL=IINLET(JN)
      IH=IEXIT(JN)
      DO 70 I=IL,IH
   70 PBALL(I,JN)=PBALL(I,JNM)
C
C     CALCULATE TOTAL POWER IN WATTS FROM VSOP INPUT
C
      QTOT=0.
      VBALL=PI*DKUGEL*DKUGEL*DKUGEL/6.
      DO 80 J=4,JNM
      IL=IMIN(J)
      IH=IMAX(J)
      DO 80 I=IL,IH
      Q=PBALL(I,J)*(1.-PROPTY(I,J,4))/VBALL
   80 QTOT=QTOT+Q
      DO 90 J=4,JNM
      I=IINLET(J)
      Q=0.5*PBALL(I,J)*(1.-PROPTY(I,J,4))/VBALL
      QTOT=QTOT+Q
      I=IEXIT(J)
      Q=0.5*PBALL(I,J)*(1.-PROPTY(I,J,4))/VBALL
   90 QTOT=QTOT+Q
      PVOL=VOLS*FLOAT(INM)
      QTOT=QTOT*1.E03*HEIGHT*RADIUS*RADIUS*PI/PVOL
C
C     CALL ROUTINE TO INTERPOLATE VSOP THERMAL POWER PROFILE
C     TO EVENLY SPACED RADIAL GRID POINTS
C
      CALL INTERP
C
C     SET STREAM FUNCTION RADIAL BOUNDARY CONDITIONS
C
      IL=IINLET(1)
      IH=IEXIT(1)
      DO 100 I=IL,IH
  100 A(I,1,1)=0.0
      IL=IINLET(JN)
      IH=IEXIT(JN)
      DO 110 I=IL,IH
  110 A(I,JN,1)=0.5
C
C     SET BOUNDARY CONDITION ON PRESSURE AT INLET
C
      DO 120 J=1,JN
      I=IINLET(J)
  120 A(I,J,4)=1.
C
```

```
C     INITIALIZE MASS-FLUX DISTRIBUTION
C
      DO 130 J=2,JN
      IL=IINLET(J)
      IH=IEXIT(J)
      DO 130 I=IL,IH
      CALL MFLUX (I,J)
  130 CONTINUE
      IL=IINLET(1)
      IH=IEXIT(1)
      DO 140 I=IL,IH
      CALL MFLUX (I,1)
  140 CONTINUE
C
C     CALCULATE CONSTANT FACTORS DEPENDENT ON INLET CONDITIONS,
C     GEOMETRY AND VOID FRACTION DISTRIBUTION
C
      DO 150 J=1,JN
      SFRACI(J)=1.-PROPTY(1,J,4)
      IL=IINLET(J)
      IH=IEXIT(J)
      DO 150 I=IL,IH
      SFRAC=1.-PROPTY(I,J,4)
      RATIO=SFRAC/PROPTY(I,J,4)**3
      PROPTY(I,J,6)=SFRAC*COEFF1/GINLET
  150 PROPTY(I,J,7)=COEFF2*RATIO/G2IN
C
C     CONVERT KW/BALL DATA TO W/BALL AND DIMENSIONLESS VOLUMETRIC
C     GENERATION RATE, QSTAR
C     CALCULATE INITIAL GUESS FOR COOLANT BULK TEMPERATURE
C     BASED ON ENTHALPY RISE
C     TEMPORARILY SET TSURFACE=TGAS
C
      DELTZ=HEIGHT/FLOAT(INM)
      GCPI=1./(GINLET*CP)
      P1=HEIGHT*HEIGHT*FKC
      DO 160 J=1,JN
      TFM=1.
      IL=IINLET(J)
      IH=IEXIT(J)
      DO 160 I=IL,IH
      PBALL(I,J)=1.E03*PBALL(I,J)
      QT=PBALL(I,J)*(1.-PROPTY(I,J,4))/(VBALL*TINLET)
      VOLCOR=1.0
      IF ((I.EQ.IL).OR.(I.EQ.IH)) VOLCOR=0.5
      A(I,J,2)=QT*VOLCOR*DELTZ*GCPI*TFM
      TFM=A(I,J,2)
      A(I,J,3)=A(I,J,2)
  160 PROPTY(I,J,9)=QT*P1
C
C     INITIALIZE BED AND COOLANT PROPERTIES (INCLUDING THE CONVECTIVE
C     HEAT TRANSFER COEFFICIENT FOR THE NEXT STEP)
C
      CALL PROPS
C
C     CALCULATE INITIAL GUESS FOR AVERAGE PEBBLE SURFACE TEMPERATURE
C     ASSUME 100 PERCENT OF THE HEAT TRANSFER IS BY CONVECTION
C
      PERCNT=1.0
      DO 170 J=1,JNM
      IL=IINLET(J)
      IH=IEXIT(J)
      DO 170 I=IL,IH
      TDROP=PROPTY(I,J,9)/(PROPTY(I,J,8)*PROPTY(I,J,5))
  170 A(I,J,3)=PERCNT*TDROP+A(I,J,2)
      IL=IINLET(JN)
      IH=IEXIT(JN)
      DO 180 I=IL,IH
  180 A(I,JN,3)=A(I,JNM,3)
C
      RETURN
      END
```

```
      SUBROUTINE STATE (P,T,RHO)
C
C     C*****************************************************************C
C     C                                                                 C
C     C          SOLVES THE BEATTIE-BRIDGEMAN EQUATION OF STATE         C
C     C                       USING NEWTONS METHOD                      C
C     C                                                                 C
C     C        REF: APPLIED NUMERICAL METHODS,                          C
C     C             B. CARNAHAN, H.A. LUTHER AND J.O. WILKES,           C
C     C             JOHN WILEY AND SONS, NY, 1964, P. 173               C
C     C                                                                 C
C     C*****************************************************************C
C
      COMMON /GAS/ AZERO, RGAS, WMOL, BBC1, BBC2, BBC3, BBC4, BBC5, BBC6
C
      TSQ=T*T
      BETA=BBC1*T-AZERO-BBC2/TSQ
      GAMMA=BBC3*T+BBC4-BBC5/TSQ
      DELTA=BBC6/TSQ
C
C     USE IDEAL GAS LAW FOR FIRST GUESS
C
      V=RGAS*T/P
C
C     BEGIN NEWTONS METHOD ITERATION ON V
C
      DO 10 I=1,20
      DELTAV=(((((-P*V+RGAS*T)*V+BETA)*V+GAMMA)*V+DELTA)*V)/(((RGAS*T*V+
     1 2.*BETA)*V+3.*GAMMA)*V+4.*DELTA)
      V=V+DELTAV
      IF (ABS(DELTAV/V).GT.1.E-06) GO TO 10
      GO TO 20
   10 CONTINUE
C
C     RECOVER DENSITY FROM MOLAR VOLUME
C
   20 RHO=WMOL/V
C
      RETURN
      END
```

```
      SUBROUTINE INTERP
C
C     C*****************************************************************C
C     C                                                                 C
C     C    INTERPOLATES POWER PER BALL DATA FROM VSOP EQUAL-VOLUME      C
C     C    RADIAL GRID POINTS TO EQUALLY SPACED RADIAL GRID POINTS      C
C     C   USING NEWTONS DIVIDED-DIFFERENCE INTERPOLATING POLYNOMIAL     C
C     C                                                                 C
C     C         REF: APPLIED NUMERICAL METHODS,                         C
C     C              B. CARNAHAN, H.A. LUTHER AND J.O.WILKES,           C
C     C              JOHN WILEY AND SONS, NY, 1964, PP. 17-26           C
C     C                                                                 C
C     C*****************************************************************C
C
      COMMON /FPOWER/ PBALL(25,22)
C
      COMMON /GEOM/ IN, INM, JN, JNM, Z(25), R(22), IINLET(22), IMIN(22)
     1 , IMAX(22), IEXIT(22), PI, VOLS, RVSOP(22), NDEG
C
      DIMENSION P(22), TABLE(22,22)
C
      M=2
      DO 30 I=1,IN
      DO 10 J=1,JN
   10 P(J)=PBALL(I,J)
      CALL DTABLE (RVSOP,P,TABLE,JN,M,TRUBL,22)
      IF (TRUBL.EQ.0.) GO TO 20
      PRINT 40
      RETURN
   20 DO 30 J=1,JN
      RARG=R(J)
   30 PBALL(I,J)=FNEWT(RVSOP,P,TABLE,JN,M,NDEG,RARG,TRUBL,22)
      RETURN
C
   40 FORMAT (/,5X,*ARGUMENT ERROR IN INTERP CALL TO DTABLE OR FNEWT*)
      END
```

```
      SUBROUTINE DTABLE (X,Y,TABLE,N,M,TRUBL,K)
C
C     C*****************************************************************C
C     C                                                                 C
C     C            SUBROUTINE REQUIRED BY SUBROUTINE INTERP             C
C     C                                                                 C
C     C*****************************************************************C
C
      DIMENSION X(N), Y(N), TABLE(K,K)
C
      IF (M.LT.N) GO TO 10
      TRUBL=1.0
      RETURN
   10 NM1=N-1
      DO 20 I=1,NM1
   20 TABLE(I,1)=(Y(I+1)-Y(I))/(X(I+1)-X(I))
      IF (M.LE.1) GO TO 40
      DO 30 J=2,M
      DO 30 I=J,NM1
      ISUB=I+1-J
   30 TABLE(I,J)=(TABLE(I,J-1)-TABLE(I-1,J-1))/(X(I+1)-X(ISUB))
   40 TRUBL=0.
      RETURN
      END
      FUNCTION FNEWT (X,Y,TABLE,N,M,NDEG,XARG,TRUBL,K)
C
C     C*****************************************************************C
C     C                                                                 C
C     C              FUNCTION REQUIRED BY SUBROUTINE INTERP             C
C     C                                                                 C
C     C*****************************************************************C
C
      DIMENSION X(N), Y(N), TABLE(K,K)
C
      IF (NDEG.LE.M) GO TO 10
      TRUBL=1.0
      FNEWT=0.
      RETURN
   10 DO 20 I=1,N
      IF (I.EQ.N.OR.XARG.LE.X(I)) GO TO 30
   20 CONTINUE
   30 MAX=I+NDEG/2
      IF (MAX.LE.NDEG) MAX=NDEG+1
      IF (MAX.GT.N) MAX=N
      YEST=TABLE(MAX-1,NDEG)
      IF (NDEG.LE.1) GO TO 50
      NDEGM1=NDEG-1
      DO 40 I=1,NDEGM1
      ISUB1=MAX-1
      ISUB2=NDEG-1
   40 YEST=YEST*(XARG-X(ISUB1))+TABLE(ISUB1-1,ISUB2)
   50 ISUB1=MAX-NDEG
      TRUBL=0.
      FNEWT=YEST*(XARG-X(ISUB1))+Y(ISUB1)
      RETURN
      END
```

```
      SUBROUTINE PROPS
C
C     C*****************************************************************C
C     C                                                                 C
C     C   COMPUTES PROPERTIES OF COOLANT AND RANDOM PACKED SPHERE BED   C
C     C                                                                 C
C     C*****************************************************************C
C
      COMMON /REACTR/ HEIGHT, RADIUS, DKUGEL, FMDOT, QTOT, TINLET,
     1 PINLET, GINLET, REYNIN, ARL, ASQ, AFRIC, BFRIC, VFNOM
C
      COMMON /PROP/ PROPTY(25,22,12), PCOND(25), CP, CSTAR, DSUBPC, EDVR
     1 , EDVA, FKC, SIGMA4, TFILMC, BETAK, GAMMAK, HENTC
C
      COMMON /GEOM/ IN, INM, JN, JNM, Z(25), R(22), IINLET(22), IMIN(22)
     1 , IMAX(22), IEXIT(22), PI, VOLS, RVSOP(22), NDEG
C
      COMMON /ANSWER/ A(25,22,10)
C
C     PARTS OF THIS ROUTINE ARE ONLY VALID FOR HELIUM COOLANT
C     CORRELATIONS USED IN THIS ROUTINE ARE FOR HIGH REYNOLDS
C     NUMBER FLOWS
C
      DO 20 J=1,JN
      IL=IINLET(J)
      IH=IEXIT(J)
      DO 20 I=IL,IH
C
C     AVOID PROPERTY UPDATE FOR UNREASONABLE VALUES OF THE
C     DEPENDENT VARIABLES
C
      IF (A(I,J,4).GT.0.95) GO TO 10
      PRINT 30, A(I,J,4),I,J
      GO TO 20
   10 IF ((A(I,J,2).LT.1.).OR.(A(I,J,3).LT.1.)) GO TO 20
      P=A(I,J,4)*PINLET
      PATM=P/1.013E05
      TFILM=(A(I,J,2)+A(I,J,3))*TFILMC
      TBULK=A(I,J,2)*TINLET
      TS=A(I,J,3)*TINLET
C
C     SOLVE BEATTIE-BRIDGEMAN EQUATION OF STATE FOR DENSITY
C
      CALL STATE (PATM,TFILM,PROPTY(I,J,1))
C
C     COMPUTE COOLANT (HELIUM) DYNAMIC VISCOSITY AND MOLECULAR
C     THERMAL CONDUCTIVITY
C     REF:  H. PETERSEN, DANISH AEC REPT. RISO-224, 1970
C
      FMU=3.674E-07*TFILM**0.7
      TEMP=TFILM**(0.71-1.426E-09*P)
      FK=2.682E-03*(1.+1.123E-08*P)*TEMP
C
C     COMPUTE EFFECTIVE THERMAL CONDUCTIVITY OF THE SOLID PHASE
C
      CALL SOLIDK (I,J,TS,FK,SKE)
      PROPTY(I,J,10)=SKE*FKC
C
C     COMPUTE FRICTION PARAMETERS
C
      PROPTY(I,J,2)=PROPTY(I,J,6)*FMU
      PROPTY(I,J,3)=PROPTY(I,J,7)/PROPTY(I,J,1)
C
```

```
C     COMPUTE EFFECTIVE THERMAL CONDUCTIVITY OF THE FLUID PHASE
C     REFS:  E. SINGER AND R. WILHELM, CHEM. ENG. PROG., 46,
C            1950, P. 343
C            B. FINLAYSON, CHEM. ENG. SCI., 26, 1971, P. 1081
C
      VOIDKF=PROPTY(I,J,4)*FK
      RHOCP=PROPTY(I,J,1)*CP
      VCON=GINLET/PROPTY(I,J,1)
      AVEL=A(I,J,9)*VCON
      ETURBR=EOVR*AVEL
      ETURBA=EOVA*AVEL
      PROPTY(I,J,11)=(VOIDKF+RHOCP*ETURBR)*FKC
      PROPTY(I,J,12)=(VOIDKF+RHOCP*ETURBA)*FKC
C
C     COMPUTE THE CONVECTIVE HEAT TRANSFER COEFFICIENT
C     REF:  H. BARTHELS, BRENNSTOFF-WARME-KRAFT, 24, 1972
C
      REYN=A(I,J,5)*GINLET*DKUGEL/FMU
      REYNM=REYN/PROPTY(I,J,4)
      COEFF=(1.-PROPTY(I,J,4))/PROPTY(I,J,4)
      H=(2.0+(COEFF*REYNM)**0.5+0.005*REYNM)*FK/DKUGEL
      IF (I.EQ.1) H=HENTC*H
   20 PROPTY(I,J,8)=H*HEIGHT*FKC
      RETURN
C
   30 FORMAT (/,2X,*UNREASONABLE PRESSURE CALCULATED, A(I,J,4) = *,F6.4,
     1 5X,*I = *,I2,5X,*J = *,I2)
      END
```

```
      SUBROUTINE SOLIDK (I,J,TS,FK,SKE)
C
C     C*****************************************************************C
C     C                                                                 C
C     C           CALCULATES EFFECTIVE THERMAL CONDUCTIVITY             C
C     C                      OF THE SOLID PHASE                         C
C     C                                                                 C
C     C     REF: D. KUNNI AND J.M. SMITH, AICHE J., 6, 1960, P. 71      C
C     C                                                                 C
C     C*****************************************************************C
C
      COMMON /REACTR/ HEIGHT, RADIUS, DKUGEL, FMDOT, QTOT, TINLET,
     1 PINLET, GINLET, REYNIN, ARL, ASQ, AFRIC, BFRIC, VFNOM
C
      COMMON /PROP/ PROPTY(25,22,12), PCOND(25), CP, CSTAR, DSUBPC, EOVR
     1 , EOVA, FKC, SIGMA4, TFILMC, BETAK, GAMMAK, HENTC
C
C     COMPUTE PEBBLE THERMAL EMISSIVITY
C     ASSUMES GRAPHITE EMISSIVITY CHANGE IS LINEAR WITH TEMPERATURE
C     REF:  WELTY, J.R., ENGINEERING HEAT TRANSFER
C           JOHN WILEY AND SONS, N.Y., 1974
C
      EMISS=0.41+1.176E-04*(TS-311.)
C
      TCUBE=TS*TS*TS
      RATIO=DKUGEL/FK
      PART1=SIGMA4*TCUBE
      PART2=PROPTY(I,J,4)/(2.*(1.-PROPTY(I,J,4)))
      HRV=PART1/(1.+PART2*((1.-EMISS)/EMISS))
      HRS=PART1*EMISS/(2.-EMISS)
      RATIOK=FK/PCOND(I)
C
C     USE CURVE FIT OF PHI1 AND PHI2 DATA
C
      PHI1=0.2770*RATIOK**0.2426
      PHI2=0.1293*RATIOK**0.3292
      PHI=PHI2+(PHI1-PHI2)*(PROPTY(I,J,4)-0.26)/0.216
      IF (PROPTY(I,J,4).LE.0.26) PHI=PHI2
      IF (PROPTY(I,J,4).GE.0.476) PHI=PHI1
C
      PARTK1=PROPTY(I,J,4)*(1.+BETAK*HRV*RATIO)
      PARTK2=1./PHI+RATIO*HRS
      PARTK3=BETAK*(1.-PROPTY(I,J,4))/(1./PARTK2+GAMMAK*RATIOK)
      SKE=FK*(PARTK1+PARTK3)
      RETURN
      END
```

```
      SUBROUTINE MFLUX (I,J)
C
C     C*****************************************************************C
C     C                                                                 C
C     C       COMPUTES STREAM FUNCTION DERIVITIVES AND RECOVERS         C
C     C            THE MASS FLUX, GSTAR, AND ITS COMPONENTS             C
C     C  ALSO APPLIES THE NO-SLIP CONDITION AT IMPERVIOUS BOUNDARIES    C
C     C                                                                 C
C     C*****************************************************************C
C
      COMMON /REACTR/ HEIGHT, RADIUS, DKUGEL, FMDOT, QTOT, TINLET,
     1 PINLET, GINLET, REYNIN, ARL, ASQ, AFRIC, BFRIC, VFNOM
C
      COMMON /GEOM/ IN, INM, JN, JNM, Z(25), R(22), IINLET(22), IMIN(22)
     1 , IMAX(22), IEXIT(22), PI, VOLS, RVSQP(22), NDEG
C
      COMMON /BDY/ DELZIN(22), DELZO(22), SFRACI(22), AXIS, AXISM
C
      COMMON /ANSWER/ A(25,22,10)
C
C     IF NON-RECTANGULAR BOUNDARIES ARE USED, EXPRESSIONS
C     EVALUATING DERIVITIVES AT THE BOUNDARIES MAY NEED TO
C     BE MODIFIED
C
      INFACE=IINLET(J)
      IOUT=IEXIT(J)
      IF (I.EQ.INFACE.OR.I.EQ.IOUT.OR.J.EQ.1.OR.J.EQ.JN) GO TO 10
      A(I,J,8)=DBYDZ(I,J,1)
      A(I,J,7)=DBYDR(I,J,1)
      GO TO 80
   10 IF (I.NE.INFACE) GO TO 20
      A(I,J,8)=(A(I+1,J,1)-A(I,J,1))/DELZIN(J)
      IF (J.EQ.1) GO TO 50
      IF (J.EQ.JN) GO TO 60
      A(I,J,7)=DBYDR(I,J,1)
      GO TO 80
   20 IF (I.NE.IOUT) GO TO 30
      A(I,J,8)=(A(I,J,1)-A(I-1,J,1))/DELZO(J)
      IF (J.EQ.1) GO TO 50
      IF (J.EQ.JN) GO TO 60
      A(I,J,7)=DBYDR(I,J,1)
      GO TO 80
   30 IF (J.NE.JN) GO TO 40
      GO TO 60
   40 A(I,J,8)=0.0
   50 A(I,J,7)=(A(I,2,1)-A(I,1,1))/R(2)
      GO TO 70
C
C     TREATMENT OF GSTAR ALONG THE IMPERVIOUS RADIAL WALL
C     APPLY THE NO-SLIP CONDITION AT ALL IMPERVIOUS BOUNDARIES,
C     I.E. GZSTAR=GRSTAR=GSTAR=0
C
   60 A(I,J,7)=0.0
      A(I,J,8)=0.0
      A(I,J,9)=0.0
      A(I,J,10)=0.0
      A(I,J,5)=0.0
      GO TO 100
C
C     TREATMENT OF GZSTAR ALONG THE AXIS OF SYMMETRY
C
   70 A(I,J,10)=0.0
      A(I,1,9)=AXIS*A(I,2,9)-AXISM*A(I,3,9)
      GO TO 90
   80 A(I,J,9)=A(I,J,7)/R(J)
      A(I,J,10)=-ARL*A(I,J,8)/R(J)
      A(I,J,5)=SQRT(ASQ*A(I,J,8)*A(I,J,8)+A(I,J,7)*A(I,J,7))/R(J)
      GO TO 100
   90 A(I,J,5)=A(I,J,9)
  100 CONTINUE
      RETURN
      END
```

```
      FUNCTION DBYDR (I,J,K)
C
C     C*************************************************************C
C     C                                                             C
C     C       COMPUTES 1ST RADIAL DERIVITIVE AT INTERIOR POINTS     C
C     C             OF VARIABLE K OF THE ARRAY A(I,J,K)             C
C     C                                                             C
C     C*************************************************************C
C
      COMMON /DERIV/ H1(25), H1D(25), H2(22), H2D(22)
C
      COMMON /ANSWER/ A(25,22,10)
C
      DBYDR=((A(I,J+1,K)-A(I,J,K))*H2(J)+(A(I,J,K)-A(I,J-1,K))/H2(J))
     1 *H2D(J)
      RETURN
      END
      FUNCTION DBYDZ (I,J,K)
C
C     C*************************************************************C
C     C                                                             C
C     C        COMPUTES 1ST AXIAL DERIVITIVE AT INTERIOR POINTS     C
C     C             OF VARIABLE K OF THE ARRAY A(I,J,K)             C
C     C                                                             C
C     C*************************************************************C
C
      COMMON /DERIV/ H1(25), H1D(25), H2(22), H2D(22)
C
      COMMON /ANSWER/ A(25,22,10)
C
      DBYDZ=((A(I+1,J,K)-A(I,J,K))*H1(I)+(A(I,J,K)-A(I-1,J,K))/H1(I))
     1 *H1D(I)
      RETURN
      END
```

```
      SUBROUTINE PDE
C
C     C*****************************************************************C
C     C                                                                 C
C     C               CONTROL ROUTINE - EQUATION SOLVER FOR             C
C     C    ELLIPTIC PARTIAL DIFFERENTIAL EQUATIONS IN STANDARD FORM     C
C     C                                                                 C
C     C      REF:  HEAT AND MASS TRANSFER IN RECIRCULATING FLOWS,       C
C     C            A.D. GOSMAN, W.M. PUN, A.K. RUNCHAL,                 C
C     C            D.B. SPALDING AND M. WOLFSHTEIN,                     C
C     C            ACADEMIC PRESS, LONDON, 1969                         C
C     C            (MODIFIED HEREIN)                                    C
C     C                                                                 C
C     C*****************************************************************C
C
      COMMON /PROP/ PROPTY(25,22,12), PCOND(25), CP, CSTAR, DSUBPC, EOVR
     1 , EOVA, FKC, SIGMA4, TFILMC, BETAK, GAMMAK, HENTC
C
      COMMON /GEOM/ IN, INM, JN, JNM, Z(25), R(22), IINLET(22), IMIN(22)
     1 , IMAX(22), IEXIT(22), PI, VOLS, RVSOP(22), NDEG
C
      COMMON /NUMER/ RP(4), RSDU(4), LOCI(4), LOCJ(4), REDUCE, IOVER
C
      COMMON /EQN/ AE, AW, AN, AS, ASUM, BE(25), BW(25), BN(22), BS(22),
     1 BBE, BBW, BBN, BBS, NSWP1, NSWP2, NSWP3, NSWP4, IUPWND
C
      COMMON /ANSWER/ A(25,22,10)
C
C     STREAM FUNCTION SUBCYCLE
C
      AE=AW=AN=AS=ASUM=0.
      DO 20 N=1,NSWP1
      RSDU(1)=0.
      DO 10 J=2,JNM
      IL=IMIN(J)
      IH=IMAX(J)
      DO 10 I=IL,IH
      IM=I-1
      IP=I+1
      JM=J-1
      JP=J+1
      CALL MFLUX (I,J)
      CALL MFLUX (IP,J)
      CALL MFLUX (IM,J)
      CALL MFLUX (I,JP)
      CALL MFLUX (I,JM)
      A(I,J,6)=(A(I,J,5)+PROPTY(I,J,2))*PROPTY(I,J,3)
      A(IP,J,6)=(A(IP,J,5)+PROPTY(IP,J,2))*PROPTY(IP,J,3)
      A(IM,J,6)=(A(IM,J,5)+PROPTY(IM,J,2))*PROPTY(IM,J,3)
      A(I,JP,6)=(A(I,JP,5)+PROPTY(I,JP,2))*PROPTY(I,JP,3)
      IF (J.EQ.JNM) A(I,JP,6)=A(I,J,6)
      A(I,JM,6)=(A(I,JM,5)+PROPTY(I,JM,2))*PROPTY(I,JM,3)
      BPP=A(I,J,6)
      BBE=(A(IP,J,6)+BPP)*BE(I)
      BBW=(A(IM,J,6)+BPP)*BW(I)
      BBN=(A(I,JP,6)+BPP)*BN(J)
      BBS=(A(I,JM,6)+BPP)*BS(J)
C
C     CALL EQUATION SOLVER ROUTINE
C
   10 CALL SOLVE (I,J,1)
C
C     ITERATE ON BOUNDARY CONDITIONS
C
      CALL BOUND1
C
   20 CONTINUE
C
```

```
C     FLUID BULK TEMPERATURE SUBCYCLE
C
      DO 40 N=1,NSWP2
      RSDU(2)=0.
      DO 30 J=2,JNM
      IL=IMIN(J)
      IH=IMAX(J)
      DO 30 I=IL,IH
      BPR=PROPTY(I,J,11)
      BPA=PROPTY(I,J,12)
      BBE=(PROPTY(I+1,J,12)+BPA)*BE(I)
      BBW=(PROPTY(I-1,J,12)+BPA)*BW(I)
      BBN=(PROPTY(I,J+1,11)+BPR)*BN(J)
      BBS=(PROPTY(I,J-1,11)+BPR)*BS(J)
C
C     CALL ROUTINE TO CALCULATE AE, AW, AN, AS AND ASUM
C
      CALL ADVEC (I,J,CSTAR)
C
   30 CALL SOLVE (I,J,2)
C
      CALL BOUND2
C
   40 CONTINUE
C
C     AVERAGE PEBBLE SURFACE TEMPERATURE SUBCYCLE
C
      AE=AW=AN=AS=ASUM=0.
      DO 60 N=1,NSWP3
      RSDU(3)=0.
      DO 50 J=2,JNM
      IL=IMIN(J)
      IH=IMAX(J)
      DO 50 I=IL,IH
      BPP=PROPTY(I,J,10)
      BBE=(PROPTY(I+1,J,10)+BPP)*BE(I)
      BBW=(PROPTY(I-1,J,10)+BPP)*BW(I)
      BBN=(PROPTY(I,J+1,10)+BPP)*BN(J)
      BBS=(PROPTY(I,J-1,10)+BPP)*BS(J)
C
   50 CALL SOLVE (I,J,3)
C
      CALL BOUND3
C
   60 CONTINUE
C
C     PRESSURE RECOVERY SUBCYCLE
C
      AE=AW=AN=AS=ASUM=0.
      DO 80 N=1,NSWP4
      RSDU(4)=0.
      DO 70 J=2,JNM
      IL=IMIN(J)
      IH=IMAX(J)
      DO 70 I=IL,IH
      BBE=2.*BE(I)
      BBW=2.*BW(I)
      BBN=2.*BN(J)
      BBS=2.*BS(J)
C
   70 CALL SOLVE (I,J,4)
C
      CALL BOUND4
C
   80 CONTINUE
C
C     UPDATE PROPERTIES BASED ON NEW VALUES OF THE DEPENDENT
C     VARIABLES
C
      CALL PROPS
C
      RETURN
      END
```

```
      SUBROUTINE SOLVE (I,J,K)
C
C     C*****************************************************************C
C     C                                                                 C
C     C            COMPUTES NEW VALUE OF VARIABLE A(I,J,K)              C
C     C      THROUGH APPLICATION OF GENERAL SUBSTITUTION FORMULA        C
C     C                                                                 C
C     C*****************************************************************C
C
      COMMON /NUMER/ RP(4), RSDU(4), LOCI(4), LOCJ(4), REDUCE, IOVER
C
      COMMON /EQN/ AE, AW, AN, AS, ASUM, BE(25), BW(25), BN(22), BS(22),
     1 BBE, BBW, BBN, BBS, NSWP1, NSWP2, NSWP3, NSWP4, IUPWND
C
      COMMON /ANSWER/ A(25,22,10)
C
C     CALCULATE THE VALUE OF D-SUBPHI
C
      CALL DTERM (I,J,K,DPHI)
C
      ANUM=(AE+BBE)*A(I+1,J,K)+(AW+BBW)*A(I-1,J,K)+(AN+BBN)*A(I,J+1,K)+
     1 (AS+BBS)*A(I,J-1,K)-DPHI
      ADNM=ASUM+BBE+BBW+BBN+BBS
      IF (ADNM.EQ.0.) GO TO 30
C
C     STORE THE OLD VALUE OF THE DEPENDENT VARIABLE K
C
      OLD=A(I,J,K)
C
C     CALCULATE THE NEW VALUE
C
      ANEW=ANUM/ADNM
      IF ((K.EQ.1).OR.(K.EQ.4)) GO TO 10
C
C     OVERRIDE NORMAL SUBSTITUTION FOR TEMPERATURES IF STABILITY
C     COULD BE A PROBLEM
C
      IF (ANEW.GT.1.0) GO TO 10
      A(I,J,K)=REDUCE*OLD
      IF (IOVER.EQ.1) PRINT 40, I,J,K,OLD,ANEW,A(I,J,K)
      GO TO 20
C
C     UNDER OR OVER RELAX IF SPECIFIED
C
   10 A(I,J,K)=OLD+RP(K)*(ANEW-OLD)
C
C     CALCULATE THE RESIDUAL
C
   20 RS=1.-OLD/ANEW
C
C     STORE THE MAXIMUM RESIDUAL AND ITS LOCATION
C
      IF (ABS(RS).LE.ABS(RSDU(K))) GO TO 30
      RSDU(K)=RS
      LOCI(K)=I
      LOCJ(K)=J
   30 CONTINUE
      RETURN
C
   40 FORMAT (/,2X,*NORMAL SUBSTITUTION OVERRIDDEN FOR STABILITY*,/,3X,*
     1I = *,I2,*, J = *,I2,*, K = *,I1,*, OLD = *,F6.3,*, NEW = *,F7.3,*
     2, A(I,J,K) = *,F6.3)
      END
```

```
      SUBROUTINE ADVEC (I,J,APP)
C
C     C*************************************************************C
C     C                                                             C
C     C    COMPUTES ADVECTION TERMS OF GENERAL SUBSTITUTION FORMULA  C
C     C                                                             C
C     C*************************************************************C
C
      COMMON /GEOM/ IN, INM, JN, JNM, Z(25), R(22), IINLET(22), IMIN(22)
     1 , IMAX(22), IEXIT(22), PI, VOLS, RVSOP(22), NDEG
C
      COMMON /EQN/ AE, AW, AN, AS, ASUM, BE(25), BW(25), BN(22), BS(22),
     1 BBE, BBW, BBN, BBS, NSWP1, NSWP2, NSWP3, NSWP4, IUPWND
C
      COMMON /ANSWER/ A(25,22,10)
C
      DV=R(J)*(Z(I+1)-Z(I-1))*(R(J+1)-R(J-1))
      GZPW=(A(I,J+1,1)-A(I,J-1,1)+A(I-1,J+1,1)-A(I-1,J-1,1))/DV
      GZPE=(A(I,J+1,1)-A(I,J-1,1)+A(I+1,J+1,1)-A(I+1,J-1,1))/DV
      GRPS=(A(I-1,J,1)-A(I+1,J,1)+A(I-1,J-1,1)-A(I+1,J-1,1))/DV
      GRPN=(A(I-1,J,1)-A(I+1,J,1)+A(I-1,J+1,1)-A(I+1,J+1,1))/DV
C
C     COMPUTE AE, AW, AN, AND AS
C
C     USER HAS OPTION OF USING UPWIND OR CENTRAL DIFFERENCES
C     CENTRAL DIFFERENCES ARE MORE ACCURATE, BUT UPWIND
C     DIFFERENCES MAY BE REQUIRED TO ENSURE CONVERGENCE
C
      IF (IUPWND.NE.1) GO TO 10
C
C     UPWIND DIFFERENCES
C
      AE=0.5*APP*(ABS(GZPE)-GZPE)
      AW=0.5*APP*(ABS(GZPW)+GZPW)
      AN=0.5*APP*(ABS(GRPN)-GRPN)
      AS=0.5*APP*(ABS(GRPS)+GRPS)
      ASUM=AE+AW+AN+AS
      RETURN
C
   10 CONTINUE
C
C     CENTRAL DIFFERENCES
C
      AE=-0.5*APP*GZPE
      AW=0.5*APP*GZPW
      AN=-0.5*APP*GRPN
      AS=0.5*APP*GRPS
      ASUM=-(AE+AW+AN+AS)
      RETURN
      END
```

```
      SUBROUTINE DTERM (I,J,K,DPHI)
C
C     C*****************************************************************C
C     C                                                                 C
C     C        COMPUTES D-SUBPHI TERM OF STANDARD ELLIPTIC FORM         C
C     C                                                                 C
C     C*****************************************************************C
C
      COMMON /REACTR/ HEIGHT, RADIUS, DKUGEL, FMDOT, QTOT, TINLET,
     1 PINLET, GINLET, REYNIN, ARL, ASQ, AFRIC, BFRIC, VFNOM
C
      COMMON /PROP/ PROPTY(25,22,12), PCOND(25), CP, CSTAR, DSUBPC, EOVR
     1 , EOVA, FKC, SIGMA4, TFILMC, BETAK, GAMMAK, HENTC
C
      COMMON /GEOM/ IN, INM, JN, JNM, Z(25), R(22), IINLET(22), IMIN(22)
     1 , IMAX(22), IEXIT(22), PI, VOLS, RVSOP(22), NDEG
C
      COMMON /ANSWER/ A(25,22,10)
C
C     SELECT THE TERM CORRESPONDING TO VARIABLE K
C
      GO TO (10,20,30,40), K
C
C     STREAM FUNCTION SUBCYCLE
C
   10 DPHI=2.*A(I,J,6)*A(I,J,7)/(ASQ*R(J))
      RETURN
C
C     FLUID BULK-TEMPERATURE SUBCYCLE
C
   20 DELTA=A(I,J,3)-A(I,J,2)
      DPHI=-PROPTY(I,J,5)*PROPTY(I,J,8)*DELTA
      RETURN
C
C     PEBBLE AVERAGE SURFACE TEMPERATURE SUBCYCLE
C
   30 DELTA=A(I,J,3)-A(I,J,2)
      DPHI=PROPTY(I,J,5)*PROPTY(I,J,8)*DELTA-PROPTY(I,J,9)
      RETURN
C
C     PRESSURE RECOVERY SUBCYCLE
C
   40 DBDZ=DBYDZ(I,J,6)
      DBDR=DBYDR(I,J,6)
      A(I,J,8)=DBYDZ(I,J,1)
      A(I,J,7)=DBYDR(I,J,1)
      DPHI=-(A(I,J,7)*DBDZ-A(I,J,8)*DBDR)*DSUBPC/R(J)
      RETURN
      END
```

```
      SUBROUTINE BOUND
C
C     C*****************************************************************C
C     C                                                                 C
C     C      ITERATES BOUNDARY CONDITIONS WHICH INCLUDE THE NORMAL      C
C     C               DERIVITIVE OF THE DEPENDENT VARIABLE              C
C     C    AND THOSE WHICH REQUIRE UPDATED VALUES OF OTHER VARIABLES    C
C     C                                                                 C
C     C*****************************************************************C
C
      COMMON /PROP/ PROPTY(25,22,12), PCOND(25), CP, CSTAR, DSUBPC, EOVR
     1 , EOVA, FKC, SIGMA4, TFILMC, BETAK, GAMMAK, HENTC
C
      COMMON /GEOM/ IN, INM, JN, JNM, Z(25), R(22), IINLET(22), IMIN(22)
     1 , IMAX(22), IEXIT(22), PI, VOLS, RVSOP(22), NDEG
C
      COMMON /BDY/ DELZIN(22), DELZO(22), SFRACI(22), AXIS, AXISM
C
      COMMON /ANSWER/ A(25,22,10)
C
C     SET UP FOR CONSTANT Z INLET FACE AT Z=0
C     AND CONSTANT Z OUTLET FACE AT Z=1
C
C     CONDITIONS CORRESPOND TO SYMMETRY AT R=0 AND R=1
C     THE RADIAL REFLECTOR IS ASSUMED IMPERVIOUS AND ADIABATIC
C
C     IT IS ASSUMED THAT THERE IS A CONSTANT PRESSURE IN THE INLET
C     PLENUM WHICH LEADS TO GRSTAR(INLET)=0 WHICH MAKES THE AXIAL
C     DERIVITIVE OF PSI ZERO
C     IT IS ASSUMED THAT FLOW AT THE OUTLET IS PURELY AXIAL, AND
C     THAT PRESSURE AT THE OUTLET FACE CORRESPONDS TO A
C     ONE-DIMENSIONAL AXIAL DROP FROM THE LAST INTERNAL GRID
C     POINT AND HAS A CONSTANT VALUE ACROSS THE OUTLET FACE
C
C     TEMPERATURE CONDITIONS AT THE INLET ARE DERIVED FROM
C     ONE-DIMENSIONAL THERMAL ENERGY BALANCES
C     TEMPERATURE CONDITIONS AT THE OUTLET REQUIRE THAT THE
C     2ND AXIAL DERIVITIVES OF THE TEMPERATURES EQUAL ZERO
C
C     STREAM FUNCTION AT INLET AND OUTLET
C
      ENTRY BOUND1
      DO 10 J=2,JNM
      A(1,J,1)=A(2,J,1)
   10 A(IN,J,1)=A(INM,J,1)
      CALL MFLUX (1,1)
      CALL MFLUX (1,JN)
      CALL MFLUX (IN,1)
      CALL MFLUX (IN,JN)
      A(1,1,6)=(A(1,1,5)+PROPTY(1,1,2))*PROPTY(1,1,3)
      A(1,JN,6)=A(1,JNM,6)
      A(IN,1,6)=(A(IN,1,5)+PROPTY(IN,1,2))*PROPTY(IN,1,3)
      A(IN,JN,6)=A(IN,JNM,6)
      RETURN
C
C     FLUID BULK TEMPERATURE AT R=0, R=1, INLET AND OUTLET
C
      ENTRY BOUND2
      DO 20 J=2,JNM
      DTFDZ=(A(2,J,2)-A(1,J,2))/DELZIN(J)
      TI1=PROPTY(1,J,8)*SFRACI(J)*(A(1,J,3)-1.)
      TI2=1./(A(1,J,5)*CSTAR)
      A(1,J,2)=TI2*(TI1+PROPTY(1,J,12)*DTFDZ)+1.
   20 A(IN,J,2)=DELZO(J)*DBYDZ(INM,J,2)+A(INM,J,2)
      DO 30 I=1,IN
      A(I,1,2)=A(I,2,2)
   30 A(I,JN,2)=A(I,JNM,2)
      RETURN
C
```

```
C     PEBBLE AVERAGE SURFACE TEMPERATURE AT R=0, R=1, INLET AND OUTLET
C
      ENTRY BOUND3
      DO 40 J=2,JNM
      DTSDZ=(A(2,J,3)-A(1,J,3))/DELZIN(J)
      TI1=PROPTY(1,J,9)*SFRACI(J)/PROPTY(1,J,5)
      A(1,J,3)=(PROPTY(1,J,10)*DTSDZ+TI1)/(PROPTY(1,J,8)*SFRACI(J))+1.
   40 A(IN,J,3)=DELZO(J)*DBYDZ(INM,J,3)+A(INM,J,3)
      DO 50 I=1,IN
      A(I,1,3)=A(I,2,3)
   50 A(I,JN,3)=A(I,JNM,3)
      RETURN
C
C     PRESSURE AT OUTLET, R=0 AND R=1
C
      ENTRY BOUND4
      JB=JNM-1
      A(IN,JB,4)=-DSUBPC*DELZO(JB)*A(IN,JB,9)*A(IN,JB,6)+A(INM,JB,4)
      DO 60 J=2,JNM
   60 A(IN,J,4)=A(IN,JB,4)
      DO 70 I=2,IN
      A(I,1,4)=A(I,2,4)
   70 A(I,JN,4)=A(I,JNM,4)
      RETURN
C
      END
```

```
      SUBROUTINE TEMPS
C
C     C*************************************************************C
C     C                                                             C
C     C            CALCULATES PEBBLE INTERNAL TEMPERATURES          C
C     C                  AND TEMPERATURE GRADIENTS                  C
C     C    FOR BOTH CONVENTIONAL AND SHELL FUEL/MODERATOR ELEMENTS  C
C     C        ALSO RE-DIMENSIONALIZES TEMPERATURES FOR OUTPUT      C
C     C                                                             C
C     C*************************************************************C
C
      COMMON /REACTR/ HEIGHT, RADIUS, DKUGEL, FMDOT, QTOT, TINLET,
     1 PINLET, GINLET, REYNIN, ARL, ASQ, AFRIC, BFRIC, VFNOM
C
      COMMON /FPOWER/ PBALL(25,22)
C
      COMMON /PROP/ PROPTY(25,22,12), PCOND(25), CP, CSTAR, DSUBPC, EOVR
     1 , EOVA, FKC, SIGMA4, TFILMC, BETAK, GAMMAK, HENTC
C
      COMMON /GEOM/ IN, INM, JN, JNM, Z(25), R(22), IINLET(22), IMIN(22)
     1 , IMAX(22), IEXIT(22), PI, VOLS, RVSOP(22), NDEG
C
      COMMON /ANSWER/ A(25,22,10)
C
      COMMON /BALL/ TEMPIN(25,22,3), IBALL, R1, R2
C
C     IT IS ASSUMED THAT THE THERMAL CONDUCTIVITY OF THE FUELED
C     MATRIX AND THE UNFUELED GRAPHITE SHELL ARE EQUAL
C     IT IS ASSUMED THAT THIS THERMAL CONDUCTIVITY VARIES AXIALLY
C     BECAUSE OF AXIAL CHANGES IN TEMPERATURE AND FAST FLUENCE
C
C     THE THERMAL CONDUCTIVITY VALUES ARE ASSIGNED IN SUBROUTINE
C     INIT, WHERE A REFERENCE IS GIVEN
C
      IF (IBALL.NE.1) GO TO 20
C
C     CONVENTIONAL BALL
C
      R3=0.5*DKUGEL
      C1=1./(4.*PI)
      C2=C1*(1./R2-1./R3)
      C3=-0.01*C1/(R2*R2)
      C4=1./(8.*PI*R2)
      DO 10 J=1,JN
      IL=IINLET(J)
      IH=IEXIT(J)
      DO 10 I=IL,IH
      TS=A(I,J,3)*TINLET
      A(I,J,3)=TS
      A(I,J,2)=A(I,J,2)*TINLET
      QOVERK=PBALL(I,J)/PCOND(I)
      TEMPIN(I,J,1)=QOVERK*C2+TS
      TEMPIN(I,J,2)=QOVERK*C3
   10 TEMPIN(I,J,3)=QOVERK*C4+TEMPIN(I,J,1)
      RETURN
```

```
C
C     SHELL BALL
C
   20 R3=0.5*DKUGEL
      C1=1./(4.*PI)
      C2=C1*(1./R2-1./R3)
      C3=1./(R2*R2*R2-R1*R1*R1)
      C4=0.5*(R2*R2-R1*R1)
      C5=R1*R1*R1*(1./R1-1./R2)
      C6=-0.01*C1/(R2*R2)
      C7=C1*C3*(C4-C5)
      DO 30 J=1,JN
      IL=IINLET(J)
      IH=IEXIT(J)
      DO 30 I=IL,IH
      TS=A(I,J,3)*TINLET
      A(I,J,3)=TS
      A(I,J,2)=A(I,J,2)*TINLET
      QOVERK=PBALL(I,J)/PCOND(I)
      TEMPIN(I,J,1)=QOVERK*C2+TS
      TEMPIN(I,J,2)=QOVERK*C6
   30 TEMPIN(I,J,3)=QOVERK*C7+TEMPIN(I,J,1)
      RETURN
      END
```

```
      SUBROUTINE RESULT
C
C     C*********************************************************************C
C     C                                                                     C
C     C                ROUTINE FOR FILM AND PRINT OUTPUT                    C
C     C                                                                     C
C     C            PLOT ROUTINES ARE INSTALLATION DEPENDENT                 C
C     C     PRINT OUTPUT FORMAT IS FOR AN 80 CHARACTER PAGE WIDTH           C
C     C    IF JN.GT.22 PRINT OUTPUT FORMAT WILL NEED TO BE MODIFIED         C
C     C                                                                     C
C     C*********************************************************************C
C
      COMMON /REACTR/ HEIGHT, RADIUS, DKUGEL, FMDOT, QTOT, TINLET,
     1 PINLET, GINLET, REYNIN, ARL, ASQ, AFRIC, BFRIC, VFNOM
C
      COMMON /FPOWER/ PBALL(25,22)
C
      COMMON /PROP/ PROPTY(25,22,12), PCOND(25), CP, CSTAR, DSUBPC, EOVR
     1 , EOVA, FKC, SIGMA4, TFILMC, BETAK, GAMMAK, HENTC
C
      COMMON /GEOM/ IN, INM, JN, JNM, Z(25), R(22), IINLET(22), IMIN(22)
     1 , IMAX(22), IEXIT(22), PI, VOLS, RVSOP(22), NDEG
C
      COMMON /ANSWER/ A(25,22,10)
C
      COMMON /BALL/ TEMPIN(25,22,3), IBALL, R1, R2
C
      COMMON /RESULT/ IOUTP(12), IFILM1, IFILM2, IFILM3, JLOCTP, ID,
     1 INDEX, KOA, NC
C
      DIMENSION OUTVAR(22,25), ZC(21)
C
      DIMENSION IOK(10), KFILM(3), JPLOT(3)
C
C     SCALE SELECTED VARIABLES FOR PRINTOUT
C
      DO 10 J=1,JN
      DO 10 I=1,IN
   10 PBALL(I,J)=PBALL(I,J)*1.E-03
      QMW=QTOT*1.E-06
      PINLET=PINLET*1.E-06
C
C     CALCULATE OUTLET PLENUM MIXED MEAN GAS TEMPERATURE, CORE PRESSURE
C     DROP, AND COMPARE COOLANT TEMPERATURE RISE ACROSS CORE WITH THAT
C     PREDICTED BY THE FIRST LAW OF THERMODYNAMICS
C
      SUMTFQ=0.
      RIN=0.
      JNMM=JNM-1
      DO 20 J=1,JNMM
      ROUT=0.5*(R(J+1)+R(J))
      AREA=ROUT*ROUT-RIN*RIN
      SUMTFQ=SUMTFQ+AREA*A(IN,J,5)*A(IN,J,2)
   20 RIN=ROUT
      AREA=1.-RIN*RIN
      SUMTFQ=SUMTFQ+AREA*A(IN,JNM,5)*A(IN,JNM,2)
      TFOMM=SUMTFQ*GINLET*RADIUS*RADIUS*PI/FMDOT
      POMM=A(IN,JNM,4)*PINLET
      DELTAT=QTOT/(FMDOT*CP)
      FSTLAW=(TFOMM-TINLET-DELTAT)*100./DELTAT
      PDROP=PINLET-POMM
C
```

```
C     LOCATE MAXIMUM AND MINIMUM VALUES IN FIELD OF SELECTED VARIABLES
C
      TFMIN=1000.
      TFMAX=0.
      TSMIN=1000.
      TSMAX=0.
      PWRMIN=10.
      PWRMAX=0.
      PMIN=1.0
      PMAX=1.0
      TMXMIN=2000.
      TMXMAX=0.
      GRADMX=0.
      DO 110 J=1,JN
      DO 110 I=1,IN
      IF (TEMPIN(I,J,3).GT.TMXMIN) GO TO 30
      TMXMIN=TEMPIN(I,J,3)
   30 IF (TEMPIN(I,J,3).LT.TMXMAX) GO TO 40
      TMXMAX=TEMPIN(I,J,3)
      ITMXM=I
      JTMXM=J
   40 IF (A(I,J,3).LT.TSMAX) GO TO 50
      TSMAX=A(I,J,3)
      ITSMAX=I
      JTSMAX=J
   50 IF (A(I,J,3).GT.TSMIN) GO TO 60
      TSMIN=A(I,J,3)
   60 IF (A(I,J,4).GT.PMIN) GO TO 70
      PMIN=A(I,J,4)
   70 IF (A(I,J,2).GT.TFMIN) GO TO 80
      TFMIN=A(I,J,2)
   80 IF (PBALL(I,J).LT.PWRMAX) GO TO 90
      PWRMAX=PBALL(I,J)
      IPWRMX=I
      JPWRMX=J
   90 IF (PBALL(I,J).GT.PWRMIN) GO TO 100
      PWRMIN=PBALL(I,J)
  100 IF (TEMPIN(I,J,2).GT.GRADMX) GO TO 110
      GRADMX=TEMPIN(I,J,2)
      IGRAD=I
      JGRAD=J
  110 CONTINUE
      DO 120 J=1,JN
      IF (A(IN,J,2).LE.TFMAX) GO TO 120
      TFMAX=A(IN,J,2)
      JHOT=J
  120 CONTINUE
      RHOTC=R(JHOT)*RADIUS
      RMPWR=R(JPWRMX)*RADIUS
      ZMPWR=Z(IPWRMX)*HEIGHT
      RMFUEL=R(JTMXM)*RADIUS
      ZMFUEL=Z(ITMXM)*HEIGHT
      RTSMAX=R(JTSMAX)*RADIUS
      ZTSMAX=Z(ITSMAX)*HEIGHT
      RGRAD=R(JGRAD)*RADIUS
      ZGRAD=Z(IGRAD)*HEIGHT
      RTFMAX=R(JHOT)*RADIUS
C
```

```
C     OUTPUT INLET PLENUM VALUES AND OTHER SELECTED VARIABLES
C
      PRINT 750, ID
      PRINT 760
      PRINT 770, FMDOT,QMW,PINLET,TINLET
      PRINT 780
      PRINT 790, RADIUS,HEIGHT,VFNOM
      IF (IBALL.EQ.1) GO TO 130
      PRINT 800
      PRINT 810, DKUGEL,R1,R2
      GO TO 140
  130 PRINT 820
      PRINT 830, DKUGEL,R2
  140 PRINT 840
      PRINT 850, PWRMAX,RMPWR,ZMPWR
      PRINT 860
      PRINT 870
      PRINT 880, REYNIN,POMM,PDROP
      PRINT 890
      PRINT 900, TFOMM,FSTLAW
      PRINT 910
      PRINT 920, TFMAX,RTFMAX
      PRINT 930
      PRINT 940, TMXMAX,RMFUEL,ZMFUEL
      PRINT 950
      PRINT 960, GRADMX,RGRAD,ZGRAD
C
C     OUTPUT VALUES OF SELECTED VARIABLES OVER ENTIRE FIELD
C
      DATA IOK /1,5,10,9,4,2,3,3,1,2/
      DO 290 IO=1,7
      K=IOK(IO)
      IF (IOUTP(IO).NE.1) GO TO 290
      JL=1
      JH=11
      DO 280 LOOP=1,2
      GO TO (150,160,170,180,190,200,210), IO
  150 PRINT 1020
      GO TO 220
  160 PRINT 1030
      GO TO 220
  170 PRINT 1040
      GO TO 220
  180 PRINT 1050
      GO TO 220
  190 PRINT 1060
      GO TO 220
  200 PRINT 1070
      GO TO 220
  210 PRINT 1080
  220 PRINT 970
      PRINT 980, (R(J),J=JL,JH)
      PRINT 990
      GO TO (230,230,230,230,230,250,250), IO
  230 DO 240 I=1,IN
  240 PRINT 1000, Z(I),(A(I,J,K),J=JL,JH)
      GO TO 270
  250 DO 260 I=1,IN
  260 PRINT 1010, Z(I),(A(I,J,K),J=JL,JH)
  270 JL=12
      JH=22
  280 CONTINUE
```

```
290 CONTINUE
    DO 360 IO=8,10
    K=IOK(IO)
    IF (IOUTP(IO).NE.1) GO TO 360
    JL=1
    JH=11
    DO 350 LOOP=1,2
    IOM=IO-7
    GO TO (300,310,320), IOM
300 PRINT 1090
    GO TO 330
310 PRINT 1100
    GO TO 330
320 PRINT 1110
330 PRINT 970
    PRINT 980, (R(J),J=JL,JH)
    PRINT 990
    DO 340 I=1,IN
340 PRINT 1010, Z(I),(TEMPIN(I,J,K),J=JL,JH)
    JL=12
    JH=22
350 CONTINUE
360 CONTINUE
    IF (IOUTP(11).NE.1) GO TO 390
    JL=1
    JH=11
    DO 380 LOOP=1,2
    PRINT 1120
    PRINT 970
    PRINT 980, (R(J),J=JL,JH)
    PRINT 990
    DO 370 I=1,IN
370 PRINT 1000, Z(I),(PBALL(I,J),J=JL,JH)
    JL=12
    JH=22
380 CONTINUE
390 CONTINUE
    IF (IOUTP(12).NE.1) GO TO 460
    JL=1
    JH=11
    DO 450 LOOP=1,2
    GO TO (400,410), INDEX
400 PRINT 1130, KOA
    GO TO 420
410 PRINT 1140, KOA
420 PRINT 970
    PRINT 980, (R(J),J=JL,JH)
    PRINT 990
    DO 440 I=1,IN
    IF (INDEX.NE.1) GO TO 430
    PRINT 1000, Z(I),(A(I,J,KOA),J=JL,JH)
    GO TO 440
430 PRINT 1000, Z(I),(PROPTY(I,J,KOA),J=JL,JH)
440 CONTINUE
    JL=12
    JH=22
450 CONTINUE
```

```
  460 CONTINUE
C
      IF (IFILM1.NE.1) GO TO 530
C
C     PREPARE DATA FILES FOR EASYPLT (LASL J5AD)
C
C     PREPARE DATA FILES FOR PLOTS OF TGAS/TSURFACE/TMAX
C     VERSUS AXIAL POSITION FOR CENTERLINE, HOT RADIUS,
C     AND USER DESIGNATED RADIUS (TAPE2 THROUGH TAPE4)
C
      PRINT 1150, JLOCTP
      IF (JLOCTP.EQ.0) JLOCTP=JTMXM
      JPLOT(1)=1
      JPLOT(2)=JHOT
      JPLOT(3)=JLOCTP
      IA=1
      IB=2
      IC=3
      DO 500 ID=1,3
      J=JPLOT(ID)
      ITAPE=ID+1
      DO 470 I=1,IN
  470 WRITE (ITAPE,1180) IA,Z(I),A(I,J,2)
      DO 480 I=1,IN
  480 WRITE (ITAPE,1180) IB,Z(I),A(I,J,3)
      DO 490 I=1,IN
  490 WRITE (ITAPE,1180) IC,Z(I),TEMPIN(I,J,3)
  500 CONTINUE
C
C     PREPARE DATA FILE FOR PLOT OF LOCAL OUTLET GAS TEMPERATURE
C     AND MIXED MEAN OUTLET GAS TEMPERATURE VERSUS RADIUS (TAPE5)
C
      DO 510 J=1,JN
  510 WRITE (5,1180) IA,R(J),A(IN,J,2)
      DO 520 J=1,JN
  520 WRITE (5,1180) IB,R(J),TFOMM
  530 CONTINUE
C
      IF (IFILM2.NE.1) GO TO 580
C
C     PREPARE DATA FILES FOR EASY3D (LASL J5AK)
C     NOTE THAT THERE IS A 961 POINT LIMIT (IN*JN)
C     DATA FILES CREATED FOR THERMAL POWER PER BALL, COOLANT BULK
C     TEMPERATURE, PEBBLE AVERAGE SURFACE TEMPERATURE, DIMENSIONLESS
C     MASS FLUX, AND MAXIMUM INTERNAL FUELED MATRIX TEMPERATURE
C     (TAPE6 THROUGH TAPE10)
C
      DATA KFILM /2,3,5/
      DO 540 J=1,JN
      DO 540 I=1,IN
  540 WRITE (6,1190) R(J),Z(I),PBALL(I,J)
      DO 560 ID=7,9
      K=KFILM(ID-6)
      DO 550 J=1,JN
      DO 550 I=1,IN
  550 WRITE (ID,1190) R(J),Z(I),A(I,J,K)
  560 CONTINUE
      DO 570 J=1,JN
      DO 570 I=1,IN
  570 WRITE (10,1190) R(J),Z(I),TEMPIN(I,J,3)
      PRINT 1160
  580 CONTINUE
```

```
C
      IF (IFILM3.NE.1) GO TO 740
C
C     CONTOUR PLOTS CALLED FOR (CONTRJB, LASL J563A)
C     FILM PLOT FILES GENERATED FOR STREAM FUNCTION, DIMENSIONLESS
C     PRESSURE, COOLANT BULK TEMPERATURE, PEBBLE AVERAGE SURFACE
C     TEMPERATURE, MAXIMUM INTERNAL FUELED MATRIX TEMPERATURE, AND
C     THERMAL POWER PER BALL
C     FILM FILE GENERATED FOR PLOT OF FINITE DIFFERENCE GRID
C
      DO 730 L=1,6
      GO TO (590,610,610,610,630,650), L
C
  590 RPSI=0.
      DO 600 IL=1,NC
      ZC(IL)=RPSI*RPSI*0.5
  600 RPSI=RPSI+1./FLOAT(NC-1)
C
C     IPLOT IS USED TO PLOT THE VARIABLE WITH THE ORIGIN IN THE UPPER
C     LEFT-HAND CORNER
C     IPLOT IS USED BECAUSE KFA DESIGNS USE DOWNFLOWING COOLANT
C
  610 DO 620 J=1,JN
      DO 620 I=1,IN
      IPLOT=IN-I+1
  620 OUTVAR(J,IPLOT)=A(I,J,L)
C
      GO TO (670,680,690,700), L
C
  630 DO 640 J=1,JN
      DO 640 I=1,IN
      IPLOT=IN-I+1
  640 OUTVAR(J,IPLOT)=TEMPIN(I,J,3)
      GO TO 710
C
  650 DO 660 J=1,JN
      DO 660 I=1,IN
      IPLOT=IN-I+1
  660 OUTVAR(J,IPLOT)=PBALL(I,J)
      GO TO 720
C
  670 CALL CONTRJB (R,JN,Z,IN,OUTVAR,JN,IN,-NC,0.0,0.5,-1.,ZC,RADIUS
     1 ,HEIGHT,-1,29HDIMENSIONLESS RADIAL POSITION,29,21HMASS FLUX STREA
     2MLINES,21,28HDIMENSIONLESS AXIAL POSITION,28)
      GO TO 730
C
  680 CALL CONTRJB (R,JN,Z,IN,OUTVAR,JN,IN,NC,TFMIN,TFMAX,-1.,ZC,RADIUS
     1 ,HEIGHT,-1,29HDIMENSIONLESS RADIAL POSITION,29,28HCOOLANT BULK TE
     2MPERATURE (K),28,28HDIMENSIONLESS AXIAL POSITION,28)
      GO TO 730
C
  690 CALL CONTRJB (R,JN,Z,IN,OUTVAR,JN,IN,NC,TSMIN,TSMAX,-1.,ZC,RADIUS
     1 ,HEIGHT,-1,29HDIMENSIONLESS RADIAL POSITION,29,38HPEBBLE AVERAGE
     2SURFACE TEMPERATURE (K),38,28HDIMENSIONLESS AXIAL POSITION,28)
      GO TO 730
C
  700 CALL CONTRJB (R,JN,Z,IN,OUTVAR,JN,IN,NC,PMIN,PMAX,-1.,ZC,RADIUS
     1 ,HEIGHT,-1,29HDIMENSIONLESS RADIAL POSITION,29,18HNORMALIZED ISOB
     2ARS,18,28HDIMENSIONLESS AXIAL POSITION,28)
      GO TO 730
C
  710 CALL CONTRJB (R,JN,Z,IN,OUTVAR,JN,IN,NC,TMXMIN,TMXMAX,-1.,ZC
     1 ,RADIUS,HEIGHT,-1,29HDIMENSIONLESS RADIAL POSITION,29,46HMAXIMUM
     2INTERNAL FUELED MATRIX TEMPERATURE (K),46,28HDIMENSIONLESS AXIAL P
     3OSITION,28)
      GO TO 730
C
  720 CALL CONTRJB (R,JN,Z,IN,OUTVAR,JN,IN,NC,PWRMIN,PWRMAX,-1.,ZC
     1 ,RADIUS,HEIGHT,-1,29HDIMENSIONLESS RADIAL POSITION,29,32HTHERMAL
     2POWER PER BALL (KW/BALL),32,28HDIMENSIONLESS AXIAL POSITION,28)
C
  730 CONTINUE
```

```
C
      CALL PLTGRD
C
      CALL ADV (2)
      PRINT 1170
  740 CONTINUE
      CALL SECOND (TIME)
      PRINT 1200, TIME
      RETURN
C
  750 FORMAT (///,13X,◆PEBBLE BED REACTOR THERMAL/HYDRAULIC ANALYSIS CAS
     1E ◆,I4,/,5X,70(◆—◆),/,5X,70(◆—◆))
  760 FORMAT (///,63X,◆MIXED MEAN◆,/,8X,◆COOLANT◆,28X,◆INLET PLENUM◆,7X,
     1 ◆INLET COOLANT◆,/,7X,◆MASS FLOW◆,8X,◆THERMAL POWER◆,8X,◆PRESSURE◆
     2 ,10X,◆TEMPERATURE◆,/,8X,◆(KG/S)◆,15X,◆(MW)◆,14X,◆(MPA)◆,15X,◆(K)◆
     3 ,/,2X,18(◆—◆),1X,18(◆—◆),1X,18(◆—◆),1X,19(◆—◆))
  770 FORMAT (8X,F5.0,15X,F5.0,13X,F5.1,15X,F4.0)
  780 FORMAT (///,15X,◆BED RADIUS◆,10X,◆BED HEIGHT◆,12X,◆NOMINAL◆,/,18X,
     1 ◆(M)◆,17X,◆(M)◆,13X,◆VOID FRACTION◆,/,11X,18(◆—◆),2X,18(◆—◆),2X,1
     2 8(◆—◆))
  790 FORMAT (18X,F4.2,16X,F4.2,16X,F4.2)
  800 FORMAT (///,27X,◆PEBBLE◆,11X,◆INNER MATRIX◆,8X,◆OUTER MATRIX◆,/,3X
     1 ,◆FUEL/MODERATOR◆,9X,◆DIAMETER◆,8X,◆INTERFACE RADIUS◆,4X,◆INTERFA
     2CE RADIUS◆,/,4X,◆ELEMENT TYPE◆,12X,◆(M)◆,18X,◆(M)◆,17X,◆(M)◆,/,1X,
     3 18(◆—◆),2X,18(◆—◆),2X,18(◆—◆),2X,18(◆—◆))
  810 FORMAT (8X,◆SHELL◆,13X,F5.3,15X,F6.4,14X,F6.4)
  820 FORMAT (//,37X,◆PEBBLE◆,11X,◆MATRIX/SHELL◆,/,13X,◆FUEL/MODERATOR◆,
     1 9X,◆DIAMETER◆,8X,◆INTERFACE RADIUS◆,/,14X,◆ELEMENT TYPE◆,13X,◆(M)
     2◆,16X,◆(M)◆,/,11X,18(◆—◆),2X,18(◆—◆),2X,18(◆—◆))
  830 FORMAT (14X,◆CONVENTIONAL◆,11X,F5.3,14X,F6.4)
  840 FORMAT (///,53X,◆LOCATION◆,/,13X,◆MAXIMUM POWER/BALL◆,15X,◆RADIUS
     1/ DEPTH FROM TOP◆,/,17X,◆(KW/BALL)◆,30X,◆(M)◆,/,10X,24(◆—◆),11X,25
     2 (◆—◆))
  850 FORMAT (19X,F4.2,28X,F5.3,◆ / ◆F5.3)
  860 FORMAT (////,32X,◆CALCULATED VALUES◆,/,5X,70(◆—◆),/,5X,70(◆—◆))
  870 FORMAT (///,35X,◆MIXED MEAN◆,13X,◆CORE◆,/,18X,◆INLET◆,10X,◆OUTLET
     1PRESSURE◆,6X,◆PRESSURE DROP◆,/,13X,◆REYNOLDS NUMBER◆,10X,◆(MPA)◆,1
     2 5X,◆(MPA)◆,/,12X,17(◆—◆),3X,17(◆—◆),3X,17(◆—◆))
  880 FORMAT (17X,F6.0,15X,F5.3,15X,F5.4)
  890 FORMAT (///,15X,◆MIXED MEAN OUTLET◆,/,14X,◆COOLANT TEMPERATURE◆,18
     1 X,◆FIRST LAW ERROR◆,/,22X,◆(K)◆,29X,◆(PERCENT)◆,/,13X,21(◆—◆),15X
     2 ,19(◆—◆))
  900 FORMAT (20X,F5.0,29X,F6.1)
  910 FORMAT (///,16X,◆MAXIMUM OUTLET◆,/,13X,◆COOLANT TEMPERATURE◆,18X,◆
     1RADIAL LOCATION◆,/,21X,◆(K)◆,32X,◆(M)◆,/,11X,24(◆—◆),10X,25(◆—◆))
  920 FORMAT (20X,F4.0,31X,F5.3)
  930 FORMAT (///,16X,◆MAXIMUM FUELED◆,/,14X,◆MATRIX TEMPERATURE◆,21X,◆L
     1OCATION,◆,/,19X,◆IN CORE◆,20X,◆RADIUS / DEPTH FROM TOP◆,/,21X,◆(K)
     2◆,32X,◆(M)◆,/,11X,24(◆—◆),10X,25(◆—◆))
  940 FORMAT (19X,F5.0,27X,F5.3,◆ / ◆,F5.3)
  950 FORMAT (///,15X,◆MAXIMUM INTERNAL◆,/,12X,◆SHELL/MATRIX INTERFACE◆,
     1 19X,◆LOCATION,◆,/,13X,◆TEMPERATURE GRADIENT◆,13X,◆RADIUS / DEPTH
     2FROM TOP◆,/,20X,◆(K/CM)◆,30X,◆(M)◆,/,11X,24(◆—◆),10X,25(◆—◆))
  960 FORMAT (20X,F5.0,26X,F5.3,◆ / ◆,F5.3)
  970 FORMAT (//,3X,◆AXIAL◆,/,2X,◆POSITION◆,28X,◆RADIAL POSITION◆,/,1X,1
     1 0(◆—◆),1X,66(◆—◆))
  980 FORMAT (11X,11F6.3)
  990 FORMAT (12X,66(◆—◆),/)
 1000 FORMAT (2X,F6.3,3X,11F6.3)
 1010 FORMAT (2X,F6.3,3X,11F6.0)
 1020 FORMAT (///,25X,◆DIMENSIONLESS STREAM FUNCTION◆,/,24X,31(◆—◆))
 1030 FORMAT (///,24X,◆DIMENSIONLESS MASS FLUX, GSTAR◆,/,23X,32(◆—◆))
 1040 FORMAT (///,14X,◆RADIAL COMPONENT OF DIMENSIONLESS MASS FLUX, GRST
     1AR◆,/,13X,53(◆—◆))
 1050 FORMAT (///,14X,◆AXIAL COMPONENT OF DIMENSIONLESS MASS FLUX, GZSTA
     1R◆,/,13X,52(◆—◆))
 1060 FORMAT (///,21X,◆DIMENSIONLESS COOLANT PRESSURE, PSTAR◆,/,20X,39(◆
     1—◆))
 1070 FORMAT (///,23X,◆COOLANT BULK TEMPERATURE, TF (K)◆,/,22X,34(◆—◆))
 1080 FORMAT (///,18X,◆PEBBLE AVERAGE SURFACE TEMPERATURE, TS (K)◆,/,17X
     1 ,44(◆—◆))
```

```
1090 FORMAT (///,16X,*MAXIMUM INTERNAL FUELED MATRIX TEMPERATURE (K)*,/
     1 ,15X,48(*-*))
1100 FORMAT (///,12X,*PEBBLE INTERNAL SHELL/MATRIX INTERFACE TEMPERATUR
     1E (K)*,/,11X,56(*-*))
1110 FORMAT (///,11X,*PEBBLE SHELL/MATRIX INTERFACE TEMPERATURE GRADIEN
     1T (K/CM)*,/,10X,59(*-*))
1120 FORMAT (///,23X,*KILOWATTS/PEBBLE INPUT FROM VSOP*,/,22X,34(*-*))
1130 FORMAT (///,22X,*AUXILIARY OUTPUT,  A(I,J,K), K = *,I2,/,21X,37(*-
     1*))
1140 FORMAT (///,19X,*AUXILIARY OUTPUT,  PROPTY(I,J,K), K = *,I2,/,18X,
     1 42(*-*))
1150 FORMAT (//,2X,*EASYPLT DATA FILES CREATED*,/,2X,*USER DESIGNATED R
     1ADIAL LOCATION,  J = *,I2)
1160 FORMAT (//,2X,*EASY3D DATA FILES CREATED*)
1170 FORMAT (//,2X,*CONTOUR PLOT FILM FILE CREATED*)
1180 FORMAT (I5,*,*,F10.4,*,*,F10.4)
1190 FORMAT (F10.4,*,*,F10.4,*,*,F10.4)
1200 FORMAT (//,2X,*TOTAL CP TIME INCLUDING COMPILATION = *,F7.3)
     END
```

```
      SUBROUTINE PLTGRD
C
C     C*************************************************************C
C     C                                                             C
C     C                 PLOTS FINITE DIFFERENCE GRID                C
C     C          MAKES CALLS TO INSTALLATION DEPENDENT ROUTINES     C
C     C                                                             C
C     C*************************************************************C
C
      COMMON /REACTR/ HEIGHT, RADIUS, DKUGEL, FMDOT, QTOT, TINLET,
     1 PINLET, GINLET, REYNIN, ARL, ASQ, AFRIC, BFRIC, VFNOM
C
      COMMON /GEOM/ IN, INM, JN, JNM, Z(25), R(22), IINLET(22), IMIN(22)
     1 , IMAX(22), IEXIT(22), PI, VOLS, RVSOP(22), NDEG
C
      DIMENSION XSCALE(2), YSCALE(2), RP(2), ZP(2)
C
C     ESTABLISH SCALES
C
      XSCALE(1)=R(1)
      XSCALE(2)=R(JN)
      YSCALE(1)=Z(1)
      YSCALE(2)=Z(IN)
C
C     CREATE LABELED BLANK GRID
C
      CALL PLOJB (XSCALE,YSCALE,2,1,1,1,1,RADIUS,HEIGHT,29HDIMENSIONLESS
     1 RADIAL POSITION,-29,22HFINITE DIFFERENCE GRID,22,28HDIMENSIONLESS
     2 AXIAL POSITION,28)
C
C     PLOT GRID LINES
C
      NP=2
      RP(1)=R(1)
      RP(2)=R(JN)
      DO 10 I=1,IN
      ZP(1)=Z(I)
      ZP(2)=Z(I)
   10 CALL PLOT (NP,RP,1,ZP,1,48,1)
      ZP(1)=Z(1)
      ZP(2)=Z(IN)
      DO 20 J=1,JN
      RP(1)=R(J)
      RP(2)=R(J)
   20 CALL PLOT (NP,RP,1,ZP,1,48,1)
C
C     PLOT BED LIMITS
C
      DO 30 J=1,JNM
      RP(1)=R(J)
      RP(2)=R(J+1)
      ZP(1)=IINLET(J)
      ZP(2)=IINLET(J+1)
      CALL PLOT (NP,RP,1,ZP,1,48,1)
      ZP(1)=IEXIT(J)
      ZP(2)=IEXIT(J+1)
   30 CALL PLOT (NP,RP,1,ZP,1,48,1)
      RETURN
      END
```

```
      SUBROUTINE DLNLN (NX,NY)
C
C     C*****************************************************************C
C     C                                                                 C
C     C              MODIFIED LASL SYSTEM ROUTINE (J529A)               C
C     C          ELIMINATES GRID LINES FROM CONTRJB OR PLOJB            C
C     C                   (LINEAR X, LINEAR Y ONLY)                     C
C     C                                                                 C
C     C*****************************************************************C
C
      COMMON /CJE07/ IXL, IXR, IYT, IYB, XL, XR, YT, YB
      CALL GYA (IYT,IYB,IXL)
      CALL GXA (IXL,IXR,IYB)
      IF (NX) 40,20,10
   10 CALL GYA (IYT,IYB,IXR)
   20 IF (NY) 40,40,30
   30 CALL GXA (IXL,IXR,IYT)
   40 RETURN
      END
      SUBROUTINE SBLIN (NNX,NK)
C
C     C*****************************************************************C
C     C                                                                 C
C     C              MODIFIED LASL SYSTEM ROUTINE (J535A)               C
C     C     MAKES PLOJB CALL TO SBLIN THE SAME AS A CALL TO STLIN       C
C     C   USED TO MAKE CONTOUR PLOT ORIGIN IN UPPER LEFT-HAND CORNER    C
C     C                                                                 C
C     C*****************************************************************C
C
      COMMON /CJE07/ IXL, IXR, IYT, IYB, XL, XR, YT, YB
C
      DIMENSION FMT(12), OUT(12)
      DATA (FMT(K),K=1,12) /2H(F,1H ,1H.,1H ,1H),8H(1PE7.0),8H(1PE8.1),8
     1 H(1PE9.2),9H(1PE10.3),9H(1PE11.4),9H(1PE12.5),9H(1PE13.6)/
C
C     DELETED FOUR LINES THAT MAKE SBLIN DIFFERENT FROM STLIN
C
      IY=IYT
      IYDEL=-12
      IF (NK.GT.9) GO TO 10
      NC=MAX0(INT(ALOG10(AMAX1(ABS(XL),ABS(XR)))+.00001)+1,1)
      IF (MIN0(XL,XR).LT.0) NC=NC+1
      IF (NK.GT.0) NC=NC+1
      NC=NC+NK
      ENCODE (10,40,FMT(2)) NC
      ENCODE (10,40,FMT(4)) NK
      K=1
      GO TO 20
   10 K=MIN0(16,MAX0(10,NK))-4
      NC=K+1
   20 ENCODE (20,FMT(K),OUT) XL
      CALL TSP (IXL,IY,1,1H+)
      IXTT=IXL-4*NC+4
      IYC=IY+IYDEL
      CALL TSP (IXTT,IYC,NC,OUT)
      IF (NNX.LE.0) RETURN
      NX=MIN0(NNX,128)
      IXC=IXL
      DDX=FLOAT(IXR-IXL)/NX
      DX=(XR-XL)/NX
      DO 30 I=1,NX
      XC=XL+I*DX
      IXT=IXTT+I*DDX
      IXC=IXL+I*DDX
      ENCODE (20,FMT(K),OUT) XC
      CALL TSP (IXC,IY,1,1H+)
   30 CALL TSP (IXT,IYC,NC,OUT)
      RETURN
C
   40 FORMAT (I2)
      END
```

```
      SUBROUTINE SLLIN (NNY,NK)
C
C     C*****************************************************************C
C     C                                                                 C
C     C              MODIFIED LASL SYSTEM ROUTINE (J533B)               C
C     C   USED TO MAKE CONTOUR PLOT ORIGIN IN UPPER LEFT-HAND CORNER    C
C     C                                                                 C
C     C*****************************************************************C
C
      COMMON /CJE07/ IXL, IXR, IYT, IYB, XL, XR, YT, YB
C
      DIMENSION FMT(14), OUT(2)
      DATA (FMT(K),K=1,14) /6H(F7.0),6H(F8.1),6H(F9.2),7H(F10.3),7H(F11.
     14),7H(F12.5),7H(F13.6),8H(1PE7.0),8H(1PE8.1),8H(1PE9.2),9H(1PE10.3
     2),9H(1PE11.4),9H(1PE12.5),9H(1PE13.6)/
      IF (NK.GT.6) GO TO 10
      K=MIN0(6,MAX0(0,NK))+1
      NC=K+6
      GO TO 20
   10 K=MIN0(16,MAX0(10,NK))-2
      NC=K-1
   20 A=FMT(K)
      ENCODE (20,A,OUT) YB
      IXT=IXL-8*NC-4
C
C     CHANGED IYB TO IYT IN CALL TO TSP
C
      CALL TSP (IXT,IYT,NC,OUT)
      CALL TSP (IXL,IYT,1,1H+)
      IF (NNY.LE.0) RETURN
      NY=MIN0(128,NNY)
C
C     CHANGED IYC=IYB TO IYC=IYT
C
      IYC=IYT
      DY=(YT-YB)/NY
      DDY=FLOAT(IYT-IYB)/NY
      DO 30 I=1,NY
      YC=YB+I*DY
C
C     IYC USED TO BE = IYB+I*DDY
C
      IYC=IYT-I*DDY
      ENCODE (20,A,OUT) YC
      CALL TSP (IXT,IYC,NC,OUT)
   30 CALL TSP (IXL,IYC,1,1H+)
      RETURN
      END
```

APPENDIX C. PRINT OUTPUT FOR ANALYSIS OF KFA DESIGN CASE 1013

```
OLD,PEBBLE
/FUN,N,I=PEBBLE
CTIME 010.417 SEC.  FUN LASL20
/SETTL,200
$SETTL,200.
/LGO

 STARTING TIME AFTER COMPILATION = 11.143
```

PROGRAM CONTROL VARIABLES

IN	JN	VOLS	NSWP1	NSWP2	NSWP3
25	22	18	1	2	5
NSWP4	**CC**	**RP(1)**	**RP(2)**	**RP(3)**	**RP(4)**
1	.00500	1.000	.250	.0025	1.000

NUMERICAL CONVERGENCE INFORMATION

MAJOR ITERATION	EXECUTION CP TIME	EQUATION NUMBER	MAXIMUM RESIDUAL	LOCATION I INDEX	LOCATION J INDEX
1	2.671 SEC	1	.001619	24	18
		2	-.079847	2	21
		3	.669533	2	7
		4	.000028	4	19
2	4.432 SEC	1	.000622	6	18
		2	-.012783	3	2
		3	.204387	3	19
		4	-.000074	24	20
3	6.184 SEC	1	.000380	22	17
		2	-.009288	5	2
		3	.104437	5	6
		4	-.000053	24	19
4	7.908 SEC	1	-.000292	7	13
		2	-.006311	6	2
		3	.078890	16	18
		4	-.000044	24	19
5	9.644 SEC	1	-.000336	8	2
		2	-.004744	8	2
		3	.074132	18	18
		4	-.000039	24	18
6	11.386 SEC	1	-.000292	10	2
		2	-.003774	10	2
		3	-.071604	10	19
		4	-.000035	24	2

7	13.114 SEC	1	-.000268	12	2
		2	-.003147	11	2
		3	-.073582	11	19
		4	-.000033	24	2
8	14.838 SEC	1	-.000256	14	2
		2	-.002558	13	2
		3	-.072965	11	19
		4	-.000031	24	2
9	16.572 SEC	1	-.000248	16	2
		2	-.002218	15	16
		3	-.069812	13	16
		4	-.000030	24	2
10	18.355 SEC	1	-.000243	18	2
		2	-.001867	16	16
		3	-.062590	15	16
		4	-.000028	24	2
11	20.104 SEC	1	-.000239	19	2
		2	-.001654	18	16
		3	-.058436	16	16
		4	-.000027	24	2
12	21.834 SEC	1	-.000238	21	2
		2	-.001470	19	16
		3	-.054289	17	16
		4	-.000026	24	2
13	23.595 SEC	1	-.000241	24	2
		2	-.001325	21	16
		3	-.050387	19	16
		4	-.000025	24	2
14	25.370 SEC	1	-.000239	24	2
		2	-.001250	24	16
		3	-.047558	20	16
		4	-.000024	24	2
15	27.105 SEC	1	-.000228	24	2
		2	-.001331	24	16
		3	-.044362	21	16
		4	-.000023	24	2
16	28.790 SEC	1	-.000213	9	3
		2	-.001266	24	16
		3	-.042301	22	16
		4	-.000022	24	2
17	30.544 SEC	1	-.000211	8	2
		2	-.001101	24	16
		3	-.040207	24	16
		4	-.000021	24	2
18	32.315 SEC	1	-.000208	8	2
		2	-.000889	24	15
		3	-.036372	24	16
		4	-.000020	24	2

19	34.044 SEC	1	-.000205	8	2
		2	-.000682	24	15
		3	-.030657	24	16
		4	-.000019	24	2
20	35.776 SEC	1	-.000201	8	2
		2	-.000499	24	15
		3	-.024584	24	15
		4	-.000018	24	2
21	37.531 SEC	1	-.000197	8	2
		2	-.000353	24	15
		3	-.018921	24	15
		4	-.000017	24	2
22	39.273 SEC	1	-.000193	8	2
		2	-.000246	24	15
		3	-.014092	24	15
		4	-.000017	24	2
23	41.052 SEC	1	-.000188	8	2
		2	-.000172	24	15
		3	-.010279	24	15
		4	-.000016	24	2
24	42.813 SEC	1	-.000184	8	2
		2	-.000123	24	15
		3	-.007435	24	15
		4	-.000016	24	2
25	44.552 SEC	1	-.000179	9	2
		2	.000095	22	2
		3	-.005402	24	15
		4	-.000015	24	2
26	46.303 SEC	1	-.000175	9	2
		2	.000088	22	2
		3	-.003989	24	15
		4	-.000015	24	2

PEBBLE BED REACTOR THERMAL/HYDRAULIC ANALYSIS CASE 1013

COOLANT MASS FLOW (KG/S)	THERMAL POWER (MW)	INLET PLENUM PRESSURE (MPA)	MIXED MEAN INLET COOLANT TEMPERATURE (K)
785	3006	4.0	523

BED RADIUS (M)	BED HEIGHT (M)	NOMINAL VOID FRACTION
4.61	5.00	.39

FUEL/MODERATOR ELEMENT TYPE	PEBBLE DIAMETER (M)	INNER MATRIX INTERFACE RADIUS (M)	OUTER MATRIX INTERFACE RADIUS (M)
SHELL	.060	.0150	.0250

MAXIMUM POWER/BALL (KW/BALL)	LOCATION RADIUS / DEPTH FROM TOP (M)
4.85	4.610 / .417

CALCULATED VALUES

INLET REYNOLDS NUMBER	MIXED MEAN OUTLET PRESSURE (MPA)	CORE PRESSURE DROP (MPA)
24009	3.930	.0700

MIXED MEAN OUTLET COOLANT TEMPERATURE (K)	FIRST LAW ERROR (PERCENT)
1259	-.2

MAXIMUM OUTLET COOLANT TEMPERATURE (K)	RADIAL LOCATION (M)
1300	3.951

MAXIMUM FUELED MATRIX TEMPERATURE IN CORE (K)	LOCATION, RADIUS / DEPTH FROM TOP (M)
1357	3.951 / 1.667

MAXIMUM INTERNAL SHELL/MATRIX INTERFACE TEMPERATURE GRADIENT (K/CM)	LOCATION, RADIUS / DEPTH FROM TOP (M)
-299	4.610 / .625

DIMENSIONLESS STREAM FUNCTION

AXIAL POSITION	RADIAL POSITION										
	0.000	.048	.095	.143	.190	.238	.286	.333	.381	.429	.476
0.000	0.000	.001	.005	.010	.018	.028	.041	.055	.072	.091	.113
.042	0.000	.001	.005	.010	.018	.028	.041	.055	.072	.091	.113
.083	0.000	.001	.005	.010	.018	.028	.041	.055	.072	.091	.113
.125	0.000	.001	.005	.010	.018	.028	.041	.055	.072	.091	.113
.167	0.000	.001	.005	.010	.018	.028	.041	.055	.072	.091	.113
.208	0.000	.001	.005	.010	.018	.028	.041	.055	.072	.091	.113
.250	0.000	.001	.005	.010	.018	.028	.041	.055	.072	.091	.113
.292	0.000	.001	.005	.010	.018	.028	.041	.055	.072	.091	.113
.333	0.000	.001	.005	.010	.018	.028	.041	.055	.072	.091	.113
.375	0.000	.001	.005	.010	.018	.028	.041	.055	.072	.091	.113
.417	0.000	.001	.005	.010	.018	.028	.041	.055	.072	.091	.113
.458	0.000	.001	.005	.010	.018	.028	.041	.055	.072	.091	.113
.500	0.000	.001	.005	.010	.018	.028	.041	.055	.072	.091	.113
.542	0.000	.001	.005	.010	.018	.028	.041	.055	.072	.091	.113
.583	0.000	.001	.005	.010	.018	.028	.041	.055	.072	.091	.113
.625	0.000	.001	.005	.010	.018	.028	.041	.055	.072	.091	.113
.667	0.000	.001	.005	.010	.018	.028	.041	.055	.072	.091	.113
.708	0.000	.001	.005	.010	.018	.028	.041	.055	.072	.091	.113
.750	0.000	.001	.005	.010	.018	.028	.041	.055	.072	.091	.113
.792	0.000	.001	.005	.010	.018	.028	.041	.055	.072	.091	.113
.833	0.000	.001	.005	.010	.018	.028	.041	.055	.072	.091	.113
.875	0.000	.001	.005	.010	.018	.028	.041	.055	.072	.091	.113
.917	0.000	.001	.005	.010	.018	.028	.041	.055	.072	.091	.113
.958	0.000	.001	.005	.010	.018	.028	.041	.055	.072	.091	.113
1.000	0.000	.001	.005	.010	.018	.028	.041	.055	.072	.091	.113

DIMENSIONLESS STREAM FUNCTION

AXIAL POSITION	RADIAL POSITION										
	.524	.571	.619	.667	.714	.762	.810	.857	.905	.952	1.000
0.000	.137	.163	.191	.222	.255	.291	.329	.368	.410	.454	.500
.042	.137	.163	.191	.222	.255	.291	.329	.368	.410	.454	.500
.083	.137	.163	.191	.222	.255	.291	.329	.368	.410	.454	.500
.125	.137	.163	.191	.222	.255	.291	.329	.368	.409	.454	.500
.167	.137	.163	.191	.222	.255	.291	.329	.368	.409	.453	.500
.208	.137	.163	.191	.222	.255	.291	.329	.368	.409	.453	.500
.250	.137	.163	.191	.222	.255	.291	.328	.368	.409	.453	.500
.292	.137	.163	.191	.222	.255	.291	.328	.368	.409	.453	.500
.333	.137	.163	.191	.222	.255	.290	.328	.368	.409	.453	.500
.375	.137	.163	.191	.222	.255	.290	.328	.368	.409	.453	.500
.417	.137	.163	.191	.222	.255	.290	.328	.367	.409	.453	.500
.458	.137	.163	.191	.222	.255	.290	.328	.367	.408	.453	.500
.500	.137	.163	.191	.222	.255	.290	.328	.367	.408	.453	.500
.542	.137	.163	.191	.222	.255	.290	.328	.367	.408	.453	.500
.583	.137	.163	.191	.222	.255	.290	.328	.367	.408	.453	.500
.625	.137	.163	.191	.222	.255	.290	.328	.367	.408	.453	.500
.667	.137	.163	.191	.222	.255	.290	.328	.367	.408	.453	.500
.708	.137	.163	.191	.222	.255	.290	.328	.367	.408	.453	.500
.750	.137	.163	.191	.222	.255	.290	.328	.367	.408	.453	.500
.792	.137	.163	.191	.222	.255	.290	.328	.367	.408	.453	.500
.833	.137	.163	.191	.222	.255	.290	.328	.367	.408	.453	.500
.875	.137	.163	.191	.222	.255	.290	.328	.367	.408	.453	.500
.917	.137	.163	.191	.222	.255	.290	.328	.367	.408	.453	.500
.958	.137	.163	.191	.222	.255	.290	.328	.367	.408	.453	.500
1.000	.137	.163	.191	.222	.255	.290	.328	.367	.408	.453	.500

DIMENSIONLESS MASS FLUX, GSTAP

AXIAL POSITION	RADIAL POSITION										
	0.000	.048	.095	.143	.190	.238	.286	.333	.381	.429	.476
0.000	.996	.996	.996	.996	.996	.996	.996	.996	.997	.998	.998
.042	.996	.996	.996	.996	.996	.996	.996	.997	.997	.998	.999
.083	.996	.996	.996	.996	.996	.996	.996	.996	.997	.997	.998
.125	.996	.996	.996	.995	.995	.996	.996	.996	.997	.997	.998
.167	.996	.996	.995	.995	.995	.995	.996	.996	.997	.997	.998
.208	.996	.995	.995	.995	.995	.995	.996	.996	.996	.997	.998
.250	.995	.995	.995	.995	.995	.995	.996	.996	.996	.997	.998
.292	.995	.995	.995	.995	.995	.995	.996	.996	.996	.997	.998
.333	.995	.995	.995	.995	.995	.995	.996	.996	.996	.997	.998
.375	.995	.995	.995	.995	.995	.995	.996	.996	.996	.997	.998
.417	.995	.995	.995	.995	.995	.995	.996	.996	.996	.997	.998
.458	.995	.995	.995	.995	.995	.995	.996	.996	.996	.997	.998
.500	.995	.995	.995	.995	.995	.995	.996	.996	.996	.997	.998
.542	.996	.995	.995	.995	.995	.995	.996	.996	.996	.997	.998
.583	.996	.995	.995	.995	.995	.996	.996	.996	.996	.997	.998
.625	.996	.996	.995	.995	.995	.996	.996	.996	.996	.997	.998
.667	.996	.996	.995	.995	.995	.996	.996	.996	.996	.997	.998
.708	.996	.996	.995	.995	.995	.996	.996	.996	.996	.997	.998
.750	.996	.996	.995	.995	.995	.996	.996	.996	.996	.997	.998
.792	.996	.996	.996	.995	.996	.996	.996	.996	.997	.997	.998
.833	.996	.996	.996	.995	.996	.996	.996	.996	.997	.997	.998
.875	.996	.996	.996	.996	.996	.996	.996	.996	.997	.997	.998
.917	.996	.996	.996	.996	.996	.996	.996	.996	.997	.997	.998
.958	.996	.996	.996	.996	.996	.996	.996	.996	.997	.997	.998
1.000	.996	.996	.996	.995	.996	.996	.996	.996	.996	.997	.997

DIMENSIONLESS MASS FLUX, GSTAR

AXIAL POSITION	RADIAL POSITION										
	.524	.571	.619	.667	.714	.762	.810	.857	.905	.952	1.000
0.000	1.000	1.001	1.004	1.006	1.009	1.012	1.004	.994	.994	.996	0.000
.042	1.000	1.001	1.004	1.006	1.009	1.012	1.004	.994	.994	.996	0.000
.083	1.000	1.001	1.004	1.006	1.009	1.012	1.004	.992	.993	.997	0.000
.125	1.000	1.001	1.004	1.006	1.009	1.013	1.003	.990	.993	.999	0.000
.167	.999	1.001	1.004	1.006	1.009	1.013	1.003	.988	.992	1.001	0.000
.208	.999	1.001	1.004	1.006	1.009	1.013	1.002	.986	.991	1.003	0.000
.250	.999	1.001	1.004	1.006	1.009	1.013	1.001	.985	.991	1.004	0.000
.292	.999	1.001	1.004	1.006	1.009	1.012	1.000	.984	.991	1.006	0.000
.333	.999	1.001	1.003	1.006	1.009	1.012	1.000	.984	.991	1.007	0.000
.375	.999	1.001	1.003	1.006	1.008	1.011	.999	.983	.991	1.008	0.000
.417	.999	1.001	1.003	1.006	1.008	1.011	.999	.983	.991	1.008	0.000
.458	.999	1.000	1.003	1.006	1.008	1.010	.998	.983	.992	1.009	0.000
.500	.999	1.000	1.003	1.006	1.008	1.010	.998	.983	.992	1.010	0.000
.542	.999	1.000	1.003	1.005	1.008	1.009	.998	.983	.992	1.010	0.000
.583	.999	1.000	1.003	1.005	1.008	1.009	.997	.983	.992	1.010	0.000
.625	.999	1.000	1.003	1.005	1.008	1.009	.997	.983	.992	1.010	0.000
.667	.999	1.000	1.003	1.005	1.007	1.008	.997	.984	.993	1.010	0.000
.708	.999	1.000	1.003	1.005	1.007	1.008	.997	.984	.993	1.010	0.000
.750	.999	1.000	1.003	1.005	1.007	1.008	.997	.984	.993	1.010	0.000
.792	.999	1.000	1.003	1.005	1.007	1.007	.997	.985	.993	1.010	0.000
.833	.999	1.000	1.003	1.005	1.007	1.007	.996	.985	.994	1.010	0.000
.875	.999	1.000	1.003	1.005	1.007	1.007	.996	.986	.994	1.010	0.000
.917	.999	1.000	1.003	1.005	1.007	1.006	.996	.986	.994	1.009	0.000
.958	.999	1.000	1.003	1.005	1.007	1.006	.996	.986	.994	1.009	0.000
1.000	.999	1.000	1.002	1.005	1.007	1.006	.996	.986	.994	1.009	0.000

AXIAL COMPONENT OF DIMENSIONLESS MASS FLUX, GZSTAR

AXIAL POSITION	RADIAL POSITION										
	0.000	.048	.095	.143	.190	.238	.286	.333	.381	.429	.476
0.000	.996	.996	.996	.996	.996	.996	.996	.996	.997	.998	.998
.042	.996	.996	.996	.996	.996	.996	.996	.997	.997	.998	.999
.083	.996	.996	.996	.996	.996	.996	.996	.996	.997	.997	.998
.125	.996	.996	.996	.995	.995	.996	.996	.996	.997	.997	.998
.167	.996	.996	.995	.995	.995	.995	.996	.996	.997	.997	.998
.208	.996	.995	.995	.995	.995	.995	.996	.996	.996	.997	.998
.250	.995	.995	.995	.995	.995	.995	.996	.996	.996	.997	.998
.292	.995	.995	.995	.995	.995	.995	.996	.996	.996	.997	.998
.333	.995	.995	.995	.995	.995	.995	.996	.996	.996	.997	.998
.375	.995	.995	.995	.995	.995	.995	.996	.996	.996	.997	.998
.417	.995	.995	.995	.995	.995	.995	.996	.996	.996	.997	.998
.458	.995	.995	.995	.995	.995	.995	.996	.996	.996	.997	.998
.500	.995	.995	.995	.995	.995	.995	.996	.996	.996	.997	.998
.542	.996	.995	.995	.995	.995	.995	.996	.996	.996	.997	.998
.583	.996	.995	.995	.995	.995	.996	.996	.996	.996	.997	.998
.625	.996	.996	.995	.995	.995	.996	.996	.996	.996	.997	.998
.667	.996	.996	.995	.995	.995	.996	.996	.996	.996	.997	.998
.708	.996	.996	.995	.995	.995	.996	.996	.996	.996	.997	.998
.750	.996	.996	.995	.995	.995	.996	.996	.996	.996	.997	.998
.792	.996	.996	.996	.995	.996	.996	.996	.996	.997	.997	.998
.833	.996	.996	.996	.995	.996	.996	.996	.996	.997	.997	.998
.875	.996	.996	.996	.996	.996	.996	.996	.996	.997	.997	.998
.917	.996	.996	.996	.996	.996	.996	.996	.996	.997	.997	.998
.958	.996	.996	.996	.996	.996	.996	.996	.996	.997	.997	.998
1.000	.996	.996	.996	.995	.996	.996	.996	.996	.996	.997	.997

AXIAL COMPONENT OF DIMENSIONLESS MASS FLUX, GZSTAR

AXIAL POSITION	RADIAL POSITION										
	.524	.571	.619	.667	.714	.762	.810	.857	.905	.952	1.000
0.000	1.000	1.001	1.004	1.006	1.009	1.012	1.004	.994	.994	.996	0.000
.042	1.000	1.001	1.004	1.006	1.009	1.012	1.004	.994	.994	.996	0.000
.083	1.000	1.001	1.004	1.006	1.009	1.012	1.004	.992	.993	.997	0.000
.125	1.000	1.001	1.004	1.006	1.009	1.013	1.003	.990	.993	.999	0.000
.167	.999	1.001	1.004	1.006	1.009	1.013	1.003	.988	.992	1.001	0.000
.208	.999	1.001	1.004	1.006	1.009	1.013	1.002	.986	.991	1.003	0.000
.250	.999	1.001	1.004	1.006	1.009	1.013	1.001	.985	.991	1.004	0.000
.292	.999	1.001	1.004	1.006	1.009	1.012	1.000	.984	.991	1.006	0.000
.333	.999	1.001	1.003	1.006	1.009	1.012	1.000	.984	.991	1.007	0.000
.375	.999	1.001	1.003	1.006	1.008	1.011	.999	.983	.991	1.008	0.000
.417	.999	1.001	1.003	1.006	1.008	1.011	.999	.983	.991	1.008	0.000
.458	.999	1.000	1.003	1.006	1.008	1.010	.998	.983	.992	1.009	0.000
.500	.999	1.000	1.003	1.006	1.008	1.010	.998	.983	.992	1.010	0.000
.542	.999	1.000	1.003	1.005	1.008	1.009	.998	.983	.992	1.010	0.000
.583	.999	1.000	1.003	1.005	1.008	1.009	.997	.983	.992	1.010	0.000
.625	.999	1.000	1.003	1.005	1.008	1.009	.997	.983	.992	1.010	0.000
.667	.999	1.000	1.003	1.005	1.007	1.008	.997	.984	.993	1.010	0.000
.708	.999	1.000	1.003	1.005	1.007	1.008	.997	.984	.993	1.010	0.000
.750	.999	1.000	1.003	1.005	1.007	1.008	.997	.984	.993	1.010	0.000
.792	.999	1.000	1.003	1.005	1.007	1.007	.997	.985	.993	1.010	0.000
.833	.999	1.000	1.003	1.005	1.007	1.007	.996	.985	.994	1.010	0.000
.875	.999	1.000	1.003	1.005	1.007	1.007	.996	.986	.994	1.010	0.000
.917	.999	1.000	1.003	1.005	1.007	1.006	.996	.986	.994	1.009	0.000
.958	.999	1.000	1.003	1.005	1.007	1.006	.996	.986	.994	1.009	0.000
1.000	.999	1.000	1.002	1.005	1.007	1.006	.996	.986	.994	1.009	0.000

RADIAL COMPONENT OF DIMENSIONLESS MASS FLUX, GRSTAR

AXIAL POSITION	RADIAL POSITION										
	0.000	.048	.095	.143	.190	.238	.286	.333	.381	.429	.476
0.000	0.000	-0.000	-0.000	-0.000	-0.000	-0.000	-0.000	-0.000	-0.000	-0.000	-0.000
.042	0.000	.000	.000	.000	.000	.000	.001	.001	.001	.001	.001
.083	0.000	.000	.000	.000	.000	.001	.001	.001	.001	.001	.001
.125	0.000	.000	.000	.000	.000	.001	.001	.001	.001	.001	.001
.167	0.000	.000	.000	.000	.000	.000	.000	.001	.001	.001	.001
.208	0.000	.000	.000	.000	.000	.000	.000	.000	.000	.001	.001
.250	0.000	.000	.000	.000	.000	.000	.000	.000	.000	.000	.000
.292	0.000	.000	.000	.000	.000	.000	.000	.000	.000	.000	.000
.333	0.000	.000	.000	.000	.000	.000	.000	.000	.000	.000	.000
.375	0.000	-.000	-.000	-.000	-.000	-.000	-.000	-.000	-.000	-.000	-.000
.417	0.000	-.000	-.000	-.000	-.000	-.000	-.000	-.000	-.000	-.000	-.000
.458	0.000	-.000	-.000	-.000	-.000	-.000	-.000	-.000	-.000	-.000	-.000
.500	0.000	-.000	-.000	-.000	-.000	-.000	-.000	-.000	-.000	-.000	-.000
.542	0.000	-.000	-.000	-.000	-.000	-.000	-.000	-.000	-.000	-.000	-.000
.583	0.000	-.000	-.000	-.000	-.000	-.000	-.000	-.000	-.000	-.000	-.000
.625	0.000	-.000	-.000	-.000	-.000	-.000	-.000	-.000	-.000	-.000	-.000
.667	0.000	-.000	-.000	-.000	-.000	-.000	-.000	-.000	-.000	-.000	-.000
.708	0.000	-.000	-.000	-.000	-.000	-.000	-.000	-.000	-.000	-.000	-.000
.750	0.000	-.000	-.000	-.000	-.000	-.000	-.000	-.000	-.000	-.000	-.000
.792	0.000	-.000	-.000	-.000	-.000	-.000	-.000	-.000	-.000	-.000	-.000
.833	0.000	-.000	-.000	-.000	-.000	-.000	-.000	-.000	-.000	-.000	-.000
.875	0.000	-.000	-.000	-.000	-.000	-.000	-.000	-.000	-.000	-.000	-.000
.917	0.000	-.000	-.000	-.000	-.000	-.000	-.000	-.000	-.000	-.000	-.000
.958	0.000	-.000	-.000	-.000	-.000	-.000	-.000	-.000	-.000	-.000	-.000
1.000	0.000	-0.000	-0.000	-0.000	-0.000	-0.000	-0.000	-0.000	-0.000	-0.000	-0.000

RADIAL COMPONENT OF DIMENSIONLESS MASS FLUX, GRSTAR

AXIAL POSITION	RADIAL POSITION										
	.524	.571	.619	.667	.714	.762	.810	.857	.905	.952	1.000
0.000	-0.000	-0.000	-0.000	-0.000	-0.000	-0.000	-0.000	-0.000	-0.000	-0.000	0.000
.042	.001	.001	.001	.000	.000	.000	-.000	.001	.002	.001	0.000
.083	.001	.001	.001	.001	.001	.000	-.000	.001	.003	.002	0.000
.125	.001	.001	.001	.001	.001	.000	-.000	.002	.004	.003	0.000
.167	.001	.001	.001	.001	.001	.001	.000	.002	.004	.003	0.000
.208	.001	.001	.001	.001	.001	.001	.001	.002	.004	.003	0.000
.250	.000	.001	.001	.001	.001	.001	.001	.002	.003	.002	0.000
.292	.000	.000	.001	.001	.001	.001	.002	.002	.003	.002	0.000
.333	.000	.000	.000	.000	.001	.001	.002	.002	.002	.002	0.000
.375	.000	.000	.000	.000	.000	.001	.001	.002	.002	.001	0.000
.417	-.000	-.000	.000	.000	.000	.001	.001	.001	.002	.001	0.000
.458	-.000	-.000	-.000	.000	.000	.000	.001	.001	.001	.001	0.000
.500	-.000	-.000	-.000	.000	.000	.000	.001	.001	.001	.001	0.000
.542	-.000	-.000	-.000	-.000	.000	.000	.001	.001	.001	.000	0.000
.583	-.000	-.000	-.000	-.000	.000	.000	.001	.001	.000	.000	0.000
.625	-.000	-.000	-.000	-.000	.000	.000	.001	.001	.000	.000	0.000
.667	-.000	-.000	-.000	-.000	-.000	.000	.001	.001	-.000	-.000	0.000
.708	-.000	-.000	-.000	-.000	-.000	.000	.001	.000	-.000	-.000	0.000
.750	-.000	-.000	-.000	-.000	.000	.000	.001	.000	-.000	-.000	0.000
.792	-.000	-.000	-.000	-.000	-.000	.000	.001	.000	-.000	-.000	0.000
.833	-.000	-.000	-.000	-.000	-.000	.000	.001	.000	-.000	-.000	0.000
.875	-.000	-.000	-.000	-.000	-.000	.000	.001	.000	-.000	-.000	0.000
.917	-.000	-.000	-.000	-.000	-.000	.000	.000	.000	-.000	-.000	0.000
.958	-.000	-.000	-.000	-.000	-.000	-.000	.000	.000	-.000	-.000	0.000
1.000	-0.000	-0.000	-0.000	-0.000	-0.000	-0.000	-0.000	-0.000	-0.000	-0.000	0.000

DIMENSIONLESS COOLANT PRESSURE, PSTAR

AXIAL POSITION	RADIAL POSITION										
	0.000	.048	.095	.143	.190	.238	.286	.333	.381	.429	.476
0.000	1.000	1.000	1.000	1.000	1.000	1.000	1.000	1.000	1.000	1.000	1.000
.042	.999	.999	.999	.999	.999	.999	.999	.999	.999	.999	.999
.083	.999	.999	.999	.999	.999	.999	.999	.999	.999	.999	.999
.125	.998	.998	.998	.998	.998	.998	.998	.998	.998	.998	.998
.167	.998	.998	.998	.998	.998	.998	.998	.998	.998	.998	.998
.208	.997	.997	.997	.997	.997	.997	.997	.997	.997	.997	.997
.250	.996	.996	.996	.996	.996	.996	.996	.996	.996	.996	.996
.292	.995	.995	.996	.996	.996	.996	.996	.996	.996	.996	.996
.333	.995	.995	.995	.995	.995	.995	.995	.995	.995	.995	.995
.375	.994	.994	.994	.994	.994	.994	.994	.994	.994	.994	.994
.417	.993	.993	.993	.993	.993	.993	.993	.993	.993	.993	.993
.458	.993	.993	.993	.993	.993	.993	.993	.993	.993	.993	.993
.500	.992	.992	.992	.992	.992	.992	.992	.992	.992	.992	.992
.542	.991	.991	.991	.991	.991	.991	.991	.991	.991	.991	.991
.583	.990	.990	.990	.990	.990	.990	.990	.990	.990	.990	.990
.625	.990	.990	.990	.990	.990	.990	.990	.990	.990	.990	.990
.667	.989	.989	.989	.989	.989	.989	.989	.989	.989	.989	.989
.708	.988	.988	.988	.988	.988	.988	.988	.988	.988	.988	.988
.750	.988	.988	.988	.987	.987	.987	.987	.987	.987	.987	.987
.792	.987	.987	.987	.987	.987	.987	.987	.987	.987	.987	.987
.833	.986	.986	.986	.986	.986	.986	.986	.986	.986	.986	.986
.875	.985	.985	.985	.985	.985	.985	.985	.985	.985	.985	.985
.917	.984	.984	.984	.984	.984	.984	.984	.984	.984	.984	.984
.958	.983	.983	.983	.983	.983	.983	.983	.983	.983	.983	.983
1.000	.982	.982	.982	.982	.982	.982	.982	.982	.982	.982	.982

DIMENSIONLESS COOLANT PRESSURE, PSTAR

AXIAL POSITION	RADIAL POSITION										
	.524	.571	.619	.667	.714	.762	.810	.857	.905	.952	1.000
0.000	1.000	1.000	1.000	1.000	1.000	1.000	1.000	1.000	1.000	1.000	1.000
.042	.999	.999	.999	.999	.999	.999	.999	.999	.999	.999	.999
.083	.999	.999	.999	.999	.999	.999	.999	.999	.999	.999	.999
.125	.998	.998	.998	.998	.998	.998	.998	.998	.998	.998	.998
.167	.998	.998	.998	.998	.998	.998	.998	.998	.998	.998	.998
.208	.997	.997	.997	.997	.997	.997	.997	.997	.997	.997	.997
.250	.996	.996	.996	.996	.996	.996	.996	.996	.996	.996	.996
.292	.996	.996	.996	.996	.996	.996	.996	.996	.996	.996	.996
.333	.995	.995	.995	.995	.995	.995	.995	.995	.995	.995	.995
.375	.994	.994	.994	.994	.994	.994	.994	.994	.994	.994	.994
.417	.993	.993	.993	.993	.993	.993	.993	.993	.993	.993	.993
.458	.993	.993	.993	.993	.993	.993	.993	.993	.993	.993	.993
.500	.992	.992	.992	.992	.992	.992	.992	.992	.992	.992	.992
.542	.991	.991	.991	.991	.991	.991	.991	.991	.991	.991	.991
.583	.990	.990	.990	.990	.990	.990	.990	.990	.990	.990	.990
.625	.990	.990	.990	.990	.990	.990	.990	.990	.990	.990	.990
.667	.989	.989	.989	.989	.989	.989	.989	.989	.989	.989	.989
.708	.988	.988	.988	.988	.988	.988	.988	.988	.988	.988	.988
.750	.987	.987	.987	.987	.987	.987	.987	.987	.987	.987	.987
.792	.987	.987	.987	.987	.987	.987	.987	.987	.987	.987	.987
.833	.986	.986	.986	.986	.986	.986	.986	.986	.986	.986	.986
.875	.985	.985	.985	.985	.985	.985	.985	.985	.985	.985	.985
.917	.984	.984	.984	.984	.984	.984	.984	.984	.984	.984	.984
.958	.983	.983	.983	.983	.983	.983	.983	.983	.983	.983	.983
1.000	.982	.982	.982	.982	.982	.982	.982	.982	.982	.982	.982

COOLANT BULK TEMPERATURE, TF (K)

AXIAL POSITION	RADIAL POSITION										
	0.000	.048	.095	.143	.190	.238	.286	.333	.381	.429	.476
0.000	537	537	537	537	537	537	537	537	537	537	537
.042	610	610	610	610	610	610	609	609	608	608	607
.083	691	691	691	691	690	690	689	688	688	686	685
.125	771	771	771	771	771	770	769	768	767	766	764
.167	847	847	847	847	847	846	845	844	842	841	838
.208	915	915	915	915	914	913	912	910	909	907	905
.250	974	974	975	975	974	973	971	970	968	966	964
.292	1026	1026	1026	1026	1026	1024	1023	1021	1019	1018	1015
.333	1071	1071	1071	1071	1070	1069	1067	1065	1063	1062	1059
.375	1108	1108	1108	1108	1107	1106	1104	1102	1100	1099	1096
.417	1139	1139	1139	1139	1139	1137	1135	1133	1131	1130	1127
.458	1165	1165	1165	1165	1164	1163	1161	1159	1157	1156	1152
.500	1186	1186	1186	1186	1186	1184	1182	1180	1179	1177	1174
.542	1204	1204	1204	1204	1203	1201	1200	1198	1196	1194	1191
.583	1218	1218	1218	1218	1217	1216	1214	1212	1210	1209	1206
.625	1230	1230	1230	1230	1229	1227	1226	1224	1222	1221	1217
.667	1240	1240	1240	1240	1239	1237	1236	1234	1232	1231	1227
.708	1248	1248	1248	1248	1247	1245	1244	1242	1240	1239	1235
.750	1254	1254	1254	1254	1253	1252	1250	1248	1247	1245	1242
.792	1260	1260	1260	1260	1259	1257	1256	1254	1252	1251	1247
.833	1264	1264	1264	1264	1263	1262	1260	1258	1257	1255	1252
.875	1268	1268	1268	1268	1267	1266	1264	1262	1261	1259	1256
.917	1272	1272	1272	1271	1271	1269	1268	1266	1264	1263	1260
.958	1275	1275	1275	1275	1274	1273	1271	1269	1268	1266	1263
1.000	1279	1279	1279	1278	1278	1276	1275	1273	1271	1270	1267

COOLANT BULK TEMPERATURE, TF (K)

AXIAL POSITION	RADIAL POSITION										
	.524	.571	.619	.667	.714	.762	.810	.857	.905	.952	1.000
0.000	536	536	536	536	535	535	536	538	537	538	538
.042	606	605	604	602	600	598	602	615	612	614	614
.083	684	682	679	676	674	669	675	698	691	691	691
.125	762	759	756	751	749	742	749	782	769	766	766
.167	836	832	829	823	820	812	821	862	844	835	835
.208	901	898	893	887	884	874	886	935	912	896	896
.250	960	956	951	944	942	931	944	998	972	949	949
.292	1011	1006	1002	993	992	980	995	1053	1023	994	994
.333	1054	1050	1045	1036	1035	1023	1038	1099	1067	1033	1033
.375	1091	1087	1082	1073	1071	1059	1076	1138	1104	1067	1067
.417	1122	1118	1113	1103	1102	1090	1107	1170	1135	1094	1094
.458	1148	1143	1138	1129	1128	1116	1134	1197	1161	1117	1117
.500	1169	1165	1160	1150	1149	1138	1157	1219	1183	1137	1137
.542	1186	1182	1177	1167	1166	1156	1175	1237	1201	1153	1153
.583	1201	1197	1191	1182	1181	1171	1191	1251	1216	1166	1166
.625	1213	1209	1203	1194	1193	1183	1204	1262	1227	1177	1177
.667	1222	1218	1213	1204	1202	1194	1215	1271	1237	1187	1187
.708	1231	1227	1221	1212	1210	1203	1224	1278	1245	1195	1195
.750	1237	1233	1228	1219	1217	1210	1232	1283	1251	1202	1202
.792	1243	1239	1233	1224	1223	1216	1238	1288	1256	1208	1208
.833	1248	1243	1238	1229	1227	1222	1243	1291	1261	1213	1213
.875	1252	1247	1242	1233	1231	1226	1248	1293	1264	1217	1217
.917	1255	1251	1246	1237	1235	1231	1252	1295	1267	1221	1221
.958	1259	1255	1249	1241	1238	1235	1256	1298	1270	1225	1225
1.000	1262	1258	1253	1244	1242	1239	1260	1300	1273	1229	1229

PEBBLE AVERAGE SURFACE TEMPERATURE, TS (K)

AXIAL POSITION	RADIAL POSITION										
	0.000	.048	.095	.143	.190	.238	.286	.333	.381	.429	.476
0.000	669	669	669	669	669	669	668	667	667	665	664
.042	756	756	756	756	755	754	753	752	751	749	748
.083	842	842	842	842	841	840	839	838	837	835	833
.125	917	917	917	917	917	915	914	912	911	909	907
.167	980	980	980	980	979	978	977	975	973	971	969
.208	1031	1031	1031	1031	1030	1029	1027	1026	1024	1022	1019
.250	1075	1075	1075	1075	1075	1073	1071	1070	1068	1066	1063
.292	1113	1113	1113	1113	1112	1110	1109	1107	1105	1103	1100
.333	1144	1144	1144	1144	1143	1142	1140	1138	1136	1135	1131
.375	1169	1169	1169	1169	1169	1167	1165	1163	1161	1160	1156
.417	1190	1190	1190	1190	1189	1188	1186	1184	1182	1181	1177
.458	1207	1207	1207	1207	1206	1204	1203	1201	1199	1197	1194
.500	1220	1220	1221	1221	1220	1218	1216	1215	1213	1211	1208
.542	1232	1232	1232	1232	1231	1230	1228	1226	1224	1223	1219
.583	1241	1241	1241	1241	1240	1239	1237	1235	1234	1232	1229
.625	1249	1249	1249	1249	1248	1246	1245	1243	1241	1240	1236
.667	1255	1255	1255	1255	1254	1253	1251	1249	1248	1246	1243
.708	1260	1260	1260	1260	1260	1258	1256	1255	1253	1251	1248
.750	1265	1265	1265	1265	1264	1263	1261	1259	1257	1256	1252
.792	1268	1268	1268	1268	1267	1266	1264	1263	1261	1260	1257
.833	1272	1272	1272	1272	1271	1269	1268	1266	1264	1263	1260
.875	1275	1275	1275	1275	1274	1272	1271	1269	1267	1266	1263
.917	1278	1278	1278	1277	1277	1275	1274	1272	1270	1269	1266
.958	1281	1281	1281	1281	1280	1279	1277	1275	1274	1272	1269
1.000	1285	1285	1285	1284	1284	1282	1281	1279	1277	1276	1273

PEBBLE AVERAGE SURFACE TEMPERATURE, TS (K)

AXIAL POSITION	RADIAL POSITION										
	.524	.571	.619	.667	.714	.762	.810	.857	.905	.952	1.000
0.000	663	661	659	656	653	648	653	674	670	675	675
.042	746	743	740	736	732	725	733	768	758	761	761
.083	830	827	823	818	814	805	814	855	837	833	833
.125	903	900	895	889	886	875	885	935	911	900	900
.167	965	961	956	949	947	934	946	1005	975	955	955
.208	1015	1011	1006	998	996	983	997	1063	1029	999	999
.250	1059	1055	1050	1041	1040	1026	1041	1107	1071	1038	1038
.292	1096	1091	1086	1077	1077	1062	1078	1146	1108	1069	1069
.333	1127	1122	1117	1107	1107	1093	1109	1178	1139	1097	1097
.375	1152	1148	1143	1132	1133	1119	1135	1204	1165	1120	1120
.417	1172	1168	1164	1153	1153	1140	1157	1226	1186	1138	1138
.458	1189	1185	1180	1170	1170	1157	1176	1244	1204	1153	1153
.500	1203	1199	1194	1184	1184	1172	1191	1258	1219	1166	1166
.542	1215	1211	1205	1195	1195	1184	1204	1269	1230	1177	1177
.583	1224	1220	1215	1205	1204	1194	1214	1277	1239	1186	1186
.625	1231	1228	1222	1213	1212	1202	1223	1284	1247	1194	1194
.667	1238	1234	1229	1219	1218	1210	1231	1289	1253	1200	1200
.708	1243	1240	1234	1225	1223	1216	1237	1292	1258	1206	1206
.750	1248	1244	1239	1229	1228	1221	1242	1295	1262	1211	1211
.792	1252	1248	1243	1233	1232	1225	1247	1298	1265	1215	1215
.833	1255	1251	1246	1237	1235	1229	1251	1299	1268	1219	1219
.875	1258	1254	1249	1240	1238	1233	1255	1301	1271	1222	1222
.917	1261	1257	1251	1243	1241	1237	1258	1302	1273	1226	1226
.958	1265	1261	1255	1246	1244	1241	1262	1304	1276	1229	1229
1.000	1268	1264	1258	1250	1248	1245	1266	1307	1279	1233	1233

MAXIMUM INTERNAL FUELED MATRIX TEMPERATURE (K)

AXIAL POSITION	RADIAL POSITION										
	0.000	.048	.095	.143	.190	.238	.286	.333	.381	.429	.476
0.000	802	802	802	802	802	801	800	799	797	795	793
.042	939	939	939	939	938	937	935	933	931	928	926
.083	1081	1081	1081	1081	1080	1079	1077	1075	1072	1070	1066
.125	1183	1183	1184	1184	1183	1181	1179	1176	1173	1171	1168
.167	1244	1244	1245	1245	1244	1242	1240	1238	1235	1233	1229
.208	1275	1275	1275	1275	1274	1272	1270	1268	1266	1264	1260
.250	1295	1295	1295	1295	1294	1292	1290	1288	1286	1284	1281
.292	1305	1305	1305	1305	1304	1302	1300	1298	1296	1294	1291
.333	1309	1309	1309	1309	1308	1306	1304	1302	1300	1299	1295
.375	1309	1309	1309	1309	1308	1306	1304	1301	1299	1298	1295
.417	1306	1306	1306	1306	1305	1303	1301	1299	1298	1297	1293
.458	1303	1303	1303	1303	1302	1300	1299	1297	1295	1293	1290
.500	1300	1300	1300	1300	1299	1297	1296	1294	1292	1290	1287
.542	1297	1297	1297	1297	1296	1295	1293	1291	1289	1288	1284
.583	1295	1295	1295	1295	1294	1292	1291	1289	1287	1286	1282
.625	1293	1293	1293	1293	1292	1290	1289	1287	1285	1284	1281
.667	1292	1292	1292	1292	1291	1290	1288	1286	1284	1283	1280
.708	1290	1290	1291	1290	1290	1288	1286	1285	1283	1281	1278
.750	1290	1290	1290	1290	1289	1287	1286	1284	1282	1281	1277
.792	1289	1289	1289	1289	1288	1287	1285	1283	1282	1281	1278
.833	1289	1289	1289	1289	1288	1287	1285	1283	1282	1280	1277
.875	1290	1290	1290	1290	1289	1288	1286	1284	1283	1281	1278
.917	1291	1291	1292	1291	1291	1289	1287	1286	1284	1283	1279
.958	1295	1295	1295	1295	1294	1293	1291	1289	1288	1286	1283
1.000	1298	1298	1298	1298	1297	1295	1294	1292	1290	1289	1286

MAXIMUM INTERNAL FUELED MATRIX TEMPERATURE (K)

AXIAL POSITION	RADIAL POSITION										
	.524	.571	.619	.667	.714	.762	.810	.857	.905	.952	1.000
0.000	790	786	782	778	772	763	772	811	803	814	831
.042	922	917	912	905	899	886	900	961	942	947	976
.083	1062	1056	1050	1041	1037	1021	1033	1103	1069	1059	1099
.125	1162	1157	1150	1140	1137	1120	1132	1215	1169	1147	1193
.167	1223	1218	1212	1201	1200	1181	1197	1291	1237	1196	1242
.208	1254	1250	1244	1231	1233	1213	1231	1331	1273	1218	1259
.250	1275	1270	1265	1252	1255	1235	1251	1345	1288	1232	1269
.292	1285	1281	1276	1263	1266	1246	1262	1354	1298	1236	1268
.333	1290	1285	1281	1268	1271	1253	1269	1357	1302	1240	1268
.375	1289	1286	1281	1268	1272	1254	1271	1356	1303	1242	1265
.417	1287	1284	1280	1267	1270	1253	1271	1354	1303	1238	1257
.458	1285	1281	1276	1265	1267	1252	1271	1353	1303	1235	1251
.500	1282	1279	1274	1262	1264	1250	1271	1349	1301	1234	1247
.542	1280	1276	1271	1259	1262	1248	1269	1343	1297	1232	1243
.583	1277	1274	1269	1258	1259	1247	1268	1338	1295	1231	1240
.625	1275	1272	1267	1257	1257	1246	1268	1335	1293	1231	1238
.667	1275	1271	1266	1255	1256	1246	1268	1331	1291	1231	1237
.708	1273	1270	1265	1254	1254	1246	1267	1327	1289	1231	1236
.750	1273	1269	1264	1254	1254	1246	1267	1324	1288	1232	1236
.792	1273	1269	1264	1254	1253	1246	1268	1321	1287	1232	1236
.833	1273	1269	1263	1254	1253	1247	1269	1320	1286	1233	1236
.875	1274	1269	1264	1255	1253	1247	1270	1318	1286	1235	1237
.917	1275	1271	1265	1256	1255	1251	1272	1318	1286	1237	1238
.958	1279	1274	1269	1260	1259	1255	1276	1320	1289	1239	1240
1.000	1281	1277	1272	1263	1262	1258	1280	1323	1293	1243	1244

PEBBLE INTERNAL SHELL/MATRIX INTERFACE TEMPERATURE (K)

AXIAL POSITION	RADIAL POSITION										
	0.000	.048	.095	.143	.190	.238	.286	.333	.381	.429	.476
0.000	726	726	726	726	726	725	724	723	722	721	719
.042	834	834	834	834	833	832	831	829	828	826	824
.083	944	944	944	944	943	942	941	939	937	935	932
.125	1031	1031	1031	1031	1030	1028	1027	1025	1023	1021	1018
.167	1093	1093	1093	1093	1092	1090	1089	1087	1085	1083	1079
.208	1135	1135	1135	1135	1134	1132	1131	1129	1127	1125	1122
.250	1169	1169	1169	1169	1168	1166	1165	1163	1161	1159	1156
.292	1194	1194	1195	1195	1194	1192	1190	1188	1186	1185	1181
.333	1214	1214	1214	1214	1213	1212	1210	1208	1206	1205	1201
.375	1229	1229	1229	1229	1228	1226	1224	1222	1220	1219	1215
.417	1240	1240	1240	1240	1239	1237	1235	1233	1231	1230	1227
.458	1248	1248	1248	1248	1247	1245	1243	1242	1240	1238	1235
.500	1254	1254	1254	1254	1253	1252	1250	1248	1246	1245	1242
.542	1260	1260	1260	1260	1259	1257	1256	1254	1252	1250	1247
.583	1264	1264	1264	1264	1263	1262	1260	1258	1256	1255	1252
.625	1267	1267	1267	1267	1267	1265	1263	1262	1260	1259	1255
.667	1271	1271	1271	1271	1270	1269	1267	1265	1263	1262	1258
.708	1273	1273	1273	1273	1272	1271	1269	1267	1266	1264	1261
.750	1275	1275	1276	1275	1275	1273	1271	1270	1268	1266	1263
.792	1277	1277	1277	1277	1276	1275	1273	1271	1270	1269	1266
.833	1279	1279	1279	1279	1278	1277	1275	1273	1272	1270	1267
.875	1281	1281	1281	1281	1280	1279	1277	1276	1274	1272	1269
.917	1283	1283	1284	1283	1283	1281	1279	1278	1276	1275	1271
.958	1287	1287	1287	1287	1286	1285	1283	1281	1280	1278	1275
1.000	1290	1290	1290	1290	1289	1288	1286	1284	1283	1281	1278

PEBBLE INTERNAL SHELL/MATRIX INTERFACE TEMPERATURE (K)

AXIAL POSITION	RADIAL POSITION										
	.524	.571	.619	.667	.714	.762	.810	.857	.905	.952	1.000
0.000	717	714	711	708	703	697	704	733	727	734	741
.042	821	817	813	808	803	794	804	850	837	840	853
.083	929	924	919	913	909	897	907	961	936	929	947
.125	1014	1009	1004	996	993	979	990	1054	1021	1005	1025
.167	1075	1071	1065	1056	1055	1039	1053	1127	1087	1058	1077
.208	1117	1113	1107	1097	1097	1081	1097	1177	1133	1093	1110
.250	1151	1147	1141	1131	1132	1115	1131	1209	1164	1121	1136
.292	1176	1172	1167	1156	1158	1141	1156	1235	1189	1140	1154
.333	1196	1192	1187	1176	1177	1161	1177	1254	1209	1158	1170
.375	1210	1206	1202	1190	1192	1176	1193	1269	1224	1172	1182
.417	1221	1218	1213	1202	1203	1188	1206	1280	1236	1181	1189
.458	1230	1226	1221	1210	1211	1197	1216	1290	1246	1188	1195
.500	1237	1233	1228	1217	1218	1205	1225	1297	1254	1195	1200
.542	1242	1238	1233	1223	1224	1211	1232	1301	1259	1200	1205
.583	1247	1243	1238	1228	1228	1217	1237	1303	1263	1205	1209
.625	1250	1246	1241	1231	1231	1221	1242	1305	1267	1210	1213
.667	1254	1250	1245	1235	1234	1225	1246	1307	1269	1213	1216
.708	1256	1252	1247	1237	1237	1228	1250	1307	1271	1216	1219
.750	1258	1255	1249	1240	1239	1231	1253	1308	1273	1220	1221
.792	1261	1257	1252	1242	1241	1234	1256	1308	1274	1222	1224
.833	1263	1258	1253	1244	1243	1237	1259	1308	1276	1225	1226
.875	1265	1261	1255	1246	1244	1239	1261	1308	1277	1228	1229
.917	1267	1263	1257	1249	1247	1243	1264	1309	1279	1230	1231
.958	1271	1266	1261	1252	1251	1247	1268	1311	1282	1234	1234
1.000	1274	1270	1264	1256	1254	1251	1272	1314	1285	1237	1237

PEBBLE SHELL/MATRIX INTERFACE TEMPERATURE GRADIENT (K/CM)

AXIAL POSITION	RADIAL POSITION										
	0.000	.048	.095	.143	.190	.238	.286	.333	.381	.429	.476
0.000	-136	-136	-136	-136	-136	-135	-135	-134	-133	-132	-131
.042	-188	-188	-188	-188	-187	-187	-186	-185	-184	-183	-182
.083	-245	-245	-245	-245	-244	-244	-243	-242	-241	-240	-239
.125	-272	-272	-272	-272	-272	-271	-271	-270	-269	-268	-267
.167	-271	-271	-271	-271	-270	-270	-269	-269	-268	-267	-266
.208	-250	-250	-250	-250	-250	-249	-248	-248	-248	-248	-246
.250	-225	-225	-225	-225	-225	-224	-223	-223	-223	-223	-222
.292	-197	-197	-197	-197	-196	-196	-196	-195	-195	-195	-195
.333	-169	-169	-169	-169	-169	-168	-168	-168	-167	-168	-168
.375	-143	-143	-143	-143	-142	-142	-142	-141	-141	-142	-141
.417	-119	-119	-119	-119	-119	-118	-118	-118	-118	-119	-118
.458	-98	-98	-98	-98	-98	-98	-98	-98	-98	-98	-98
.500	-81	-81	-81	-81	-81	-81	-81	-81	-81	-81	-81
.542	-67	-67	-67	-67	-67	-67	-67	-67	-67	-67	-67
.583	-55	-55	-55	-55	-55	-55	-55	-55	-55	-55	-55
.625	-45	-45	-45	-45	-45	-45	-45	-45	-45	-46	-45
.667	-37	-37	-37	-37	-37	-37	-37	-37	-37	-37	-37
.708	-31	-31	-31	-31	-31	-31	-31	-31	-31	-31	-31
.750	-25	-25	-25	-25	-25	-25	-25	-25	-25	-25	-25
.792	-21	-21	-21	-21	-21	-21	-21	-21	-21	-22	-22
.833	-18	-18	-18	-18	-18	-18	-18	-18	-18	-18	-18
.875	-16	-16	-16	-16	-16	-16	-16	-16	-16	-16	-16
.917	-14	-14	-14	-14	-14	-14	-14	-14	-14	-14	-14
.958	-14	-14	-14	-14	-14	-14	-14	-14	-14	-14	-14
1.000	-13	-13	-13	-13	-13	-13	-13	-13	-13	-13	-13

PEBBLE SHELL/MATRIX INTERFACE TEMPERATURE GRADIENT (K/CM)

AXIAL POSITION	RADIAL POSITION										
	.524	.571	.619	.667	.714	.762	.810	.857	.905	.952	1.000
0.000	-130	-128	-126	-124	-121	-117	-121	-140	-136	-141	-159
.042	-180	-178	-176	-173	-171	-165	-171	-197	-188	-190	-220
.083	-237	-235	-232	-229	-228	-221	-224	-254	-237	-231	-272
.125	-265	-263	-261	-257	-257	-250	-253	-286	-264	-252	-299
.167	-264	-263	-262	-258	-259	-252	-256	-292	-267	-246	-293
.208	-245	-244	-243	-239	-242	-235	-239	-275	-250	-224	-266
.250	-221	-220	-220	-216	-220	-214	-215	-243	-221	-198	-237
.292	-194	-193	-193	-190	-194	-188	-189	-213	-194	-171	-203
.333	-167	-167	-167	-164	-167	-163	-163	-183	-166	-147	-175
.375	-141	-141	-142	-139	-143	-138	-138	-155	-141	-124	-148
.417	-118	-118	-119	-117	-120	-116	-116	-131	-119	-102	-122
.458	-98	-98	-98	-97	-99	-97	-98	-111	-101	-84	-100
.500	-81	-81	-82	-80	-82	-80	-81	-93	-84	-69	-82
.542	-67	-67	-67	-66	-68	-66	-67	-76	-69	-57	-67
.583	-55	-55	-55	-55	-56	-55	-55	-63	-57	-47	-55
.625	-45	-45	-46	-45	-46	-45	-46	-52	-47	-38	-46
.667	-37	-38	-38	-37	-38	-38	-38	-43	-38	-32	-37
.708	-31	-31	-31	-30	-32	-31	-31	-35	-31	-26	-31
.750	-25	-26	-26	-25	-26	-26	-25	-29	-27	-21	-25
.792	-21	-21	-22	-21	-22	-21	-21	-24	-22	-18	-21
.833	-18	-18	-18	-18	-18	-18	-18	-21	-18	-15	-17
.875	-16	-16	-16	-15	-15	-15	-15	-17	-15	-13	-15
.917	-14	-14	-14	-14	-15	-14	-14	-16	-14	-11	-13
.958	-14	-14	-14	-14	-15	-14	-14	-16	-14	-10	-11
1.000	-13	-13	-13	-13	-14	-14	-14	-17	-15	-11	-11

KILOWATTS/PEBBLE INPUT FROM VSOP

AXIAL POSITION	RADIAL POSITION										
	0.000	.048	.095	.143	.190	.238	.286	.333	.381	.429	.476
0.000	4.000	4.000	4.000	4.000	3.994	3.982	3.971	3.949	3.925	3.897	3.866
.042	4.100	4.100	4.100	4.100	4.092	4.077	4.061	4.044	4.025	3.997	3.972
.083	4.360	4.360	4.360	4.360	4.354	4.342	4.331	4.314	4.298	4.284	4.256
.125	4.280	4.280	4.280	4.280	4.274	4.262	4.251	4.234	4.219	4.212	4.192
.167	3.950	3.950	3.950	3.950	3.946	3.938	3.930	3.919	3.909	3.902	3.882
.208	3.500	3.500	3.500	3.500	3.496	3.488	3.480	3.475	3.470	3.470	3.452
.250	3.080	3.080	3.080	3.080	3.076	3.068	3.060	3.055	3.050	3.050	3.044
.292	2.660	2.660	2.660	2.660	2.658	2.654	2.650	2.645	2.640	2.640	2.634
.333	2.270	2.270	2.270	2.270	2.268	2.264	2.260	2.255	2.251	2.258	2.254
.375	1.910	1.910	1.910	1.910	1.908	1.904	1.900	1.895	1.891	1.898	1.894
.417	1.590	1.590	1.590	1.590	1.588	1.584	1.580	1.580	1.581	1.588	1.584
.458	1.310	1.310	1.310	1.310	1.310	1.310	1.310	1.310	1.310	1.310	1.310
.500	1.080	1.080	1.080	1.080	1.080	1.080	1.080	1.080	1.080	1.080	1.080
.542	.890	.890	.890	.890	.890	.890	.890	.890	.890	.890	.890
.583	.730	.730	.730	.730	.730	.730	.730	.730	.731	.738	.734
.625	.600	.600	.600	.600	.600	.600	.600	.600	.601	.608	.604
.667	.500	.500	.500	.500	.500	.500	.500	.500	.500	.500	.500
.708	.410	.410	.410	.410	.410	.410	.410	.410	.410	.410	.410
.750	.340	.340	.340	.340	.340	.340	.340	.340	.340	.340	.340
.792	.280	.280	.280	.280	.280	.280	.280	.280	.281	.288	.290
.833	.240	.240	.240	.240	.240	.240	.240	.240	.240	.240	.240
.875	.210	.210	.210	.210	.210	.210	.210	.210	.210	.210	.210
.917	.190	.190	.190	.190	.190	.190	.190	.190	.190	.190	.190
.958	.190	.190	.190	.190	.190	.190	.190	.190	.190	.190	.190
1.000	.180	.180	.180	.180	.180	.180	.180	.180	.180	.180	.180

KILOWATTS/PEBBLE INPUT FROM VSOP

AXIAL POSITION	RADIAL POSITION										
	.524	.571	.619	.667	.714	.762	.810	.857	.905	.952	1.000
0.000	3.827	3.777	3.720	3.660	3.575	3.455	3.574	4.129	4.010	4.167	4.680
.042	3.937	3.895	3.846	3.780	3.729	3.606	3.724	4.312	4.107	4.144	4.800
.083	4.222	4.185	4.140	4.080	4.064	3.937	3.998	4.522	4.217	4.111	4.850
.125	4.162	4.132	4.100	4.034	4.041	3.927	3.974	4.497	4.149	3.959	4.700
.167	3.856	3.840	3.820	3.760	3.785	3.677	3.734	4.264	3.903	3.591	4.270
.208	3.431	3.420	3.404	3.350	3.396	3.297	3.350	3.846	3.501	3.134	3.720
.250	3.026	3.018	3.014	2.965	3.016	2.926	2.947	3.325	3.033	2.717	3.240
.292	2.621	2.618	2.618	2.575	2.626	2.546	2.554	2.877	2.620	2.311	2.750
.333	2.241	2.242	2.248	2.205	2.249	2.194	2.191	2.459	2.239	1.974	2.350
.375	1.885	1.892	1.898	1.865	1.912	1.854	1.854	2.081	1.895	1.668	1.980
.417	1.575	1.582	1.592	1.560	1.602	1.554	1.556	1.755	1.593	1.371	1.630
.458	1.305	1.308	1.316	1.295	1.328	1.293	1.304	1.490	1.347	1.125	1.340
.500	1.080	1.088	1.092	1.070	1.101	1.072	1.086	1.244	1.122	.928	1.100
.542	.890	.894	.896	.880	.911	.882	.895	1.019	.916	.760	.900
.583	.730	.734	.740	.730	.748	.731	.733	.836	.755	.621	.740
.625	.600	.604	.610	.600	.618	.601	.611	.694	.625	.513	.610
.667	.500	.504	.506	.495	.511	.501	.502	.571	.512	.423	.500
.708	.410	.414	.416	.405	.421	.411	.413	.468	.419	.345	.410
.750	.340	.344	.346	.340	.354	.341	.340	.388	.354	.287	.340
.792	.285	.284	.290	.285	.294	.281	.284	.325	.289	.237	.280
.833	.240	.240	.240	.235	.244	.240	.241	.275	.243	.198	.230
.875	.210	.210	.210	.205	.207	.200	.205	.233	.206	.168	.200
.917	.190	.190	.190	.185	.194	.190	.185	.213	.186	.148	.170
.958	.190	.190	.190	.185	.194	.190	.188	.215	.186	.140	.150
1.000	.180	.180	.180	.175	.184	.180	.188	.223	.196	.142	.150

```
  EASYPLT DATA FILES CREATED
  USER DESIGNATED RADIAL LOCATION,  J = 21

  EASY3D DATA FILES CREATED

  CONTOUR PLOT FILM FILE CREATED

  TOTAL CP TIME INCLUDING COMPILATION =  77.378
STOP
/
```

APPENDIX D. PRINT OUTPUT FOR ANALYSIS OF ORNL PBRE BED 13FCa

```
/OLD,B13FC
/FUN,N,I=B13FC
CTIME 007.457 SEC.  FUN LASL20
/SETTL,200
$SETTL,200.
/LGO
 STIME = 8.177000

OPTIONS FOR PROGRAM AND OUTPUT CONTROL

 IN = 51    JN = 21    CC = .00500000    RP(1) = 1.285000
 RP(4) = 1    NSWP1 = 5    NSWP4 = 2
 IZSTEP = 1    IRSTEP = 1    IPRESS = 1    IVOID = 1
 IAXIAL = 1    IRAD = 1    IFILM1 = 0    IFILM2 = 1
 IFILM3 = 0    IFILM4 = 1

MAXIMUM RESIDUALS IN FIELD

 ITER = 1    RSDU(1) = -62.26226    RSDU(4) = -.00251299
 RUNTIME = 4.242000
 ITER = 2    RSDU(1) = -.180238    RSDU(4) = -.00150810
 RUNTIME = 8.515000
 ITER = 3    RSDU(1) = -.0173049    RSDU(4) = -.00142899
 RUNTIME = 12.46900
 ITER = 4    RSDU(1) = -.0114268    RSDU(4) = -.00140124
 RUNTIME = 16.44500
 ITER = 5    RSDU(1) = -.00850163    RSDU(4) = -.00135949
 RUNTIME = 20.44300
 ITER = 6    RSDU(1) = -.00681434    RSDU(4) = -.00136906
 RUNTIME = 24.40500
 ITER = 7    RSDU(1) = -.00570949    RSDU(4) = -.00137142
 RUNTIME = 28.37300
 ITER = 8    RSDU(1) = -.00488158    RSDU(4) = -.00134158
 RUNTIME = 32.34300


PREDICTIONS FOR OAK RIDGE PBRE BED-13FCA
 VALUES OF GEOMETRY AND INLET VARIABLES (S.I. UNITS)

 HEIGHT = 1.351725    RADIUS = .381000    DKUGEL = .0381000
 FMDOT = 1.438000    GINLET = 3.153255    VELIN = 2.775681
 REYN = 6275.847    POUT = 100000    TINLET = 316    FRICF = 5.607955
 AFRIC = 24.50000    BFRIC = .175400    ANGREP = .401426
```

STREAM FUNCTION

AXIAL POSITION	RADIAL POSITION										
	0.000	.050	.100	.150	.200	.250	.300	.350	.400	.450	.500
0.000	0.000	0.000	0.000	0.000	0.000	0.000	.049	.049	.049	0.000	0.000
.008	0.000	0.000	0.000	0.000	0.000	0.000	.049	.050	.054	.068	0.000
.016	0.000	0.000	0.000	0.000	0.000	0.000	.049	.053	.060	.073	.086
.024	0.000	0.000	0.000	0.000	0.000	0.000	.049	.058	.065	.077	.091
.033	0.000	0.000	0.000	0.000	0.000	.035	.047	.060	.069	.081	.095
.041	0.000	0.000	0.000	0.000	.020	.031	.044	.060	.071	.085	.099
.049	0.000	0.000	0.000	.008	.016	.028	.041	.057	.073	.088	.103
.057	0.000	0.000	0.000	.005	.013	.025	.039	.054	.072	.091	.108
.065	0.000	0.000	.001	.004	.011	.021	.037	.053	.071	.091	.112
.073	0.000	.000	.001	.004	.010	.020	.036	.052	.071	.091	.113
.081	0.000	.000	.001	.005	.010	.020	.035	.052	.071	.091	.115
.090	0.000	.000	.002	.005	.011	.020	.035	.052	.071	.092	.116
.098	0.000	.000	.002	.005	.011	.022	.036	.053	.071	.093	.117
.106	0.000	.001	.002	.006	.013	.023	.037	.053	.072	.093	.117
.151	0.000	.001	.003	.008	.016	.027	.040	.055	.072	.093	.118
.197	0.000	.001	.004	.010	.018	.028	.041	.055	.072	.093	.117
.242	0.000	.001	.005	.010	.018	.029	.041	.056	.072	.093	.116
.288	0.000	.001	.005	.010	.018	.029	.041	.055	.072	.092	.116
.334	0.000	.001	.005	.010	.018	.029	.041	.055	.072	.092	.116
.379	0.000	.001	.005	.010	.018	.029	.041	.055	.072	.092	.115
.425	0.000	.001	.005	.010	.018	.029	.041	.055	.072	.092	.115
.470	0.000	.001	.005	.010	.018	.029	.041	.055	.072	.092	.115
.516	0.000	.001	.005	.010	.018	.029	.041	.055	.072	.092	.115
.561	0.000	.001	.005	.010	.018	.029	.041	.055	.072	.092	.115
.607	0.000	.001	.005	.010	.018	.029	.041	.055	.072	.092	.115
.653	0.000	.001	.005	.010	.018	.029	.041	.055	.071	.092	.115
.698	0.000	.001	.005	.010	.018	.029	.041	.055	.071	.091	.115
.744	0.000	.001	.005	.010	.018	.028	.041	.055	.071	.091	.114
.789	0.000	.001	.004	.010	.018	.028	.040	.054	.070	.090	.113
.835	0.000	.001	.004	.010	.018	.027	.039	.053	.068	.088	.110
.880	0.000	.001	.004	.009	.017	.026	.038	.051	.066	.084	.105
.886	0.000	.001	.004	.009	.017	.026	.037	.050	.065	.083	.104
.892	0.000	.001	.004	.009	.016	.026	.037	.050	.065	.082	.102
.898	0.000	.001	.004	.009	.016	.025	.036	.049	.064	.081	.101
.904	0.000	.001	.004	.009	.016	.025	.036	.048	.063	.080	.099
.910	0.000	.001	.004	.009	.016	.024	.035	.048	.062	.078	.097
.916	0.000	.001	.004	.009	.015	.024	.034	.047	.061	.077	.094
.922	0.000	.001	.004	.009	.015	.023	.034	.046	.059	.075	.092
.928	0.000	.001	.004	.008	.015	.023	.033	.044	.058	.073	.089
.934	0.000	.001	.004	.008	.014	.022	.032	.043	.056	.070	.087
.940	0.000	.001	.003	.008	.014	.021	.031	.042	.054	.068	.084
.946	0.000	.001	.003	.007	.013	.021	.029	.040	.052	.065	0.000
.952	0.000	.001	.003	.007	.013	.020	.029	.038	.050	0.000	0.000
.958	0.000	.001	.003	.007	.012	.019	.027	.036	0.000	0.000	0.000
.964	0.000	.001	.003	.006	.011	.018	.025	0.000	0.000	0.000	0.000
.970	0.000	.001	.003	.006	.010	.016	0.000	0.000	0.000	0.000	0.000
.976	0.000	.001	.002	.005	.010	0.000	0.000	0.000	0.000	0.000	0.000
.982	0.000	.001	.002	.005	0.000	0.000	0.000	0.000	0.000	0.000	0.000
.988	0.000	.001	.002	0.000	0.000	0.000	0.000	0.000	0.000	0.000	0.000
.994	0.000	.000	0.000	0.000	0.000	0.000	0.000	0.000	0.000	0.000	0.000
1.000	0.000	0.000	0.000	0.000	0.000	0.000	0.000	0.000	0.000	0.000	0.000

STREAM FUNCTION

AXIAL POSITION	RADIAL POSITION										
	.500	.550	.600	.650	.700	.750	.800	.850	.900	.950	1.000
0.000	0.000	0.000	0.000	0.000	0.000	0.000	0.000	0.000	0.000	0.000	0.000
.008	0.000	0.000	0.000	0.000	0.000	0.000	0.000	0.000	0.000	0.000	0.000
.016	.086	0.000	0.000	0.000	0.000	0.000	0.000	0.000	0.000	0.000	0.000
.024	.091	.104	0.000	0.000	0.000	0.000	0.000	0.000	0.000	0.000	0.000
.033	.095	.109	.123	0.000	0.000	0.000	0.000	0.000	0.000	0.000	0.000
.041	.099	.113	.129	.153	0.000	0.000	0.000	0.000	0.000	0.000	0.000
.049	.103	.120	.138	.161	.192	0.000	0.000	0.000	0.000	0.000	0.000
.057	.108	.127	.147	.172	.202	.233	0.000	0.000	0.000	0.000	0.000
.065	.112	.133	.155	.181	.211	.243	.275	0.000	0.000	0.000	0.000
.073	.113	.138	.162	.189	.219	.252	.286	.322	0.000	0.000	0.000
.081	.115	.140	.169	.197	.228	.261	.296	.334	.372	0.000	0.000
.090	.116	.142	.171	.203	.235	.269	.305	.344	.386	.427	0.000
.098	.117	.143	.173	.206	.242	.278	.313	.352	.397	.436	.500
.106	.117	.144	.174	.207	.244	.286	.321	.353	.408	.443	.500
.151	.118	.146	.175	.204	.235	.267	.305	.342	.387	.439	.500
.197	.117	.144	.172	.200	.229	.259	.295	.331	.377	.427	.500
.242	.116	.143	.170	.197	.226	.256	.292	.327	.373	.422	.500
.288	.116	.142	.169	.196	.225	.255	.290	.326	.372	.421	.500
.334	.116	.142	.169	.196	.225	.254	.290	.326	.372	.421	.500
.379	.115	.142	.169	.195	.224	.254	.290	.325	.372	.421	.500
.425	.115	.142	.169	.195	.224	.254	.289	.325	.372	.421	.500
.470	.115	.142	.169	.195	.224	.254	.289	.325	.372	.421	.500
.516	.115	.141	.169	.195	.224	.254	.289	.325	.372	.421	.500
.561	.115	.141	.169	.195	.224	.254	.289	.325	.371	.421	.500
.607	.115	.141	.169	.195	.224	.254	.289	.325	.371	.421	.500
.653	.115	.141	.168	.195	.224	.254	.289	.325	.371	.421	.500
.698	.115	.141	.168	.195	.224	.253	.289	.325	.371	.420	.500
.744	.114	.140	.167	.194	.223	.252	.288	.324	.371	.420	.500
.789	.113	.139	.166	.192	.221	.251	.286	.323	.369	.419	.500
.835	.110	.136	.162	.188	.216	.246	.282	.318	.366	.416	.500
.880	.105	.128	.153	.178	.206	.235	.269	.306	.353	.404	.500
.886	.104	.126	.151	.176	.203	.232	.266	.303	.346	.397	0.000
.892	.102	.124	.148	.173	.199	.229	.261	.297	.337	0.000	0.000
.898	.101	.122	.145	.169	.196	.224	.256	.291	0.000	0.000	0.000
.904	.099	.119	.142	.166	.192	.220	.250	0.000	0.000	0.000	0.000
.910	.097	.117	.138	.162	.187	.214	0.000	0.000	0.000	0.000	0.000
.916	.094	.114	.135	.158	.183	0.000	0.000	0.000	0.000	0.000	0.000
.922	.092	.111	.132	.154	0.000	0.000	0.000	0.000	0.000	0.000	0.000
.928	.089	.108	.128	0.000	0.000	0.000	0.000	0.000	0.000	0.000	0.000
.934	.087	.104	0.000	0.000	0.000	0.000	0.000	0.000	0.000	0.000	0.000
.940	.084	0.000	0.000	0.000	0.000	0.000	0.000	0.000	0.000	0.000	0.000
.946	0.000	0.000	0.000	0.000	0.000	0.000	0.000	0.000	0.000	0.000	0.000
.952	0.000	0.000	0.000	0.000	0.000	0.000	0.000	0.000	0.000	0.000	0.000
.958	0.000	0.000	0.000	0.000	0.000	0.000	0.000	0.000	0.000	0.000	0.000
.964	0.000	0.000	0.000	0.000	0.000	0.000	0.000	0.000	0.000	0.000	0.000
.970	0.000	0.000	0.000	0.000	0.000	0.000	0.000	0.000	0.000	0.000	0.000
.976	0.000	0.000	0.000	0.000	0.000	0.000	0.000	0.000	0.000	0.000	0.000
.982	0.000	0.000	0.000	0.000	0.000	0.000	0.000	0.000	0.000	0.000	0.000
.988	0.000	0.000	0.000	0.000	0.000	0.000	0.000	0.000	0.000	0.000	0.000
.994	0.000	0.000	0.000	0.000	0.000	0.000	0.000	0.000	0.000	0.000	0.000
1.000	0.000	0.000	0.000	0.000	0.000	0.000	0.000	0.000	0.000	0.000	0.000

DIMENSIONLESS PRESSURE

AXIAL POSITION	RADIAL POSITION										
	0.000	.050	.100	.150	.200	.250	.300	.350	.400	.450	.500
0.000	0.000	0.000	0.000	0.000	0.000	0.000	1.031	1.031	1.031	0.000	0.000
.008	0.000	0.000	0.000	0.000	0.000	0.000	1.031	1.031	1.031	1.031	0.000
.016	0.000	0.000	0.000	0.000	0.000	0.000	1.031	1.031	1.031	1.031	1.031
.024	0.000	0.000	0.000	0.000	0.000	0.000	1.031	1.031	1.031	1.031	1.031
.033	0.000	0.000	0.000	0.000	0.000	1.031	1.031	1.031	1.031	1.031	1.031
.041	0.000	0.000	0.000	0.000	1.031	1.031	1.031	1.031	1.030	1.030	1.030
.049	0.000	0.000	0.000	1.031	1.031	1.031	1.031	1.031	1.030	1.030	1.030
.057	0.000	0.000	1.031	1.031	1.031	1.031	1.031	1.031	1.030	1.030	1.030
.065	0.000	1.031	1.032	1.031	1.031	1.031	1.031	1.030	1.030	1.030	1.030
.073	1.031	1.031	1.030	1.030	1.030	1.030	1.030	1.030	1.030	1.030	1.030
.081	1.030	1.030	1.029	1.030	1.030	1.030	1.030	1.030	1.030	1.030	1.029
.090	1.029	1.029	1.029	1.029	1.029	1.030	1.030	1.030	1.030	1.029	1.029
.098	1.029	1.029	1.029	1.029	1.029	1.029	1.029	1.029	1.029	1.029	1.029
.106	1.029	1.029	1.029	1.029	1.029	1.029	1.029	1.029	1.029	1.029	1.029
.151	1.027	1.027	1.027	1.027	1.028	1.028	1.028	1.028	1.028	1.027	1.027
.197	1.026	1.026	1.026	1.026	1.026	1.026	1.026	1.026	1.026	1.026	1.026
.242	1.025	1.025	1.025	1.025	1.025	1.025	1.025	1.025	1.025	1.025	1.025
.288	1.023	1.023	1.023	1.023	1.023	1.023	1.023	1.023	1.023	1.023	1.023
.334	1.022	1.022	1.022	1.022	1.022	1.022	1.022	1.022	1.022	1.022	1.022
.379	1.020	1.020	1.020	1.020	1.020	1.020	1.020	1.020	1.020	1.020	1.020
.425	1.019	1.019	1.019	1.019	1.019	1.019	1.019	1.019	1.019	1.019	1.019
.470	1.017	1.017	1.017	1.017	1.017	1.017	1.017	1.017	1.017	1.017	1.017
.516	1.016	1.016	1.016	1.016	1.016	1.016	1.016	1.016	1.016	1.016	1.016
.561	1.014	1.014	1.014	1.014	1.014	1.014	1.014	1.014	1.014	1.014	1.014
.607	1.013	1.013	1.013	1.013	1.013	1.013	1.013	1.013	1.013	1.013	1.013
.653	1.011	1.011	1.011	1.011	1.011	1.011	1.011	1.011	1.011	1.011	1.011
.698	1.010	1.010	1.010	1.010	1.010	1.010	1.010	1.010	1.010	1.010	1.010
.744	1.008	1.008	1.008	1.008	1.008	1.008	1.008	1.008	1.008	1.008	1.008
.789	1.007	1.007	1.007	1.007	1.007	1.007	1.007	1.007	1.007	1.007	1.007
.835	1.005	1.005	1.005	1.005	1.005	1.005	1.005	1.005	1.005	1.005	1.005
.880	1.004	1.004	1.004	1.003	1.003	1.003	1.003	1.003	1.003	1.004	1.003
.886	1.003	1.003	1.003	1.003	1.003	1.003	1.003	1.003	1.003	1.003	1.003
.892	1.003	1.003	1.003	1.003	1.003	1.003	1.003	1.003	1.003	1.003	1.003
.898	1.003	1.003	1.003	1.003	1.003	1.003	1.003	1.003	1.003	1.003	1.003
.904	1.003	1.003	1.003	1.003	1.003	1.003	1.003	1.003	1.003	1.003	1.002
.910	1.003	1.003	1.003	1.003	1.003	1.003	1.003	1.003	1.002	1.002	1.002
.916	1.003	1.003	1.003	1.003	1.003	1.003	1.002	1.002	1.002	1.002	1.002
.922	1.002	1.002	1.002	1.002	1.002	1.002	1.002	1.002	1.002	1.002	1.001
.928	1.002	1.002	1.002	1.002	1.002	1.002	1.002	1.002	1.001	1.001	1.001
.934	1.002	1.002	1.002	1.002	1.002	1.002	1.002	1.001	1.001	1.001	1.000
.940	1.002	1.002	1.002	1.002	1.002	1.001	1.001	1.001	1.001	1.000	1.000
.946	1.002	1.002	1.002	1.001	1.001	1.001	1.001	1.001	1.000	1.000	0.000
.952	1.001	1.001	1.001	1.001	1.001	1.001	1.001	1.000	1.000	0.000	0.000
.958	1.001	1.001	1.001	1.001	1.001	1.001	1.000	1.000	0.000	0.000	0.000
.964	1.001	1.001	1.001	1.001	1.001	1.000	1.000	0.000	0.000	0.000	0.000
.970	1.001	1.001	1.001	1.000	1.000	1.000	0.000	0.000	0.000	0.000	0.000
.976	1.000	1.000	1.000	1.000	1.000	0.000	0.000	0.000	0.000	0.000	0.000
.982	1.000	1.000	1.000	1.000	0.000	0.000	0.000	0.000	0.000	0.000	0.000
.988	1.000	1.000	1.000	0.000	0.000	0.000	0.000	0.000	0.000	0.000	0.000
.994	1.000	1.000	0.000	0.000	0.000	0.000	0.000	0.000	0.000	0.000	0.000
1.000	1.000	0.000	0.000	0.000	0.000	0.000	0.000	0.000	0.000	0.000	0.000

DIMENSIONLESS PRESSURE

AXIAL POSITION	RADIAL POSITION										
	.500	.550	.600	.650	.700	.750	.800	.850	.900	.950	1.000
0.000	0.000	0.000	0.000	0.000	0.000	0.000	0.000	0.000	0.000	0.000	0.000
.008	0.000	0.000	0.000	0.000	0.000	0.000	0.000	0.000	0.000	0.000	0.000
.016	1.031	0.000	0.000	0.000	0.000	0.000	0.000	0.000	0.000	0.000	0.000
.024	1.031	1.031	0.000	0.000	0.000	0.000	0.000	0.000	0.000	0.000	0.000
.033	1.031	1.031	1.031	0.000	0.000	0.000	0.000	0.000	0.000	0.000	0.000
.041	1.030	1.031	1.031	1.031	0.000	0.000	0.000	0.000	0.000	0.000	0.000
.049	1.030	1.030	1.031	1.031	1.031	0.000	0.000	0.000	0.000	0.000	0.000
.057	1.030	1.030	1.031	1.031	1.031	1.031	0.000	0.000	0.000	0.000	0.000
.065	1.030	1.030	1.030	1.031	1.031	1.031	1.031	0.000	0.000	0.000	0.000
.073	1.030	1.029	1.029	1.030	1.030	1.031	1.031	1.031	0.000	0.000	0.000
.081	1.029	1.029	1.029	1.029	1.030	1.030	1.030	1.031	1.031	0.000	0.000
.090	1.029	1.029	1.029	1.029	1.029	1.029	1.030	1.030	1.031	1.031	0.000
.098	1.029	1.029	1.029	1.028	1.028	1.028	1.029	1.029	1.029	1.030	1.031
.106	1.029	1.029	1.028	1.028	1.028	1.027	1.028	1.028	1.028	1.029	1.029
.151	1.027	1.027	1.027	1.027	1.027	1.026	1.026	1.026	1.026	1.026	1.026
.197	1.026	1.026	1.026	1.026	1.026	1.026	1.026	1.026	1.026	1.026	1.026
.242	1.025	1.025	1.025	1.025	1.025	1.025	1.025	1.025	1.025	1.025	1.025
.288	1.023	1.023	1.023	1.023	1.023	1.023	1.023	1.023	1.023	1.023	1.023
.334	1.022	1.022	1.022	1.022	1.022	1.022	1.022	1.022	1.022	1.022	1.022
.379	1.020	1.020	1.020	1.020	1.020	1.020	1.020	1.020	1.020	1.020	1.020
.425	1.019	1.019	1.019	1.019	1.019	1.019	1.019	1.019	1.019	1.019	1.019
.470	1.017	1.017	1.017	1.017	1.017	1.017	1.017	1.017	1.017	1.017	1.017
.516	1.016	1.016	1.016	1.016	1.016	1.016	1.016	1.016	1.016	1.016	1.016
.561	1.014	1.014	1.014	1.014	1.014	1.014	1.014	1.014	1.014	1.014	1.014
.607	1.013	1.013	1.013	1.013	1.013	1.013	1.013	1.013	1.013	1.013	1.013
.653	1.011	1.011	1.011	1.011	1.011	1.011	1.011	1.011	1.011	1.011	1.011
.698	1.010	1.010	1.010	1.010	1.010	1.010	1.010	1.010	1.010	1.010	1.010
.744	1.008	1.008	1.008	1.008	1.008	1.008	1.008	1.008	1.008	1.008	1.008
.789	1.007	1.007	1.007	1.007	1.007	1.007	1.007	1.007	1.007	1.007	1.007
.835	1.005	1.005	1.005	1.005	1.005	1.005	1.004	1.004	1.004	1.004	1.004
.880	1.003	1.003	1.003	1.003	1.002	1.002	1.001	1.001	1.001	1.001	1.000
.886	1.003	1.003	1.003	1.002	1.002	1.001	1.001	1.001	1.001	1.000	0.000
.892	1.003	1.003	1.002	1.002	1.002	1.001	1.001	1.000	1.000	0.000	0.000
.898	1.003	1.002	1.002	1.002	1.001	1.001	1.000	1.000	0.000	0.000	0.000
.904	1.002	1.002	1.002	1.001	1.001	1.000	1.000	0.000	0.000	0.000	0.000
.910	1.002	1.002	1.001	1.001	1.000	1.000	0.000	0.000	0.000	0.000	0.000
.916	1.002	1.001	1.001	1.000	1.000	0.000	0.000	0.000	0.000	0.000	0.000
.922	1.001	1.001	1.000	1.000	0.000	0.000	0.000	0.000	0.000	0.000	0.000
.928	1.001	1.000	1.000	0.000	0.000	0.000	0.000	0.000	0.000	0.000	0.000
.934	1.000	1.000	0.000	0.000	0.000	0.000	0.000	0.000	0.000	0.000	0.000
.940	1.000	0.000	0.000	0.000	0.000	0.000	0.000	0.000	0.000	0.000	0.000
.946	0.000	0.000	0.000	0.000	0.000	0.000	0.000	0.000	0.000	0.000	0.000
.952	0.000	0.000	0.000	0.000	0.000	0.000	0.000	0.000	0.000	0.000	0.000
.958	0.000	0.000	0.000	0.000	0.000	0.000	0.000	0.000	0.000	0.000	0.000
.964	0.000	0.000	0.000	0.000	0.000	0.000	0.000	0.000	0.000	0.000	0.000
.970	0.000	0.000	0.000	0.000	0.000	0.000	0.000	0.000	0.000	0.000	0.000
.976	0.000	0.000	0.000	0.000	0.000	0.000	0.000	0.000	0.000	0.000	0.000
.982	0.000	0.000	0.000	0.000	0.000	0.000	0.000	0.000	0.000	0.000	0.000
.988	0.000	0.000	0.000	0.000	0.000	0.000	0.000	0.000	0.000	0.000	0.000
.994	0.000	0.000	0.000	0.000	0.000	0.000	0.000	0.000	0.000	0.000	0.000
1.000	0.000	0.000	0.000	0.000	0.000	0.000	0.000	0.000	0.000	0.000	0.000

DIMENSIONLESS MASS FLUX

AXIAL POSITION	RADIAL POSITION										
	0.000	.050	.100	.150	.200	.250	.300	.350	.400	.450	.500
0.000	0.000	0.000	0.000	0.000	0.000	0.000	0.000	0.000	0.000	0.000	0.000
.008	0.000	0.000	0.000	0.000	0.000	0.000	0.000	.278	.660	.701	0.000
.016	0.000	0.000	0.000	0.000	0.000	0.000	0.000	.527	.676	.686	.631
.024	0.000	0.000	0.000	0.000	0.000	0.000	.683	.588	.623	.663	.618
.033	0.000	0.000	0.000	0.000	0.000	1.099	.879	.635	.590	.637	.610
.041	0.000	0.000	0.000	0.000	1.187	1.109	1.013	.796	.640	.651	.648
.049	0.000	0.000	0.000	1.255	1.155	1.108	1.010	.936	.783	.718	.717
.057	0.000	0.000	0.000	.960	1.065	1.132	1.034	.955	.907	.820	.785
.065	0.000	0.000	.451	.710	.878	1.083	1.071	.982	.940	.919	.865
.073	0.000	.138	.360	.639	.817	1.023	1.080	1.000	.968	.950	.948
.081	.069	.166	.481	.649	.758	1.004	1.076	1.011	.987	.976	.976
.090	.265	.347	.541	.600	.765	1.011	1.062	1.013	.998	.993	.997
.098	.378	.433	.490	.617	.862	1.018	1.018	1.007	1.003	1.005	1.013
.106	.406	.441	.504	.703	.916	.984	.991	.997	1.004	1.013	1.024
.151	.566	.600	.702	.865	.952	.951	.929	.925	.968	1.030	1.058
.197	.801	.818	.870	.916	.936	.925	.901	.897	.941	1.001	1.026
.242	.912	.914	.918	.921	.928	.915	.889	.884	.925	.984	1.008
.288	.922	.922	.922	.922	.926	.911	.884	.878	.918	.976	1.000
.334	.921	.921	.921	.921	.924	.909	.882	.875	.915	.974	.998
.379	.920	.920	.920	.919	.923	.908	.881	.874	.914	.972	.996
.425	.919	.919	.920	.919	.922	.907	.880	.873	.914	.972	.996
.470	.919	.919	.919	.918	.922	.907	.880	.873	.914	.972	.996
.516	.919	.919	.919	.918	.922	.907	.880	.873	.913	.972	.996
.561	.918	.919	.919	.918	.921	.906	.879	.873	.913	.972	.996
.607	.918	.918	.918	.917	.921	.906	.879	.873	.913	.971	.995
.653	.917	.917	.917	.916	.920	.905	.878	.872	.912	.971	.995
.698	.914	.914	.915	.914	.918	.903	.876	.870	.911	.969	.994
.744	.909	.909	.909	.909	.912	.898	.872	.866	.907	.965	.990
.789	.898	.898	.898	.898	.901	.887	.862	.856	.898	.957	.982
.835	.878	.878	.878	.877	.881	.867	.842	.837	.877	.935	.962
.880	.847	.847	.846	.845	.848	.836	.814	.806	.833	.878	.902
.886	.841	.840	.839	.838	.836	.829	.815	.811	.829	.857	.874
.892	.832	.831	.830	.828	.825	.820	.812	.811	.822	.840	.852
.898	.821	.821	.819	.817	.814	.810	.805	.805	.812	.824	.832
.904	.809	.809	.807	.805	.802	.798	.795	.796	.801	.809	.814
.910	.796	.795	.793	.791	.788	.786	.784	.784	.788	.793	.798
.916	.780	.779	.778	.776	.773	.771	.770	.771	.773	.778	.782
.922	.762	.762	.760	.758	.757	.755	.755	.755	.758	.762	.766
.928	.743	.742	.741	.739	.738	.737	.738	.739	.742	.746	.751
.934	.721	.720	.719	.718	.718	.718	.719	.722	.725	.730	.732
.940	.697	.696	.696	.695	.696	.697	.700	.704	.708	.710	.723
.946	.670	.670	.669	.670	.672	.675	.679	.685	.687	.701	0.000
.952	.641	.641	.641	.643	.647	.652	.658	.662	.676	0.000	0.000
.958	.608	.608	.609	.613	.620	.628	.634	.649	0.000	0.000	0.000
.964	.572	.572	.574	.581	.591	.601	.618	0.000	0.000	0.000	0.000
.970	.531	.531	.535	.547	.560	.581	0.000	0.000	0.000	0.000	0.000
.976	.484	.485	.493	.511	.537	0.000	0.000	0.000	0.000	0.000	0.000
.982	.428	.430	.447	.481	0.000	0.000	0.000	0.000	0.000	0.000	0.000
.988	.354	.364	.406	0.000	0.000	0.000	0.000	0.000	0.000	0.000	0.000
.994	.347	.332	0.000	0.000	0.000	0.000	0.000	0.000	0.000	0.000	0.000
1.000	.342	0.000	0.000	0.000	0.000	0.000	0.000	0.000	0.000	0.000	0.000

DIMENSIONLESS MASS FLUX

AXIAL POSITION	RADIAL POSITION										
	.500	.550	.600	.650	.700	.750	.800	.850	.900	.950	1.000
0.000	0.000	0.000	0.000	0.000	0.000	0.000	0.000	0.000	0.000	0.000	0.000
.008	0.000	0.000	0.000	0.000	0.000	0.000	0.000	0.000	0.000	0.000	0.000
.016	.631	0.000	0.000	0.000	0.000	0.000	0.000	0.000	0.000	0.000	0.000
.024	.618	.577	0.000	0.000	0.000	0.000	0.000	0.000	0.000	0.000	0.000
.033	.610	.590	.681	0.000	0.000	0.000	0.000	0.000	0.000	0.000	0.000
.041	.648	.650	.783	.930	0.000	0.000	0.000	0.000	0.000	0.000	0.000
.049	.717	.755	.873	.981	1.010	0.000	0.000	0.000	0.000	0.000	0.000
.057	.785	.824	.910	.997	.985	.959	0.000	0.000	0.000	0.000	0.000
.065	.865	.864	.919	.971	.982	.965	.959	0.000	0.000	0.000	0.000
.073	.948	.922	.936	.971	.984	.979	.976	.983	0.000	0.000	0.000
.081	.976	.990	.978	.981	.992	.992	.996	.997	1.141	0.000	0.000
.090	.997	1.010	1.034	1.019	1.006	1.006	1.000	1.026	1.042	1.238	0.000
.098	1.013	1.025	1.044	1.072	1.051	1.020	.984	1.006	1.017	1.128	0.000
.106	1.024	1.036	1.052	1.074	1.130	1.069	.876	1.024	1.058	1.002	0.000
.151	1.058	1.037	.964	.924	.907	.933	.934	.972	1.084	1.188	0.000
.197	1.026	1.000	.921	.875	.856	.883	.902	.964	1.060	1.294	0.000
.242	1.008	.981	.903	.859	.841	.871	.893	.960	1.050	1.335	0.000
.288	1.000	.974	.898	.855	.838	.870	.893	.963	1.055	1.346	0.000
.334	.998	.972	.896	.853	.837	.870	.893	.965	1.057	1.350	0.000
.379	.996	.971	.895	.853	.837	.870	.894	.966	1.058	1.351	0.000
.425	.996	.971	.895	.853	.837	.870	.894	.966	1.058	1.352	0.000
.470	.996	.971	.895	.853	.837	.870	.894	.966	1.059	1.352	0.000
.516	.996	.971	.895	.853	.837	.870	.894	.966	1.059	1.352	0.000
.561	.996	.971	.895	.853	.837	.870	.894	.966	1.059	1.353	0.000
.607	.995	.970	.895	.853	.837	.870	.894	.967	1.059	1.353	0.000
.653	.995	.970	.894	.853	.837	.871	.895	.967	1.060	1.354	0.000
.698	.994	.969	.894	.853	.837	.871	.896	.968	1.061	1.356	0.000
.744	.990	.967	.892	.852	.838	.872	.897	.971	1.065	1.361	0.000
.789	.982	.960	.888	.850	.837	.874	.901	.978	1.074	1.375	0.000
.835	.962	.942	.875	.842	.834	.876	.907	.991	1.093	1.414	0.000
.880	.902	.897	.854	.827	.829	.862	.911	.993	1.142	1.581	0.000
.886	.874	.875	.855	.834	.838	.859	.913	.972	1.128	1.656	0.000
.892	.852	.852	.842	.834	.840	.862	.906	.952	1.175	0.000	0.000
.898	.832	.833	.828	.826	.834	.854	.889	.942	0.000	0.000	0.000
.904	.814	.816	.815	.816	.825	.840	.878	0.000	0.000	0.000	0.000
.910	.798	.800	.801	.804	.810	.832	0.000	0.000	0.000	0.000	0.000
.916	.782	.785	.788	.789	.803	0.000	0.000	0.000	0.000	0.000	0.000
.922	.766	.770	.771	.782	0.000	0.000	0.000	0.000	0.000	0.000	0.000
.928	.751	.752	.763	0.000	0.000	0.000	0.000	0.000	0.000	0.000	0.000
.934	.732	.744	0.000	0.000	0.000	0.000	0.000	0.000	0.000	0.000	0.000
.940	.723	0.000	0.000	0.000	0.000	0.000	0.000	0.000	0.000	0.000	0.000
.946	0.000	0.000	0.000	0.000	0.000	0.000	0.000	0.000	0.000	0.000	0.000
.952	0.000	0.000	0.000	0.000	0.000	0.000	0.000	0.000	0.000	0.000	0.000
.958	0.000	0.000	0.000	0.000	0.000	0.000	0.000	0.000	0.000	0.000	0.000
.964	0.000	0.000	0.000	0.000	0.000	0.000	0.000	0.000	0.000	0.000	0.000
.970	0.000	0.000	0.000	0.000	0.000	0.000	0.000	0.000	0.000	0.000	0.000
.976	0.000	0.000	0.000	0.000	0.000	0.000	0.000	0.000	0.000	0.000	0.000
.982	0.000	0.000	0.000	0.000	0.000	0.000	0.000	0.000	0.000	0.000	0.000
.988	0.000	0.000	0.000	0.000	0.000	0.000	0.000	0.000	0.000	0.000	0.000
.994	0.000	0.000	0.000	0.000	0.000	0.000	0.000	0.000	0.000	0.000	0.000
1.000	0.000	0.000	0.000	0.000	0.000	0.000	0.000	0.000	0.000	0.000	0.000

AXIAL COMPONENT OF MASS FLUX

AXIAL POSITION	RADIAL POSITION										
	0.000	.050	.100	.150	.200	.250	.300	.350	.400	.450	.500
0.000	0.000	0.000	0.000	0.000	0.000	0.000	0.000	0.000	0.000	0.000	0.000
.008	0.000	0.000	0.000	0.000	0.000	0.000	0.000	.161	.452	.607	0.000
.016	0.000	0.000	0.000	0.000	0.000	0.000	0.000	.317	.479	.587	.546
.024	0.000	0.000	0.000	0.000	0.000	0.000	.660	.475	.470	.566	.541
.033	0.000	0.000	0.000	0.000	0.000	.952	.842	.631	.528	.569	.547
.041	0.000	0.000	0.000	0.000	1.028	.990	.956	.773	.621	.603	.576
.049	0.000	0.000	0.000	1.086	.991	1.008	.954	.897	.783	.681	.637
.057	0.000	0.000	0.000	.856	.957	1.036	.998	.939	.903	.813	.724
.065	0.000	0.000	.435	.681	.849	1.036	1.057	.976	.939	.919	.846
.073	0.000	.137	.359	.638	.816	1.017	1.076	.999	.968	.950	.945
.081	.069	.165	.453	.627	.757	1.003	1.076	1.011	.987	.975	.973
.090	.265	.323	.500	.595	.760	.998	1.061	1.013	.998	.992	.995
.098	.378	.404	.481	.614	.843	.996	1.015	1.006	1.003	1.004	1.011
.106	.406	.430	.502	.698	.889	.970	.988	.996	1.003	1.012	1.023
.151	.566	.599	.699	.861	.949	.949	.927	.925	.968	1.030	1.058
.197	.801	.818	.868	.914	.935	.925	.901	.897	.941	1.001	1.026
.242	.912	.914	.918	.921	.928	.915	.889	.884	.925	.984	1.008
.288	.922	.922	.922	.922	.926	.911	.884	.878	.918	.976	1.000
.334	.921	.921	.921	.921	.924	.909	.882	.875	.915	.974	.998
.379	.920	.920	.920	.919	.923	.908	.881	.874	.914	.972	.996
.425	.919	.919	.920	.919	.922	.907	.880	.873	.914	.972	.996
.470	.919	.919	.919	.918	.922	.907	.880	.873	.914	.972	.996
.516	.919	.919	.919	.918	.922	.907	.880	.873	.913	.972	.996
.561	.918	.919	.919	.918	.921	.906	.879	.873	.913	.972	.996
.607	.918	.918	.918	.917	.921	.906	.879	.873	.913	.971	.995
.653	.917	.917	.917	.916	.920	.905	.878	.872	.912	.971	.995
.698	.914	.914	.915	.914	.918	.903	.876	.870	.911	.969	.994
.744	.909	.909	.909	.909	.912	.898	.872	.866	.907	.965	.990
.789	.898	.898	.898	.898	.901	.887	.862	.856	.897	.956	.982
.835	.878	.878	.878	.877	.881	.867	.842	.836	.876	.934	.960
.880	.847	.847	.846	.845	.847	.834	.812	.805	.833	.876	.896
.886	.841	.840	.839	.837	.835	.826	.813	.810	.828	.854	.865
.892	.832	.831	.830	.827	.824	.817	.808	.807	.818	.834	.839
.898	.821	.821	.819	.816	.812	.806	.801	.800	.806	.814	.815
.904	.809	.809	.806	.803	.799	.794	.790	.788	.791	.795	.793
.910	.796	.795	.792	.789	.785	.780	.776	.774	.775	.775	.772
.916	.780	.779	.777	.773	.769	.765	.761	.758	.756	.754	.751
.922	.762	.761	.759	.755	.751	.747	.743	.739	.736	.733	.729
.928	.743	.742	.739	.736	.732	.727	.723	.719	.715	.711	.707
.934	.721	.720	.717	.714	.710	.705	.701	.696	.692	.688	.684
.940	.697	.696	.693	.690	.686	.681	.677	.672	.668	.664	.666
.946	.670	.669	.666	.663	.659	.655	.651	.647	.643	.645	0.000
.952	.641	.640	.637	.633	.630	.627	.623	.620	.622	0.000	0.000
.958	.608	.607	.604	.601	.598	.596	.593	.597	0.000	0.000	0.000
.964	.572	.570	.567	.565	.564	.563	.569	0.000	0.000	0.000	0.000
.970	.531	.529	.525	.525	.526	.535	0.000	0.000	0.000	0.000	0.000
.976	.484	.482	.478	.481	.494	0.000	0.000	0.000	0.000	0.000	0.000
.982	.428	.427	.424	.443	0.000	0.000	0.000	0.000	0.000	0.000	0.000
.988	.354	.359	.373	0.000	0.000	0.000	0.000	0.000	0.000	0.000	0.000
.994	.347	.306	0.000	0.000	0.000	0.000	0.000	0.000	0.000	0.000	0.000
1.000	.342	0.000	0.000	0.000	0.000	0.000	0.000	0.000	0.000	0.000	0.000

AXIAL COMPONENT OF MASS FLUX

AXIAL POSITION	RADIAL POSITION										
	.500	.550	.600	.650	.700	.750	.800	.850	.900	.950	1.000
0.000	0.000	0.000	0.000	0.000	0.000	0.000	0.000	0.000	0.000	0.000	0.000
.008	0.000	0.000	0.000	0.000	0.000	0.000	0.000	0.000	0.000	0.000	0.000
.016	.546	0.000	0.000	0.000	0.000	0.000	0.000	0.000	0.000	0.000	0.000
.024	.541	.499	0.000	0.000	0.000	0.000	0.000	0.000	0.000	0.000	0.000
.033	.547	.513	.590	0.000	0.000	0.000	0.000	0.000	0.000	0.000	0.000
.041	.576	.553	.654	.805	0.000	0.000	0.000	0.000	0.000	0.000	0.000
.049	.637	.629	.696	.830	.875	0.000	0.000	0.000	0.000	0.000	0.000
.057	.724	.712	.760	.845	.864	.831	0.000	0.000	0.000	0.000	0.000
.065	.846	.785	.808	.858	.884	.856	.831	0.000	0.000	0.000	0.000
.073	.945	.893	.854	.877	.896	.892	.868	.851	0.000	0.000	0.000
.081	.973	.983	.947	.907	.911	.911	.912	.891	.988	0.000	0.000
.090	.995	1.005	1.027	.993	.939	.926	.931	.959	.923	1.196	0.000
.098	1.011	1.022	1.040	1.067	1.030	.941	.924	.988	.933	1.087	0.000
.106	1.023	1.034	1.050	1.072	1.128	1.023	.833	1.023	1.004	.974	0.000
.151	1.058	1.037	.964	.923	.904	.927	.928	.969	1.079	1.187	0.000
.197	1.026	1.000	.921	.875	.855	.882	.900	.963	1.059	1.293	0.000
.242	1.008	.981	.903	.859	.841	.871	.892	.960	1.050	1.335	0.000
.288	1.000	.974	.898	.854	.838	.870	.893	.963	1.055	1.346	0.000
.334	.998	.972	.896	.853	.837	.870	.893	.965	1.057	1.350	0.000
.379	.996	.971	.895	.853	.837	.870	.894	.966	1.058	1.351	0.000
.425	.996	.971	.895	.853	.837	.870	.894	.966	1.058	1.352	0.000
.470	.996	.971	.895	.853	.837	.870	.894	.966	1.059	1.352	0.000
.516	.996	.971	.895	.853	.837	.870	.894	.966	1.059	1.352	0.000
.561	.996	.971	.895	.853	.837	.870	.894	.966	1.059	1.353	0.000
.607	.995	.970	.895	.853	.837	.870	.894	.967	1.059	1.353	0.000
.653	.995	.970	.894	.853	.837	.871	.895	.967	1.060	1.354	0.000
.698	.994	.969	.894	.853	.837	.871	.895	.968	1.061	1.356	0.000
.744	.990	.967	.892	.852	.838	.872	.897	.971	1.065	1.361	0.000
.789	.982	.960	.887	.849	.837	.874	.901	.977	1.074	1.375	0.000
.835	.960	.940	.872	.839	.831	.873	.904	.989	1.092	1.413	0.000
.880	.896	.882	.832	.810	.810	.851	.889	.981	1.095	1.552	0.000
.886	.865	.856	.826	.809	.812	.839	.881	.945	1.054	1.623	0.000
.892	.839	.830	.811	.801	.805	.826	.861	.894	1.082	0.000	0.000
.898	.815	.808	.795	.788	.792	.807	.830	.867	0.000	0.000	0.000
.904	.793	.787	.777	.772	.774	.783	.809	0.000	0.000	0.000	0.000
.910	.772	.766	.758	.754	.754	.766	0.000	0.000	0.000	0.000	0.000
.916	.751	.745	.739	.735	.739	0.000	0.000	0.000	0.000	0.000	0.000
.922	.729	.724	.718	.720	0.000	0.000	0.000	0.000	0.000	0.000	0.000
.928	.707	.702	.703	0.000	0.000	0.000	0.000	0.000	0.000	0.000	0.000
.934	.684	.685	0.000	0.000	0.000	0.000	0.000	0.000	0.000	0.000	0.000
.940	.666	0.000	0.000	0.000	0.000	0.000	0.000	0.000	0.000	0.000	0.000
.946	0.000	0.000	0.000	0.000	0.000	0.000	0.000	0.000	0.000	0.000	0.000
.952	0.000	0.000	0.000	0.000	0.000	0.000	0.000	0.000	0.000	0.000	0.000
.958	0.000	0.000	0.000	0.000	0.000	0.000	0.000	0.000	0.000	0.000	0.000
.964	0.000	0.000	0.000	0.000	0.000	0.000	0.000	0.000	0.000	0.000	0.000
.970	0.000	0.000	0.000	0.000	0.000	0.000	0.000	0.000	0.000	0.000	0.000
.976	0.000	0.000	0.000	0.000	0.000	0.000	0.000	0.000	0.000	0.000	0.000
.982	0.000	0.000	0.000	0.000	0.000	0.000	0.000	0.000	0.000	0.000	0.000
.988	0.000	0.000	0.000	0.000	0.000	0.000	0.000	0.000	0.000	0.000	0.000
.994	0.000	0.000	0.000	0.000	0.000	0.000	0.000	0.000	0.000	0.000	0.000
1.000	0.000	0.000	0.000	0.000	0.000	0.000	0.000	0.000	0.000	0.000	0.000

RADIAL COMPONENT OF MASS FLUX

AXIAL POSITION	RADIAL POSITION										
	0.000	.050	.100	.150	.200	.250	.300	.350	.400	.450	.500
0.000	0.000	0.000	0.000	0.000	0.000	0.000	0.000	0.000	0.000	0.000	0.000
.008	0.000	0.000	0.000	0.000	0.000	0.000	0.000	-.227	-.481	-.350	0.000
.016	0.000	0.000	0.000	0.000	0.000	0.000	0.000	-.421	-.477	-.356	-.315
.024	0.000	0.000	0.000	0.000	0.000	0.000	.177	-.347	-.408	-.346	-.299
.033	0.000	0.000	0.000	0.000	0.000	.550	.252	-.069	-.263	-.287	-.270
.041	0.000	0.000	0.000	0.000	.593	.500	.335	.190	-.153	-.244	-.297
.049	0.000	0.000	0.000	.628	.594	.459	.330	.266	-.003	-.227	-.330
.057	0.000	0.000	0.000	.434	.467	.457	.271	.174	.084	-.105	-.303
.065	0.000	0.000	-.119	.201	.223	.316	.175	.109	.040	-.015	-.181
.073	0.000	-.013	-.030	-.025	.054	.111	.084	.052	.010	-.034	-.080
.081	0.000	-.015	-.161	-.168	-.025	-.024	.011	.006	-.013	-.042	-.077
.090	0.000	-.127	-.207	-.074	-.087	-.163	-.047	-.027	-.028	-.045	-.069
.098	0.000	-.156	-.093	-.055	-.180	-.212	-.079	-.044	-.034	-.042	-.059
.106	0.000	-.095	-.047	-.085	-.219	-.166	-.082	-.045	-.030	-.034	-.047
.151	0.000	-.027	-.060	-.085	-.080	-.062	-.042	-.021	-.005	.001	-.001
.197	0.000	-.022	-.049	-.052	-.038	-.026	-.017	-.009	-.001	.005	.012
.242	0.000	-.010	-.016	-.014	-.010	-.006	-.003	.000	.003	.006	.009
.288	0.000	-.001	-.001	-.001	-.000	.000	.001	.002	.003	.004	.005
.334	0.000	.000	.000	.000	.001	.001	.001	.002	.002	.002	.003
.379	0.000	.000	.000	.000	.001	.001	.001	.001	.001	.001	.001
.425	0.000	.000	.000	.000	.000	.000	.000	.001	.001	.001	.001
.470	0.000	.000	.000	.000	.000	.000	.000	.000	.000	.000	.000
.516	0.000	.000	.000	.000	.000	.000	.000	.000	.000	.000	.000
.561	0.000	.000	.000	.000	.000	.000	.000	.000	.000	.000	.000
.607	0.000	.000	.000	.000	.001	.001	.001	.001	.001	.001	.001
.653	0.000	.000	.001	.001	.001	.001	.002	.002	.002	.002	.002
.698	0.000	.001	.001	.002	.003	.003	.004	.004	.004	.005	.005
.744	0.000	.001	.003	.004	.005	.006	.008	.009	.010	.011	.011
.789	0.000	.002	.005	.007	.010	.013	.015	.017	.020	.022	.025
.835	0.000	.004	.008	.012	.017	.022	.026	.029	.034	.041	.050
.880	0.000	.008	.016	.025	.035	.056	.054	.041	.027	.056	.110
.886	0.000	.009	.019	.030	.042	.062	.064	.053	.044	.074	.127
.892	0.000	.012	.023	.036	.050	.067	.074	.074	.077	.104	.147
.898	0.000	.013	.027	.042	.056	.072	.083	.090	.102	.128	.165
.904	0.000	.015	.031	.047	.063	.080	.094	.107	.124	.150	.183
.910	0.000	.017	.035	.053	.071	.089	.106	.123	.144	.170	.201
.916	0.000	.020	.039	.059	.080	.100	.119	.140	.162	.189	.218
.922	0.000	.022	.044	.066	.089	.111	.133	.156	.180	.208	.236
.928	0.000	.024	.049	.074	.098	.123	.147	.172	.199	.226	.255
.934	0.000	.027	.054	.081	.109	.135	.162	.189	.217	.245	.262
.940	0.000	.030	.060	.090	.120	.149	.178	.207	.236	.253	.283
.946	0.000	.033	.066	.099	.132	.164	.195	.225	.244	.274	0.000
.952	0.000	.036	.073	.110	.146	.180	.213	.234	.264	0.000	0.000
.958	0.000	.039	.081	.122	.161	.197	.223	.254	0.000	0.000	0.000
.964	0.000	.043	.091	.136	.178	.210	.241	0.000	0.000	0.000	0.000
.970	0.000	.046	.103	.154	.193	.227	0.000	0.000	0.000	0.000	0.000
.976	0.000	.050	.120	.172	.210	0.000	0.000	0.000	0.000	0.000	0.000
.982	0.000	.055	.142	.188	0.000	0.000	0.000	0.000	0.000	0.000	0.000
.988	0.000	.058	.159	0.000	0.000	0.000	0.000	0.000	0.000	0.000	0.000
.994	0.000	.130	0.000	0.000	0.000	0.000	0.000	0.000	0.000	0.000	0.000
1.000	0.000	0.000	0.000	0.000	0.000	0.000	0.000	0.000	0.000	0.000	0.000

RADIAL COMPONENT OF MASS FLUX

AXIAL POSITION	RADIAL POSITION										
	.500	.550	.600	.650	.700	.750	.800	.850	.900	.950	1.000
0.000	0.000	0.000	0.000	0.000	0.000	0.000	0.000	0.000	0.000	0.000	0.000
.008	0.000	0.000	0.000	0.000	0.000	0.000	0.000	0.000	0.000	0.000	0.000
.016	-.315	0.000	0.000	0.000	0.000	0.000	0.000	0.000	0.000	0.000	0.000
.024	-.299	-.288	0.000	0.000	0.000	0.000	0.000	0.000	0.000	0.000	0.000
.033	-.270	-.290	-.340	0.000	0.000	0.000	0.000	0.000	0.000	0.000	0.000
.041	-.297	-.342	-.431	-.465	0.000	0.000	0.000	0.000	0.000	0.000	0.000
.049	-.330	-.418	-.528	-.524	-.505	0.000	0.000	0.000	0.000	0.000	0.000
.057	-.303	-.416	-.500	-.530	-.473	-.480	0.000	0.000	0.000	0.000	0.000
.065	-.181	-.361	-.439	-.455	-.428	-.446	-.480	0.000	0.000	0.000	0.000
.073	-.080	-.228	-.382	-.417	-.406	-.404	-.445	-.492	0.000	0.000	0.000
.081	-.077	-.114	-.242	-.374	-.394	-.393	-.400	-.449	-.570	0.000	0.000
.090	-.069	-.097	-.119	-.230	-.361	-.392	-.364	-.365	-.483	-.320	0.000
.098	-.059	-.078	-.095	-.102	-.209	-.395	-.339	-.189	-.406	-.302	0.000
.106	-.047	-.062	-.072	-.072	-.061	-.313	-.270	-.034	-.332	-.235	0.000
.151	-.001	-.001	.009	.036	.065	.110	.097	.078	.104	.054	0.000
.197	.012	.019	.026	.033	.040	.047	.052	.052	.048	.035	0.000
.242	.009	.012	.015	.017	.019	.020	.020	.020	.017	.019	0.000
.288	.005	.006	.007	.008	.008	.008	.007	.007	.005	.004	0.000
.334	.003	.003	.003	.003	.003	.003	.003	.002	.002	.001	0.000
.379	.001	.001	.001	.001	.001	.001	.001	.001	.001	.000	0.000
.425	.001	.001	.001	.001	.001	.001	.000	.000	.000	.000	0.000
.470	.000	.000	.000	.000	.000	.000	.000	.000	.000	.000	0.000
.516	.000	.000	.000	.000	.000	.000	.000	.000	.000	.000	0.000
.561	.000	.000	.000	.000	.000	.000	.000	.000	.000	.000	0.000
.607	.001	.001	.001	.001	.001	.001	.001	.001	.000	.000	0.000
.653	.002	.002	.002	.002	.002	.002	.002	.001	.001	.001	0.000
.698	.005	.005	.005	.005	.005	.005	.004	.003	.002	.001	0.000
.744	.011	.012	.012	.012	.012	.011	.010	.008	.006	.004	0.000
.789	.025	.027	.028	.029	.028	.027	.025	.022	.017	.012	0.000
.835	.050	.059	.065	.066	.067	.066	.066	.062	.058	.049	0.000
.880	.110	.167	.195	.166	.175	.138	.203	.154	.324	.301	0.000
.886	.127	.183	.218	.201	.209	.186	.239	.227	.403	.330	0.000
.892	.147	.193	.227	.233	.242	.247	.283	.326	.459	0.000	0.000
.898	.165	.203	.233	.247	.262	.281	.318	.368	0.000	0.000	0.000
.904	.183	.216	.244	.263	.284	.304	.343	0.000	0.000	0.000	0.000
.910	.201	.231	.258	.280	.295	.325	0.000	0.000	0.000	0.000	0.000
.916	.218	.247	.273	.287	.314	0.000	0.000	0.000	0.000	0.000	0.000
.922	.236	.264	.279	.305	0.000	0.000	0.000	0.000	0.000	0.000	0.000
.928	.255	.270	.298	0.000	0.000	0.000	0.000	0.000	0.000	0.000	0.000
.934	.262	.291	0.000	0.000	0.000	0.000	0.000	0.000	0.000	0.000	0.000
.940	.283	0.000	0.000	0.000	0.000	0.000	0.000	0.000	0.000	0.000	0.000
.946	0.000	0.000	0.000	0.000	0.000	0.000	0.000	0.000	0.000	0.000	0.000
.952	0.000	0.000	0.000	0.000	0.000	0.000	0.000	0.000	0.000	0.000	0.000
.958	0.000	0.000	0.000	0.000	0.000	0.000	0.000	0.000	0.000	0.000	0.000
.964	0.000	0.000	0.000	0.000	0.000	0.000	0.000	0.000	0.000	0.000	0.000
.970	0.000	0.000	0.000	0.000	0.000	0.000	0.000	0.000	0.000	0.000	0.000
.976	0.000	0.000	0.000	0.000	0.000	0.000	0.000	0.000	0.000	0.000	0.000
.982	0.000	0.000	0.000	0.000	0.000	0.000	0.000	0.000	0.000	0.000	0.000
.988	0.000	0.000	0.000	0.000	0.000	0.000	0.000	0.000	0.000	0.000	0.000
.994	0.000	0.000	0.000	0.000	0.000	0.000	0.000	0.000	0.000	0.000	0.000
1.000	0.000	0.000	0.000	0.000	0.000	0.000	0.000	0.000	0.000	0.000	0.000

STREAM FUNCTION CONTOUR PLOT CREATED

ISOBAR PLOT CREATED

RUNTIME = 39.08500 SESSION = 47.26200
STOP
/

☆U.S. Government Printing Office: 1979 — 677-013/41

Printed in the United States of America. Available from
National Technical Information Service
US Department of Commerce
5285 Port Royal Road
Springfield, VA 22161

Microfiche $3.00

001-025	4.00	126-150	7.25	251-275	10.75	376-400	13.00	501-525	15.25
026-050	4.50	151-175	8.00	276-300	11.00	401-425	13.25	526-550	15.50
051-075	5.25	176-200	9.00	301-325	11.75	426-450	14.00	551-575	16.25
076-100	6.00	201-225	9.25	326-350	12.00	451-475	14.50	576-600	16.50
101-125	6.50	226-250	9.50	351-375	12.50	476-500	15.00	601-up	

Note: Add $2.50 for each additional 100-page increment from 601 pages up.